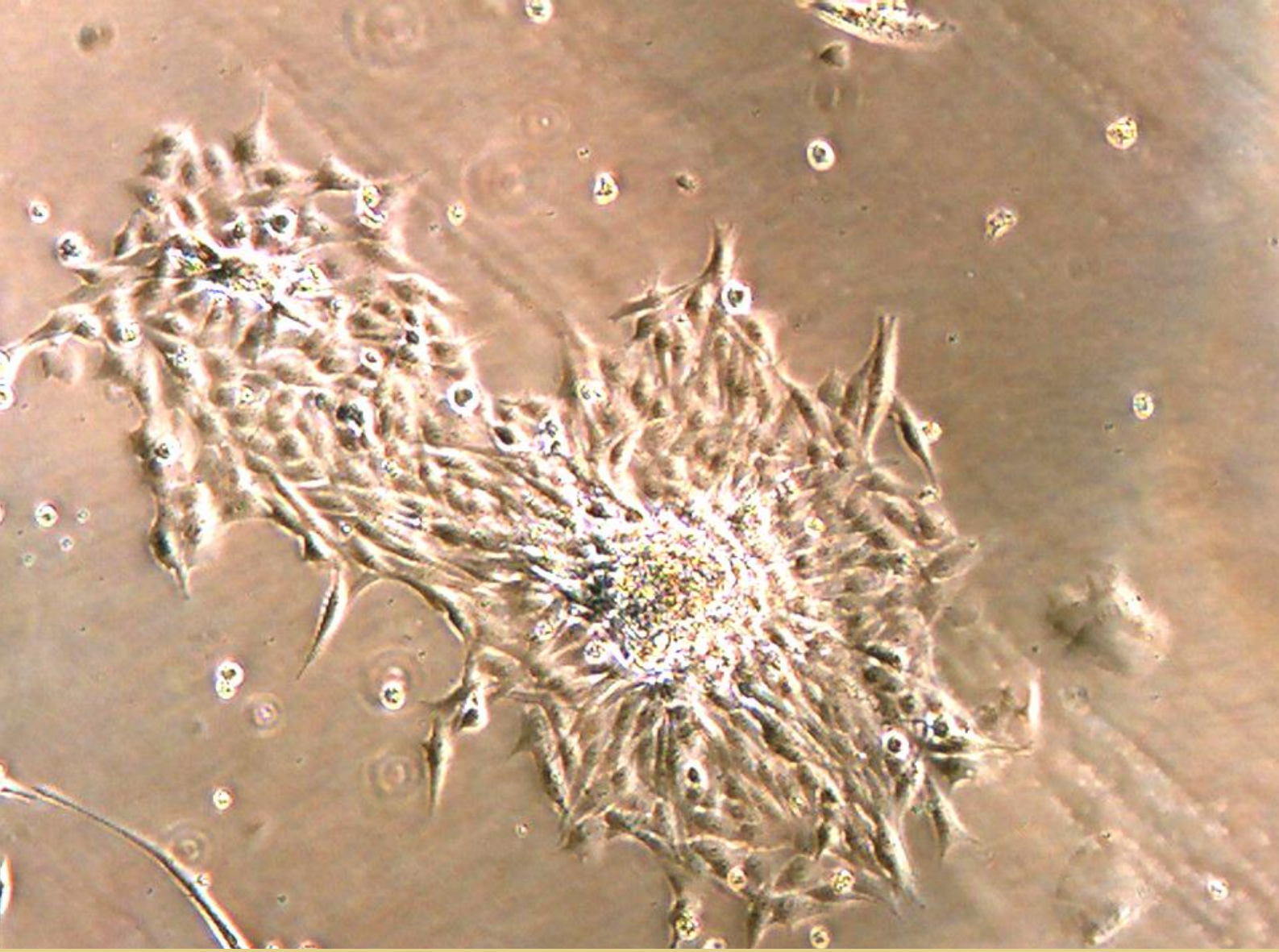

Carlos Fernando Dias Rodrigues

Hexavalent Chromium and Cancer Stem Cells: a view to a kill!

Doctoral Dissertation in the scientific field of Biosciences with specialization in Cellular and Molecular Biology, under the supervision of Maria Carmen Alpoim, PhD, presented to the Department of Life Sciences from the Faculty of Sciences and Technology of University of Coimbra

September 2013

· U C ·

Universidade de Coimbra

Hexavalent Chromium and Lung Cancer: a view to a kill!

UNIVERSIDADE DE COIMBRA

Carlos F. D. Rodrigues, BSc

School of Sciences and Technology
University of Coimbra

Dissertation submitted in partial fulfilment of the requirements for candidature for degree of

PhD in Biosciences
Specialization in Cellular and Molecular Biology

Coimbra, September 2013

rodriguescfd@gmail.com

Cover Illustration Credit: Carlos F. Dias Rodrigues

Published in Portugal on September 2013

To my parents.

Aos meus pais.

“Há um tempo em que é preciso abandonar as roupas usadas, que já têm a forma do nosso corpo. E esquecer os nossos caminhos, que nos levam sempre aos mesmos lugares. É o tempo da travessia… e se não ousarmos fazê-la, teremos ficado, para sempre, à margem de nós mesmos.”

Fernando Pessoa

This work was peformed in the Centre for Neurosciences and Cell Biology, Department of Life Sciences, University of Coimbra, Coimbra, Portugal, under the supervision of Maria Carmen Alpoim, PhD.

Finantial support for this project was attained from the Portuguese Foundation for Science and Technology (FCT) in the form of a PhD fellowship addressed to the author (SFRH/BD/33884/2009) and of a research grant addressed to Maria Carmen Alpoim (PTDC/BBB-BQB/2450/2012), and also from Centro de Investigação em Meio Ambiente, Genética e Oncobiologia (CIMAGO) in the form of a research grant addressed to Maria Carmen Alpoim (16/06).

Abstract

Bypassing all the research advances made in the last decades, cancer remains as a major public health problem affecting millions of people worldwide. The most recent advance in the tumor biology field was the discovery of cancer stem cells (CSCs) and of their implication in the metastatic disease, the main cause of cancer patients' mortality. CSCs were shown to drive tumorigenesis and differentiation, contributing to tumors' heterogeneity and to their chemo- and radiotherapy resistance and eventually relapse. Although targeted therapeutic approaches have been developed to abolish them, CSCs managed to reemerge through dedifferentiation of other tumor cells, condemning these therapies. The mechanisms behind dedifferentiation process are still unclear and were part of the main focus of this project.

Lung cancer is one of the most common neoplasias worldwide. Its prevalence is increasing due to the widespread smoking habits and increasing accumulation of atmosphere pollutants. In this work hexavalent chromium [Cr(VI)] was selected as a model for lung carcinogenesis mainly due to is increasing occupational relevance. The non-malignant human bronchial epithelial airway system 2B (BEAS-2B) was malignantly transformed into the RenG2 cell line using low density culture in the presence of Cr(VI). A parallel control cellular system (Cont1) was produced under the same conditions, though, in the absence of Cr(VI). Two additional derivative cell lines were attained following serial rounds of injection in immunocompromised mice, and named DRenG2 and DDRenG2, respectively. A panoply of techniques was then used to characterize the attained cellular systems leading to the hypothesis of CSCs involvement in Cr(VI)-driven BEAS-2B malignant transformation. The sphere-formation assay tested this hypothesis and allowed the isolation of CSC spheres (SC-DRenG2 and SC-DDRenG2 cells, respectively), but only from the derivative cell lines. These results suggested that a dedifferentiation process featured CSCs' formation during RenG2 derivation in nude mice.

The involvement of the mouse stroma in the dedifferentiation process was uncovered by surgical isolation of lumbar stromal cells (FR fibroblasts) from the subcutaneous compartment and their subsequent co-culture with RenG2 cells. Following two months, RenG2 cells were isolated from the upper compartment (iRenG2) and tested for their ability to form spheres. Gene and protein expression analysis were used to compare iRenG2 cells' signature with those of RenG2, DRenG2 and SC-DRenG2, showing that iRenG2 cells were no longer similar to RenG2 but rather more close to both DRenG2 and SC-DRenG2. Finally, the study of the conditioned media from co-cultured cells identified interleukin-6 (IL-6), granulocyte colony-stimulating factor (G-CSF) and Activin-A as the potential paracrine orchestrators of this stromal-induced dedifferentiation process.

Resumo

Contornando os avanços científicos feitos nas últimas décadas, o cancro prevalece como um grande problema de saúde pública que afeta milhões de pessoas por todo o mundo. O avanço mais recente feito no campo da oncobiologia foi a descoberta das células estaminais tumorais (CETs) e do seu envolvimento na doença metastática, a principal causa de morte em doentes oncológicos. Subsequentemente ficou demonstrado que as CETs regulam a tumorigenicidade e o grau de diferenciação tumoral, sendo ainda responsáveis pela resistência às terapias convencionais e pelas recidivas. Mais recentemente foram desenvolvidas terapias direcionadas especificamente a estas células que, no entanto, não surtiram o efeito esperado, uma vez as CETs conseguem regenerar-se por dediferenciação a partir de outras células do tumor. Os mecanismos subjacentes ao processo de dediferenciação são ainda desconhecidos, constituindo a sua caracterização parte dos objetivos deste trabalho.

O cancro do pulmão é uma das neoplasias mais frequentes. A sua prevalência tem aumentado nos últimos anos, principalmente devido ao acréscimo dos hábitos tabágicos e à acumulação de poluentes atmosféricos. Neste trabalho utilizou-se o crómio hexavalente [Cr(VI)], um agente carcinogénico cujos níveis atmosféricos e relevância ocupacional têm aumentado significativamente nos últimos anos. Para os nossos estudos selecionámos uma linha celular não maligna de epitélio bronquial humano (BEAS-2B), a qual foi malignizada por cultura a baixa densidade na presença de Cr(VI), originando a linha celular RenG2. Em paralelo, uma linha controlo cultivada a baixa densidade na ausência de Cr(VI) (Cont1) foi também estabelecida. Visando aumentar o seu potencial maligno, as células RenG2 foram injetadas em murganhos imunocomprometidos e uma nova linha celular (DRenG2) foi estabelecida a partir do tumor formado. Este processo foi repetido com as células DRenG2, tendo-se obtido as células DDRenG2. Diversas técnicas de biologia celular e molecular foram então utilizadas para caracterizar os vários sistemas celulares, tendo os resultados obtidos sugerido o envolvimento de

CETs na malignização das células BEAS-2B. Esta hipótese foi testada usando o ensaio de formação de esferas, no qual se observou a formação de colónias SC-DRenG2 e SC-DDRenG2, apenas nos dois sistemas derivados, DRenG2 e DDRenG2, respetivamente. Os resultados obtidos sugeriram que a formação de CETs na população de RenG2 injetada em murganhos imunocomprometidos decorreu de um processo de dediferenciação, provavelmente orquestrado pelas células do estroma do compartimento subcutâneo do animal. Para testar esta teoria, foram isoladas cirurgicamente células da região lombar de murganhos singénicos aos anteriores, e uma linha primária de fibroblastos (FR) foi estabelecida. A sua subsequente co-cultura com as células RenG2 durante dois meses levou à formação de uma população de CETs no seio das células RenG2 isoladas (iRenG2), cuja posterior caracterização mostrou serem mais semelhantes às DRenG2 e SC-DRenG2 do que às suas progenitoras RenG2. Por fim, o estudo dos meios condicionados das células em co-cultura identificou a Interleucina-6 (IL-6), o Factor estimulador de colónias derivado de granulócitos (G-CSF) e a Activina-A como potenciais mediadores parácrinos do processo de dediferenciação induzido pelas células do estroma do murganho.

Acknowledgements

My first acknowledgment is to **Professor Maria Carmen Alpoim**. More than just a supervisor, she was a mentor and a good friend. She taught me that only being humble I could understand biology and life, and that the search for excellence may sometimes deprive us of attaining the good. Always eager to listen to my ideas and unsubstantiated theories, she fueled my creativity with her wise opinions and always sent me to collect the good of our joint work. Words will never be enough to say how much I have enjoyed these years and how grateful I am for having her mentoring and friendship.

I would also like to acknowledge the **Portuguese Foundation for Science and Technology** for my PhD fellowship. I like to think that I have used it properly while building my (yet) little family's home.

To **Professor Isabel Marques Carreira** I want to express my gratitude for accepting me in her laboratory, trusting me, and never making me fell an outsider. Even with her restricted agenda, she always maneuvered to have time for my existential doubts and never neglected helping when I needed. I just hope this work makes her proud of her investment.

This project was performed in many laboratories, in different cities and with the help of different persons. As so, it would not have been possible otherwise and because of that, I am eternally grateful to everyone involved. Initially we were three, with **Professor Ana Urbano**, then we joined the **Cytogenetics laboratory** and I must admit those were some of the best years of my life. **Professor Filomena Botelho** and **Master Margarida Abrantes** were fundamental in the mice experiments, and **Professor Lina Carvalho** was tireless in accepting my slides for analysis and spending entire afternoons with me in the microscope. **Professor Carolino Monteiro** and **Doctor Margarida Alves** performed the microsatellite analysis and **Professor Artur Paiva** and his team introduced me to flow cytometry and real time PCR. Last, but not less important, **Doctor Célia Gomes** presented me to the world of cancer stem cells and **Doctor Antero**

Abrunhosa allowed me to perform the metabolic studies in his laboratory. You will always have my gratitude and recognition.

A good team always helps attaining a good performance. That being said, I cannot forget our home-made masters **Mariana Val** and **João Fonseca**. I know it can be difficult to work with me and that I may have sometimes pushed you more than you have liked. I believe you understand that my goal was to help you starting your future and I hope I have succeeded.

The best motivation for me to work is perhaps to know that at the end of the day I will have a programme with friends. If you have not noticed yet, you are a very important part of my life, upon which I tremendously depend. And that became even clearer for me during this writing period when I have been more deprived from your company. So let's go, without any special order, but respecting the chivalric traditions.

My little **Pat**, you will always be for me an example of motivation and determination. I guess I do not need to say how much I love to talk to you, to laugh with you and how delightful is our capacity of brainstorming on science (or whatever other subject!) at anytime or stage of tiredness. It has been a pleasure to be your friend!

Filhota, having your company during the last moths was absolutely decisive for me to have everything ready at time. Whatever are the future designs, they will certainly not erase what we have shared together, and I am pretty much optimistic that they may meet some of our shared dreams. Gonçalinho, my favourite biochemist, I would never had survived without your help in formatting this Thesis. Thank you for spending part of your vacations helping me.

Réu, my acquired brother! Faculty was just the beginning of our journey together. Yet separated by a couple thousands of miles, you have always managed to make yourself present. Plus, I could have never survived without you sending me papers!

Carlitis, my dear friend, there is no way I can express in words how much important our friendship was in the last years. Our weakly dinners followed by a couple of beers and a lot of talk made everything easier.

After all of you, it is only missing my family. The one that built me and the one I built. Yes, I am talking to you, **Joana and Gonçalo**. In fact, I have just placed you on the place that you already occupy for long. Thank you for all the dinners, teas, concerts, talks, walks, phone calls, postcards, everything. Thank you for being part of our lives and making us be better persons.

Inês. My friend, my love, my wife, my accomplice. This project is over! And we have done it together. It has not been easy to hold back our projects and dreams hoping for a better future, even more being separated. But there is a time for everything, and these years were for the future. Now is time to abandon the worn clothes and recover the invested time. Let's get married again!

Mãe e Pai, esta Tese é inteiramente dedicada a vós. Espero que vos faça sentir orgulhosos, mas por vocês, pois ela é o resultado do vosso trabalho, empenho, dedicação e amor. Obrigado soará sempre a pouco…Amo-vos incondicionalmente.

Contents

List of Figures

List of Tables

List of Abbreviations

- Cell passage number.

^{18}FDG - [^{18}F]-fluoro-2-deoxyglucose.

α -SMA - α-smooth muscle actin.

AB(s) - Antibody(ies).

Abs - Absorbance.

ACS- American Cancer Society.

AD12 - Adenovirus 12.

ALDH1 - Aldehyde dehydrogenase 1.

Angptl4 - Angiopoitin-like-4.

AP - Apurinic/Apyrimidinic.

APC - Adenomatous polyposis coli.

APE - Apurinic/Apyrimidinic endonuclease.

ATM - Ataxia-telangiectasia mutated protein.

AURKA - Aurora kinase A.

AURKB - Aurora kinase B.

AVCs - Angiogenic vascular cells.

BAGE - B melanoma antigen.

BASC - Bronchioalveolar stem cells.

BBB - Blood-brain barrier.

BC - Before Christ.

BCR-ABL - C-Abl Oncogene 1, non-receptor tyrosine kinase.

BER - Base excision repair.

BM - Bone marrow.

bFGF - Basic fibroblast growth factor.

BSA - Bovine serum albumin.

CAFs - Cancer-associated fibroblasts.

CAV-1 - Caveolin-1.

CCL-n - chemokine (C-C motif) ligand n.

CCND1 - Cyclin D1 gene.

CDn - Cluster of differentiation n.

CETs - Células estaminais tumorais.

CHO - Chinese hamster ovary.

CI5 - Cancer Incidence in Five Continents.

Cis - Cisplatin.

CK1 - Casein kinase 1.

CK7 - Cytokeratin 7.

Clara^{V} - Variant Clara cells.

CLL - Chronic lymphoid leukemia.

CML - Chronic myeloid leukemia.

COX-2 - Cyclooxygenase-2.

Cr(III) - Trivalent chromium.

Cr(VI) - Hexavalent chromium.

CSCs - Cancer stem cells.

CTCs - Circulating tumor cells.

CTLs - Cytotoxic T lymphocytes.

CXCLn - C-X-C chemokine ligand n.

CXCRn - C-X-C chemokine receptor type n.

Cyn - Cyanine n.

DAB - Diaminobenzidine tetrahydrochloride.

DALYs - Disability-adjusted life years.

DAPI - 4',6-Diamidino-2-phenylindole.

DLL4 - Delta-like 4 ligand.

DMSO - Dimethyl sulfoxide.

DNA - Deoxyribonucleic acid.

DPCs - DNA-protein crosslinks.

DSB - Double strand breaks.

DT - Doubling time.

ECs - Endothelial cells.

ECCAC - European collection of cell cultures.

ECM - Extracellular matrix.

EDN1 - Endothelin 1.

EGF - Epidermal growth factor.

ELAC2 - ElaC homolog 2.

ELISA - Enzyme-linked immunosorbent assay.

EMT - Epithelial to mesenchymal transition.

EPCs - Endotelial precursor cells.

EXO1 - Exonuclease 1.

FA - Fanconi anemia.

FACS - Fluorescence associated cell sorting.

FANCD2 - Fanconi anemia complementation group D.

FBS - Fetal bovine serum.

FELASA - Federation for Laboratory Animal Science Associations.

Fzd - Frizzled.

G-CSF - Granulocyte colony-stimulating factor.

Gem - Gemcitabine.

GM-CSF - Granulocyte macrophage colony-stimulating factor.

GFP - Green fluorescent protein.

GI - Genomic instability.

GSK3-β - Glycogen synthase kinase 3 beta.

GWAS - Genome wide association studies.

HBE - Human bronchial epithelium.

hESCs - Human embryonic stem cells.

HGF - Hepatocyte growth factor.

HIF-1α - Hypoxia-inducible factor 1α.

HIF-1β - Hypoxia-inducible factor 1β.

HLA-A,B,C - Major histocompatibility complex, class I, A, B and C.

HR - Homologous recombination.

IARC - International Agency for Research on Cancer.

ICLs - Inter/intrastrand crosslinks.

IICs - Infiltrating immune cells.

IL-n - Interleukin n.

INF-γ - Interferon gamma.

IP - Interferon gamma-induced protein.

IPs - Inducible pluripotent stem cells.

ITS - Insulin, transferrin and selenium pyruvate solution.

JAK - Janus kinase.

LC - Lung cancer.

LEF - Lymphoid enhancer factor.

LOX - Lysyl oxydase.

mAb(s) - Monoclonal antibody(ies).

MAPK - Mitogen-activated protein kinase 1.

MCP-1 - Monocyte chemotactic protein-1.

mESCs - Mouse embryonic stem cells.

MIP - Macrophage inflammatory protein.

MLH - Human MutL-homolog protein.

MLL - Myeloid/Lymphoid Or Mixed-Lineage Leukemia gene.

MMP-n - Metalloproteinase n.

MMR - Mismatch repair.

MSH - Human MutS-homolog protein.

MSI - Microsatellite instability.

MTT - 3-[4, 5-dimethylthiazol-2-yl]-2, 5-diphenyltetrazolium bromide.

MTX - Methotrexate.

MYC -Myelocytomatosis viral oncogene homolog.

MYCT1 - MYC target 1

NAD^+/NADH - Nicotinamide adenine dinucleotide.

NER - Nucleotide excision repair system.

NFATC1 - Nuclear Factor Of Activated T-Cells, Cytoplasmic, Calcineurin-Dependent 1.

NF_KB - Nuclear factor of kappa light polypeptide gene enhancer.

NGFR - Nerve growth factor receptor.

NK - Natural killer.

NSCLC - Non-small cell lung cancer.

OCT-3/4 - Octamer-binding protein ¾.

OGG1 - 8-oxo-guanine DNA glycosylase 1.

PBS - Phosphate-buffered saline.

PDGF - Platelet-derived growth factor.

PE - Plating efficiency.

PET - Positron emission tomography.

PFA - Paraformaldehyde.

Pgp - P-glycoprotein.

PI3K - Phosphoinositide-3-kinase.

PMN - Pre-metastatic niche.

PNEC - Pulmonary neuroendocrine cells.

Poly-HEMA - Poli-(2-hydroxyethyl methacrylate).

Polβ - DNA polymerase β.

RAF - Raf-1 murine leukemia viral oncogene homolog 1.

RAS - Rat sarcoma.

RANTES - Regulated on activation, normal T cell expressed and secreted protein.

RB1 - Retinoblastoma gene 1.

ROS - Reactive oxygen species.

Rpm - Revolutions per minute.

RT - Room temperature.

SCs - Stem cells.

SCID - Severe combined immunodeficiency.

SCLC - Small-cell lung cancer.

SMO - Smoothened.

SNAI3 - Snail homolog 3.

SORCS1 - Sortilin-related VPS10 domain containing receptor 1.

SOX2 - SRY-box containing gene 2.

SRC - Sarcoma (Schmidt-Ruppin A-2) viral oncogene homolog.

SSB - Single strand break.

STAT - Signal transducer and activator of transcription.

SV40 - Simian virus 40.

TAMs - Tumor-associated macrophages.

TBC1D7 - TBC1 domain family, member 7.

TCA - Tricarboxilic acid.

TCF - T-cell factor.

TFAP2A - Transcription factor AP-2 alpha.

TGF-β - Tumor growth factor β.

TMEM - Tumor microenvironment of metastases.

TNF-α - Tumor necrosis factor α.

TP53 - Tumor protein P53.

USEPA - United States Environmental Protection Agency.

VE-Cadherin - Vascular endothelium cadherin.

VEGF - Vascular endothelial growth factor.

VEGFR1 - Vascular endothelium growth factor receptor 1.

VEGFR2 - Vascular endothelium growth factor receptor 2.

VPS10 - Vacuolar protein sorting 10.

XP - *Xeroderma pigmentosum*.

XRCC1 - X-ray cross-complementing group 1.

WNT - Wingless-type mouse mammary tumor virus integration site family.

ZC3HAV1 - Zinc finger CCCH-type antiviral 1 gene.

PART I

General Introduction

Chapter 1

Cancer

Cancer is probably one of the most intriguing mysteries of biology and medicine. With its intricate pathways and deceiving strategies, it has always managed to defeat its aggressors and win the battle against cure. Acting as a professional spy, cancer keeps evading the tremendous amount of knowledge that has been acquired on the biology of tumors, avoiding even the most elegant and fine-tuned therapeutic approach.

1.1 From Pre-historic times to the XXI century: an historic perspective

Paleopathological reports indicate that tumors could be found in animals that inhabited Earth long before men, during the pre-historic times (Haddow, 1936). The first evidence of tumors in men's evolutionary lineage came out this year by the hand of an American anthropologist who reported the discovery of a Neanderthal skeleton in Croatia with a rib that preserves bony indications of a fibrous dysplastic tumor (Monge et al., 2013). The next references to malignant growths in men appear in the Edwin Smith Papyrus, dated from 3000 BC, where breast tumor was described as a grave disease to which no treatment was available (Hajdu, 2011a). After that, the next reference came from the Ebers Papyrus, dated from circa 1500 BC, mentioning an ulcerative soft-tissue tumor, treated at the time with the Egyptian ointment, an arsenical paste used until the XIX centu-

ry (Garrison, 1926; Hajdu, 2011a). This second papyrus also referred to the identification of skin, uterus, stomach, and rectum tumors (Hajdu, 2011a).

Tumor treatment was firstly approached by the Egyptians. Besides the arsenical past, Egyptians tried to use salts to prevent the malignant growth (Hajdu, 2011a). Afterwards, Indians introduced the use of knifes to surgically resect the more exuberant and localized malignant masses (Garrison, 1926), followed again by Egyptians who redesigned the surgical technique by introducing the cautery and describing specific surgical protocols very alike to the ones still practiced today (Hajdu, 2011a; Papavramidou et al., 2010; Sudhakar, 2009). At the same time, other oriental civilizations like Indian, Hebrew and Chinese also contributed with their insights to the malignant growth prevention by introducing some herbal remedies like tea, figs, boiled cabbage, and fruit juices, as well as pastes of iron, copper, sulfur, and mercury in more extreme cases (Hajdu, 2011a).

The advent of Greek civilization was accompanied by profound changes in the way that life was seen by ancient populations. Disease started to be learned as a natural biological process and not as a mere God punishment for improper conduct or the result of dark magic, as a consequence, major important advances occurred in the fields of pathophysiology and therapy. Hippocrates (460-375 BC) was the first personality of history to use the words ***carcinoma*** and ***cancer*** to differentiate between malignant and ulcerative malignant tumors, respectively (Hajdu, 2011a). These words root from the Greek word *karkinos* that means *crab*, highlighting the similarities that Hippocrates found between the growth of a tumor throughout the human body and the movement of a crab in the sand. In his works, he also introduced the term ***scirrhus*** or *hard tumor*, to depict tumors with uncertain malignant potential, and described anorectal condylomas and polyps aided by the use of a speculum (Hajdu, 2011a). Regarding therapy, Hippocrates introduced the notion and practice of palliative cares for tumors he classified untreatable and surgical removal for the others. He also advised lotions and cautery use for superficial lesions and knife extraction for deep tumors (Hajdu, 2011a).

After the decline of the Greek empire, Romans ascended to the power. Roman physicians essentially continued the traditions of the Greek colleagues, despite introducing their own new philosophies, one being the change of the scientific language to Latin. Aulus Celsus (25 BC-50 AD), the first eminent roman physician working on cancer, made reference to tumors of visceral and parenchymal organs and described a wide range of superficial cancers (Haddow, 1936). He also differentiated cancer from other non-malignant cellular proliferations and highlighted the involvement of the axillary glands in mammary carcinoma (Garrison, 1926). Even though already aware of metastatic dissemination of primary tumors, particularly of the breast, Celsus kept on with the Hippocratic assumption that cancer resulted from an excess or deprivation of blood, mucus, bile, and/or other body secretions (the humors), particularly at old age, the so called **Humoral Theory** (Sudhakar, 2009). In agreement, Claudius Galen (130-200 AD), another physician of Rome, declared cancer as disease of the sick that should be treated with purgatives to diminish the accumulation of black bile (Hajdu, 2011a). He also agreed with the *cancer* denomination attributed by Hippocrates, as he once said that "as a crab is furnished with claws on both sides of its body, so, in this disease, the veins which extend from the tumor represent with it a figure much like that of a crab" (Haddow, 1936). This Greek physician was also responsible for the attribution of the name *sarcoma* to the tumors with the appearance of raw meat (in Greek *sarkos*) (Garrison, 1926).

Following the decline of the Western Roman Empire, progress of medicine was left in the hands of the Byzantine Empire. By combining oriental medicine principles with the theoretical knowledge propagated from Greece, this population produced a great deal of knowledge regarding the different tumor types. The first insights into the cancer of the uterus were done by Aretaeus (81-138 AD), who made a comprehensive description of signs and symptoms commonly associated to these tumors. Later on, Oribasius of Baghdad (325-403) observed that cancers were not as red as inflammatory lesions and were habitually

painless. Aetius (527-565) introduced the treatment of breast cancer by amputation of the entire breast and established that ulcerated cancers should be given no treatment. Simultaneously, the cancer of the esophagus was approached by Avenzoar (1070-1162). Lanfranc (1252-1315) firstly described how to differentiate benign tumors of the breast from cancer and proclaimed that cancer "could only be cured by entire removal, along with its roots" (Garrison, 1926; Hajdu, 2011a).

The almost 1000-year-old theory of the humors of Galen was publically rejected for the first time by Henri de Mondeville (1260-1320), who stressed that scirrhus and carcinoma mean the same and that both of them were cancer. The French physician was responsible for introducing some organization in the field of oncology. He realized that the history of prior lesions was essential for the understanding of tumors and proposed a classification of cancers based on their size, anatomic site, and whether the tumors were superficial or deep in location. On break with the prevailing paradigm, Mondeville firstly introduced the idea of *external carcinogens* which according to the author could make their way to the body through the orifices of the glands (Hajdu, 2011a).

In 1315, in Bologna, Italy, the first public *postmortem* dissection of two human cadavers took place and the first steps for autopsy studies were taken. Nearly a century later, in 1450, Johannes Guttenberg (1395-1468) developed the movable-type printing. These two independent events marked the beginning of the Renascence, a period that was marked by an intense knowledge production, mainly based on experimental science (Hajdu, 2011b). The introduction of autopsies as current practice rendered the cause of many deaths and highly increased the knowledge on anatomy, allowing a better understanding of cancer in its different perspectives, as, for instance, epidemiology. In agreement, Ambroise Paré (1510-1590) in his cadaver dissection studies observed that malignant tumors were far more common and more dangerous in women than in men (Garrison, 1926).

By the early 1600s, anatomic dissections and scientific illustration had been so perfected that very few anatomic details remained undisclosed. The illustration of tumors in particular was pioneered by Marco Aurelio Severino (1580-1656) who made dozens of images depicting some of the largest carcinomas and sarcomas he had operated on (Hajdu, 2011b). The movable-type printing turned out a very professional way of diffusing this knowledge among the scientific community in a fast and efficient manner.

The microscopy studies and the establishment of the cellular theory by Robert Hook (1635-1703), pretty much influenced by the work of other contemporary microscopists, led Marie Xavier Bichat (1771-1802) to reveal the lobular nature of cancer, which he ascribed to the proliferation of the connective tissue, and also to differentiate between the tumor parenchyma, or nutritive base, and its stroma, or degenerated element (Garrison, 1926). As a consequence of these observation, the microscope was introduced as a tool for diagnosis of tumors by Michael Etmullerus (1644-1683) and Bichat postulated that cancer forms as the result of pathologic changes in the tissues (Hajdu, 2011b). This observation was further corroborated by Johannes Müller (1801-1858) who demonstrated that rather of being made of lymph, cancer was made of cells grouped within the connective tissue of an organ with profound affection or infection of whole system through vascular dissemination – the **Blastema Theory** (Garrison, 1926; Sudhakar, 2009). He was the first author to demonstrate a nuclear epithelium in cancerous tissues and to establish a classification of the different carcinomas based on detailed microscopic observation of tumor samples (Hajdu, 2012a). As a disciple of Müller, Rudolph Virchow (1821-1902) continued to study the cellular origins of cancer and postulated a new theory according to which tumors are the result of the proliferation of connective tissue's cells in response to a chronic irritating element or secretion – **The Chronic Irritation Theory** (Garrison, 1926; Sudhakar, 2009).

The term ***metastasis*** to describe the dissemination of the primary tumor to other locations in the body was first introduced by Joseph Recamier (1774-1852) (Hajdu, 2012a). At the time it was believed that some unidentified fluid and not cells conducted the metastatic process (Sudhakar, 2009), and that the lymphatic system played a crucial role in the process (Garrison, 1926). Later on, Karl Thiersch (1822-1895) showed that cancers metastasize through the spread of malignant cells and subsequently, Theodor Billroth (1829-1894) first recognizing that carcinomas spread preferentially through the lymphatic vessels while sarcomas preferably use blood vessels. John Birkett (1815-1904) observed for the first time malignant epithelial cells breaking through the basement membrane of an epithelium to initiate the metastatic process, a step called microinvasion (Hajdu, 2012a).

The XX century was a period during which the knowledge on oncology sciences grew exponentially. In accordance, Steven Hajdu and Farbod Darvishian recently stated that "in the three decades from 1910 to 1940, more progress took place in cancer research and the diagnosis and treatment of cancers than during the prior centuries combined" (Hajdu and Darvishian, 2013). As a matter of fact, the technological boom observed at the time greatly propelled scientific advance as new and better cell laboratory conditions and techniques were established. Alexis Carrel (1873-1944) gave the first steps in the culture of tumor cells while Theodor Boveri (1862-1915) set the basis for the **Chromosomal Theory of Cancer** by evidencing that cancer can be triggered by chromosomal mutations (Hajdu and Darvishian, 2013). Animals started to be used to xenotransplant tumors which resulted in the observation that some tumors are specie-specific while others are not. Also chemical- and radiation-induced tumors were discovered as were some biological agents capable of inducing neoplastic growth. During the 20's, James Ewing (1866-1943) reconfirmed inflammation as a main cause of cancer and advised early diagnosis as the better approach to treat cancer, which should be done using a multidisciplinary approach combining radiological

screening with clinical examination and microscopic observation of tumor biopsies. Ewing was the first to indicate that large number of tumor cells in mitosis, cellular pleomorphism, hypervascularity, and tumor necrosis were biomarkers of increased malignancy (Hajdu and Darvishian, 2013).

Following the discovery of the DNA structure by James Watson and Francis Crick in 1953, the unspoken world of molecular biology started to gain form and the field of genetics prospered. The concept of gene introduced in the beginning of the century by the botanist Wilhelm Johannsen (1857-1927) acquired a new dimension, and the works on heredity made by Gregor Mendel (1822-1884) were finally accepted, as consequently were the rumors of the hereditary behavior of some tumors. One of the last big discoveries on the field was made when the genetic basis of cancer were established. In 1969, Robert Huebner and George Todaro identified genes that were normally activated (sometimes hyperactivated) in cancer and highlighted their malignant potential by calling them ***oncogenes*** (Huebner and Todaro, 1969). The first oncogene to be discovered was the sarcoma (Schmidt-Ruppin A-2) viral oncogene homolog (*SRC*), by Steve Martin in a chicken retrovirus (Martin, 2004). Some years later, a group of scientists from the University of California observed that oncogenes were activated genes that pre-existed in the normal cellular genome and as such termed them ***proto-oncogenes*** (Stehelin et al., 1976). Conversely, genes with tumor suppressive ability, predictably underexpressed in tumors, were also found. The first of those called ***tumor suppressor genes*** to be discovered was the *retinoblastoma-1* (*RB1*) which plays a key role in cell cycle progression from G1 to S phase (Murphree and Benedict, 1984).

The implication of mutations as key players in the tumorigenic process opened the hunt period for new cancer-related mutations. Several oncogenes and proto-oncogenes were identified, as was a plethora of tumor suppressors. As a consequence, a big paradigm shift was made and the **Somatic Mutation Theory** for cancer origin, also known as ***stochastic*** or ***clonal evolution model***, was postu-

lated. According to this theory, cancer derives from a single somatic cell that accumulated multiple DNA mutations. These mutations often affect genes that control proliferation and cell cycle, thus inducing hyperproliferation (Soto and Sonnenschein, 2004).

The last three decades of cancer research were marked by an extraordinary increase in the input of scientific knowledge on the different aspects of cancer biology. Every day new genes are discovered as are new features and abilities of cancer cells. Tumor stroma fired from being a mere supporter of tumor cells to adopt a key function in either tumor cells' survival or metastization. The velocity at which information is generated long overcame our capacity of overall integration and in the apogee of the genomic era integrative strategies and multidisciplinary teams are still scarce in cancer research.

1.1.1 Cancer Epidemiology and Etiologies

Bernardino Ramazzini (1633-1714) was the first to seed the roots of cancer epidemiology. The Italian physician, considered the father of occupational medicine, established the first correlation between individual lifestyles and cancer development when he realized that celibate nuns almost never develop cervical cancer while breast cancer was a common malignancy among them (Felton, 1997). Almost fifty years later, Percival Pott (1714-1788) highlighted the enormous incidence of cancer of the scrotum in chimney sweeps, caused by soot accumulation in the skin folds of the scrotum (Brown and Thornton, 1957). These two studies lighted the fuse for the search and identification of new occupational carcinogens and various reports came out in the scientific literature at the time.

The industrial revolution repainted the skies of the metropolitan centers of the epoch. With the use of coal as the source of energy for the new designed machines, black smoke started to deposit in the atmosphere

above the industrialized cities and cancer incidence increased (Firket, 1958; Hajdu, 2012b). Literature reports indicate that despite the higher prevalence of lung and skin cancers, malignant processes were documented in most of the human tissues and organs as a consequence of chemical pollution (Ames and Gold, 1997). The most popular human carcinogen in the late nineties was the tobacco, whose recently discovered prejudices to health largely overcame the benefices predicted in the previous decades (Loeb, 1989).

Parasitic origins of cancer were proposed during the advent of microbiology back in XIX century. Reginald Harrison (1838-1908) was the first to establish a correlation between parasitic infections, in this case the urinary system parasite *Schistosoma haematobium*, and an extraordinary elevated frequency of bladder carcinoma. The second parasite associated with cancer was the *Clonorchis sinensis*, whose infection was correlated with the bile ducts' tumors (Hajdu, 2012b). Over the last decades many other microorganisms including virus and bacteria were correlated with cancer development, being the most recent the Nobel laureate association between *Helicobacter pylori* and gastric cancer (Marshall and Warren, 1984).

The view of cancer as a hereditary disease appeared with Recamier who believed that disposition to breast and many other cancers might derive from family predisposition, even though he could not identify the exact source. Later on, Virchow also unrevealed the hereditary nature of some gastric tumors (Hajdu, 2012a). With the discovery of oncogenes and tumor suppressor genes, the hereditary nature of cancer was better understood. Retinoblastoma was definitely established as a hereditary tumor that needs two mutations to develop, but in which the presence of an inherited mutation already predisposes to the development of the second, and consequently, to the onset of the disease (Murphree and Benedict, 1984).

More recently, cancer was also proposed to result from endogenous homeostasis dysregulation. The first evidence on this endogenous origin of cancer was implicit in the Ramazzini observations of nuns' higher incidence of breast cancer. As a corollary of his observations, the author hypothesized that sexual hormones and hormonal cycles in females may predispose them, somehow, to the development of breast cancer (Felton, 1997). From there on, many other endogenous carcinogens capable of inducing mutations in the DNA have been discovered (Loeb, 1989). For instance, the disequilibrium of oxidant and anti-oxidant species as a result of excessive reactive oxygen species (ROS) production may cause DNA damage, which, if unrepaired, can drive cell's malignant transformation (Ralph et al., 2010).

Nowadays, despite the huge increase in the number and availability of carcinogenic agents produced, the etiologies of cancer remain essentially the same, with proportional differences between developed and developing countries (Figure 1.1). Tobacco and dietary habits account for the major slice of all cancers worldwide, followed by other unspecified sources and microorganism infections (American Cancer Society, 2011).

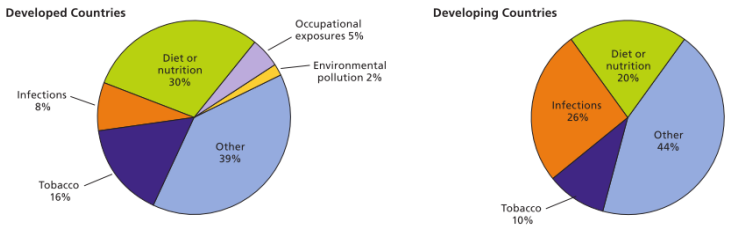

Figure 1.1 - Graphic representation of the proportions of the different cancer causes and their correlation with economic development. In developing countries microorganism infections represent a major risk factor for cancer development, while in developed countries dietary habits and tobacco

are responsible for almost 50% of all tumors. Adapted from American Cancer Society, 2011.

1.1.2 Cancer Statistics

For a disease like cancer that affects so many people all over the world and so many tissues and/or organs in the human body, statistical analysis is a complicated task. Trying to shed some light in the subject, the American Cancer Society (ACS) organized a council that estimates roughly every year the numbers of new cancer cases and the expected cancer-related deaths for the United States, and published an annual public report on the collected data (Siegel et al., 2013). However, no such a thing exists at a planet scale and consequently, the data on worldwide cancer statistics is scarce.

In an attempt to fulfill the need for cancer statistical information, international consortiums were established to scrutinize the available data on cancer incidence, etiologies and survival in as much countries of the world as possible. One of the first consortiums was the Cancer Incidence in Five Continents (CI5), whose main aim was to make available comparable data on cancer incidence from a wide range of geographical locations. Later on, in early 2000's, information from a group of 184 countries was combined and used to build an online database under the control of international project GLOBOCAN. The aim of the project was to provide contemporary estimates of the incidence of cancer, and the mortality, prevalence and disability-adjusted life years (DALYs) from the major cancer types at the national level. Nowadays it represents a very helpful open-access web tool that allows researchers from all over the world to perform several statistical combinations according to their specific needs. All these databases are now grouped and available online at the CANCER*Mondial* webpage, supervised by the International Agency for Research on Cancer (IARC).

Through the compilation of some information from GLOBOCAN 2008 the IARC, working with the Cancer Research UK, constructed a map depicting the worldwide incidence of cancer (Figure 1.2). Through its analysis it becomes evident that cancer incidence still correlates with the higher industrialized or polluted countries. In agreement, the countries with higher cancer incidence are Australia and EUA, while the lower rates are placed in Northern and Middle Africa and in the South Central Asia.

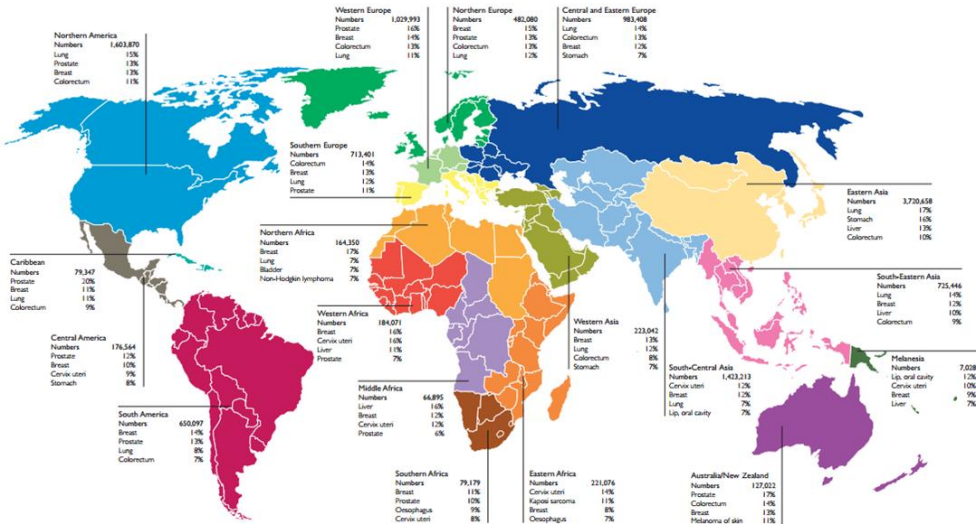

Figure 1.2 - Worldwide incidence of cancer. Cancer has a higher incidence Australia and North America and a lower incidence in Northern and Middle Africa. Adapted from Cancer Research UK website.

According to a publication from the ACS, the rate of cancer incidence is increasing worldwide, with particular emphasis on developed countries (American Cancer Society, 2011). This regionalized behavior of cancer incidence seems to depend upon the adoption of the so-called western lifestyle. In fact, the popularized smoking and poor-diet habits are directly correlated with higher cancer development rates, as are some reproductive factors like the increased medium age for first pregnancy.

The risk of being diagnosed with cancer seams to increase substantially with age. In agreement, 78% of all newly diagnosed cancer cases in developed countries occur at age 55 and older. Also true is the fact that men seem to have more susceptibility for cancer than women, as higher rates of almost all the different tumor types are observed in men (Figure 1.3). Epidemiological studies also revealed a higher mortality rate among men (American Cancer Society, 2011).

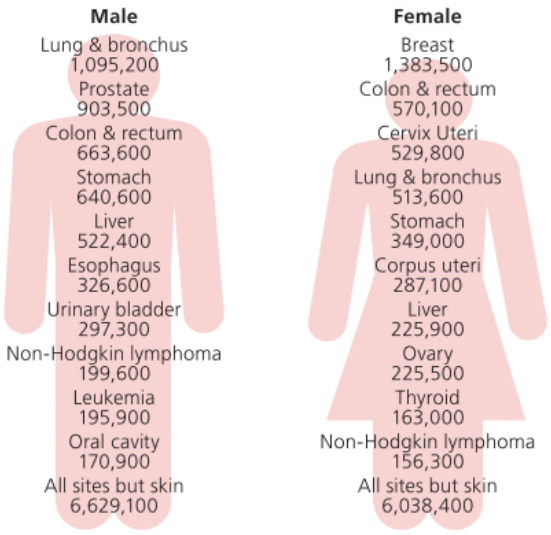

Figure 1.3 - Cancer incidence in men *versus* women. Cancer is normally more common among men, either when analyzed in general or each type in particular. Adapted from American Cancer Society, 2011.

Cancer should now be regarded as an epidemic disease. In fact, it is spread for all over the planet and affects all kinds of animals reaping more lives than any other disease. The costs of cancer are tremendous; a report from the ACS indicated that cancer has the most devastating economic impact of any cause of death worldwide (American Cancer Society and

Livestrong, 2010). Of note is the fact that these costs are not only due to the treatments at health institutions, but also due to the loss of economic output as a consequence of a decrease in work production by the affected population.

1.1.3 The hallmarks of cancer: an overview of the transformation process

Cancer biology is a vast and active field of research that receives input from virtually all the other scientific areas. As a matter of fact, cancer can be approached from different perspectives such as immunology, genetics or cellular biology; however the attained results and deduced outlines should not be left imprisoned in their own fields but for contrarily, they should be included into the other's attainments in order to complete the full picture of cancer.

In an attempt to provide cancer field with some consensus and clarify several uncorrelated results, Hanahan and Weinberg published a review article in which they ruled out six hallmarks all cancer cells have and which are responsible for their malignant properties (Hanahan and Weinberg, 2000). More recently, two additional hallmarks were added to the list, as were two enabling characteristics (Figure 1.4) (Hanahan and Weinberg, 2011).

The most prominent characteristics of tumor cells are their sustained proliferative signaling and their ability to resist cell death, which combined confer cells replicative immortality. Some tumors acquire these hallmarks solely by the loss-of-function of the tumor suppressor *tumor protein P53* (*TP53*), while others depend upon the collaboration of two or more independent genetic changes to attain the same features (Hanahan and Weinberg, 2000). This observation implies that there is not a rigid pro-

gramme followed by a cell in its rout for malignancy, or in other words, the acquisition of the hallmark capabilities in the different tumor types happens by distinct means and at various times along the multistep tumorigenesis (Hanahan and Weinberg, 2011).

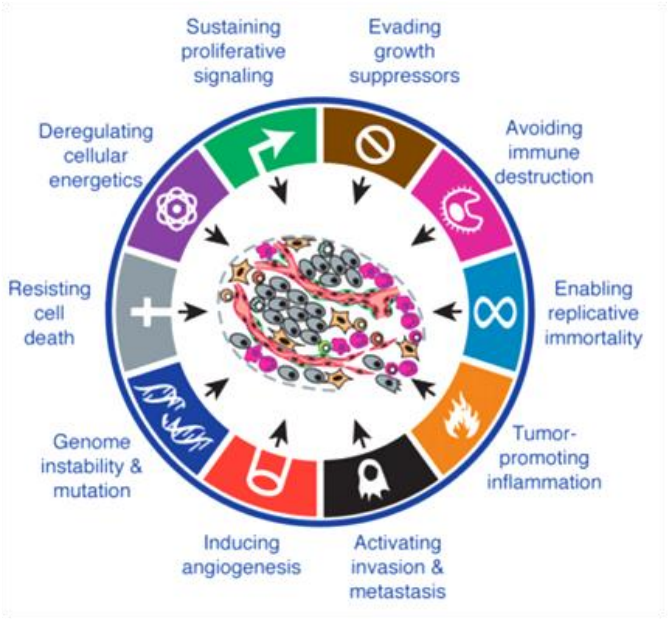

Figure 1.4 - The hallmarks of cancer and their enabling characteristics proposed by Hanahan and Weinberg. The eight hallmarks and the two enabling characteristics are transversal to almost all tumors and largely contribute for the understanding of the tumors' biology. Adapted with permission from Hanahan and Weinberg, 2011.

Successive rounds of genetic alterations must happen in the genome of pre-malignant cells in order to provide them with the full set of the cancer hallmarks. Between rounds, natural selection acts over the mutated cells selecting the clones with higher survival potential (Khong and Restifo, 2002). As a consequence, tumors become comprised of heterogeneous cell populations, each of them with a different arsenal of mutations,

and the prominent cell clone within the tumor may vary along time in tune with changes in the environment.

A good and diverse arsenal of mutations may, in periods of stress, represent a backup escape for keeping cellular integrity. For instance, while a primary tumor is growing and angiogenesis has not yet been triggered in the tumor bed, or when the vasculature of the tumor is leaky and did not ensure cell's needs, **genomic instability** (GI) may hide the exit for an oxygen-independent metabolism, thus allowing cells to survive oxygen deprivation. In accordance, activated oncogenes such as the *rat sarcoma* (*RAS)* and the *myelocytomatosis viral oncogene homolog* (*MYC)*, or silenced tumor suppressors like *TP53,* have been implicated in potentiating glycolysis under such conditions (DeBerardinis et al., 2008; Kamphorst et al., 2013). Hypoxia response system is also implicated by upregulating glucose transporters at cell's surface in response to low oxygen pressures (Semenza, 2010; Fakhrejahani and Toi, 2012). Recent reports further confirmed that when these actions are blocked, the metabolic switch did not take place and tumor's progression is abrogated (Kim et al., 2013a; Zirath et al., 2013).

The establishment of a tumor-dedicated vascular web is essential to ensure malignant cells' energetic needs and to appropriately remove the byproducts of their metabolism. This net originates from both **angiogenesis**, *i.e.*, the sprouting of pre-existing vessels, and **vasculogenesis**, stating for the *in situ* formation of blood vessels by the recruitment of bone marrow (BM)-derived endothelial precursor cells (EPCs) (Figure 1.5) (Carmeliet and Jain, 2011; Lyden et al., 2001). However, the activation of these programs seems to differ considerably among different tumors, apparently in a type-specific manner (De Palma and Hanahan, 2012).

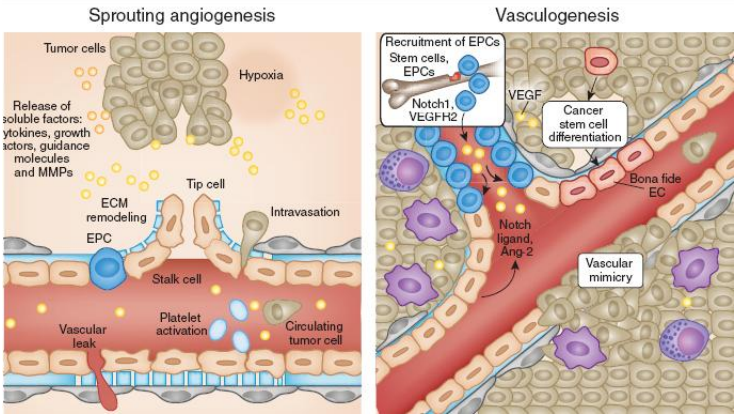

Figure 1.5 - Angiogenesis *versus* Vasculogenesis. Tumor angiogenesis is based on the sprouting of pre-existing vessels driven by a tip cell that was chemically selected to be so (left). Vasculogenesis represents the formation of vessels through the recruitment of BM-derived EPCs. Adapted with permission from Weis and Cheresh, 2011.

Contrarily to what may be thought tumor vascularization is induced very early during the tumorigenic process in a process called ***angiogenic switch*** (Hanahan and Folkman, 1996). In accordance to this observation, Vivek Mittal's group showed that green fluorescent protein $(GFP)^+$ BM-derived cells infiltrate subcutaneous tumors implanted in GFP^+ BM-replaced mice as soon as 4-6 days after tumor implantation (Nolan et al., 2007). The observed cellular mobilization resulted from a breakdown of the balance between pro- and anti-angiogenic factors in the tumor bed which triggers the hyperproliferation of tumor cells and the formation of hypervascularized tumors (Baeriswyl and Christofori, 2009). The mobilized GFP^+ cells documented in Mittal's work, characterized as being vascular endothelial growth factor receptor 2 ($VEGFR2^+$), vascular endothelium cadherin $(VE\text{-}cadherin)^+$ and $CD31^{low}$, incorporate into the initially sprouting vessels and differentiate into mature endothelial cells (ECs), albeit their overall small percentage (5-10%) in the tumor vasculature. This observation led to the understanding that EPCs' action is critical during the initia-

tion of the angiogenesis, providing structural support and guidance for the nascent vessels, but less important in the subsequent growth of the stubs, which is ascribed to other cellular populations (Nolan et al., 2007; Okazaki et al., 2006).

Vascular endothelial growth factor (VEGF) is by far the most common angiogenic switch trigger; however, some tumors revealed less dependent upon VEGF and use noncanonical pathways to activate vascular growth and fulfill their needs. Such is the case of tumors arising in very vascularized tissues, like brain gliomas (Holash, 1999) or melanomas in the skin (Hillen and Griffioen, 2007). In these tumors, cells divide and grow along pre-existing tissue vessels without evoking an angiogenic response, in a process called **vascular co-option** (Holash, 1999). Alternatively, tumor cells can also mimic endothelial cells by altering their gene expression profile, and integrating themselves into the tumor vasculature. This process of **vascular mimicry** is common among more undifferentiated tissue tumors like glioblastomas and melanomas (Maniotis et al., 1999; Soda et al., 2011). Finally, one last alternative is the induction of CSCs differentiation into endothelial cells. These cells then embody the tumor vasculature even though they normally carry some cytogenetic abnormalities (Wang et al., 2010). The role of this specific cell population will be dissected in detail in Chapter 3. Figure 1.6 highlights the main differences between the aforementioned strategies that tumors can use to access vascular supply.

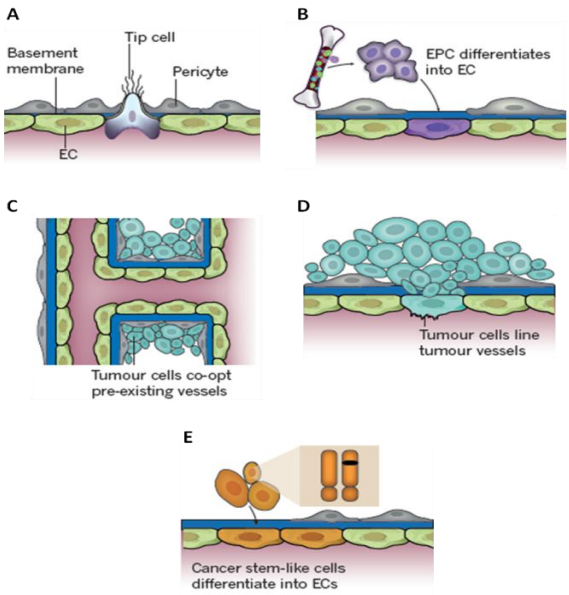

Figure 1.6 - Different strategies used by tumors to access vascular supply. A. Sprouting angiogenesis based upon a tip cell differentiation from an endothelial cell of a pre-existing vessel. **B.** Vasculogenesis dependent on BM-derived cells, namely EPCs. **C.** Vessel co-option by tumors growing in the neighborhoods of pre-existing vessels. This strategy did not involve an angiogenic response. **D.** Vascular mimicry portrayed by tumor cells that attempt to differentiate into endothelial cells. **E.** Endothelial cell differentiated form CSCs, which carry chromosomal mutations and integrate tumor vasculature. Adapted with permission from Carmeliet and Jain, 2011.

The activation of the migration and metastases programme is commonly assumed as the last pace in the process of multistep carcinogenesis. Contrary to this belief, research made over the last decade indicates that at least dissemination may not occur as late as predicted, but instead very early during tumor establishment (Joyce and Pollard, 2009). **Invasive niches**, comprised of a mixture of cancer and tumor-co-opted microenvironment cells called ***tumor microenvironment of metastases*** (TMEM), were observed to form within the primary tumor prompting them for dissemination (Robinson et al., 2009). The increased density of these

niches over time, along with their ability to paracrinely communicate with neighbor endothelial cells, facilitate migrating cells' intravasation and can be directly correlated with the appearance of **circulating tumor cells** (CTCs) (Joyce and Pollard, 2009).

Nowadays the metastatic disease is the main cause of cancer-related deaths, accounting for more than 90% of the mortality rate of this disease. The main reason for our inability to target metastases relies on their systemic nature and on the increased chemo- and radioresistance of CTCs (Valastyan and Weinberg, 2011).

The collection of the cellular and molecular events driving the formation of metastases by **carcinomas**, meaning the human tumors of epithelial nature, is theoretically divided into seven steps, in a process termed **invasive-metastasis-cascade**. These steps encompass: (1) invasion of the local microenvironment and breakdown of the basement membrane, (2) intravasation, (3) survival in the bloodstream, (4) arrest at distant organs, (5) extravasation, (6) survival in a foreign territory and (7) reactivation of the proliferative programs and subsequent metastatic growth (Valastyan and Weinberg, 2011).

As reviewed by Joyce and Pollard, "*tens of thousands of cancer cells can be shed into circulation every day, yet less than 0.01% will survive to produce metastases"* (Joyce and Pollard, 2009). This observation, besides clearly reflecting the inefficiency of the metastatic process, uncovers the difficulties endured by CTCs while in the bloodstream. One of the first selective pressures that CTCs would have to overcome after intravasation is the survival to the absence of anchorage. As is widely known normal cells die without integrin-mediated adhesion to extracellular matrix (ECM) and the consequently activated downstream signaling pathways. The activated programmed cell death pathway is characteristic of the metastatic pro-

gramme and is called "***anoikis***". Many strategies adopted by tumor cells to avoid anoikis have recently been summarized by Paoli and collaborators (Paoli et al., 2013).

Another main disadvantage of being inhabitant of the bloodstream is the omnipresence of immune cells and the continuous need to avoid them. As a matter of fact, if it was not for the deceiving strategies that CTCs employ to hide from natural killer (NK) cells, for example, through an innate immune response, CTCs will be killed within minutes after intravasation (Palumbo et al., 2005). One such effective and elaborated strategy used by CTCs is the elaboration of a platelet shield. It has been demonstrated that CTCs are able to release paracrine factors that act over platelets inducing the formation of a platelet shield around them. These activated platelets were also shown to release themselves other factors that potentiate CTCs' survival in a paracrine loop communication (Goubran et al., 2013). An alternative, albeit most complex, strategy is the fusion of CTCs with macrophages, which provides them with myeloid cell traits favoring the success of metastatic process (Lu and Kang, 2009; Pawelek and Chakraborty, 2008).

The leaky and tortuous vasculature and the tumor-associated cells, characteristics of the primary tumor sites, are absent at metastatic places hampering the extravasation process. As a consequence, CTCs must overcome alone the physical barrier imposed by the capillaries to access the tissue parenchyma. However, this barrier has not the same composition throughout the body, and some places are more prone to metastases than others (Figure 1.7). This is the case of BM, where capillaries, specifically called sinusoids, are lined with fenestrated endothelium which provides virtually none friction to the extravasation of CTCs. In contrast, brain parenchyma is efficiently protected by the blood-brain barrier (BBB) which requires specifically adapted strategies to be transposed.

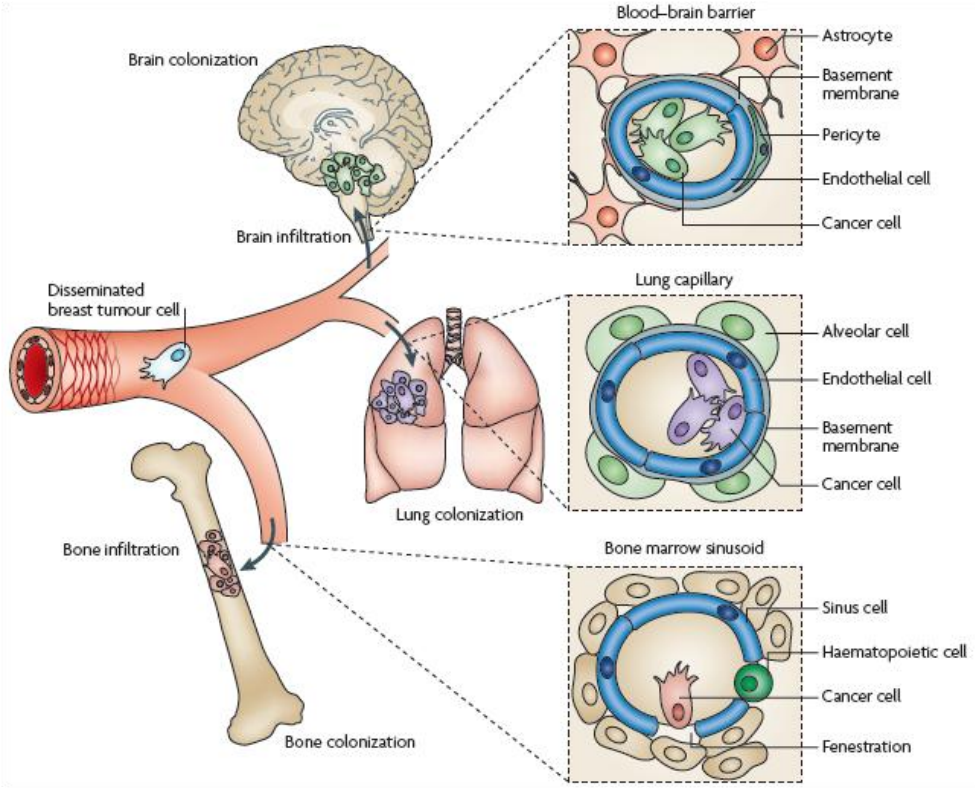

Figure 1.7 - Different vascular barriers imposed to extravasating CTCs. CTCs lodged at distant organs may encounter different capillary barriers depending on the organ. In the case of bone, fenestrated capillaries easily allow CTCs to extravasate into the bone trabeculae. Lung capillaries, however, are less permissive for metastases due to the presence of a basement membrane (resultant from the fusion of the basal lamina of both the endothelium and of the respiratory epithelium). Finally, the brain is the organ that imposed the higher degree of difficulty for metastization due to the presence of the BBB composed by tightly-connected endothelial cells covered with the foot-processes of the astrocytes. Adapted with permission from Nguyen et al., 2009.

In the last decades debate was installed over the tropism of metastases formation. Although it has long been recognized that some tumors often metastized to the same organs (Valastyan and Weinberg, 2011), the prevailing idea that the dynamics of the circulatory system may justify the tropism of metastases lacked robustness and no better idea emerged until Stephen Paget first proposed that cancer cells (the *seeds*) would only colonize tissues or organs (the *soils*) that allow their growth (Paget, 1889).

However, this observation, later known as the "***seed and soil theory***", while providing the first hint into the organ-specific theory of metastases gave no clues about the molecular mechanisms underlying the process.

Knowledge produced over the last decades indicate that primary tumors are able to secrete cytokines into the bloodstream that will influence the microenvironment of distant organs, eventually inducing vascular hyperpermeability (Valastyan and Weinberg, 2011). One such example is angiopoitin-like-4 (Angptl4) which besides remodeling the vasculature of the lung prompting it for extravasation of CTCs (Gupta et al., 2007), was also shown to promote breast cancer derived CTCs' extravasation specifically to the lung parenchyma (Padua et al., 2008). Erler and collaborators also verified that the release of lysyl oxydase (LOX) by the primary tumor induced the production of fibronectin by the fibroblasts at the secondary site (Erler et al., 2009), which was shown to increase the survival and proliferative ability of metastatic cells (Knowles et al., 2013). These and other similar observations lead David Lyden's group to propose that primary tumors are able to induce changes in the parenchyma of the secondary metastatic sites prior to the extravasation of CTCs, thus minimizing the impact of a foreign microenvironment over extravasated CTCs. This concept became known as the ***pre-metastatic niche*** (PMN) formation (Psaila and Lyden, 2009).

Much alike to what was done concerning the first steps of the tumorigenic process, specific metastases-related genes have been searched for. In a review published in the *The New England Journal of Medicine*, Chiang and Massagué divided the known metastatic-related genes into three categories: (1) metastases initiation genes, (2) metastases progression genes and (3) metastases virulence genes (Figure 1.8) (Chiang and Massagué, 2008). The action of the two first categories-grouped genes could very easily be deduced from their group names; however, expression

of genes clustered in the third group has been shown to confer cells the essential features needed for organ-specific metastization (Chiang and Massagué, 2008). Because the expression of metastases virulence genes can only be found in cancer cells that metastasize to specific tissues, the attainment of such a list of genes would most probably provide markers that could help clinicians to predict tumor relapses, and more importantly, organ-specific relapse.

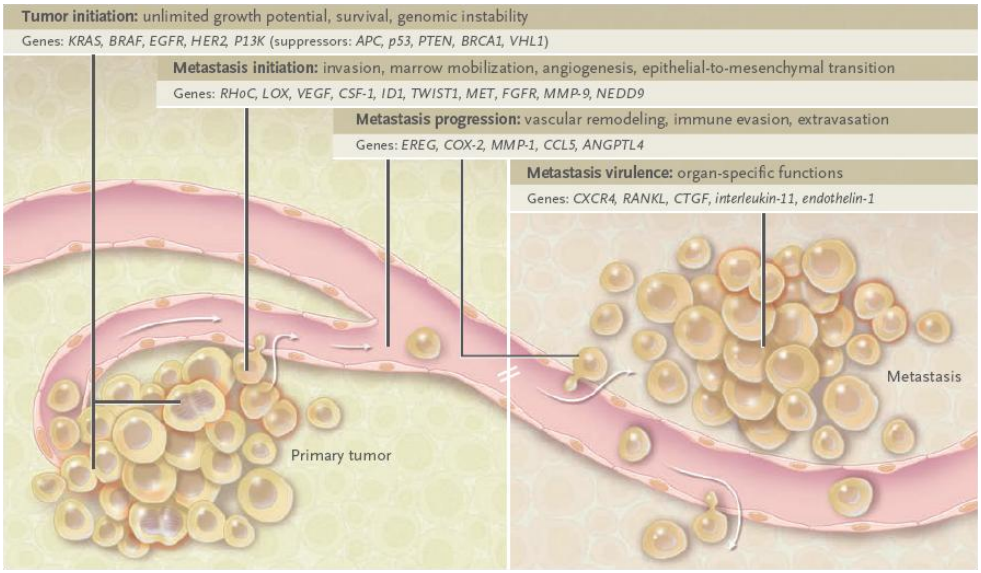

Figure 1.8 - Groups of genes involved in the different steps of the tumorigenic process. The genes involved in the different steps of tumor progression can be separated into different categories. Regarding metastases, there are three categories, the third of which containing the genes responsible for tissue-specific metastization. Adapted with permission from Chiang and Massagué, 2008.

1.1.4 The tumor microenvironment: a crowded and agitated battlefield

The assumption that a tumor is not a mere aggregate of homotypic cells brought in the necessity of identifying and dissecting as much cell populations as possible from the wide diversity that inhabit the tumor bed.

As a result, much became known about tumor microenvironment, and in a paradigm shift tumors started to be interpreted as organs, perhaps even more complex than some anatomical ones.

During the last decades different cell populations in different stages of differentiation were identified within the tumor microenvironment. In a recent report, Hanahan and Coussens grouped these warriors into three general classes, namely, (1) angiogenic vascular cells (AVCs), (2) infiltrating immune cells (IICs) and cancer-associated fibroblasts (CAFs), which are fundamental in sustaining the hallmark capabilities of tumors (Hanahan and Coussens, 2012).

As previously discussed, tumor's vascularization is one of the main growth-limiting steps in tumor progression, mainly because adult blood vessels are usually in a quiescent state (Carmeliet and Jain, 2011). In fact, only during the female menstrual cycle or in certain pathophysiological responses angiogenesis is triggered in an adult body and this normal physiological answer relays mostly on the same pathways as the angiogenic switch in cancer, and invariably involves stromal cells. In the particular case of tumors, IICs and CAFs have been implicated.

Tumor-co-opted IICs produce a wide range of soluble mediators that act over endothelial cells inducing angiogenesis. Particular subsets of myeloid cells named tumor-associated macrophages (TAMs) have been described to have a key role in the overall angiogenic process. In agreement, TAMs were shown to directly stimulate angiogenesis via the production of VEGF-A, a ligand of the VEGFR2 present in endothelial cells inducing their sprouting (Baeriswyl and Christofori, 2009); or indirectly by protease secretion, namely metalloproteinase-9 (MMP-9), that disassemble the ECM and release the ECM-sequestered VEGF-A (Carmeliet and Jain, 2011). Mast cells represent another important IIC population found in tumor's stroma that

has the ability to trigger angiogenesis. These cells, can also act directly over the pre-existing endothelium, by releasing a battery of potent pro-angiogenic mediators including VEGF, angiotensin-1, histamine, heparin and interleukin (IL)-8, also called C-X-C chemokine ligand (CXCL)-8 (Coussens et al., 1999). Alternatively, recent evidence demonstrated that mast cells may also induce angiogenesis by cleaving the protease-activated receptor-2 on CAFs, which in turns activates pro-angiogenic pathways (Khazaie et al., 2011).

The most intuitive warriors of the tumor microenvironment would be perhaps the IICs, intended to combat infections and cancer. However, these cells are very soon co-opted by the tumor, and the factors that they then release sustain tumor growth, rather than activating suppressive pathways (Hanahan and Weinberg, 2011). According to Peyton Rous, tumors developed from "*subthreshold neoplastic states*" previously induced by viral or chemical carcinogens (Rous and Kidd, 1941), described by Dvorak as "*wounds that never heal"* (Dvorak, 1986). Following this first association between cancer and inflammation, evidence continued to accumulate and no doubt remains regarding the immune system responsibility on identifying and eliminating emerging tumors (Hanahan and Weinberg, 2011; Schiavoni et al., 2013; Schreiber et al., 2011). Moreover, mice models engineered to portray ablated, isolated or combined immune cell populations showed increased susceptibility to develop tumors, as recently reviewed by Schiavoni and collaborators (Schiavoni et al., 2013). However, pretty much contradicting these observations are the increasing body of evidences showing that highly immunogenic tumors are able to evade the immune system bullets, thus surviving unharmed the immunological traps in a process called **cancer immunoediting** (Vesely and Schreiber, 2013). Among the deceiving strategies employed by tumors to avoid the immune surveillance is the secretion by the tumor cells of anti-inflammatory cytokines, such as

tumor growth factor β(TGF-β), which paralyze tumor-infiltrating $CD8^+$ cytotoxic T lymphocytes (CTLs) and NK cells, thus blocking their action (Wilson et al., 2011b; Yang et al., 2010). Subsequent studies further corroborated this observation by showing that inhibiting TGF-β signaling in fibroblasts enhanced the growth and oncogenic potential of adjacent epithelia (Cheng et al., 2005).

Other similar paracrine loops between tumor and microenvironment cells have been shown to influence a wide repertoire of tumor's actions. For example, Bose and collaborators recently demonstrated that IL-6 produced by stromal cells is able to co-opt pericytes from tumor vasculature inducing them to produce negative regulators of $CD4^+$ T effector cells (Bose et al., 2013), one of the principal cellular framework of antitumor immune response (Hung et al., 1998). Finally, the previously referred tumor recruited myeloid cells also play important roles in mediating immune-evasion responses as depicted in Figure 1.9 (Pistoia et al., 2013).

A link between the metabolic switch observed in progressing tumors and the microenvironment has also been established. In a recent review, Pavlides and collaborators highlighted the role o CAFs in mediating this switch. According to the authors, CAFs are educated during tumor progression to shift their metabolism towards the independency from mitochondria by favoring glycolysis, while tumor cells keep their oxidative metabolism. This way, the big amounts of L-lactate produced by CAFs as a consequence of their anaerobic metabolism, are released to the extracellular space and enter the tumor cells via monocarboxylate transporters. Once inside tumor cells L-lactate is used in the tricarboxilic acid (TCA) cycle, which allows its full oxidation and subsequent ATP synthesis. This parasitic relation between CAFs and tumor cells was named "**Reverse Warburg Effect**" as it opposes the initial idea of Otto Warburg of an increased glycolytic metabolism in tumor cells even in normoxic conditions (Pavlides et al.,

2012; Warburg, 1956), and seems to relay on the loss of Caveolin-1 (Cav-1) by the stromal CAFs during their education by tumor cells (Pavlides et al., 2012).

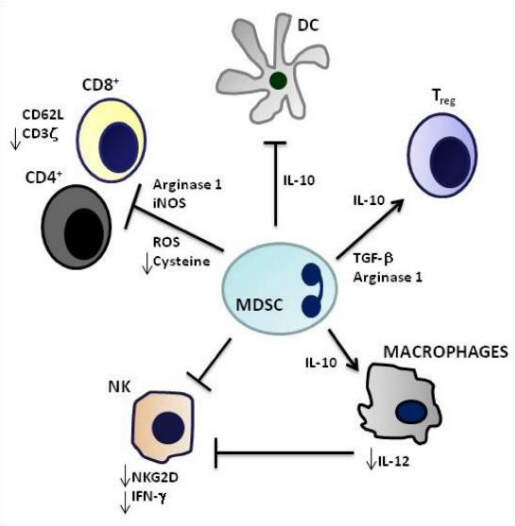

Figure 1.9 - The role of myeloid-derived cells in tumor immune evasion. Myeloid-derived suppressor cells (MDSC) can help cancer immunoediting by acting over the immune cells and inhibiting their anti-tumoral activities. Adapted with permission from Pistoia et al., 2013.

Strong evidence also supports a connection between microenvironment and metastases. In a special issue from Nature magazine dedicated to migration and metastases, Joyce and Pollard dissected the theory of the microenvironment-based regulation of metastases formation and highlighted the particularly important role played by TAMs in this step of tumor progression, mostly due to their ability to produce the aforementioned invasive niches within the primary tumor (Joyce and Pollard, 2009). It has also been hypothesized, yet not completely proved, that TAMs are the guides of tumor cells during the intravasation process. As a matter of fact, IL-4 produced by metastatic-competent tumor cells was shown to induce

TAM-phenotype in the macrophages of the primary tumor stroma, which in turn secrete cathepsin. This protease has a potent ECM-degrading activity thus favoring the migration of the tumor cells towards the circulatory system (Gocheva et al., 2010). Nevertheless, previous results have shown that the touristic trip to circulation, rather than being guided by TAMs, is guided by CAFs (Gaggioli et al., 2007).

Regardless of ongoing debates on the role of specific microenvironment cells in the different tumor progression steps, no arguments are raised against their having any role at all. However, future research in the field, particularly in the recent field of cancer immunology, is expected to substantiate most of the available knowledge on each cell's task during tumor progression, thus allowing redefining and improving therapeutic strategies, and consequently better outcomes.

Chapter 2

Lung Cancer

In the last decades cancer prevailed as one of the most common human diseases with lung cancer (LC) on the top 3 ranking (American Cancer Society, 2011). Notwithstanding the advances made, much is still unknown about the malignant transformation of the human bronchial epithelium (HBE) and the number of LC-related deaths is still astonishing.

2.1 Lung Cancer Statistics, Epidemiology, Etiology and other relevant facts

The statistical and epidemiological discussions on LC are hampered by the scarceness of recent reports, particularly at the worldwide scale. Nevertheless, some things never (or almost never) change, and according to Parkin and collaborators, LC has been the most common neoplasia diagnosed each year since 1985 (Parkin et al., 2005). As to nowadays, it keeps topping the list of tumors diagnosed among men and retreats to the fourth place in the case of women (Figure 3) (American Cancer Society, 2011).

There is a strong association between LC and smoking habits. As a matter of fact, the geographical distribution of LC, especially among men, can easily be interpreted by following the introduction of tobacco as a social habit in the dif-

ferent countries, as well as following the modifications that tobacco suffered over time. Supporting these observations are the higher rates of LC registered among men in North America, Australia, New Zealand, and many North-Western Europe countries during the eighties (Youlden et al., 2008). Also in agreement are the still increasing or tending to plateau LC rates of the emerging economies, like the Chinese, the Japanese and the Eastern European countries where tobacco is still an habit of the wealthy circles (Devesa et al., 2005). Moreover, the introduction of filters in the cigarettes during the sixties along with the alteration of the tobacco's composition also had a tremendous impact in LC cancer rates and histological features (Brooks et al., 2005). These alterations imprinted a worldwide unbalance of LC not only in terms of geography but also between genders.

Surprisingly, the introduction of tobacco also changed the landscape of prominent LC histological types (Stellman et al., 1997; Wynder and Muscat, 1995). Classically, lung tumors are divided in two major histological types: **small cell LC** (SCLC) and **non-small cell LC** (NSCLC) (Walter and Pryce, 1955). The first type of tumors encompasses the most aggressive forms of LC which are strongly associated with smoking habits (>95% patients). These tumors characteristically grow in the hilar region of the lung and have a strong tendency for early dissemination (Jackman and Johnson, 2005). Conversely, NSCLC is a more heterogeneous group of lung tumors that comprise three distinct subtypes, namely, **adenocarcinomas**, **squamous cell carcinomas** and **large cell carcinomas**. Large cell carcinomas are relatively rare and can differentiate into a neuroendocrine phenotype (Harada et al., 2002). The other two subtypes account for the majority of NSCLCs and tend to develop at the periphery of the lungs (Goldstraw et al., 2011).

Epidemiological data attained between 1998 and 2002 revealed that squamous cell carcinoma was the most frequent LC histological subtype among men, while adenocarcinomas occupy that position among women (Youlden et

al., 2008). However, the incidence of lung adenocarcinoma has been increasing gradually in most countries, having already displaced squamous cell carcinomas from the prime position (Nakamura and Saji, 2013). This tendency has long been accepted to be driven by tobacco, in particular by the changes in different physical and chemical properties of the cigarettes introduced during the past decades (Brooks et al., 2005; Thun et al., 1997). The decrease in the concentration of tar and nicotine and the introduction of filters in the cigarettes made smokers increase the puff volume, frequency, or duration in order to attain the desired stimulation. However, due to the presence of the filters, the particles entering the lungs were smaller, thus gaining more access to the periphery of the organs where adenocarcinomas normally develop. Finally, the increased nitrosamination of the tobacco also predisposes to adenocarcinomas (Gabrielson, 2006; Hecht, 1998).

But tobacco is far from being the only human lung carcinogen. Many other substances have been described over the last century, either chemical or physical, natural or artificial, and much more remain unknown. There are, however, identified endangered populations; for instance, workers of certain professions or people living in specific environments are known to be more prone to develop LC than others. One example would be people living near dust incineration sites or highways, who are continuously exposed to chemical combustion-derived smokes and would have a higher incidence of LC than those living near the ocean (Brugge et al., 2007; Sharma et al., 2013). Similarly, metallurgic industry workers and airport ground staff are considered very high-risk populations to develop LC, and their work conditions are, or at least should be, very strictly controlled (Clapp et al., 2008). Finally, radiation may also induce cancer. The first case of radiation-induced cancer was reported in 1902 on the hand of an X-ray technician, who died four years after the diagnostic of a metastatic squamous cell carcinoma (Hajdu, 2012b).

Independently of its etiology, LC is the worldwide leading cause of cancer death in men and the second cause in women. This fact mainly reflects the late stage of the tumor at the time of diagnosis, when almost no therapeutic options are available but palliative care (Spiro and Silvestri, 2005; Youlden et al., 2008). Nonetheless, despite still being very elevated, the incidence and mortality rates of LC have been slightly decreasing in the last years, with more pronounced decline observed among men (Figure 2.1) (American Cancer Society, 2011).

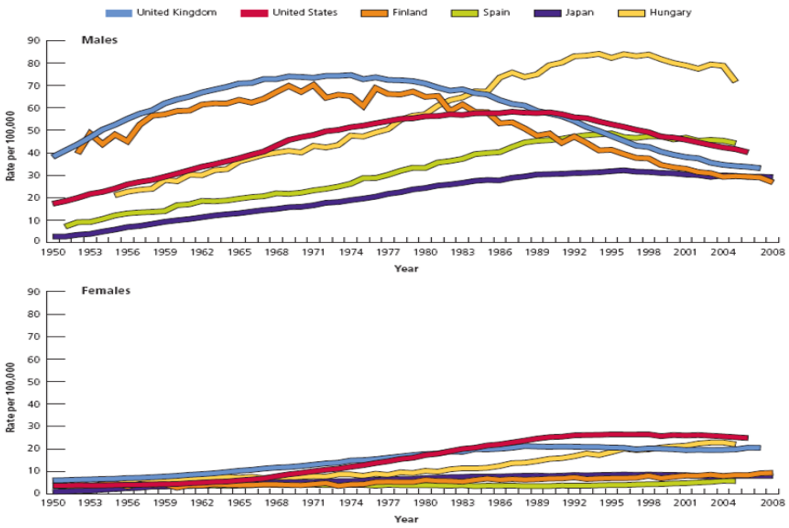

Figure 2.1 - Worldwide lung cancer death rates analyzed by sex. Lung cancer-related deaths decreased in the last decades, most markedly among men. Adapted from American Cancer Society, 2011.

The principal reason for the decrease in the incidence and mortality rates of LC is believed to relay on the increased awareness of the world population to this infirmity which is translated into a reduction in the risk behaviors and in a more dedicated medical surveillance. Anti-tobacco campaigns and the elevated price of the cigarettes were very helpful on alerting adult populations for this disease, and benefits are already visible. As a matter of fact, American States that introduced very rigid anti-tobacco policies are viewing the consumption of

tobacco decreasing at the same time that the rate of LC and other lung pathologies are diminishing. The most ironic subtleness of LC is that among the different human neoplasias, it is one of the most preventable (American Cancer Society, 2011).

2.2 Hexavalent Chromium and Lung Cancer: a view to a kill!

Chromium is a natural element discovered in 1797 by Louis Vauquelin. It is relatively abundant on Earth, being mostly found in the mineral form combined with iron and oxygen ($FeCr_2O_4$) (Urbano et al., 2008). Its name derived from the Greek word "*chroma*" which means "color", mirroring its ability to form colored compounds (Kotaś and Stasicka, 2000).

Ruled by the minimum energy principle, chromium only exists naturally in its most stable oxidation states: the trivalent and the hexavalent (Cr(III) and Cr(VI), respectively) (Urbano et al., 2012, 2008). Cr(III) is a very stable oxidation state for chromium. Under this form it produces large octahedral complexes and chelates with other substances, thus hampering its ability to enter the cells and reducing its cytotoxicity (Urbano et al., 2012, 2008). In agreement, studies using human fibroblasts showed that Cr(III) compounds were one thousand-fold less cytotoxic than Cr(VI) compounds (Biedermann and Landolph, 1990). In opposition, Cr(VI) is normally found in aqueous solutions under the form of chromate (CrO_4^{2-}) or dichromate ($Cr_2O_7^{2-}$) oxyanions, being the prominent ion strongly dependent upon the pH of the solution. At normal physiological pH (7.4) there is a predominance of the chromate oxyanion which has a tetrahedral structure very similar to that of sulphate and phosphate at the same pH (Urbano et al., 2012, 2008). Provided with this ability to structurally mimic such ubiquitary endogenous anions, Cr(VI) can easily move across the cellular membranes using the equally ubiquous non-specific anion-exchangers (Alexander and Aaseth, 1995;

O'Brien et al., 2003). Once inside the cells, Cr(VI) is rapidly reduced to Cr(III) through mechanisms dependent on the reducing conditions of the medium, mainly the concentration of ascorbate (Figure 2.2) (Wong et al., 2012b). Because Cr(III) is too large, cells become a playground from where it can no longer exit, thus being available to induce damage to the cellular constituents. In support of this observation are a wide range of reports in the literature outlining the repertoire of lesions induced by Cr(III) trapped inside the cells. Among the more dangerous are the Cr(III)-DNA adducts and protein-crosslinks which may corrupt cells function and drive their malignant transformation (Nickens et al., 2010; O'Brien et al., 2003).

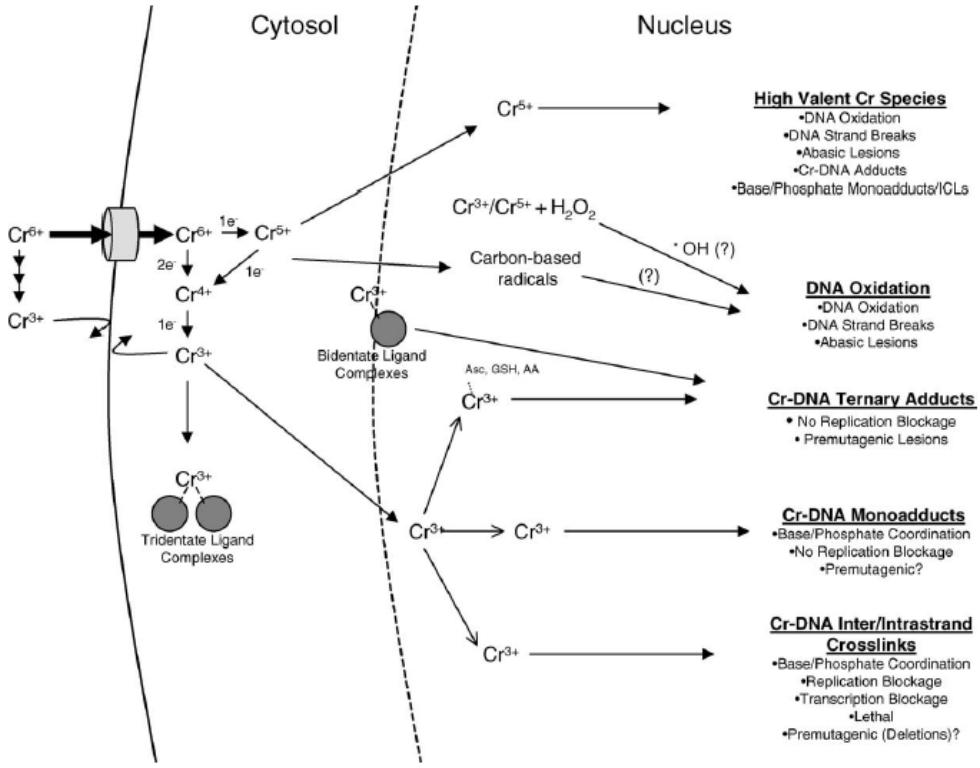

Figure 2.2 - The intracellular reduction of Cr(VI) and the consequent genetic lesions. After entering the cells Cr(VI) is immediately reduced by ascorbate to Cr(III). Due to its bigger size, Cr(III) can no longer exit the cells and moves to the nucleus where is interacts with the DNA, either directly with its bases and/or the phosphate backbone or indirectly with DNA-associated proteins. The result of these interactions

is the formation of wide panoply of DNA lesions, ranging in size and importance. Also of note is the formation of intermediate chromium oxidation states during the reduction process of Cr(VI), which can also induce genetic lesions. Adapted with permission from O'Brien et al., 2003.

The hypothesis of a possible link between Cr(VI) exposition and LC first appeared during the late XIX century, when a higher rate of LC was registered among the Scottish chrome pigment workers (Barceloux, 1999). This discovery triggered the search for the mechanisms of Cr(VI)-induced LC and in the subsequent year piles of reports came out in the literature dissecting the pathophysiology and molecular pathways underlying this disease. Currently, Cr(VI) is classified by both the IACR and the United States Environmental Protection Agency (USEPA) as a human lung carcinogen of Group I and Group A, respectively (Urbano et al., 2008).

In the last century the atmospheric levels of Cr(VI) increased, mainly due to the release of chromium-containing compounds from industrial waste disposal, Portland cement, concrete pavement, milling, demolition, cigarette smoke, fuel combustion and other known, and most probably unknown, sources (Urbano et al., 2008). The immediate and drastic consequence of these elevated Cr(VI) levels was that the size of the population at risk of developing Cr(VI)-induced lung cancer increased from just the employees of specific jobs to the worldwide population. As a matter of fact Cr(VI)-induced LC have already been reported among people unpredictable of being affected by the disease (Kotaś and Stasicka, 2000).

Regardless of the source of Cr(VI), the pathophysiology of the disease is essentially the same. After being inhaled, Cr(VI) nanoparticles with a diameter ranging from 0.2 to 10 µm fly into the lungs and tend to accumulate at the bronchial bifurcations (Ishikawa et al., 1994a, 1994b; Kotaś and Stasicka, 2000). The deposited nanoparticles may persist in the lung for decades, slowly releasing

Cr(VI) oxyanions to the lung parenchyma and thus promoting a chronic exposition to the carcinogen (Ishikawa et al., 1994a, 1994b). The majority of the released ions are immediately reduced to Cr(III) by the ascorbate present in the lung interstitial fluid; however, some Cr(VI) bypasses ascorbate-driven reduction and enters the cell via the non-specific anion-exchangers, as previously described. Microscopic analysis of lungs or biopsy samples from chromate industry workers revealed that Cr(VI)-induced LC tends to develop at the sites of chromium accumulation (Kondo et al., 2003). The *postmortem* studies of Ishikawa and collaborators, where autopsies were made to thirteen chromate industry ex-worker men, further showed that the most frequent histological type of Cr(VI)-induced LC is the squamous cell carcinoma, and that tumors tend to develop centrally in the lung (Ishikawa et al., 1994b).

The plethora of genetic lesions resumed in Figure 11 and described by the group of Patierno was unquestionably confirmed to occur both in the lungs' cells of the chromate industry workers and in cultured cells exposed to different concentrations of Cr(VI) (Arakawa et al., 2012; Figgitt et al., 2010; Ishikawa et al., 1994a, 1994b; Kondo et al., 2003; Nickens et al., 2012; O'Brien et al., 2003; Reynolds et al., 2012; Thompson et al., 2012; Wise et al., 2010). Moreover, these lesions are also established activators of most of the DNA repair systems, in a lesion-dependent manner. In agreement, chromium-DNA monoadducts and induced-oxidized DNA are preferably repaired by the **Base Excision Repair** (BER) system in coordination with the Apurinic/Apyrimidinic (AP) site repair system (Brooks et al., 2008). The cooperation of these two repair systems results in the excision of the damaged base by a DNA glycosylase (normally the 8-oxo-guanine DNA glycosylase 1 (OGG1)), with the consequent formation of an AP site. This site is then recognized by AP endonuclease (APE) which cleaves the phosphodiester backbone forming a transitory single strand break (SSB) that is promptly repaired by the cooperative action of the DNA polymerase β (Polβ) and the X-ray cross-complementing group 1 (XRCC1) complex (Robertson et al.,

2009). Major Cr(VI)-induced genetic lesions, such is the case of DNA-protein crosslinks (DPCs) and DNA inter/intrastrand crosslinks (ICLs), imply the recruitment of more complex DNA repair systems as is the case of **Nucleotide Excision Repair** (NER) system (O'Brien et al., 2005). Provided with a set of protein groups called *xeroderma pigmentosum* (XP) complementation groups, this system proceeds with the excision of a fragment of injured DNA and replaces it by a normal equivalent polymerized using as a template the intact strand (Shuck et al., 2008). Not surprisingly, mutations in key proteins involved in these DNA repair systems have been described both in Cr(VI)-induced LC patients and in cultured cells exposed to the oxyanion. One example is the impaired ability to remove chromium-DNA adducts and the increased sensitivity to Cr(VI) of Chinese hamster ovary (CHO) cells engineered to carry an inactive NER system (O'Brien et al., 2005).

Notwithstanding the unquestionable importance of the role played by BER and NER systems in keeping genome's integrity, it is the Mismatch Repair (MMR) system that leads the fight against genetic instability. MMR is a complex system that encompasses dozens of heterodimeric proteins acting sequentially to repair the mismatched DNA (Figure 2.3). Briefly, the injured DNA is recognized by the human MutS-homolog protein (MSH) heterodimeric complex that binds to the lesion and recruits the human MutL-homolog protein (MLH) complex. This second complex, in turn, recruits the exonuclease 1 (EXO1) that excises the mismatched DNA bases along with some adjacent bases at each side of the lesion, thus forming a temporary DNA SSB with loss of some genetic material. Finally, the same EXO1 resynthesize the gap in the DNA having as template the intact DNA strand (Harfe and Jinks-Robertson, 2000; Li, 2008).

One of the main hallmarks of Cr(VI)-induced lung tumors is their characteristic GI. As a matter of fact, the tumors that relay on Cr(VI) malignant potential can be distinguished from the other types of lung squamous cell carcinomas through their high incidence of **microsatellite instability** (MSI), a particular type of GI that specifically affects the microsatellites (Hirose et al., 2002; Takahashi et

al., 2005; Urbano et al., 2008). Although the exact mechanisms underlying Cr(VI)-induced GI are still largely unknown, the damage that takes place in the DNA, particularly DNA single and double strand breaks (SSB and DSB, respectively), and the consequent activation of the DNA repair systems, seem to play an important role in this effect.

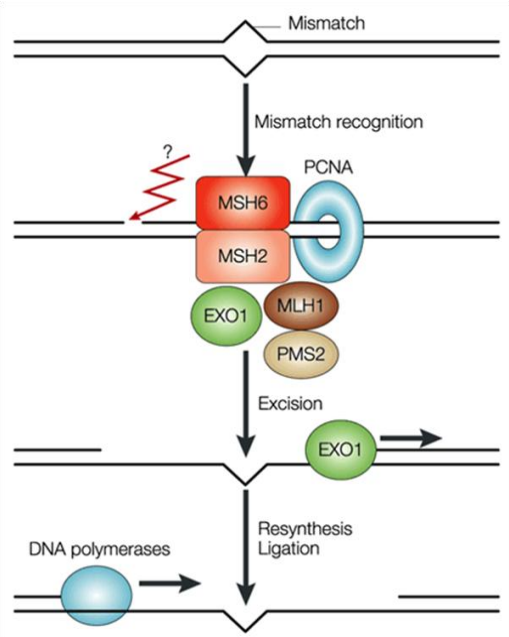

Figure 2.3 - Mismatch Repair System. Following recognition of the mismatched bases by the MSH heterocomplex, a scaffolding protein heterocomplex including an exonuclease 1 (EXO1) is recruited to remove the injured DNA along with some adjacent bases. Subsequently DNA polymerase fills the gap having as template the non-injured strand. Adapted with permission from Martin and Scharff, 2002.

Following a genomic insult, cells usually trigger a cell cycle arrest, thus gaining time to repair the damage. This arrest normally occurs during the S or G2 phases of the cell cycle and is characterized by an intense activation of the cellular repair mechanisms. However, when cells immediately sense that the DNA damage is extensive, instead of arresting their growth, they promptly block cell

cycle progression and eventually trigger apoptosis. In a very accurate work, O'Brien and collaborators applied the abovementioned cellular strategies to Cr(VI)-expositions and concluded that the cellular response to Cr(VI) depends on the concentration of the ion (Figure 2.4) (O'Brien et al., 2003).

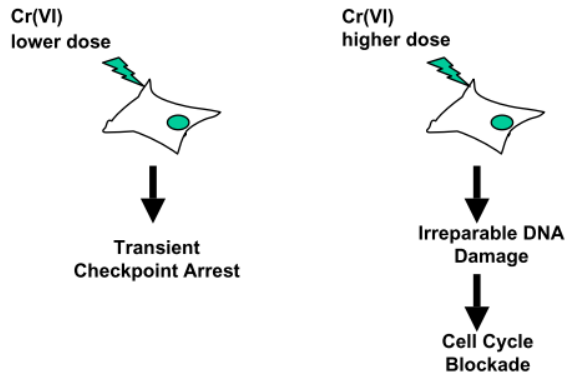

Figure 2.4 - Cellular responses to different Cr(VI) concentrations. Depending on the dose, Cr(VI)-exposed cells may either activate a transient cell cycle arrest or block cell cycle progression. Adapted with permission from O'Brien et al., 2003.

Cells' fate after S/G2-cell cycle arrest mainly depends on the extent of the induced lesions and on the time needed to repair them. Various *in vitro* studies on Cr(VI)-induced genetic injuries demonstrated that following Cr(VI) exposition, MMR is most often the cellular repair system to be activated (Jiang et al., 2010; Reynolds and Zhitkovich, 2007; Reynolds et al., 2007). Furthermore, these studies also showed that lung fibroblasts and epithelial cells exposed to low concentrations of Cr(VI) have a higher incidence of DSB formation (identified by the γ-H2AX foci formation), thus unveiling a potential link between the activation of the MMR system and the formation of these lesions (Reynolds et al., 2007, 2009; Zecevic et al., 2009). Nonetheless, because the formation of DSB in the Cr(VI)-exposed cells occurred faster than following alkylating agents exposures, the idea that a mechanism rather than the production of persistent SSB following

EXO1 mismatch removal may drive the collapse of the DNA replications forks and the consequent DSB formation emerged. In confirmation of this idea, studies from the Zhitkovich's laboratory showed that the DSB formation results from a replication fork collapse induced by the chromium-ascorbate-DNA-induced bulky lesions, rather than from EXO1-promoted SSB formation (Reynolds et al., 2007, 2009). Moreover, these studies also postulated that DSB formation under physiologically relevant Cr(VI) concentrations only requires the progression of the cell cycle from late S to early G2 phase and the specific action of MSH3 protein (Urbano et al., 2012).

DSBs' repair during the S and G2 phases is entrusted to the **homologous recombination** (HR) repair system. This mechanism is described by Urbano and collaborators as a series of interrelated molecular pathways that intervene in the recovery of stalled or broken replication forks and in the repair of DSBs and ICLs (Urbano et al., 2012). In agreement, HR activation is based upon the recognition of the γ-H2AX foci by the scaffolding protein 53BPI and ataxia-telangiectasia mutated protein (ATM). The downstream actions of the ATM protein involve the crosstalk between different molecular pathways and the consequent induction of different cellular responses. As an example, the activation of the HR system depends on the activation of the Fanconi anemia (FA) complementation group D (FANCD2) protein and on its interplay with RAD51 (Taniguchi et al., 2002).

In addition to the direct Cr(VI)-induced genetic lesions and to those induced by the action of the repair systems, GI may also result of an uncoupling of the cell cycle from centrosome duplication (Urbano et al., 2008; Xie et al., 2005). The molecular mechanisms underlying this uncoupling are mostly unknown; however it apparently results from a delayed S/G2-induced cell cycle arrest (Figure 2.5). Wise's group exhaustively explored this subject and concluded that chronic exposure of cells to lead chromate induces centrosome amplification, which drives Cr(VI) clastogenic effects, namely the formation of aneuploid cells (Holmes et al., 2010). Wise's laboratory also reported the formation of tetraploid

cells following chronic exposures to Cr(VI), which is in line with the theory explored by Pellman's laboratory, stating that a link exists between tetraploidy, aneuploidy and cancer (Ganem et al., 2007; Gordon et al., 2012; Pellman, 2007).

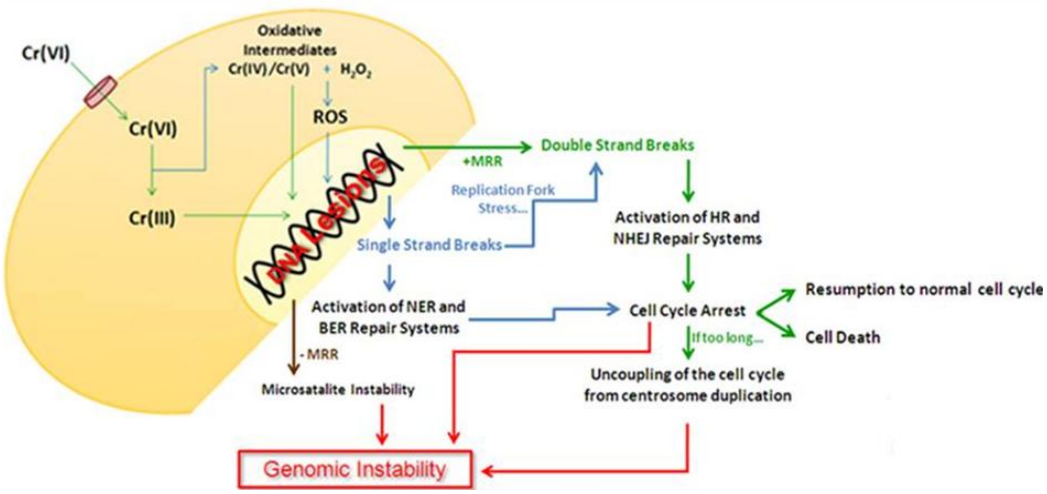

Figure 2.5 - Different pathways for genomic instability formation following Cr(VI) exposure. Cells with DSBs and SSBs may repair their DNA by the activation of cell cycle checkpoints and DNA damage repair systems while cells with extensive damage may trigger cell death to be eliminated. Impairment of these systems can lead to genomic instabilities including chromosomal aberrations. Note should be given to the important role played by MMR in the formation of genetic instability.

However much became known regarding Cr(VI) carcinogenicity in the last decades, the use of inadequate study designs hampered the translation between the bench and the clinic and no big advances were done in terms of therapeutics. So far there are no solution for Cr(VI)-induced lung tumors and we are still recurring to the same therapeutic interventions used in the nineties, mainly based on the administration of ascorbate and soft metal chelating agents (Barceloux, 1999).

Chapter 3

Cancer Stem Cells and the Hierarchical Theory of Cancer

With the accumulating knowledge on the diverse areas of cancer, the stochastic model started to be questioned. By assuming the tumor to be a mass of hyperproliferative cells equally provided with the ability to drive tumor's growth, this model justifies cellular heterogeneity and malignant progression mainly by the action of adaptive selective pressures acting over new genetic mutations or environmental alterations (Garvalov and Acker, 2011). However, evidence suggesting that tumor initiation and maintenance may only be ascribed to a limited population of cells within the tumor, along with the identification of cells with progressive degrees of differentiation shook the foundations of this theory and drove the edification of new ones.

The **hierarchical model of cancer** emerged as an alternative theory trying to explain the presence of high degrees of cellular heterogeneity within the tumors. According to this model, tumors are hierarchically organized heterogeneous entities coordinated by a small subset of cells with self-renewal and multilineage differentiation abilities, named CSCs (Chen et al., 2010; Medema, 2013). These cells are more tumorigenic and capable of generating a serially transplantable phenocopy of the human tumor when xenotransplanted into immunocompromised mice (Garvalov and Acker, 2011). Also, much alike normal stem cells (SCs), they divide asymmetrically to provide tissues with

progenitor cells while keeping the pool of endogenous SCs (Padilla-Nash et al., 2012). Moreover, they inhabit discreet niches within the tumor, where a very complex network of communication with the tumor stroma exists (Vermeulen et al., 2012). As a consequence of this intense crosstalk, CSCs become extremely plastic and they can differentiate or not into progenitor and eventually terminally differentiated tumor cells depending on the signals released by the stromal cells (Vermeulen et al., 2012).

An immediate corollary of the CSCs model is that, notwithstanding the fact that tumors are comprised of heterogeneous cell populations, only the small fraction of CSCs have the ability to self-renew and to produce phenotypically diverse populations and thus to metastasize (Garvalov and Acker, 2011). The link between CSCs and metastases has also been supported by several studies even though only a few of them have directly tested the metastatic capability of putative CSCs *in vivo* (Singh and Settleman, 2010). Nonetheless, the attained results showed that even though *in vitro* the CSCs phenotype alone may exhibit invasive properties, *in vivo* this phenotype may not be enough to determine or predict metastases formation. In fact, albeit two distinct $CD133^{+}$ pancreatic CSCs sub-populations with tumorigenic potential can be isolated, just the subpopulation concomitantly positive for CD133 and C-X-C chemokine receptor (CXCR) type 4 (CXCR4) caused liver metastases (Hermann et al., 2007).

3.1 On the origin of CSCs: theories, myths and speculations

Since the XIX century that it has been hypothesized that tumors are maintained by a discreet and eccentric population of cells that inhabit them (Trosko and Chang, 1989). These cells would portray stem properties and underline the malignant features of tumors (Wicha et al., 2006). However, the first time CSCs were isolated from tumor samples was in 1994 when Lapidot and coworkers identified a cell population able to initiate human acute myeloid leukemia following transplantation into severe combined immunodeficient (SCID) mice (Lapidot

et al., 1994). From there on, CSCs have been identified and characterized in virtually all human neoplasias (Vermeulen et al., 2012).

It was initially proposed that CSCs originate following the mutational transformation of tissue-endogenous SCs, inducing dysregulated self-renewal properties in these cells and selectively driving tumor growth (Visvader, 2011). However, alternative evidence further suggested that CSCs may also arise from restricted progenitors likewise due to oncogenic mutations (Pardal et al., 2003). More recently, however, this mostly unidirectional view of CSCs formation was questioned and an active role was attributed to the microenvironment. The works of Takahashi and Yamanaka showing that cells portraying pluripotent properties can be attained by artificial inducing these properties in differentiated cells through genetic manipulation (Yamanaka and Blau, 2010), made the central dogma of stem cell biology to collapse. Consequently a big paradigm shift took place in what regards the understanding of the CSCs biology. For the first time it was hypothesized that in addition to the abovementioned pathways to originate CSCs, these cells may also be obtained through dedifferentiation of tumor differentiated cells (Figure 3.1) (Vermeulen et al., 2012).

Previous studies from the Weinberg's group further supported the dedifferentiation theory as they showed that CSCs' features result from an epithelial to mesenchymal transition (EMT) happening in the tumor (Mani et al., 2008). In fact, authors showed that EMT induces deep phenotypic changes in cells, which are accompanied by the expression of CSCs markers and an increase in the self-renewal and tumor formation abilities (Mani et al., 2008). Besides suggesting EMT as a possible intermediary step in the route to CSCs' formation, these results also unveiled that that process may depend upon alterations in the expressome of cells (Medema, 2013). In agreement, Vermeulen and collaborators showed that myofibroblasts-secreted hepatocyte growth factor (HGF) is a potent inducer of EMT, which acts through the activation of the EMT-promoting

factors SNAIL and TWIST, resulting in the induction of CSCs' formation through dedifferentiation of tumor cells (Vermeulen et al., 2010; Wu and Yang, 2011).

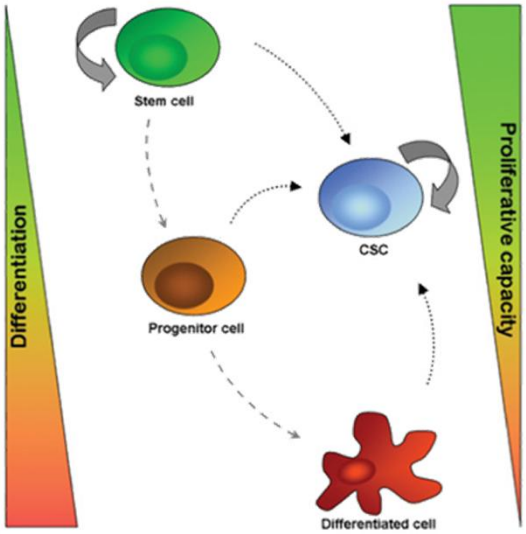

Figure 3.1 - Possible different origins of CSCs. CSCs can be attained from tissue-endogenous normal SCs through the accumulation of oncogenic mutations or, in a similar way, from restricted progenitor cells. More recently, it was proved that CSCs may also result from the stromal-orchestrated dedifferentiation of differentiated tumor cells. Adapted with permission from Welte et al., 2010.

Whether CSCs arise from pre-existing tissue SC, restricted progenitors or dedifferentiation of terminally differentiated cells is currently accepted to depend on the context. In agreement, the accumulating knowledge on the field led the group of Medema to redesign the hierarchical model of cancer by introducing the microenvironment as a key player. According to their **Emerging Dynamic CSCs Model**, CSCs' physiology depends mostly on stromal cells-released molecules that strongly modulate their phenotype. Authors depict CSCs as very plastic entities that can be interconverted into any cell type of the tumor hierarchy. Heterogeneity is the result of CSCs' asymmetric division that originates progeni-

tor cells, which ultimately will differentiate in a wide range of differentiated tumor cells. Alternatively, the stromal cell population comprised of myofibroblasts, endothelial cells, stellate cells and monocytes may also induce stem cell symmetric division and consequently enrich the CSCs pool of the tumor. As to the origins of CSCs, this model perfectly accommodates both the mutagenic and the dedifferentiation hypothesis, but attributes a coordination role to the microenvironment cells (Figure 3.2) (Borovski et al., 2011; Vermeulen et al., 2012).

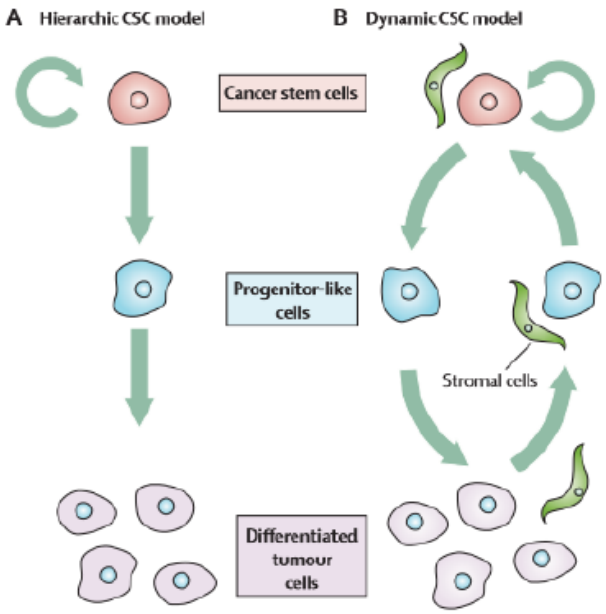

Figure 3.2 - The CSCs-based models for cancer formation. Recent evidence suggests that CSCs may form in response to microenvironmental clues released by stromal cells. Adapted from Vermeulen and Melo, 2012.

3.2 CSCs' biology and underlying cellular pathways

CSCs' undifferentiated status mainly relays on the integrity of their niches. Recent evidence shows that this integrity is mainly sustained by the same

molecular pathways that govern normal SCs' biology, thus supporting the theories of Weinberg and Medema on an overlapping gene expression signature between normal and CSCs (Garvalov and Acker, 2011; Mani et al., 2008; Seidel et al., 2010; Vermeulen et al., 2010).

Wnt signaling cascade plays a central role in inducing and keeping CSCs populations. This highly conserved signaling pathway is essential during the early phases of embryonic development. It belongs to the family of *morphogens*, a group of molecules responsible for the attainment of the bodies' shapes (Clevers, 2006). In adults, however, Wnt signals work on keeping tissues' homeostasis preferably acting over the endogenous SCs and controlling their division. For example, the weekly renewal of the intestinal epithelium is mainly regulated by the action of the Wnt signaling pathway over the intestinal SCs living in the bottom of the intestinal crypts (Medema and Vermeulen, 2011).

The Wnt cascade can be subdivided into a canonical and a non-canonical signaling pathway, being the first more important regarding CSCs' biology (De Sousa E Melo and Medema, 2012). The canonical Wnt signaling pathway is driven by β-catenin, whose levels and cellular localization are extremely well regulated as they strongly affect the activation of the signaling cascade. In fact, Wnt axis is generally turned off in a normal cell and, as a consequence, beyond the β-catenin captive in the intercellular adhesion membrane complexes, all the remaining β-catenin molecules are targeted for proteasomal degradation by the adenomatous polyposis coli (APC) complex following phosphorylation at specific serine residues by the glycogen synthase kinase 3 beta (GSK3-β)/casein kinase 1 (CK1) complex (MacDonald et al., 2009). In the presence of Wnt ligands, however, frizzled (Fzd) receptor is activated and the canonical pathway is turned on. As a consequence, the assembly of APC/GSK3-β/CK1 complex is blocked and β-catenin is left free to migrate to the nucleus to work as a transcription factor (Figure 3.3) (MacDonald et al., 2009). The transcription activities of β-catenin are mediated by the T-cell factor (TCF)/ lymphoid enhancer factor (LEF) complex and

modulate the expression of genes involved in cellular proliferation and differentiation, namely, *MYC* and *cyclin D1* (*CCND1*) (MacDonald et al., 2009). Recent reports in the literature unveiled the role of the wingless-type mouse mammary tumor virus integration site family (Wnt) axis in the development and maintenance of tumor CSCs populations. For instance, Vermeulen and collaborators showed that the stemness of colon CSCs is regulated by microenvironment-released Wnt signals while the Huelsken's laboratory proved that skin CSCs' maintenance is dependent on β-catenin signaling (Malanchi et al., 2008; Vermeulen et al., 2010). More recently, evidence came out implicating the involvement of Wnt/β-catenin in brain (Gong and Huang, 2012), lung (Xu et al., 2013) and breast (Cai et al., 2013) CSCs' homeostasis as well as in mediating leukemias' resistance to therapy (Yeung et al., 2010).

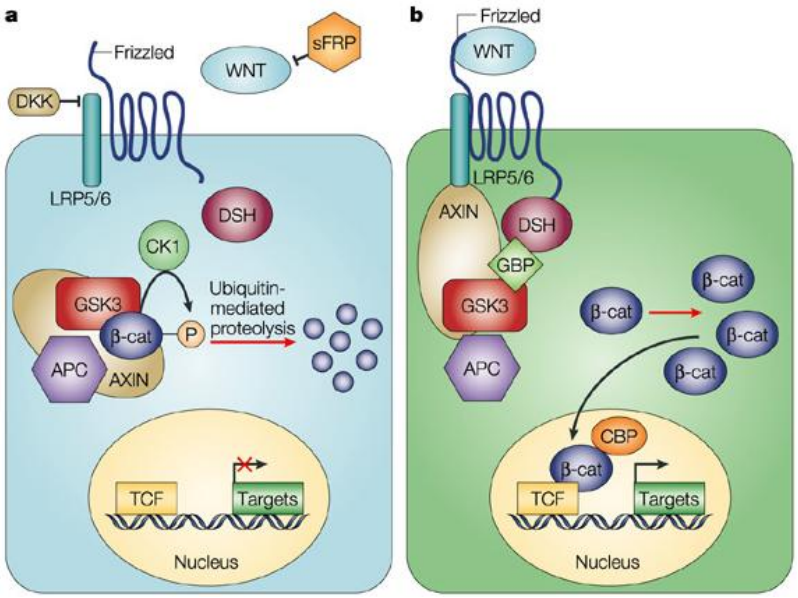

Figure 3.3 - Wnt/β-catenin canonical signaling pathway. a) In the absence of WNT-frizzled ligands the excess of β-catenin in the cells is phosphorylated by the APC/GSK3/CK1 complex and subsequently targeted for proteasomal degradation. **b)** In the presence of Wnt-frizzled ligands, however, β-catenin phosphorylation is prevented and the transcription factor translocates to the nucleus where it activates the transcription of targeted genes. Adapted with permission from Moon et al., 2004.

Another important signaling cascade activated by CSCs is the **Notch pathway**. Similarly to Wnt, this pathway is also very important during early embryogenesis; however, differently, its activation is mediated by juxtacrine signalization (Bolós et al., 2007). In adults, Notch signaling plays a crucial role in the preservation of adult SCs' properties, as illustrated by the studies of van Es and colleagues showing that silencing of this cascade resulted in the lost of the stem potential of intestinal SCs and an increase in the pool of differentiated cells (van Es et al., 2005). Regarding CSCs, Notch signaling has also been said fundamental for their function. In agreement, Zhang and collaborators showed that the activation of the Notch signaling pathway drives hyperproliferation and the formation of neural stem cell-like colonies in human glioma cells (Zhang et al., 2008), while Hovinga and colleagues showed that its inhibition in glioblastoma targets CSCs (Hovinga et al., 2010). Moreover, experimental therapeutic approaches using inhibition of Notch signaling through the use of neutralizing antibodies (ABs) against delta-like 4 ligand (DLL4) results in an accentuated decrease of CSC's populations in human tumors (Hoey et al., 2009).

Hedgehog signaling cascade is fundamental in determining dorsoventral body axis and in tissue repair during early embryonic phases. Conversely, in adult bodies the dysregulation of this pathway is a potent driver of tumorigenesis (Coni et al., 2013). This may happen due to the role of Hedgehog signaling in governing CSCs' expressome with tremendous implications for their proliferation. In agreement, the laboratory of You showed that the downregulation of Hedgehog pathway in lung tumors induces a significant reduction in the CSCs population (Zhang et al., 2012). Also corroborating this observation are recent reports from Huang and Rodova showing that abrogation of Hedgehog signaling in pancreatic CSCs decreased the ability of this cell population to self-renewal (Huang et al., 2012; Rodova et al., 2012), and a study from the Eberhart laboratory revealing the dependency on the Hedgehog signaling for the maintenance of the CSCs population in gliomas (Bar et al., 2007).

CSCs not only relay on the activation of stem-associated cellular pathways, like the abovementioned, but they may also co-opt stromal cells to produce paracrine inducers of alternative signaling pathways. This is the case of **Activin/Nodal signaling pathway**, essential for the sustained growth of CSCs, which is activated by stellate cell-released factors following co-option by CSCs. Alternatively, Activin/Nodal may also be produced by CSCs and act over themselves in an autocrine loop (Lonardo et al., 2011).

3.3 The search for a specific marker

The implication of the aforementioned pathways in CSCs physiology strongly supported the search for specific markers of CSCs. The recognition of such markers would allow the understanding of CSCs biology and dynamics in the tumor, as they permit to specifically identify and isolate this population of cells. So far CSCs have been isolated based on some of their physiological properties. The classically used protocol is the selection and purification of CSCs based on their ability to form tridimensional spheres when cultured under low-adherence conditions with appropriate mediums and supplements, the so-called **sphere-forming assay** (Eramo et al., 2008). Alternatively, CSCs can also be separated by fluorescence associated cell sorting (FACS) based on their capacity to extrude Hoechst dyes through the ABC membrane pumps family (Goodell, 2005; Goodell et al., 1996). Although both methods exhibit advantages and weaknesses, none of them is enough to identify CSCs *per si* and must be completed by the additional use of specific molecular markers.

An ideal marker should only be expressed in a fully-stem CSCs and be lost as soon as differentiation begins (Medema, 2013). As a consequence, the markers proposed so far are typically intermediate molecules of the differentiation signaling pathways. The most renewed example is CD133 which is allegedly a marker of colorectal, lung, brain, pancreatic, breast and ovarian CSCs (reviewed

by Garvalov and Acker, 2011 and Medema, 2013). Corroborating CD133 utility as a CSCs marker are two studies from 2007 showing that only the $CD133^+$ colorectal cancer cells are able to initiate tumors (O'Brien et al., 2007; Todaro et al., 2007). In the next year, Medema's group further showed that just one $CD133^+$ cell is able to give rise to a sphere that induces a perfect phenocopy of the original tumor following subcutaneous implantation in immunosuppressed mice (Vermeulen et al., 2008a). Nonetheless, the same group also alerted more recently that it is possible to find $CD133^+$ non-CSCs due to the fact that differentiation from $CD133^+$ CSCs is not accompanied by a downregulation of CD133 but from a change in the AC133 epitope, thus imposing prudence when using this protein as a marker (Kemper et al., 2010).

More recently aldehyde dehydrogenase 1 (ALDH1) has also been proposed as a marker for CSCs. Effectively, high levels of ALDH activity have been documented in CSCs isolated from diverse tumor samples, thus favoring the hypothesis that this enzyme, or at least its antigen expression may be used as a tag for CSCs (Chen et al., 2009; Huang et al., 2009). Nonetheless, regardless of the use of ALDH1 as a marker of CSCs, the physiological meaning of its higher expression in CSCs is yet to be uncovered.

3.4 Therapeutic implications of CSCs

Therapy resistance has classically been ascribed to a small population of cells inhabiting the tumor that acquired an arsenal of pro-survival genetic mutations. Following the destruction of the bulk of tumor cells, this population would clonally expand and recapitulate the tumor, usually with a more aggressive phenotype (Vermeulen et al., 2012). Studies corroborating this theory can be encountered throughout the literature in virtually all tumor types. The most exuberant example is the behavior of chronic lymphoid leukemia (CLL) following therapy. A recent paper from Ouillette and colleagues showed that the replace-

ment of CLL *TP53* mutation-harboring cells following therapy is dominated by the outgrowth of clones portraying very complex genetic alterations (Ouillette et al., 2013). But the advent of CSCs revolutionized the concept of tumor relapse by introducing the idea that CSCs may respond differently to therapy. In fact, many studies have shown that CSCs are substantially more resistant to therapeutical agents (either chemical or radiation) than the bulk of tumor cells, regardless of sharing the same genetic background (Al-Hajj et al., 2004). In agreement, an *in vitro* study from the group of Gomes recently showed that a CSCs population, isolated from an osteosarcoma cell line, has a relatively higher drug and radiation resistance when compared to the progenitor cell line, as well as a higher tumorigenic ability (Martins-Neves et al., 2012).

By accepting the hierarchical model of cancer, or more correctly, the dynamic CSCs model of cancer, researchers inherently assigned CSCs to the position of survivors following therapy cycles and thus of drivers of tumors' relapse. Experimental evidence strongly supported this suspicion by showing, for example, that following the chemotherapeutical treatment of colorectal tumors there is an increment of the CSCs population (Wilson et al., 2011a). Similar observations were additionally found for lung (Huang et al., 2013), breast (Ithimakin et al., 2013; Lee et al., 2011), prostate (Wang et al., 2013) and pancreatic tumors (Izumiya et al., 2012) among others, leading the scientific community to understand that current therapeutic approaches are actually the responsible for tumor relapses as they only target the bulk of tumor cells, leaving untouched the CSCs population and their arranged niches (Figure 3.4) (Garvalov and Acker, 2011; Vermeulen et al., 2012).

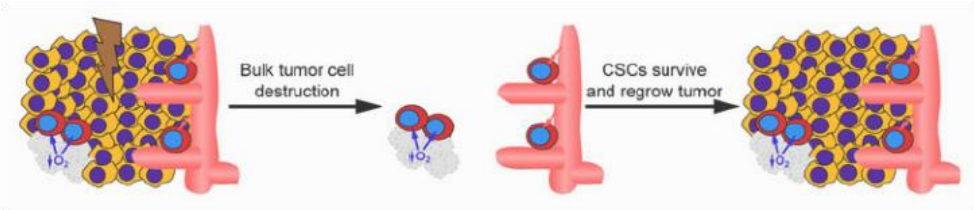

Figure 3.4 - The effect of conventional cancer therapies over CSCs. Conventional therapies, either chemical- or radiation-based tend to target the bulk of tumor cells leaving untouched the CSC's pool and their niches. Consequently, tumor relapse often occurs as CSCs may repopulate the tumor bed most of the times displaying even more aggressive properties. Adapted with permission from Garvalov and Acker, 2011.

The understanding of the cellular basis of CSCs mediated tumor relapse prompted the search for therapeutic approaches that can effectively prevent tumor regrowth. Initially, it was believed that CSCs-targeted therapies would resolve the problem of tumor relapse and a plethora of new CSCs-targeted drugs have been developed. These drugs, much alike the CSCs' markers, mainly target the signaling pathways involved in the homeostasis of the CSCs' pool (Figure 3.5). For instance, blockage of the Hedgehog signaling pathway using cyclopamide, an antagonist of the Hedgehog co-receptor smoothened (SMO), results in the abrogation of the CSCs' population in chronic myeloid leukemia (CML) (Zhao et al., 2009). Alternative targets on CSCs were also surveyed, as reviewed by the groups of Frank and Acker (Frank et al., 2010; Garvalov and Acker, 2011). In agreement, Gupta and colleagues performed a high-throughput screening to identify selective inhibitors of CSCs from which they spot **salinomycin** as a potent reducer of the CSCs population, killing 100-fold more cells than common chemotherapeutic drugs (Gupta et al., 2009). Ongoing studies are dissecting the molecular targets of salinomycin and the signaling pathways it activates, prior to its test for introduction in clinical practice (Arafat et al., 2013; Koo et al., 2013; Li et al., 2013).

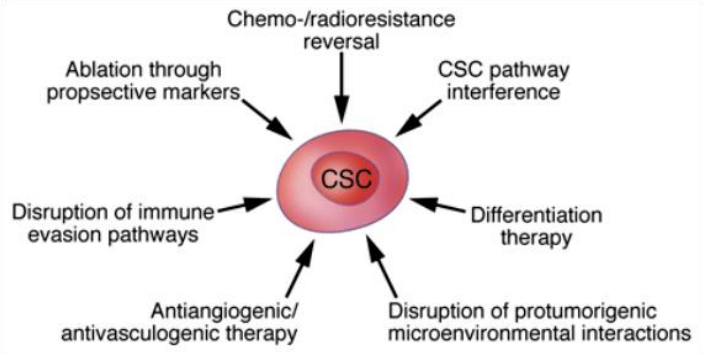

Figure 3.5- Multi-ways of therapeutically targeting CSCs. Following the identification of CSCs as the drivers of tumor relapse, many targeted therapies have been tried. So far the most effective relay on the interference with the signalling pathways underlying CSCs' homeostasis. Adapted with permission from Frank et al., 2010.

Most surprisingly, the results from the first CSCs-based therapy assays immediately revealed that solely by targeting CSCs tumors are not abrogated. In fact, due to the abovementioned ability of tumors to replenish their CSCs population through dedifferentiation of differentiated tumor cells (Figure 3.6), CSCs-targeted therapies were condemned at birth (Garvalov and Acker, 2011). A recent study from Chaffer and colleagues provided the first experimental confirmation that dedifferentiation takes place in human tumors, thus providing a route for therapy resistance following CSCs' hit (Chaffer et al., 2011).

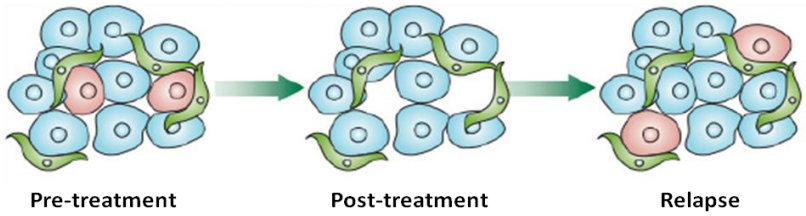

Figure 3.6 - The effect of CSC-targeted therapies. Due to the ability of CSCs to be attained by dedifferentiation of differentiated tumor cell, CSCs-targeted therapies fail to abrogate tumors as they replenish the population that sustains their growth. Adapted from Vermeulen and Melo, 2012.

Ongoing work now focuses on the development of combined therapies to target simultaneously the CSCs, their niches and the bulk of differentiated tumor cells (Figure 3.7). Successful studies both *in vitro* and in animal models have already been documented, as is the case of the use of salinomycin combined with gemcitabine to target pancreatic tumor cells (Zhang et al., 2011). In accordance to the dynamic cancer stem cell model, microenvironment-focused therapies have also been designed, particular those targeting the CSCs' niches. For instance, the perivascular sites are preferable niches for CSCs as they are enriched in both high levels of oxygen and high concentrations of nutrients. Moreover, an intricate paracrine signaling between endothelial cells and CSCs seems to be involved in keeping CSCs' undifferentiation properties and in potentiating their robustness, thus rendering cells more resistant to therapy (Borovski et al., 2011). In light of these facts, anti-angiogenic therapies combined with cytotoxic drugs have been designed to eradicate tumors, and in the case of gliomas, they have been shown to render CSCs more susceptible to therapeutic agents (Folkins et al., 2007). However, contradictory results have been published regarding the impact of anti-angiogenic therapies in tumors' growth and progression and additional studies must be done to clarify their potentials (Pàez-Ribes et al., 2009).

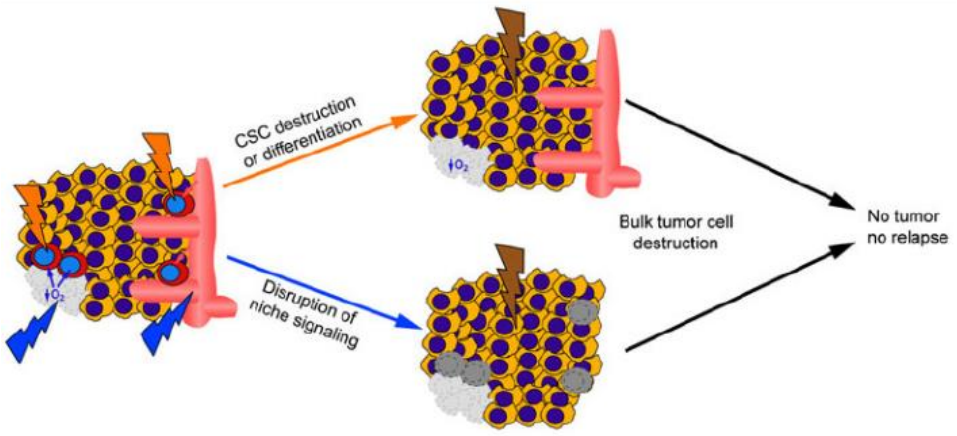

Figure 3.7 - The ideal CSCs-targeted therapeutic approaches. Tumor abrogation can only be attained through a combined therapy. One therapy may consist

of either target or induce differentiation of CSCs followed by hitting the bulk of tumor cells using a conventional cytotoxic drug. Alternatively, the CSCs' niches may be disrupted by interfering with either environmental conditions or the concentration of paracrine molecules to target CSCs, followed again by a conventional cytotoxic drug to kill the bulk of the remaining tumor cells. Adapted with permission from Garvalov and Acker, 2011.

3.5 Lung CSCs: the resident evil

The first time cancer stem-like cells were identified in and isolated from LC samples was in 2008 by the group of de Maria (Eramo et al., 2008). Growing evidence on the potential existence of such cells drove the authors' search and in agreement to the actual ideals, they managed to isolate a population of $CD133^+$ cells that exhibit the capacity of growing indefinitely as tumor spheres in appropriately supplemented serum-free medium (Eramo et al., 2008). From there on, many other laboratories corroborated these findings, although debate persists over the molecular markers of lung CSCs.

The normal lung parenchyma, like virtually any other human tissue, comprises a small population of undifferentiated cells. In the particular case of lung, which is an internal vital organ in intimate contact with the extracorporeal environment, these cells are of extreme importance in restoring the respiratory epithelium following environment-induced injuries (Rivera et al., 2011). In the proximal bronchial airways, **basal cells** have been proposed to represent this population of cells, as they have the potential to restore a fully differentiated epithelium (Hong et al., 2004). These cells lay in the most internal layer of the pseudostratified respiratory epithelium and are the primary source of cells during lung healing after injury (Musah et al., 2012). Nevertheless, as one approaches the respiratory sections of the lung, the pseudostratified epithelium progressively turns to columnar and then cubic, and its cellular composition changes. In the more distal portions of the air conductive system, **Clara cells** become more abundant and inherit the responsibility of tissue repair. In agreement, these cells

have been proved to self-renew and generate ciliated cells in response to epithelial injury (Rawlins et al., 2009). More internally, terminal bronchioles give rise to respiratory bronchioles lined by a very tiny epithelial layer comprised of a single sheet of cells. These cells can either be type I or type II **pneumocytes** (also known as alveolar cells), being the former more abundant and the latter the responsible for the surfactant production. Type II pneumocytes are also the undifferentiated cells of the respiratory epithelium, with long confirmed ability to both self-renew and differentiate into type I pneumocytes (Adamson and Bowden, 1974). More distally, an additional population of relatively undifferentiated variant Clara ($Clara^{V}$) cells lay near pulmonary neuroendocrine cells (PNEC), with which they establish an intimate communication to maintain epithelial diversity after injury (Giangreco et al., 2002). Finally, a subset of these $Clara^{V}$ cells, independent of PNECs and displaying more undifferentiated properties, lay in the transition between the conductive and respiratory epithelium **bronchioalveolar stem cells** (BASC) and are considered the true stem cells of the bronchiole (Rivera et al., 2011). Figure 3.8 further provides a geographical idea of the distribution of the different cell population throughout the respiratory system.

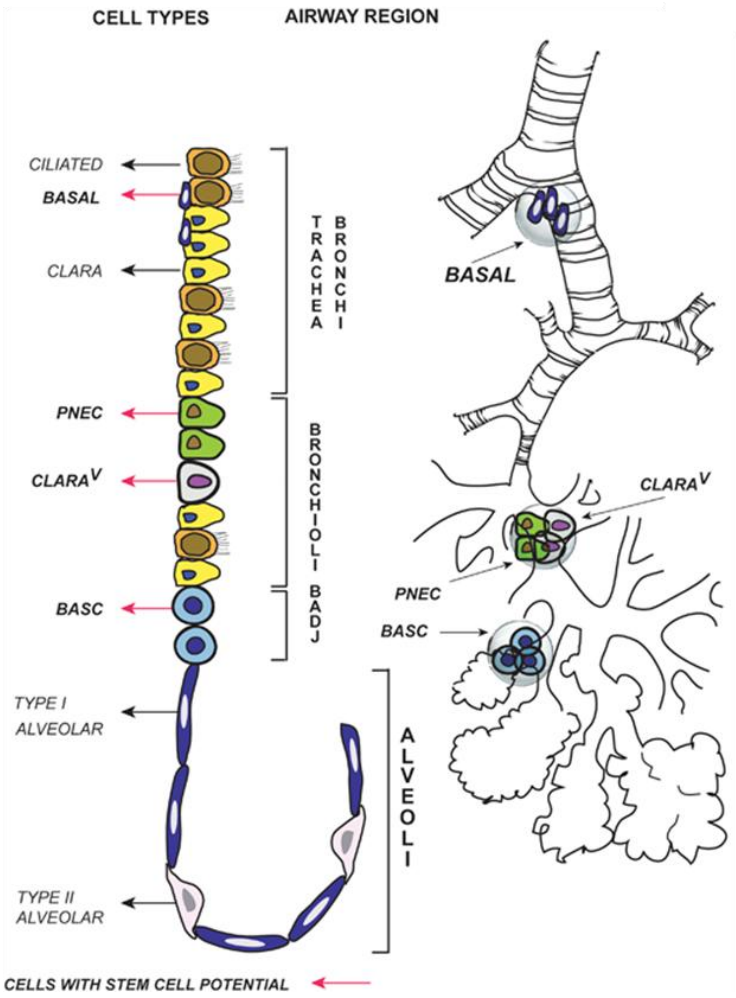

Figure 3.8 - The different cell types along the respiratory system. While penetrating into the lung, the pseudostratified respiratory epithelium changes towards a simple squamous epithelium. This structural modification is accompanied by an alteration in the cellular constitution: basal cells disappear and their function is ensured by Clara cells; BASC establish at the transition between the conductive and respiratory epitheliums and finally, alveoli are lined by pneumocytes. Adapted from Eramo et al., 2010.

The current literature on the origins of CSCs in lung tumors does not indicate any particular source, but many. For instance, Kim and collaborators showed that BASCs are a potential source, as these cells are expanded in lung tumors sustaining their malignant proliferation (Kim et al., 2005). Moreover, the group of Crystal just showed that lung basal cells may be reprogrammed during

early phases of cigarette-induced LC in favor of the development of highly aggressive lung tumors (Shaykhiev et al., 2013). Finally, dedifferentiation may also represent an alternative pathway for the development of LC CSCs, as cells similar to Clara, but with decreased secretory ability, have been isolated from lung preneoplastic lesions and seem to sustain the subsequent malignant progression (Rivera et al., 2011). Nonetheless, regardless of their origins, lung CSCs have already a couple of well defined characteristics that may allow their identification. They can be isolated through the sphere-forming assay and are positive for the octamer-binding transcription factor 3 and 4 (OCT-3/4), the SRY-box containing gene 2 (SOX2) and the NANOG (Kitamura et al., 2009; Rivera et al., 2011). Additionally, the majority of the papers in the literature describe lung CSCs as being $CD133^+$ (Kitamura et al., 2009; Medema, 2013; Rivera et al., 2011). However, this positivity is still arguable as independent studies have shown that $CD133^-$ glioblastoma cells have equivalent tumor initiation ability in mice to $CD133^+$ cells (Beier et al., 2007; Joo et al., 2008). Finally, lung CSCs also express ALDH, and the isoforms 1A1 and 3A1 seem to be specific of NSCLC (Patel et al., 2008).

Similarly to the populations of CSCs identified in other tumors, lung CSCs are more resistance to conventional therapies than the bulk of differentiated tumor cells. In agreement, Barr and colleagues showed that the treatment of these cells with therapeutic doses of cisplatin, a common cytotoxic drug used in the chemotherapy of NSCLC, targets the bulk of cells but leaves untouched the CSCs' population (Barr et al., 2013). Moreover, combined therapeutic strategies have also been designed for LC with very promising results. For instance, the group of Gorelik recently showed that the combination of the cisplatin treatment with an inhibitor of the c-Kit receptor make the lung tumor cells more sensitive to therapy, thus favoring tumor eradication (Levina et al., 2010).

Coming years will be crucial in defining an effective therapeutic approach for LC. The wide arsenal of arrays, along with genome wide association studies (GWAS), and the improvement and continuous development of new molecules

to be used as therapeutic agents are providing knowledge at such a high rate that it is expectable that very soon the complete picture of CSCs, their role in cancer and the different efficient ways to target them is completed. Never like now men was so eager and so able to go deep into the cell and dissect its intricacies. This can only result in a positive outcome, translated in effective therapeutic approaches and improvement of the quality of life of oncologic patients.

Chapter 4

Hypothesis and Goals

Regardless of the efforts to unravel the cellular and molecular mechanisms underlying Cr(VI)-induced LC, much is yet to be undisclosed. The main obstacle seems to be the absence of uniformity among the experimental designs used in different laboratories, as well as the use of inadequate cellular systems and exposure regimens.

Aiming to outline the abovementioned lacuna, the first goal of this project was to establish an adequate cellular system for the study of Cr(VI) carcinogenesis that adequately mimics both the physiological and the epidemiological aspects of the process.

Chapter 6 describes the developed strategy to attain such a system departing from a normal human bronchial epithelial cell line, and exposing it to a epidemiologically relevant concentration of Cr(VI).

A second major aim of this project was to exhaustively characterize the different aspects of the malignization process, hoping to identify the drivers of the transformation, which could become potential therapeutical targets.

In agreement, Chapter 7 presents the rational used to increase the malignant potential of the Cr(VI)-derived malignant system aiming to exacerbate the Cr(VI)-induced features. Moreover, the different approaches used to dissect the malignant progression

are also presented, with particular reference to the metabolic and gene expression profiles.

Driven by the results attained during the characterization of the Cr(VI)-induced malignant cellular systems, the last hypothesis proposed was that CSCs may have been involved in the transformation process mobilized by Cr(VI). To test this hypothesis a battery of assays were performed.

Chapter 8 groups the results attained during the search for a CSC population within the malignant systems. A comparative analysis is also presented in order to provide an integrative picture of the malignization process and of the Cr(VI) effects over the lung epithelial cells.

The ultimate aim of the work depicted in this thesis is to clarify the cellular and molecular mechanisms underlying the carcinogenesis of Cr(VI), giving particular emphasis to the role played by the stroma and the CSCs in that process. Ultimately, the attained results are believed to provide a better understanding on the different stages of Cr(VI)-induced lung carcinogenesis: onset, progression and metastases formation. As a consequence, they will represent a step-forward not only in chromium carcinogenesis but also in the understanding of the overall cancer biology.

PART II

Laboratory Procedures

Chapter 5

Material and Methods

5.1 Reagents, Solutions & Mediums

The reagents used in the various experiments throughout this work were either of analytical grade or cell culture recommended and were acquired from Sigma-Aldrich (Sintra, Portugal) unless specifically stated. Conversely, all cell culture media and supplements were from Gibco® (Life Technologies, Carlsbad, CA, USA) unless the contrary is referred. Ultrapure water (milli-Q) was used anytime water was needed, in particular for the preparation of aqueous solutions. Plastics used for cell culture were attained from either Corning (Lowell, MA, USA) or SPL Life Sciences (Eumhyeon-ri, Korea). The protocols for the preparation of stock and secondary solutions are collectively grouped in the Appendix A of this thesis.

5.1.1 Potassium Dichromate Aqueous Solution for Culture

For the culture of cells in the presence of Cr(VI), the oxyanion was added as a 50 µM potassium dichromate ($K_2Cr_2O_7$) aqueous solution, prepared from dilution from a 2.5 mM stock solution. The solution was filtered prior to use to ensure sterilization.

5.1.2 Gelatin Coating Solution

According to manufacturer's instructions, BEAS-2B should be cultured on the top a type-B gelatin from bovine skin solution. This solution was prepared by diluting the commercialized 2 % gelatin solution in 25 % of 1x-phosphate-buffered saline (PBS) and 5 % of 2 % bovine serum albumin (BSA) solution.

5.1.3 F12 Supplemented Growth Medium

To prepare 500 mL of this cell culture medium, 5 mL of penicillin (5000 U/mL)-streptomycin (5000 µg/mL), 1 mL Ultroser G (Pall Corporation, Port Washington, NY, USA), 100 µl of amphotericin B and 97,9 mL of Ham's F12 medium.

5.1.4 CSCs' Isolation Medium

The liquid matrix of this medium was prepared by mixing 250 mL of DMEM:F12 (1:1) cell culture medium, with 5 mL of penicillin (5000 U/mL)-streptomycin (5000 µg/mL), 10 µl of 1mM progesterone solution (Sigma-Aldrich) and 5 mL of the commercialized insulin, transferrin, selenium (ITS) sodium pyruvate solution. Subsequently, 0.6 g of sodium bicarbonate ($NaHCO_3$) was dissolved in the liquid phase, along with 0.08 g of putrescine. 2 % methylcellulose solution was then used to perform the final volume of 500 mL.

5.1.5 Preparation of Low Adherence 6-well Plates for CSCs' Isolation

Low adherence conditions are mandatory for the isolation of CSCs. To attain them, one can either buy commercially available low-adherence supports or prepare them in the laboratory. For our experiments we choose to prepare ourselves the 6-well plates by coating them with a 2 % poli-(2-hydroxyethyl methacrylate) (poli-HEMA) solution.

To prepare 100 mL of a 2 mg/mL coating solution, 2 g of poli-HEMA were added to 100 mL of 95 % ethanol in a glass flask, and allowed to dissolve over a stirring plate with mild agitation for circa 8 h at room temperature (RT). After complete dissolution, 6-well plates were coated with 0.4 mL/well of this solution and allowed to dry at room temperature, in a sterile atmosphere over a stable bench. Following drying, plates were further sterilized by exposing them to UV light for 20 min. Whenever plates were not immediately necessary, they were sealed with Parafilm® and stored at 4 ºC.

5.1.6 N2 Medium for CSCs' Growth

500 mL of the N2 medium were prepared by mixing 5 mL of penicillin (5000 U/mL)-streptomycin (5000 µg/mL) with 5 mL of the ITS solution, 100 µl of amphotericin B and 10 µl of the 1mM progesterone solution. Subsequently, 0.6 g of $NaHCO_3$ and 0.08 g of putrescine were dissolved in the medium. Sterility was ensured by filtration.

5.1.7 DMEM Cell Culture Medium Supplemented with 10 % FBS

500 mL of this medium were prepared by mixing 444.9 mL of DMEM cell culture medium with 50 mL of fetal bovine serum (FBS), 5 mL of penicillin (5000 U/mL)-streptomycin (5000 µg/mL) and 100 µl of amphotericin B.

5.1.8 Freezing Solution

The solution used to freeze cells was prepared by mixing cell culture medium:FBS:dimethyl sulfoxide (DMSO) at the proportion of 7:2:1.

5.2 Cells and Cell Culture Procedures

From the nine different cellular systems used in this work, only BEAS-2B was attained from a commercial source. The remaining eight cell lines were produced under the scope of this project using original protocols. Minor description will be provided in this section regarding the novel cell lines, as it is an integrant part of both the results and discussion of Part III.

5.2.1 Bronchial Epithelial Airway System-2B (BEAS-2B)

BEAS-2B cells were obtained from the European Collection of Cell Cultures (ECCAC, Salisbury, UK; ECCAC no. 95102433). This system has been produced in 1988 by the group of Curtis Harris through the use of an adenovirus 12 (AD12)-simian virus 40 (SV40) hybrid virus. The resultant immortalized human bronchial epithelial cells were proved to retain the ability to form an epithelium in deepithelialized rat tracheas, as well as to produce mucin when inoculated onto a collagen matrix (Reddel et al., 1988).

Cells grown as adherent monolayers were maintained in either Clonetics™ BEGM medium (Lonza, Basel, Switzerland) supplemented with bovine insulin, bovine pituitary extract, epinephrine, human epidermal growth factor, hydrocortisone, retinoic acid, triiodothyronine, transferrin and the antibiotics amphotericin-B sulphate and gentamicin (Lonza) or LHC-9 medium, a recently produced equivalent from Gibco. Cells were kept at 37 ºC in a 95 % air/5 % CO_2 incubator. Vented culture flasks were coated with gelatin solution 2 h before use, and except otherwise stated cells were seeded at a the recommended initial density of $4x10^3$ cells/cm^2. Sub-culture was performed using a 0.25 % trypsin-1 mM EDTA solution (Biochrom, Cambridge, UK) whenever cultures reached 80 % confluence.

Continuous culture in the presence of 1.0 μM Cr(VI) described in Chapter 6 started at passage (#) 4. Control cultures, grown in the absence of Cr(VI), were always maintained in parallel.

5.2.2 RenG2, Cont1, DRenG2, DDRenG2, SC-DRenG2, SC-DDRenG2 and iRenG2 Cellular Systems

The attention of the RenG2 following a low density culture of the BEAS-2B cells in the presence of 1.0 μM of Cr(VI) is of part of the novelty of this work and will be explored in the Part III of this manuscript. Suffice to say now that these cells, along with their non-malignant controls, the Cont1 system (BEAS-2B cells cultured at low density but in the absence of Cr(VI) oxyanions), were cultured in the same conditions and manipulated using the same protocols established for BEAS-2B cells.

All the remaining cell lines were attained following manipulation of the RenG2 system. They are all malignant and some of them portray stem-like properties. The derivative systems (DRenG2 and DDRenG2) were produced by direct *in vivo* isolation of RenG2- and DRenG2-xenograft-

derived cells, and following their establishment were cultured using the same protocol as their progenitors, but in F12 supplemented growth medium. Conversely, due to their similarities with RenG2, iRenG2 were cultured in LHC-9 cell culture medium.

5.2.3 Mouse Fibroblasts (FR) Primary Cell Line

For the co-culture studies, a primary mouse stromal cell line was needed. To attain it, a mouse from the same colony as the ones used for the production of the derivative cellular systems was anesthetized using a 77 % ketamine (Ketalar®, Pfizer, New York City, NY, USA), 23 % chlorpromazine (Largactil®, Laboratórios Vitória, Amadora, Portugal) solution, and cells from the thoracolumbar aponeurosis were surgically isolated. Tissue fragments' were then washed several times with PBS and divided into smaller pieces which were distributed throughout the basis of a T_{25} cell culture flask. A small drop of FBS was next added to each of the fragments to help them attach to the plastic surface of the flask and to provide them with nutrients. Finally, the flask was turned upside-down and 5 mL of DMEM cell culture medium supplemented with 10 % FBS were added to the top surface of the flask. Fragments were allowed to attach upside-down for 24 h in the incubator and after that period the flask was gently turned to the upright position allowing cells to contact with the cell culture medium. In the subsequent days cells slowly started to detach from the fragments and to form a monolayer of cells that ended up covering almost all the bottom surface of the flask. Following trypsinization cells were sub-cultured and amplified and various aliquots criopreserved for subsequent use.

5.3 Clonogenic Assays

This cell biology technique evaluates the ability of a single cell to grow at unfavorable low densities in the form of a colony. It allows to compare different cell populations, malignant vs. non-malignant or cells derived from different treatment regimens (Franken et al., 2006). Moreover, increased clonogenic ability is frequently associated with a malignant phenotype (Barr et al., 2013).

The optimized clonogenic assay used encompassed the plating of 13 cells/cm^2 onto 100 mm Petri dishes. Cells were allowed to grow for 15 days and then fixed and stained with crystal violet according to the protocol established by the group of van Bree (Franken et al., 2006). Surviving colonies (containing more than 10 cells) were scored to assess cloning efficiency and the complete protocol was repeated at least three times.

Plating efficiency (PE) was calculated according to Equation 1 and the results were presented as a mean of three independent assays.

$$PE = \frac{\text{no.of colonies formed}}{\text{no.of cell seeded}} \text{ x } 100\ \% \qquad \textit{Equation 1}$$

5.4 Generation of the Subclonal Cell Lines: RenG2 and Cont1

The low density culture in the presence of Cr(VI) resulted in the formation of numerous dense clumps with deeply altered morphology. For the generation of subclonal cell lines, several of these clumps were isolated using glass cloning rings (Figure 5.1) and then reseeded onto 150 mm Petri dishes to be cultured again in the presence of 1 µM Cr(VI). 10 days later, three morphologically altered colonies were isolated and transferred into 3 different wells of a 6-well plate. When cultures reached near 80% confluence, cells were trypsinized and reseeded onto T_{25}

flasks, again in the presence of 1 μM Cr(VI). In the case of BEAS-2B control cultures the cloning rings were used to isolate randomly chosen colonies, as none displayed particular morphological features. The cells thus isolated were subjected to the same treatment as the Cr(VI)-treated cells.

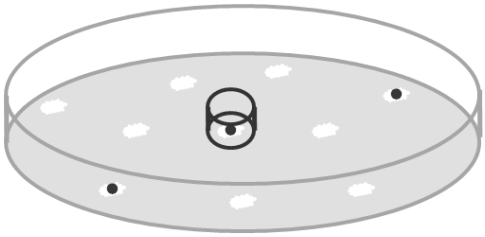

Figure 5.1 - Colony isolation using cloning rings. Cloning rings are small glass rings that can be placed around cellular colonies in order to isolate them. The protocol of isolation encompassed a normal tripsinization followed by cells' collection using PBS. This proceeding was cautiously done inside the ring.

Following expansion of the isolated colonies in the 6-well plate, three subclonal cell lines were established for either Cr(VI)-exposed and control cells. Karyotype and gene expression profiles were equivalent among the colonies, so we randomly choose one of each condition to continue the studies. From Cr(VI)-exposed isolated colonies, **RenG2** cellular system was produced; the system obtained from the control low-density colonies was named **Cont1**.

5.5 Cytogenetic Analys1s

For cytogenetic analysis cells were cultured in 75 cm^2 flasks and allowed to reach approximately 75 % confluence. The preparation of metaphase chromosomes was carried out according to standard procedures optimized to our cul-

tures. Briefly, cells' cycle was stopped in pro-metaphase by the addition of 200 µl of colcemid to the cell culture flask followed by a 25 min incubation period at 37 ºC/95 % air/5 % CO_2. After this period, the cell culture medium was discarded and cells were washed using PBS. Cells were then dethatched by tripsinization and collected using PBS to a 10 mL centrifuge tube.

To get rid of remaining cellular debris or trypsin, tubes were centrifuged for 5 min at 1000 revolutions per minute (rpm) and the supernatants were discarded. Cells were then resuspended in 1 mL of FBS, to inactivate any remaining trypsin, plus 9 mL of a 5 mM potassium chloride (KCl) hypotonic solution. Cells and their elements were allowed to swell for 17 min at 37 ºC.

After swelling, fixation was initiated by the addition of 1 mL of an ice-cold methanol:acetic acid (3:1) fixation solution to the tube containing the hypotonic solution. This step was of extreme importance to prepare and preserve the structure of the chromosomes for the next fixation steps. The hypotonic solution was then removed by centrifugation, 5 min at 1000 rpm, and 10 mL of the fixation solution were used to ressuspend the pellet. Fixation was promoted by placing the tubes at 4 ºC for 1 h. Passed that time, tubes were again centrifuged 5 min at 1000 rpm and the pellets resuspended in 10 mL of the fixation solution. Tubes were kept at 4 ºC until the preparation of the metaphase spreads.

Metaphase spreads were prepared by dropping small volumes of the resuspended fixed cells into microscope slides. This process induced the mechanic rupture of the cells' membrane, thus allowing the spread of the chromosomes (Figure 5.2).

Chromosomes were giemsa-banded (GTG-banding) in order to organize them into karyotypes. The initial banding protocol step relays on the action of trypsin over the different types of chromatin. Therefore, microscope slides were immersed in a 0.4 % trypsin solution for a period of time optimized for each cell line everytime time the protocol was performed. Trypsin only digested the more

decondensed chromatin (the euchromatin), leaving untouched the heterochromatin. Subsequently, slides were washed and the striped chromosomes were labeled with giemsa by immersing the slides into the dye for as much time as the estimated in the optimization steps.

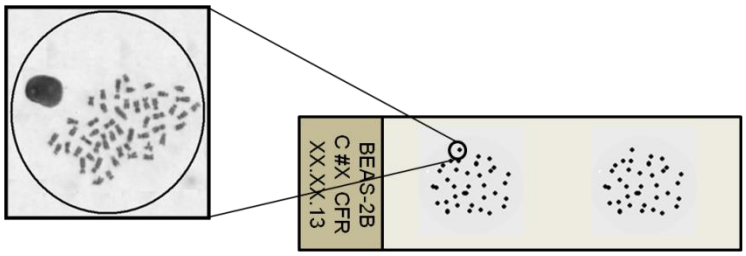

Figure 5.2 - Preparation of metaphase spreads. Following cells' fixation, metaphase spreads were prepared by dipping a small drop of the fixed cellular suspension over the microscope slides.

For each passage or cell line studied at least 50 metaphase spreads were analyzed and 20 karyotypes constructed using a Nikon microscope (Nikon Portugal, Lisbon, Portugal) coupled with Applied Imaging® CytoVision® software (Genetix, New Milton, UK).

5.6 Gene Expression Analysis by Reverse Transcriptase-quantitative Polymerase Chain Reaction (RT-qPCR)

A very accurate and reliable way to monitorize malignant transformation-associated changes is to evaluate the expression of some genes involved in the underlying processes. That can be attained by isolating the messenger ribonucleic acid (mRNA) from cells and subsequently analyze its contents, which would represent the cells' expressome at a certain time point.

For mRNA isolation, $1x10^6$ cells were initially collected in RNAlater® RNA stabilization reagent (Bioportugal, Porto, Portugal) and stored at -20 ºC. For total RNA isolation, the RNAeasy® Mini Kit (Qiagen, Venlo, Netherlands) was used. To quantify the RNA extracted and verify its integrity, samples were analyzed using the RNA 6000 Nano Chip® Kit (Agilent Technologies, Santa Clara, CA, USA) in an Agilent 2100 Bioanalyzer with the 2100 Expert Software (Agilent Technologies), according to the manufacturer's instructions.

1 µg of total RNA was reverse transcribed using the SuperScript™ III First-Strand Synthesis System for RT-PCR (Invitrogen, Carlsbad, CA, USA). The reactions were carried out in a GeneAmp PCR System 9600 Thermal Cycler (Perkin Elmer, Waltham, MA, USA). Reaction products were digested with 1 µL RNase A (Amresco, Solon, OH, USA).

Relative quantification of gene expression by qPCR was performed in a 7900 HT Sequence Detection System (Applied Biosystems, Foster City, CA, USA). For normalization purposes, optimal housekeeping genes for this study were selected using the geNorm™ Housekeeping Gene Selection Kit (PrimerDesign, Southampton, UK) and the geNorm™ software (Ghent University Hospital, Ghent, Belgium). Real-time PCR reactions used QuantiTect® Primer Assays (Qiagen) for each of the different genes. PCR reactions were carried using 100 ng of cDNA sample, 1× QuantiTect® Primer Assay and 1× iTaq™ Universal SYBR® Green Supermix (BioRad, Hercules, CA, USA), in a total volume of 10 µL, using the following thermal profile: 15 min at 95 ºC (PCR initial activation step) and 40 cycles of 15 s at 95 ºC, 30 s at 60 ºC and 30 s at 72 ºC. RT-qPCR results were analyzed using RQ Manager 1.2.1 software (Applied Biosystems) and the $2^{-\Delta\Delta Ct}$ method (Livak and Schmittgen, 2001).

The primers used in this study were GAPDH_2_SG, TOP1_1_SG, CCNB1_1_SG, LDHA_1_SG, HIF1α_1_SG, SLC2A1_1_SG, MYC_1_SG, SPARC_1_SG,

EGFR_1_SG, MAPK14_1_SG, MAP2K4_1_SG, MAPK1_1_SG, XRCC1_1_SG, XRCC3_1_SG, XRCC5_1_SG, RAD51_1_SG, MSH2_1_SG, CAV1_1_SG, DNMT1_1_SG, MLH1_1_SG. They have all been acquired from Qiagen and their sequence is depicted in Table III of Appendix A.

5.7 Microsatellite (MSI) Analysis

The pentaplex PCR of five mononucleotide repeats (NR-21, NR-24, NR-27, BAT-25 and BAT-26) is commonly used to establish the MSI status of human cells, being 100 % sensitive and specific (Buhard et al., 2004). In our samples, these mononucleotide repeats were amplified in a pentaplex PCR reaction using a T3 Thermocycler (Biometra, Göttingen, Germany). Primer sequences were as previously described (Buhard et al., 2004). All the reverse primers (Thermo Scientific, Waltham, MA, USA) were 5'-labelled with a fluorescent tag (HEX for markers NR-24, NR-27 and BAT-26, and 6-FAM for NR-21 and BAT-25) to allow for microsatellite detection using an Applied Biosystems 3730XL DNA Analyzer (Applied Biosystems). The PCR reaction was carried out in a total volume of 25 µl that contained 1× GoTaq® Flexi Buffer (Promega, Madison, WI, USA), 0.2 mM dNTPs, 2.5 mM magnesium dichloride ($MgCl_2$), 8 pmol of primers NR-21, NR-24 and NR-27, 10 pmol of primer BAT-25, 12 pmol of primer BAT-26, 0.75 U of GoTaq® Flexi A DNA Polymerase (Promega) and 5 µl of genomic DNA.

Genomic DNA was extracted from the cells with the Puregene® DNA Isolation Kit (Qiagen), according to the manufacturer's instructions. After an initial denaturation at 95 ºC for 5 min, PCR steps were as follows: 35 cycles of denaturation at 94 ºC for 30 s, annealing at 54 ºC for 45 s and extension at 72 ºC for 30 s. Final extension was carried out at 72 ºC for 10 min. Successful amplification was confirmed by electrophoresis on a 3.5 % agarose gel and PCR products were sent to Macrogen Inc. (Seoul, Korea) (http://www.macrogen.com) for fragment analysis.

Allelic sizes estimation and MSI analysis were made using the GeneMarker® software (SoftGenetics, State College, PA, USA). The Cr(VI)-exposed cell line would be considered MSI positive if, at least, 2 out of 5 markers showed band shifting, when compared to the control, non-exposed one.

5.8 *In vivo* Studies

Animal studies were mentored by category C researchers credited by the Federation for Laboratory Animal Science Associations (FELASA). All the procedures were in agreement with the European Convention for the Protection of Vertebrate Animals used for Experimental and Other Scientific Purposes (CETS no. 123), as well as the Portuguese rules (DL 129/92).

Two types of animals have been used in this project. For the evaluation of the RenG2's malignant potential, 10^7 cells suspended in 100 µl of PBS were subcutaneously injected into four 6-week-old BALB/c-nu/nu mice. 3 control mice injected with 100 µl of PBS were kept in parallel. Animals were maintained in eurostandard type III-H cages (Tecniplast, Buguggiate, Italy) coupled to a 1291H support and ventilation system (Tecniplast) to ensure appropriate conditions. Animals were weekly screened for tumors by observation, palpation, and indirectly by weight measurement. Two months after the injection tumors were resected and fixed in formalin.

The derivative systems were also attained using BALB/c-nu/nu mice. To this end, one of the tumors formed during the evaluation of RenG2's malignant potential was divided into 2 parts: half of it was used to identify the histological type of the tumor, and the other half was divided into small fragments and used to establish a primary culture out of it. The protocol used was equal to that used for the establishment of the FR primary cell line, exception made to the cell culture medium, which here was the F12 supplemented growth medium. The attained culture

turned out to be immortal and was baptized as **DRenG2** (first derivative cell line). The second derivative system, the **DDRenG2** cell line, was similarly produced by subcutaneously injection of 10^7 DRenG2 cells into BALB/c-nu/nu mice and establishment of a primary culture out of fragments collected from the induced tumors.

5.9 Histopathological Analysis

Whenever tumors developed in mice, they were resected and sent for pathological analysis. An experienced pathologist performed current histopathological examination on the collected samples. For that end, formalin fixed tumors were embedded in paraffin and thinly sliced using a RM2135 Minot microtome (Leica, Solms, Germany). Tumor slices were then stained with hematoxylin and eosin for microscopic evaluation of their major morphological features. Immunohistochemistry was subsequently performed in order to attain the histological type of the developed tumor. The markers used were LCA (lymphoma marker; clone 2B11 + PD7/26), HMB-45 (melanosome marker), MNF116 (cytokeratin AB marker for carcinomas; clone MNF116), and Vimentin (mesenchymal marker; clone Vim 3B4), all of them obtained from Dako Corporation (Carpinteria, CA, USA).

5.10 Metabolic Studies: ^{18}FDG uptake

The metabolic status of each cellular system was accessed using [^{18}F]-fluoro-2-deoxyglucose (^{18}FDG), a radiopharmaceutical glucose analogue designed for positron emission tomography (PET), routinely used in clinical PET imaging studies.

1.5 mL of single-cell suspensions containing $2x10^6$ cells/mL were prepared in each cell's culture medium, from either adherent-growing cell lines or tridimensional spheres. The suspensions were placed in 10 mL centrifuge tubes and left for

recovery for 60 min at 37°C. Subsequently, a calculated volume of 37 ºC-heated ^{18}FDG was added to each tube in order to attain a final concentration of 0.75 MBq/m. Tubes were gently homogenized and then conserved at 37 ºC under a heat plate (FALC, Treviglio, Italy). After 60 min of incubation, samples of 200 µL were collected to 1.5 mL microcentrifuge tubes containing 500 µL of ice-cold PBS. Tubes were then centrifuged 1 min at 10000 rpm in an Eppendorf miniSpin Centrifuge (Eppendorf, Hamburg, Germany) and the supernatants were collected into glass tubes. 500 µL of ice-cold PBS were added to the pellets to wash any remaining radioactive medium and tubes were again centrifuged for 1 min at 10000 rpm. Supernatants were collected to the same glass tube as previous and cell pellets were preserved. Finally, both the supernatants and the pellets were assayed for radioactivity using a Radioisotope Calibrator Well Counter (CRC-15W Capintec, Savannah, GA, USA) narrowed to the ^{18}F sensitivity energy window (400-600 keV). All cell populations were studied in triplicate in at least three sets of independent experiments. The attained results represent the percentage of cells' radioactivity relatively to the total radioactivity added, normalized *per* million of cells.

5.11 Flow Cytometry-based Cellular Characterization

A molecular signature for each cell line was searched for using basic flow cytometry assays. To this end, 300 µL of single-cell suspensions containing 1x10^5 cells were prepared. Four different cytometry tubes were prepared *per* cellular system, two tubes destined to be the blank controls and the other two to be incubated with the selected panel of fluorescence-labeled monoclonal antibodies (mABs) as schematized in Table I. The mABs used were CD31 (WM59, BD Biosciences, San Jose, CA, USA), NGFR (C40-1457, BD Biosciences), CD14 (M5E2, BD Biosciences), CD13 (Immu103.44, Beckman Coulter, Pasadena, CA, USA), CD133 (293C3, Miltenyi Biotec, Bergisch Gladbach, Germany), CD11b (ICRF44, BD Biosci-

ences), CD45 (HI30, Invitrogen), CD106 (51-10C9, BD Biosciences), CD105 (1G2, Beckman Coulter) and HLA A, B, C (G46-2.6, BD Biosciences). The volumes of each mAB were selected according to manufacturer's recommendations and are listed in Table I.

Table I - Markers and fluorophore used in the flow cytometry-based cellular characterization studies.

	Tube 1		Tube 2	
FITC	CD31	10 µL	CD106	10 µL
PE	NGFR	10 µL	CD30	10 µL
PerCP5.5	CD14	2.5 µL	-	-
PeCy7	CD13	2.5 µL	CD13	2.5 µL
APC	CD133	10 µL	HLA-A,B,C	10 µL
PB	CD11b	2.5 µL	CD11	2.5 µL
PO	CD45	2.5 µL	CD45	2.5 µL

FITC – Fluorescein isothiocyanate; PE – Phycoerythrin; PerCP – Peridinin-cholophyll-protein complex; PeCy7 – Phycoerythrin Cy7-conjugated; APC – Allophycocyanin; PB – Pacific blue; PO – Pacific orange.

Following the addition of the mABs, tubes were incubated for 15 min in the dark at RT. 2 mL of PBS were then added to each tube to help removing the excess of fluorophore, and the tubes were centrifuged for 5 min at 1500 rpm. After centrifugation, pellets were resuspended in circa 200 µL of the supernatant. Control tubes were also centrifuged and resuspended, albeit the washing step with PBS was avoided. Sample readings were carried out in a FACS Canto II Flow Cytometer (BD Biosciences) and the attained results were analyzed using the CellQuest software (BD Biosciences).

5.12 Immunocytochemistry

AB-based assays are very powerful techniques in the dissection of cellular constituents. In this project, immunocytochemistry was mostly used to highlight cell lines' specific features that may be responsible for the observed physiological differences, and consequently, may had driven Cr(VI)-induced BEAS-2B malignant transformation and the formation of a CSC population within the derivative systems.

$4x10^3$ cells/cm^2 were seeded on the top of 2 % gelatin-coated microscope slides placed inside a 100 mm cell culture dish and cells were allowed to grow until the cultures reach approximately 80 % confluence. By then, the medium was aspired and the slides were rinsed twice with PBS and collected into centrifuge tubes containing 50 mL of 95% ethanol. Tubes were stored at 4 ºC until slides were processed.

To quench the endogenous peroxidase activity slides were incubated for 15 min in a 3 % hydrogen peroxide (H_2O_2) solution. Subsequently, blockage was promoted by allowing the cells to contact for 5 min with the Ultra V Block solution (Ultra Vision Kit, Thermo Scientific). Staining encompassed incubating the slides with an optimized primary AB solution for 1 h at RT. Slides were then washed with PBS and incubated with the biotin-labeled secondary AB (Ultra Vision Kit, Thermo Scientific) for 15 min at RT. Revelation was made by adding the peroxidase-conjugated streptavidin (Ultra Vision Kit, Thermo Scientific) along with the chromogen diaminobenzidine tetrahydrochloride (DAB), and counterstaining was promoted by incubating slides with hematoxylin. Finally, slides were dehydrated and mounted using the Tissue-Tek Glas Mounting Medium (1408, Sakura, Torrance, CA, USA).

The primary ABs used to stain all the cell lines were Vimentin (Vim3B4, Dako Corporation, Carpinteria, CA, USA) and α-Smooth muscle actin (αSM-1,

Leica). Cells' were observed in a Nikon Eclipse 80i microscope and photographs were taken using a Nikon Digital DXM1200F coupled camera.

5.13 Scratch Assay

The scratch assays are widely used to infer on the ability of cells to migrate. Liang and collaborators provided the first protocol for the technique and highlighted the inexpensiveness and easiness with which it can be accomplished (Liang et al., 2007). Even though it encompasses some limitations, when carefully interpreted in the context of other results, it often provides valuable information.

To perform the scratch assay, $4x10^3$ cells/cm^2 were added to previously 2 % gelatin-coated 60 mm cell culture dishes and cells were allowed to growth until forming a complete monolayer. Subsequently, a linear scratch was made in the monolayer using a p200 pipet tip. Cultures were then rinsed with PBS to remove any cellular debris and the medium was replaced. Marks were done in the dishes to ensure the photos were taken in approximately the same site over time. Cells were allowed to grow, and photographs were taken at 0 h, 12 h, 19 h, 24 h, 27 h, 37 h, 49 h, 60 h, 73 h, 82 h, 93 h, 176 h and 200 h using a Moticam 2300 3.0 M Pixel USB 2.0 camera (Motic, Xiamen, China) coupled to a AE31 microscope (Motic).

5.14 Drug Resistance Studies

Resistance to both chemo- and radiotherapy is a particular feature commonly attributed to CSCs. To test the differential chemoresistance of the isolated CSCs, proliferating spherical clones were dissociated into a single-cell suspension and plated into a 24-well plate in N2 cell culture medium. Concomitantly, all the five cell lines previously amplified in T_{75} flasks were also platted in 24-well plates. The optimized initial cellular density for all cell lines was $8x10^3$ cells/cm^2. 24 hours after seeding the cells, 10 µL of each drug solution [cisplatin (Cis, CG6413, Gene-

ris®, Amadora, Portugal), methotrexate (MTX, Teva Pharmaceutical Industries) and gemcitabine (Gem, Gemzar®, Lilly, Indianapolis, IN, USA)] were administered to attain the desired final concentration (0.0 µM, 0.1 µM, 10 µM and 50 µM). For each condition, including the controls, three independent assays were carried in triplicate. Cells' viability was assessed every 24 h, during 3 days using the 3-[4, 5-dimethylthiazol-2-yl]-2, 5-diphenyltetrazolium bromide (MTT) reduction assay (Figure 5.3).

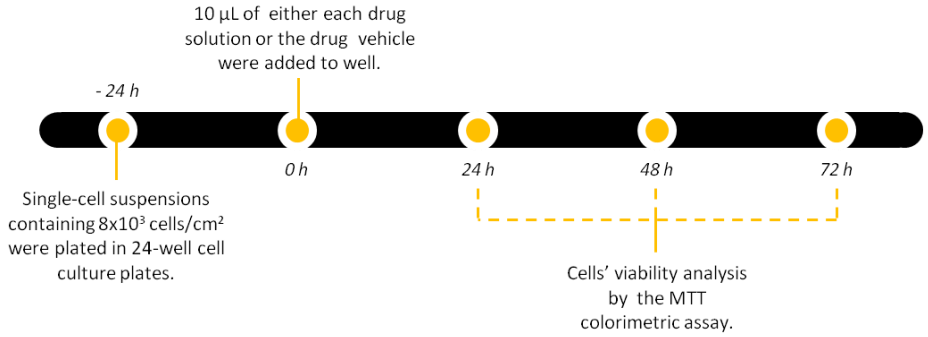

Figure 5.3 - Experimental design of the drug resistance studies. Cells were seeded at the optimized density 24 h prior to the beginning of the study. At 0 h, equal volume of either the drug solutions or the drug vehicle was added to each well. Viability was assessed 24 h, 48 h and 72 h after the beginning of the incubation period.

The ability of cells to reduce MTT is fundamentally based on the integrity of their mitochondria. Consequently, any harm directed towards these organelles or anything that compromises cells' viability is translated into a diminished ability of cells to reduce MTT (van Meerloo et al., 2011). The calculation of cells' viability relatively to the controls was made according to Equation 2, where the Abs Sample means the absorbance (Abs) of the solution collected from treated cells minus the absorbance of the dissolution vehicle and the Abs Control means the same from the control, untreated cells.

$$\text{Viable cells} = \frac{\text{Abs Sample}}{\text{Abs Control}} \text{ x } 100\ \% \qquad \textit{Equation 2}$$

In order to circumvent bias resultant from differences in mitochondria number between cell lines, which would provide false positive viability values, direct cell counting using trypan blue was used. To this end, samples of cellular suspensions were collected and diluted in appropriate volumes of trypan blue staining. Cells were counted under a microscope in a Neubauer's chamber.

5.15 Cellular Doubling Times

The doubling time (DT) of a culture intends to mirror the time individual cells need to travel their cycle one complete turn. There are various ways to assess cells' viability, but the colorimetric assay based on MTT's reduction is still the one of the most used, as it represents a very easy and inexpensive technique.

For the MTT assay, cells were seeded into 24-well plates at an optimized initial cellular density of $8x10^3$ cells/cm^2. At the desired time points (Figure 5.4) cell culture medium was discarded and the wells were rinsed with 200 µL PBS. 500 µL of 0.5 mg/mL MTT were then added to each well and cells were left in the incubator for 4 h. Subsequently, the MTT solution was cautiously removed, leaving untouched the violet formazan crystals to be dissolved in 500 µL of acid isopropanol. The samples' absorbance was measured at 570 nm in a multiplate reader according to manufacturer's instructions.

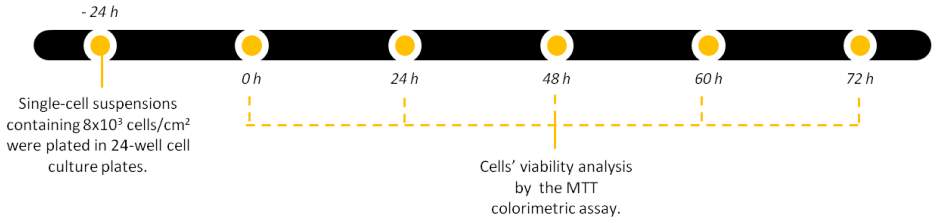

Figure 5.4 - Experimental design of the cellular duplication time study. Cells were seeded at the optimized density 24 h prior to the beginning of the study. At 0 h, 24 h, 48 h, 60 h and 72 h cells viability was assessed. The time needed to duplicate the viability reflects cell's DT.

Each cell line DT was attained using the Equation 3, where *t* means time, *N(0)* means cells' viability at 0 h and *k* represents the growth rate (number of doublings that occur *per* unit of time). Calculations were made using the Doubling Time software at Doubling Time webpage (V. 2006).

$$DT = N_0 \times e^{kt} \qquad \textit{Equation 3}$$

Similarly to what has been described for drug resistance studies, cellular proliferation was monitorized by trypan blue direct cell counting in a Neubauer's chamber.

5.16 Sphere-forming Assay and the SC-DRenG2 and SC-DDRenG2 Cell Lines

In light of the results attained during the characterization of the malignant cellular systems, it seemed logical that an eventual stem-like population living inside the BEAS-2B cellular system may have responded to Cr(VI) by amplifying itself and giving birth to a CSCs pool in the malignant systems. To test this hypothesis, the sphere-forming assay was used. This assay takes advantage of an intrinsic

property of CSCs, i.e., their ability to form tridimensional spheres when cultured under low-adherence conditions with appropriate mediums and supplements, to efficiently isolate that individual cell population. The use of the sphere-forming assays meets consensus throughout the scientific community as it has been widely used to isolate CSCs from different tumor types.

Except for FR mice cells, all the cell lines under study were scrutinized for the presence of CSCs. Low adherence 6-well plates were prepared according to the previously described protocol (section 5.1.5) as was the isolation medium (section 5.1.4). For the isolation, a cellular suspension containing $3x10^4$ cells/mL was prepared in CSCs' isolation medium and 2 mL of this suspension were added to each well of the plate. Isolation medium was supplemented with 10 ng/mL of both human EGF (E9644, Sigma-Aldrich) and bFGF (100-18B, PeproTech, London) and cells were allowed to grow under normal conditions. Supplements' concentration was replaced twice a week.

Whenever sphere formation was observed, and when spheres reached a satisfactory volume (which normally happens circa 15 day after platting), they were collected, washed with PBS, and plated in a T_{25} cell culture flasks provided with 5 mL of N2 medium. Cells were allowed to attach and expand, and when they attained nearly 80 % confluence, the protocol of isolation was repeated. The procedure was repeated until third generation spheres were attained, as these cells are considered a pure clonal-derived CSCs population.

The spheres isolated from **DRenG2** and **DDRenG2** cellular systems gave rise to the SC-DRenG2 and SC-DDRenG2 cell lines, respectively.

5.17 Comparative Genome Hybridization Array (aCGH)

aCGH is a molecular cytogenetic tool that identifies unbalanced chromosomal rearrangements with a resolution in the range of Kb (Darai-Ramqvist et al., 2006). The use of aCGH for analysis of solid tumors has revealed a number of recurrent chromosomal copy number aberrations including micro-deletions and micro-amplifications that had not been previously detected by any existing conventional cytogenetic technique.

This method provides a comparative genomic analysis between two DNA samples. Most often, one compares normal and tumor cells-derived DNAs; however, in this work, BEAS-2B were initially compared with a normal standard masculine control (DD7101, Promega) and the remaining six cell lines (Cont1, RenG2, DRenG2, DDRenG2, SC-DRenG2 and SC-DDRenG2) were conversely compared with BEAS-2B cells.

For the aCGH analysis of our systems, DNA was extracted using the High Pure PCR Template Preparation Kit (11796828001, Roche Applied Science, Basel, Switzerland), according to manufacturer's instructions. Then BEAS-2B-extracted DNA was labeled with the cyanin (Cy) 3 (Cy3) fluorophore, while DNA derived from the remaining systems was labeled with Cy5. The labeling step was attained using the SureTag Complete DNA Labeling Kit (5190-4240, Agilent Technologies). DNA samples were subsequently fragmented and mixed with unlabeled human COT-1 DNA (EA-020, Kreatech Diagnostics, Amsterdam, Netherlands) to suppress repetitive DNA sequences. Finally, the DNA mixture was hybridized to a SurePrint G3 Human CGH Microarray 180 K (G4449A, Agilent Technologies) containing hundreds or thousands of printed defined DNA probes. The fluorescence ratio along the chromosomes was measured in a DNA microarray scanner C (Agilent Technologies). DNA regions containing fluorescence unbalances were spotted for further analysis, as they represent regions of gains or losses of genetic material, compared

to the reference sample. Data was processed using the Feature Extraction Software version 10.7 (Agilent Technologies) and results were analyzed using the Agilent Genomic Workbench life edition 6.0 aCGH data analyzing software (Agilent Technologies).

5.18 Co-culture of RenG2 and FR: The Attainment of the iRenG2 System.

As it was only possible to isolate spheres out of DRenG2 and DDRenG2 cell lines, we hypothesized that the cells in the mice lumbar subcutaneous compartment may have driven RenG2 cells' dedifferentiation. To assess this hypothesis FR cells were cultured in a 6 well plate equipped with 4.5 cm^2 Transwell® insert (CLS3450, Corning) containing RenG2 cells, as illustrated in Figure 5.5. The ultimate goal of this co-culture was to mimic as much as possible the conditions that RenG2 cells faced in mice lumbar subcutaneous compartment, when these cells were injected to attain the derivative systems. As so, co-cultures were kept in the incubator for two months and mediums were changed every 15 days. The conditioned mediums of both compartments were preserved and stored at 4 ºC until further analysis.

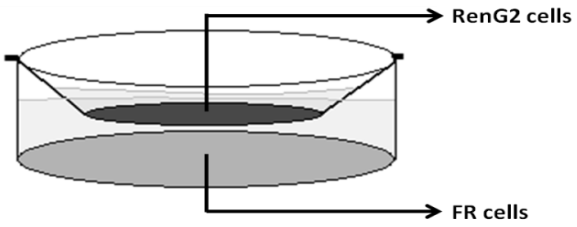

Figure 5.5 - Co-culture experimental design. Using a 6-well plated adapted transwell system, RenG2 and FR cells were co-cultured for 2 months. FR cells were cultured in DMEM in the lower compartment, while RenG2 cells were housed in the upper compartment in LHC-9.

After 2 months in co-culture, RenG2 cells were isolated and re-baptized **iRenG2**. Their ability to for spheres was assessed as described in section 5.16 and their molecular signature was also searched for as in sections 5.6 and 5.11.

5.19 Multiplex Cytokine Array: The Search for the Guilty!

To further test the hypothesis of a stromal-driven crosstalk and to search for its potential orchestrators, the BioPlex® multiplex cytokine array (BioRad) was performed in the conditioned media of the co-cultured cells. Our results were further validated by simultaneously analyzing conditioned media collected from other control standard cultures and co-cultures. The complete experiment layout is depicted in Figure 5.6.

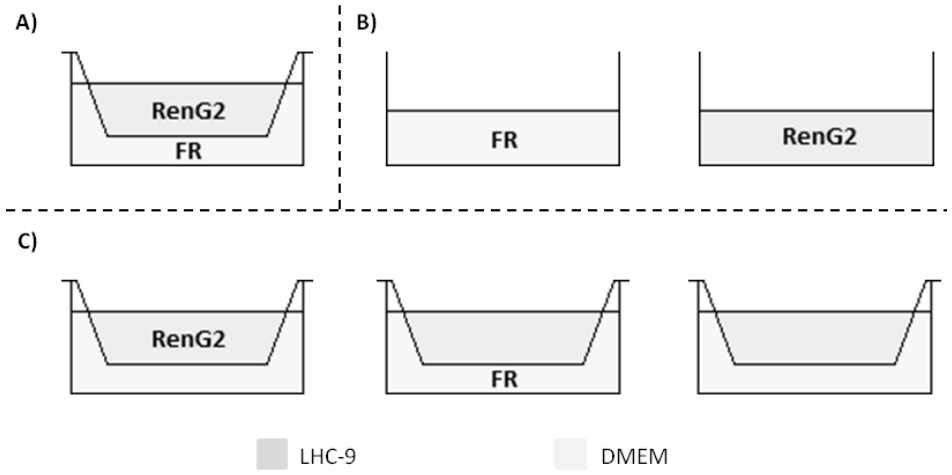

Figure 5.6 - Experimental layout to attain the different conditioned media. A) Co-culture of RenG2 with FR cells to test the hypothesis of stromal-induced dedifferentiation. B) Standard control cultures of both FR and RenG2 cells. C) Control co-cultures of RenG2 cells with FR cell culture media, of FR cells with LHC-9 media and of both media, without cells. All cultures were left for 2 months and media were changed every 15 days.

FR cells-derived cytokines were searched for using the Bio-Plex Pro™ Mouse Cytokine 23-plex Assay Kit (#M60-009RDPD, BioRad), which contains beads to detect eotaxin, granulocyte colony-stimulating factor (G-CSF), granulocyte macrophage colony-stimulating factor (GM-CSF), interferon gamma (INF-γ), IL-1α, IL-1β, IL-2, IL-3, IL-4, IL-5, IL-6, IL-9, IL-10, IL-12p40, IL-12p70, IL-13, IL-17A, KC (also known as CXCL1), monocyte chemotactic protein-1 (MCP-1, also known as chemokine (C-C motif) ligand (CCL) 2, CCL2), macrophage inflammatory protein (MIP) 1α (MIP-1α), MIP-1β, regulated on activation, normal T cell expressed and secreted (RANTES, also known as CCL5) and tumor necrosis factor α (TNF-α).

Samples were studied in triplicate in a Bio-Plex® 200 System (BioRad) according to manufacturer's instructions, and the attained results were analyzed using the Bio-Plex Manager™ Software, Standard Edition (BioRad).

5.20 Enzyme-linked immunosorbent assay (ELISA)

Considering that BioRad did not have commercially available multiplex beads for activin-A analysis, we assayed the levels of this cytokine in our conditioned media by ELISA. To this end, the Human/Mouse/Rat Activin-A Quantikine ELISA Kit (#DAC00B, R&D Systems, Minneapolis, MN, USA) was acquired and our samples were processed according to manufacturer's instructions.

5.21 Data Processing and Statistics

Unless stated otherwise, data here presented result from at least three independent experiments carried out in triplicate, and the results' statistical analysis was carried out using the Graph Pad Prism software version 5 (GraphPad Inc., San Diego, CA, USA).

Whenever possible, data normality was tested using the Kolmogorov-Smirnov test with Dallal-Wilkinson-Lillefor correction. To assess statistical significance between means of the cell lines under study a one-way ANOVA was used followed by correction for multiple comparisons. Thus, Bonferroni's pos-hoc test was applied for comparisons between all cell lines while Dunnett's test was used to compare cell lines to BEAS-2B in the clonogenic assay. A two-way ANOVA followed by a Bonferroni pos-hoc test was specifically used in the analysis of the results from the gene expression study as both the gene and the cell line variations were to be considered simultaneously. A 5 % level was defined as the threshold of significance for the differences and the *P* value was categorized according to their interval of confidence.

PART III

Experimental Results

Chapter 6

Attainment of a Reliable Cellular System

6.1 Introduction

In the last half century many studies were conducted on Cr(VI)-induced lung carcinogenesis. Different experimental designs and systems (both *in vitro* and *in vivo*) have been developed, as well as different exposure regimens to the oxyanion. However, and as previously dissected in Chapter 2, regardless of the advantages and disadvantages of each system and the valuable information provided, the molecular mechanisms underlying Cr(VI)-induced LC are still undisclosed.

Chemical and biochemical processing of Cr(VI) have been exhaustively studied *in vitro*. However, significant divergence is observed among the results attained in different laboratories or study designs. The main reason underlying this divergence may relay on the fact that very few studies utilized epithelial lung cells and most of them used excessive concentrations of Cr(VI). In agreement, the majority of Cr(VI)-based studies employed lung malignant cell lines, whose physiology is already deeply altered by the transformation process. Additionally, some laboratories also used cell lines from other regions of the respiratory system, which may also differ greatly from epithelial cells in what concerns Cr(VI)-uptake and intracel-

lular actions. Finally, Cr(VI) concentration is also of great importance, as cellular effects of low and high Cr(VI) levels greatly differ and evoke dramatically different cellular responses (Nickens et al., 2010).

Based on the epidemiological studies available, as well as on previous results attained in our laboratory (Costa et al., 2010), we set the concentration of Cr(VI) in 1.0 μM. This concentration appropriately mimics an occupational exposure to low concentrations of atmospheric Cr(VI). Furthermore, we choose a non-malignant immortalized human bronchial epithelial cell line (BEAS-2B), cultured in a cell culture media that avoids Cr(VI) reduction in the extracellular space (Borthiry et al., 2008).

The main goal of this study was to develop an adequate and reliable system for the study of Cr(VI) carcinogenesis. Our driving hypothesis was that by promoting a chronic exposure of BEAS-2B cells to 1.0 μM of Cr(VI) and monitoring our cultures for morphological, karyotypic and gene expression changes we would be able to reach our goal.

6.2 Results

6.2.1 Characterization of BEAS-2B cells

The karyotypic study of BEAS-2B cells along time in culture was mostly prompted by the lack of detailed information on their cytogenetic constitution and the first karyotypes immediately showed a group of constant chromosomal alterations. In fact, all low-passage BEAS-2B cells presented an isochromosome of the long arm of chromosome 5 [i(5)(q10)], a terminal deletion of the short arm of chromosome X (Xp^-) and additional material on the short arm of chromosomes 15 ($15p^+$), 16 ($16p^+$) and 22 ($22p^+$) (Figure 6.1). Additionally, chromosomal alterations presented as mosaics were documented. For instance, chromosome 20 trisomy

[tris(20)], found in 80 % of the analyzed metaphases, and a chromosome 14 with additional material in its short arm ($14p^+$) in 70 %. Finally, structural alterations of the banding pattern of the long arm of chromosome 2 [der(2)] were documented in 20 % of the metaphases studied.

Figure 6.1 - Representative karyotype of BEAS-2B cell line at #15. At this passage, i(5)(q10)del(qter) was already present along with all the other chromosomal alterations. At least 20 karyotypes were constructed for each cell passage analyzed.

The mosaicism observed for both the tris(20) and the $14p^+$ tended to decrease along the time in culture, being completely eliminated between #25 and #41. The opposite was observed for the der(2), which reached 100 % prevalence at #25. Finally, a terminal deletion on i(5)(q10) [i(5)(q10)del(qter)], probably resulting from the culture protocol, arises between #12 and #25 and at #41 was definitely established in all cells. Figure 6.2 illustrates the proportional variation of these alterations along BEAS-2B's time in culture.

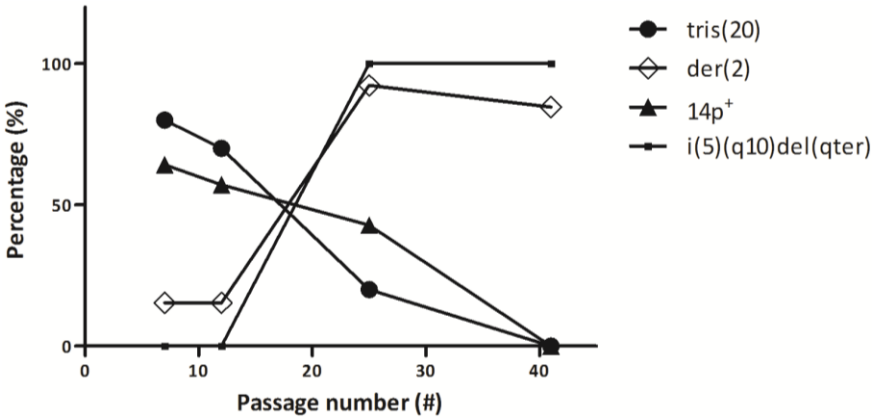

Figure 6.2 - Structural chromosomal changes of BEAS-2B cells along time in culture. While the population of cells portraying the i(5)(q10)del(qter) and the der(2) tend to be amplified along time, $14p^+$- and tris(20)-carrying cells tend to disappear. The results are expressed in percentage in relation to a normal diploid cell line and were obtained from at least 20 karyotypes constructed per #.

Cells' ploidy stability was also analyzed to validate the results attained by Reddel and collaborators, according to which 72 % of the BEAS-2B cells remain near diploid until #29 (Reddel et al., 1988). Giemsa-colored counts of at least 50 metaphase spreads further confirmed those results, as depicted in Figure 6.3. Initial passages of BEAS-2B cells still retained tris(20), which was translated into a higher proportion of hyperdiploid cells. However, as previously mentioned, this mosaic cellular population tended to be eliminated and the percentage of hyperdiploid cells concomitantly diminished. The fraction of hyperdiploid and hypodiploid cells that was observed in latter passages potentially represents culture-induced chromosomal unbalances.

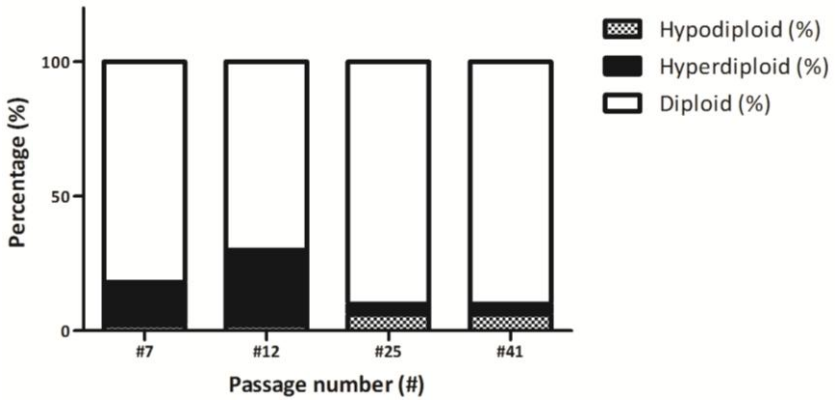

Figure 6.3 - Ploidy analysis of control BEAS-2B cells over time. In agreement with previous observations, BEAS-2B cells remained mostly diploid throughout the time in culture. Yet, an initial increased percentage of hyperdiploid cells potentially represented the mosaic tris(20) population identified in karyotypic studies. For this study at least 50 giemsa-stained metaphase spreads were counted for each cell passage.

In order to attain their better characterization, the gene panel whose expression was later used to monitor Cr(VI)-induced malignant transformation was also applied to BEAS-2B cells. The gene expression profile at different passages of BEAS-2B cells was compared with BEAS-2B #5 cells' profile using the $2^{-\Delta\Delta Ct}$ method. The attained results are depicted in Figure 6.4.

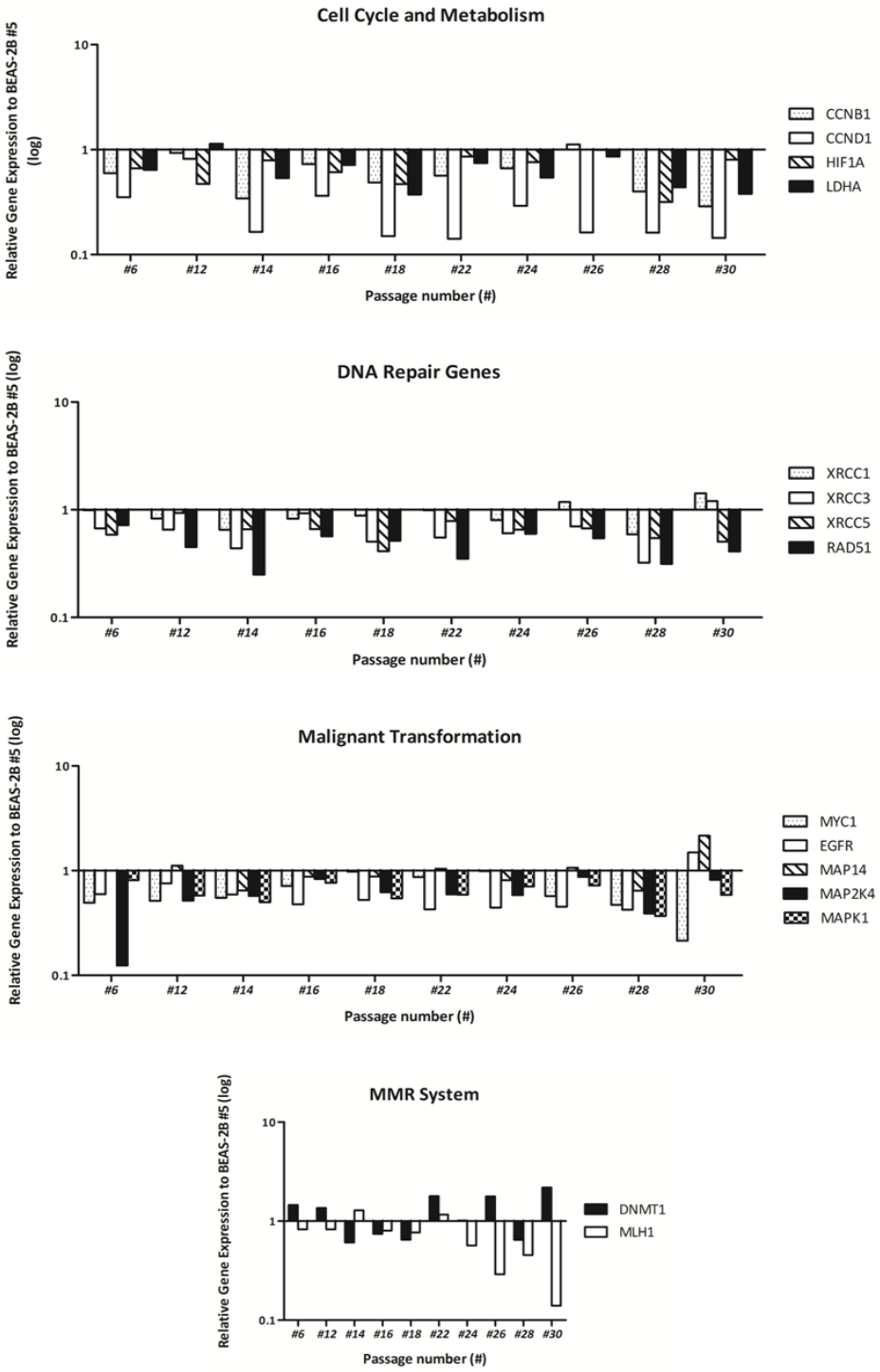

Figure 6.4 - Relative gene expression quantification of BEAS-2B cells' passages to BEAS-2B #5. The majority of the analyzed genes tended to be down-regulated, thus corroborating the non-malignant signature of BEAS-2B cells. MMR system revealed to be functional, even though with no consistent pattern of activation. Bars represent means. Bars represent means (N=1).

Despite some negligible exceptions at isolated passages, the expression of the selected genes was globally downregulated thus confirming the non-malignant nature of BEAS-2B. Moreover, the fluctuations of the expression of *MLH1* gene unveiled a functional MMR System.

6.2.2 Exposure of BEAS-2B to 1.0 µM Cr(VI)

Aiming to malignantly transform BEAS-2B cells by the action of Cr(VI), a concentration of 1.0 µM was endorsed. Our choice was sustained by both epidemiologic studies (Davies, 1984; Langård, 1990) and the observation that this concentration is only slightly cytotoxic (Costa et al., 2010). Control cultures of BEAS-2B cells were kept in parallel to monitor eventual changes occurred in the absence of Cr(VI).

After the first 10 passages in culture, both control and Cr(VI)-treated BEAS-2B cells, seeded at the regular cellular density ($4x10^3$ cells/cm^2), displayed similar morphologies, although the former cultures tended to became increasingly less resistant to trypsinization. Following 12 passages in the presence of Cr(VI), BEAS-2B cultures became non-homogeneous (Figure 6.5, right), with discrete collections of cells displaying a growth pattern and/or distinct morphologic appearance from those of the normal diamond-shaped epithelial cells. As illustrated in Figure 6.5 (left), control cultures retained cells' normal morphology.

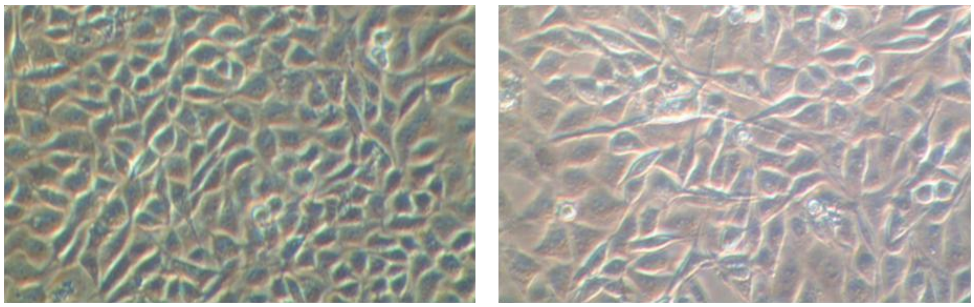

Figure 6.5 - Effect of Cr(VI) on the morphology and growth pattern of BEAS-2B cells. BEAS-2B cells grown in the absence of Cr(VI) (left) displayed an organized growth pattern with cells portraying a diamond-shaped morphology. Cr(VI) (right) induces cellular disorganization and deep morphological changes, with spindle-like shaped cells being particularly abundant. A magnification of 100x was used in both panels.

Nevertheless, besides the morphologic alterations, no additional karyotypic changes where induced by the exposure of BEAS-2B cells to 1.0 µM of Cr(VI) when cells were cultured at the recommended cellular density (Figure 6.6). Moreover, no major alterations were observed in the behavior of these structural chromosomal alterations along the time in culture of Cr(VI)-exposed BEAS-2B (Figure 6.7). Conversely, Cr(VI) did seemed to affect cells' ploidy as Cr(VI)-exposed cells showed an increase in the percentage of hyperdiploid cells in the early passages (#7 and #12) and an increase in the fraction of hypodiploid cells after more prolonged culture (>#25) (Figure 6.8). These results were in agreement with previous similar studies attained using human bronchial fibroblasts exposed to Cr(VI) (Holmes et al., 2006).

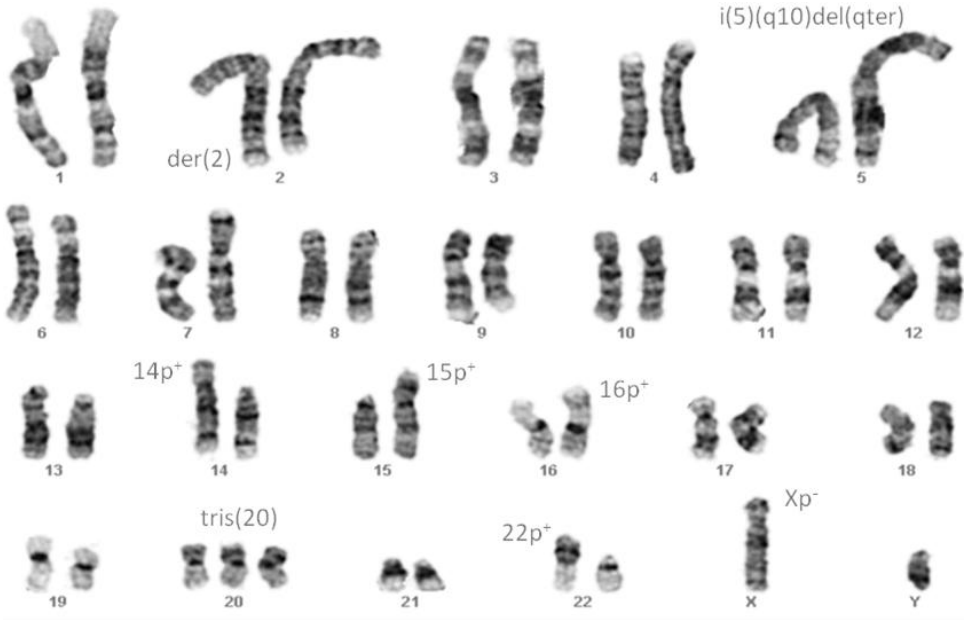

Figure 6.6 - Representative karyotype of Cr(VI)-exposed BEAS-2B cell line at #17. The analysis of the karyotype showed that no additional alterations were induced in BEAS-2B cells by the presence of 1.0 µM Cr(VI), when the cells were cultured at the normal cellular density. At least 20 karyotypes were constructed for each cell passage analyzed.

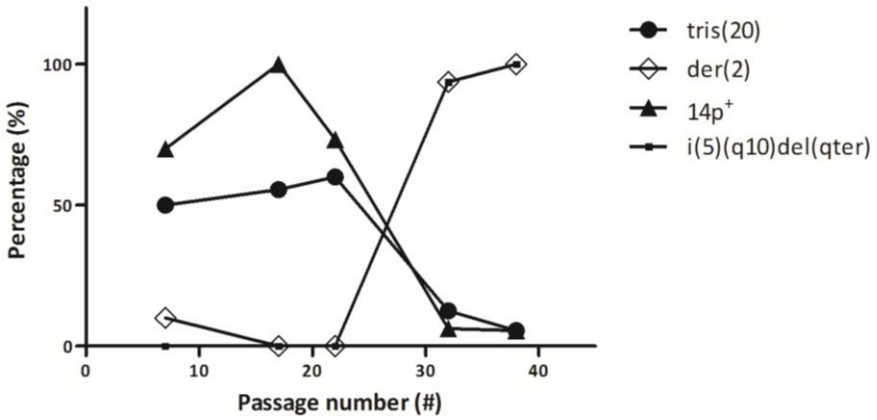

Figure 6.7 - Behaviour of structural chromosomal changes along time in Cr(VI)-exposed BEAS-2B cells. While the population of cells portraying the i(5)(q10)del(qter) and the der(2) tend to be amplified along time, $14p^+$- and tris (20)-carrying cells tend to disappear. The results are expressed in percentage in relation to a normal diploid cell line and were obtained from at least 20 karyotypes constructed per #.

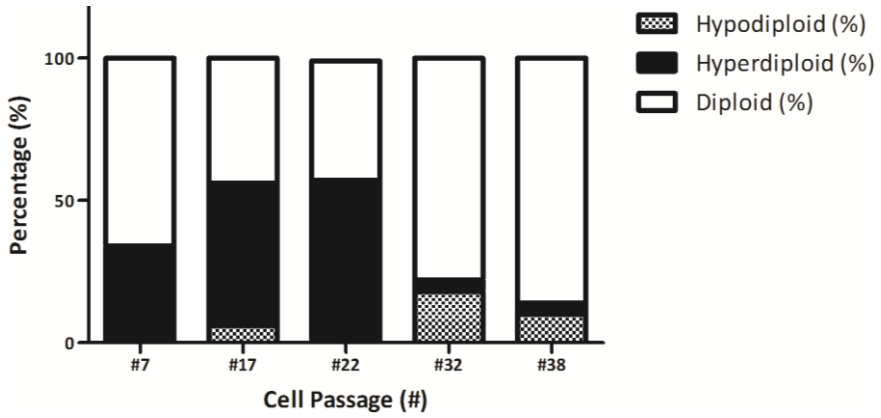

Figure 6.8 - Ploidy analysis of Cr(VI)-exposed BEAS-2B cells over time. The observed increase in hyperdiploid cells during the early passages of BEAS-2B cells resulted from Cr(VI)-induced genetic damage. Also observable was an increase in the percentage of hypodiploid cells in latter passages, what may also be attributed to Cr(VI), as it has been previously observed in human bronchial fibroblasts. For this study at least 50 giemsa-stained metaphase spreads were counted for each cell passage.

Gene expression analysis of the Cr(VI)-exposed cells revealed a pattern that although slightly different from that of control BEAS-2B cells, did not patronize a malignant phenotype (Figure 6.9). Again, an exception should be emphasized, now for the genes involved in the DNA repair systems who were shown to be upregulated, most probably as a consequence of Cr(VI)-mediated genotoxic effects. Taken together these observations further corroborated the failure of the employed strategy to malignantly transform BEAS-2B cells.

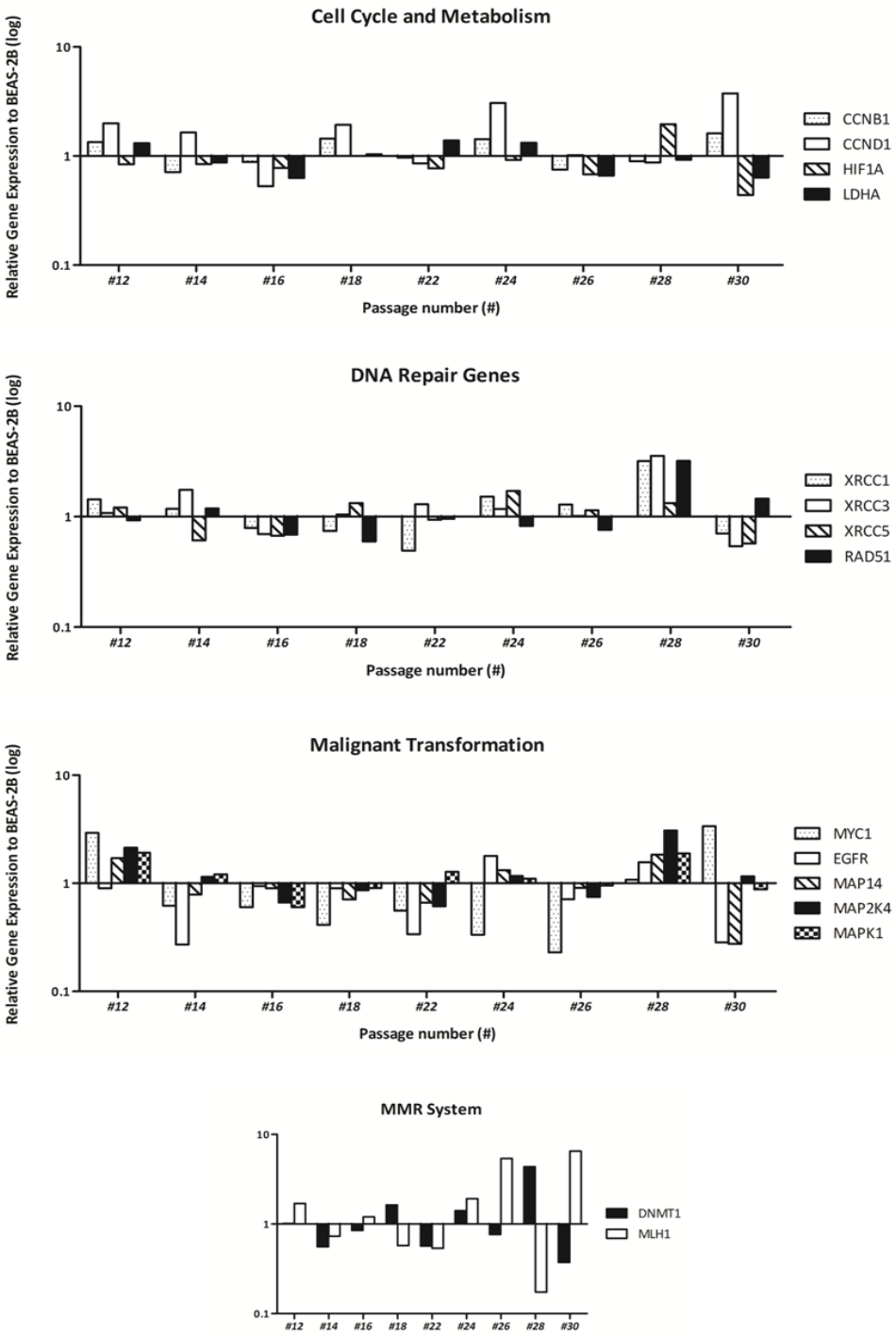

Figure 6.9 - Relative gene expression quantification of Cr(VI)-exposed BEAS-2B cells to BEAS-2B cells at the same passage. Overall there is no consistent pattern of expression among the analyzed genes. Genes associated to malignant transformation tended to be downregulated and the MMR system follows the random tendency of the remaining genes. Bars represent means (N=1).

6.2.3 Low density cultures in the presence of Cr(VI) and establishment of the subclonal cell lines

Once the adopted strategy did not succeed on malignantly transform BEAS-2B cells, alternative approaches were investigated. Following an exhaustive review of the pathophysiology dynamics of Cr(VI)-induced lung tumors, we realized that notwithstanding the fact that the overall concentration of Cr(VI) in the entire lung is very low, that same concentration at bronchial bifurcations is incredibly high. This means that the availability of Cr(VI) oxyanions *per* cell is greatly increased at these sites in comparison with the rest of the lung parenchyma. It was hypothesized that by increasing each cell surface area to Cr(VI) we would be able to increase the availability of Cr(VI) *per* cell, thus better mimicking the reality of Cr(VI)-exposed individuals.

To attain our goal we decided to culture Cr(VI)-exposed BEAS-2B cells at a very low density (13 cells/cm^2), in the presence of 1.0 μM of Cr(VI). As expected, the increased availability of Cr(VI) *per* cell deeply accentuated its effects, as profoundly morphologically altered cells, with an abnormal growth pattern, were visible in many areas of the culture. Several dense clumps containing cells with clearly altered morphologies were also documented (Figure 6.10, right). Conversely, control BEAS-2B cells cultured at the same cellular density showed no changes on their morphology and growth pattern (Figure 6.10, left).

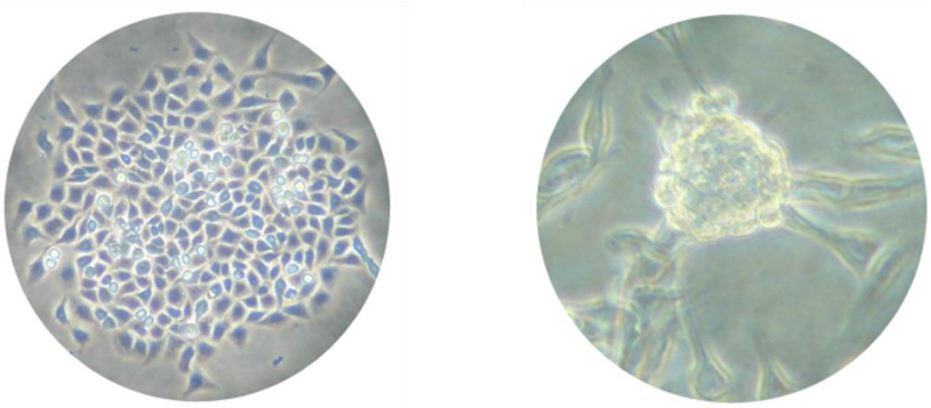

Figure 6.10 - The effects of Cr(VI) on the culture of both control and Cr(VI)-exposed BEAS-2B cells at low cellular density. When cultured at very low density, control BEAS-2B cells (left) formed colonies that retained the appearance of a normal epithelium. In contrast, Cr(VI)-exposed cells (right) tended to form dense cellular aggregates of approximately spherical shape. A magnification of 100x was used in both panels.

The deep contrast observed between the morphology of control and Cr(VI)-exposed colonies revealed that the employed strategy succeeded in transforming BEAS-2B cells.

6.2.4 Characterization of the Cont1 and RenG2 subclonal systems

To verify our hypothesis, three dense clumps from low density cultured Cr(VI)-exposed BEAS-2B cells, as well as 3 BEAS-2B control colonies were ring-cloned. Following isolation, Cr(VI)-treated cells were expanded and the resulting cell lines named RenG1, RenG2 and CrossG1. Similarly, the isolated control colonies were given the names Cont1, Cont2 and Cont3.

Initial characterization studies based on morphologic and karyotypic analysis of the expanded colonies revealed that, even though isolated from different foci, the RenG1, RenG2 and CrossG1 systems portrayed very simi-

lar features. Likewise, Cont1, Cont2 and Cont3 were equivalent. These observations lead us to randomly choose the RenG2 and Cont1 cell lines to continue our studies.

The cytogenetic analysis of the Cont1 cell line revealed a karyotype rather similar to that of the BEAS-2B cells. In fact, the same karyotypic alterations could be found in the subclonal systems, excepting the tris(20). RenG2 cells, on contrary, showed a marked karyotypic alteration (Figure 6.11) with cells carrying circa 82 chromosomes, the majority in tetrasomy.

Figure 6.11 - Representative karyotype of RenG2 cells at #4. Most of the chromosomes showed four copies. The alterations observed in the parental cell line, e.g., the i(5)(q1.0)del(qter), allowed to hypothesize that an intermediate tetraploid may have been generated during the malignization of Cr(VI)-exposed BEAS-2B cells. At least 20 karyotypes were constructed for each # analyzed.

As to the gene expression profile, it revealed that Cont1 cells' expression pattern overlapped with that of BEAS-2B cells. In contrast, RenG2

cells presented almost all the analyzed genes overexpressed in comparison to Cont1 cells (Figure 6.12).

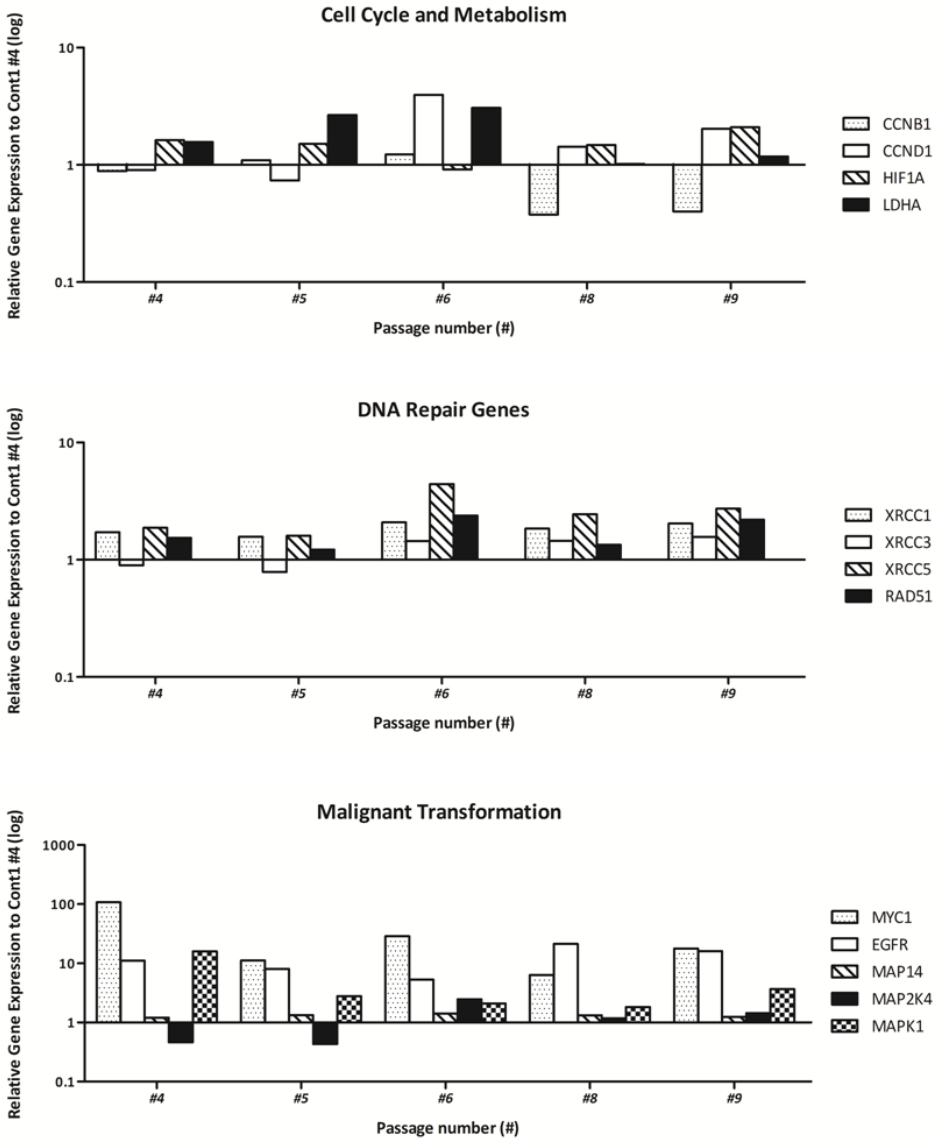

Figure 6.12 - Relative gene expression quantification of RenG2 cells to Cont1 #4. The gene expression profile of RenG2 cells corroborated the karyotype analysis, thus supporting a malignant nature for this cell line. Regardless minor exceptions, all genes grouped as malignant transformation-related genes were overexpressed. DNA repair genes were constitutively upregulated probably as a result of both Cr(VI) presence and GI. Bars represent means (N=1).

The evident overexpression of the *MYC* gene along with the karyotypic drift observed in RenG2 cells strongly suggested the success of the implemented strategy on malignantly transforming BEAS-2B cells. Moreover, the overall activation of the MAP kinases' pathways suggested their recruitment during the transformation process, corroborating the findings of Chuang and Yang (Chuang and Yang, 2001). Finally, *EGFR* activation also seemed to have played a pivotal role in the malignization process, further substantiating the observations of Lonardo and colleagues (Lonardo et al., 1999).

6.2.5 MMR activation status and MSI Analysis of RenG2 cells

As previously mentioned, Cr(VI) may lead to MMR system inactivation, consequently driving MSI development in chromate tumors (Takahashi et al., 2005). To assess whether Cr(VI)-driven BEAS-2B cells' malignant transformation involved MSI formation pentaplex PCR analysis of the MSI-associated repeats was carried out in RenG2 cells.

Figure 6.13 depicts the chromatograms attained from the MSI screening of RenG2 cells. As only the NR-24 repeat showed a significant shift banding from the control, according to the established criteria, no MSI was present in the RenG2 system.

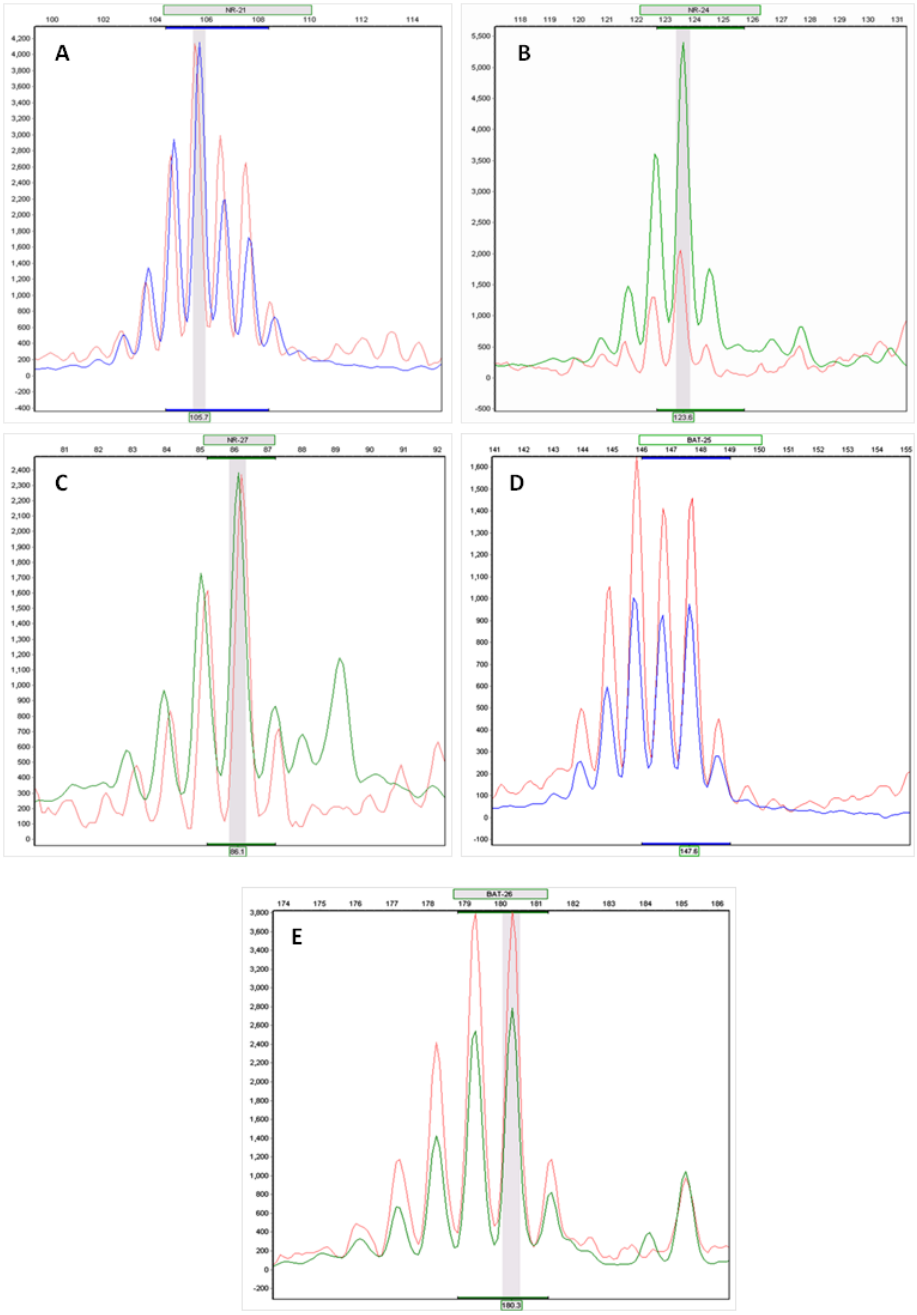

Figure 6.13 - MSI analysis of RenG2 cell line. The chromatograms showed a comparison between BEAS-2B control cell lines (red) and RenG2 cells (green or blue). Only for the NR-24 repeat a significant drift was observed relative to BEAS-2B cells, meaning that no MSI was present in the genome of RenG2 cells. Red line represent the control and Green/Blue lines represent the samples.

In agreement with a fully functional MMR system, RT-qPCR analysis of *MLH1* in RenG2 cells revealed its upregulation in comparison to BEAS-2B cells (Figure 6.14). However, because the action of demethylase 1 may also drive MMR inactivation through epigenetic silencing of MMR-related genes, the expression level of *DNMT1* was simultaneously assessed (Figure 6.14).

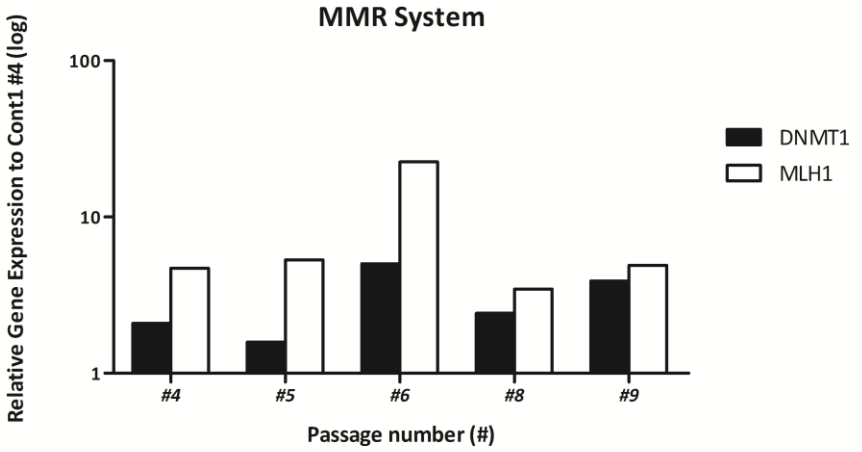

Figure 6.14 - Relative gene expression analysis of *DNMT1* and *MLH1* genes. In agreement with the absence of MSI, both *MLH1* and *DNMT1* proteins were being actively transcribed in RenG2 cells, indicating an active MMR system. Bars represent means (N=1).

Taken together, our results showed that in spite of the slight *DNMT1* overexpression, *MLH1* was not silenced and thus no MSI was developed in RenG2 cells.

6.2.6 Tumorigenic potential of RenG2 cells

In vivo tumorigenicity assays are the gold standard for the evaluation of cells' tumorigenic potential. Therefore, BALB/c-nu/nu mice were used to confirm RenG2 cells' malignant potential.

None of the three male mice subcutaneously injected in the lumbar region with control BEAS-2B cells developed tumors, thus highlighting the non-tumorigenic nature of these cells and further confirming Reddel's observations (Reddel et al., 1988). RenG2 cells, however, succeeded at inducing tumors in three out of the four injected mice.

Histopathological analysis of the tumors revealed negative staining for LCA and HMB45, and positive staining for MNF116 (Figure 6.15). The positivity of MNF116, an epithelial pan-cytokeratin marker, along with the slight and ubiquous expression of the mesenchymal marker vimentin, reveals the epithelial nature of the attained tumors.

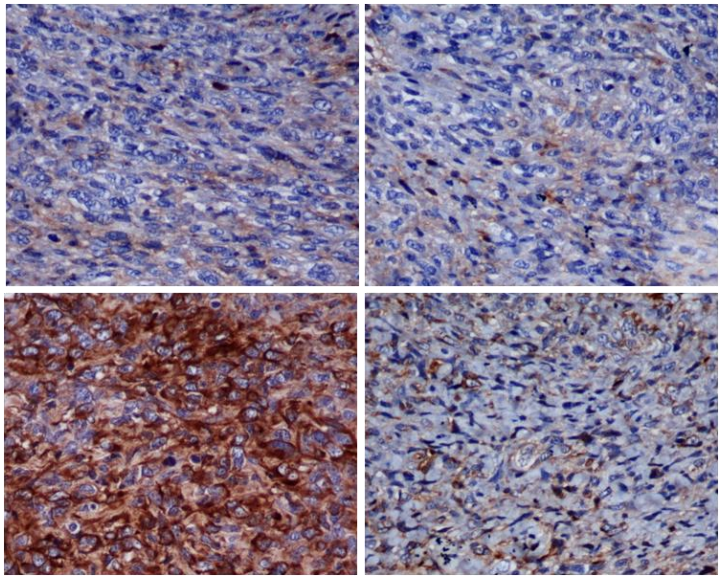

Figure 6.15 - Histopathological analysis of the RenG2-induced tumors. The positivity of MNF116 (bottom left), the slight ubiquous

positivity of vimentin (bottom right) and the negativity of both LCA (top left) and HMB45 (top right) identified the epithelial nature of the RenG2 induced tumors. A magnification of 400x was used in all panels.

6.3 Discussion

Most frequently the studies on carcinogenesis begin with the selection of a malignant cellular system, whose intricacies are then exhaustively dissected while searching for the pathways underlying its sustained malignant potential. Eventually, therapeutic strategies are designed and tested, and the recovery of the system is attempted. Despite the fact that much of what is actually known on tumor biology was attained by the employment of similar strategies, potentially precious information may actually be lost when the malignization process is bypassed.

Due to the lack of an adequate system, and to prevent losing any important clue, it was decided to initiate the studies by transforming a non-malignant immortalized human bronchial epithelial cell line. Moreover, primary cultures were not compatible with the intended prolonged exposures to sub-lethal concentrations of Cr(VI) as they have short lifespans. BEAS-2B cells were chosen as they represented the commercially available system that better mimic normal human lung epithelium. However, regardless of all the advantages BEAS-2B cells may have, attention should be given to the fact that they were obtained following a SV40-based immortalization protocol whose success relays on the sequestration of the P53 protein, the so-called guardian of the genome. The involvement of P53 in human cancers is amply accepted, so it could be thought that the immortalization by SV40 might *per si* drive the malignant transformation of BEAS-2B cells. Yet, this and other studies revealed that P53 sequestration alone is not sufficient for the neoplastic transformation of BEAS-2B cells, as non-treated BEAS-2B cells were neither malignant nor tumorigenic (Reddel et al., 1988).

As the induction of aneuploidy and the morphological transformation observed in this study parallels the results obtained with other human and rodent SV40-immortalized cells (Li et al., 1997; Zhu and Gooderham, 2002), and with a SV40-transgenic mouse model (Ornitz et al., 1987), following exposure to chemical carcinogens, we cannot exclude that P53 deficiency may had pre-disposed RenG2 Cr(VI)-damaged cells to aneuploidy. In fact, loss of P53, either by gene disruption or small interfering RNA-mediated depletion, is known to sensitize cells to aurora kinase B (AURKB) inhibition, promoting mitotic slippage (Marxer et al., 2013). Additionally, as the P53-dependent post-mitotic checkpoint is also important for preventing genome reduplication after mitotic slippage (Marxer et al., 2013), cells with DNA damage may have continued to divide, being subjected to asymmetric chromosome segregation. Aneuploid genomes similar to that of RenG2 cells have been found in a wide range of tumor cells and their development was hypothesized to underline malignant transformation (reviewed by Potapova et al., 2013).

Even though the mutagenic effect of carcinogens is generally accepted as the driving force of malignant transformation, changes in ploidy and the consequent imbalance in gene expression also seem to play an important role (Nguyen and Ravid, 2006). The group of David Pellman has been successfully dissecting the theory of a tetraploid intermediate during the route for malignancy (Ganem et al., 2007). Based on Shi and King, who observed that cell lines with relatively high spontaneous rates of chromosome non-disjunction in late mitosis tend to give rise to tetraploid cells, Pellman's laboratory further discovered that these tetraploid cells may be the source of the full malignant aneuploid tumor cells (Shi and King, 2005). They realized that problems during cell division, for instance induced by a carcinogenic agent, may result in karyo- and/or cytokinesis abrogation. Consequently, if the cells had already duplicated their DNA content, tetraploid cells would be formed. These cells were shown to have increased resistance to the microenvironment stresses (Castedo et al., 2006) and, most frequently, to be provided with an additional set of centrosomes (Ganem et al., 2007). The presence of

twice the number of centrosomes may be responsible, in a subsequent cellular division, for the development of a catastrophic mitosis resultant from a multipolar spindle establishment (Ganem et al., 2007). Cells that successfully escape these mitotic catastrophes may enter in asymmetrical cell division, thus driving the formation of an aneuploid progeny vested with high malignant potential (Ganem et al., 2007, 2009; Godinho et al., 2009).

Considering the abovementioned observations it became clear that cancer development may not necessarily require mutations in cancer related genes, but an imbalance in the dosage of thousands of normal genes, caused by random aneuploidization and consequent GI development (Duesberg and Li, 2003; Nguyen and Ravid, 2006). In other words, such observations state that cells may become transformed in the absence of mutations on tumor suppressor genes and/or oncogenes.

Wise's laboratory have long been working on a link between Cr(VI)-exposure and aneuploidy development. Using a clonal cell line derived from normal human bronchial fibroblasts exposed to different concentrations of lead chromate, Holmes and colleagues showed for the first time that particulate chromate induces aneuploidy (Holmes et al., 2006). Moreover, authors also showed that the aneuploid cells resulted from multipolar mitosis established following centrosome amplification (Holmes et al., 2006). It thus seemed reasonable that the karyotypic drift observed in RenG2 cells, that showed many chromosomes in tetrasomy, may have resulted from an abrogated cell division that lead to the formation of tetraploid cells harboring extra centrosomes. The subsequent division of these tetraploids may then have occurred through a multipolar mitosis favoring the formation of the aneuploid malignant RenG2 cells (Figure 6.16). Additional studies should be done to further confirm this hypothesis.

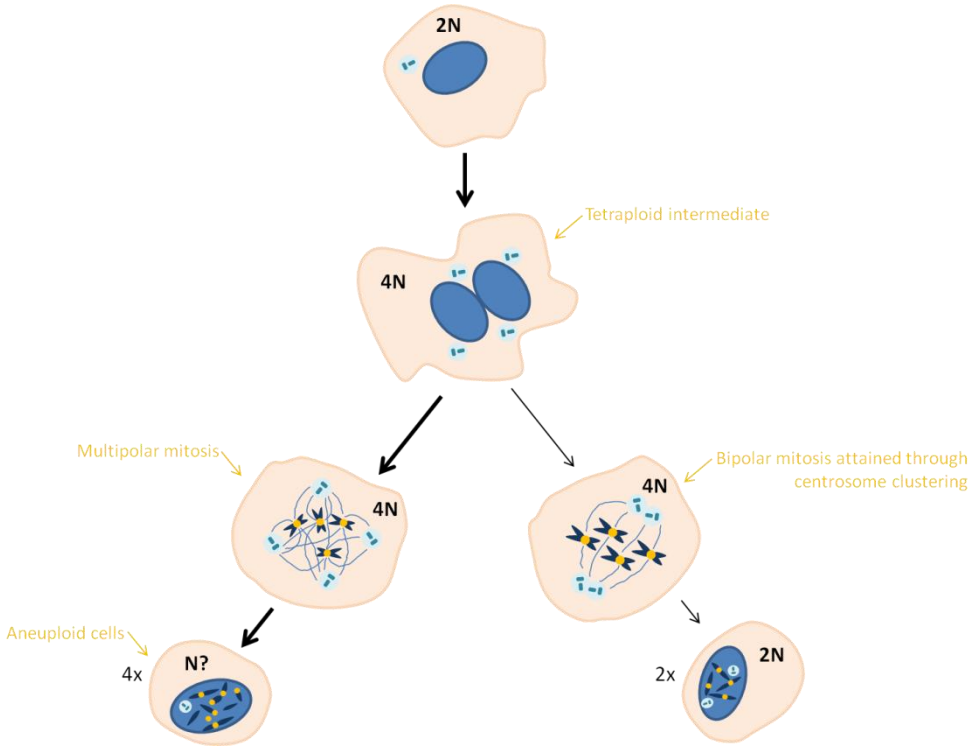

Figure 6.16 - Proposed model for the development of RenG2's aneuploid genome. Following culture at very low density in the presence of Cr(VI), BEAS-2B may have abrogated their cellular division ending up forming tetraploid cells. The development of a tetraploid genome eventually boosted cells' survival under Cr(VI)-sustained adverse conditions, but when these cells attempted to divide, multipolar mitoses may have occurred as a consequence of the increased number of centrosomes. The cells that survived aberrant mitosis portrayed an aneuploid genome and the morphological features of malignant cells. These cells were named RenG2 cells.

However, the malignant transformation of BEAS-2B cells following low density culture and prolonged exposure to Cr(VI) cannot be ascribed solely to Cr(VI) effects on chromosome segregation and GI. In fact, the upregulation of the genes associated to the most important DNA repair systems (BER, HR and NHEJ) observed in the RenG2 system indicated that DNA damage played an important role in the overall process of transformation. Contradicting the assertion that GI only develops in cells whose DNA repair pathways are seriously compromised (Grlickova-Duzevik et al., 2006; Stackpole et al., 2007; Vilcheck et al., 2002), our

hypothesis was further reinforced by other unpublished observations showing that BEAS-2B cells exposed for only five passages to Cr(VI) preserved a normal phenotype, even when cultured at very low cell density. Moreover, the fact that chronic exposure of BEAS-2B cells to Cr(VI) increased their duplication time most probably reflects the action of DNA repair systems in attempting to repair Cr(VI)-induced DNA damage (Costa et al., 2010).

Studies on diverse human cellular systems showed that MMR is fundamental on mediating cellular responses to Cr(VI), and that chronic exposures to toxic doses of the oxyanion may result in the selective outgrowth of MMR-deficient cells (Peterson-Roth et al., 2005; Reynolds and Zhitkovich, 2007; Reynolds et al., 2007, 2009; Zecevic et al., 2009). Moreover, this deficiency has been associated with high spontaneous mutagenesis rates, as well as with a high incidence of MSI among chromate cancers (Hirose et al., 2002; Kondo et al., 2006; Takahashi et al., 2005), which lead to the hypothesis that chromate cancer cells express the mutator phenotype, *i.e.*, a tendency to undergo a cascade of further mutations caused by the loss of the MMR system (Loeb et al., 2008; Salnikow and Zhitkovich, 2008). Our findings, however, did not sustain this hypothesis, as the malignant RenG2 system expressed high levels of the *MLH1* transcript and did not exhibit MSI. Nevertheless, our observations were in agreement with previous ones indicating that reduced DNMT1 activity correlated with increased MSI development (Kim et al., 2004), which seemed to happen due to loss of efficiency of the MMR system (Loughery et al., 2011). Moreover, increased *DNMT1* transcript levels were previously reported to correlate with increased MYC mRNA levels in gastric cancers (Fang et al., 2004), as well as with transformation of NIH 3T3 cells (Wu et al., 1993).

The absence of neoplastic transformation of BEAS-2B cells after prolonged exposure to Cr(VI) at normal cell density indicates that low density culture provided the adequate conditions for the selection of transformation-susceptible Cr(VI) variants. We believe that those conditions relay on the physiology of cellular Cr(VI)

uptake. Previous studies showed that this uptake represents a very fast and efficient process that reaches a maximum load within the first 3 h of exposure (Xie et al., 2004). Besides, it seems to be limited by the ratio Cr(VI)/cell (Xie et al., 2004). By increasing this ratio, the low density conditions influenced the rate of Cr(VI) uptake, and consequently, imposed a stronger environmental pressure on BEAS-2B cells being cultured at unfavorable low densities. As a natural Darwinian response, only the cells with the most resistant cellular phenotypes survived the adverse conditions. Similarly to the acquisition of drug resistance, the selection process may has encompassed multi-stages and resulted in GI development, which then provided a supply of mutants for another round of natural selection (Blagosklonny, 2002). This theory is in agreement with the actual thinking according to which mutations themselves are irrelevant if there is not a microenvironment change that selects the cells carrying such mutations (Barcellos-Hoff et al., 2013).

6.4 Conclusion

Similarly to chronic contact to cigarette smoke, prolonged exposure to Cr(VI) induces sustained DNA damage and growth inhibition, thus driving the malignant transformation of the bronchial epithelium. These direct effects of the oxyanion over cells' DNA set the conditions for the selection of cytotoxicity-resistant altered cells. It seems that the development of Cr(VI) resistance, more than the mutagenic potential of Cr(VI), paved the way for the accumulation of mutations through the selection of the most resistant variants. It is thus possible that this process of selection may drive the onset of chromate lung tumors through the activation of the resistance phenotype pathway.

Note

The results presented in this chapter are already published as an original paper:

Rodrigues CFD, Urbano AM, Matoso E, Carreira IM, Almeida A, Santos P, Botelho MF, Carvalho L, Alves M, Monteiro C, Costa A, Moreno V and Alpoim MC. Cr(VI)-induced malignant transformation of a human bronchial epithelial cell line. Mutat. Res 670(1-2):42-52.

Chapter 7

Derivation and Characterization of RenG2 cells

1.1. Introduction

Cancer is typically characterized by series of progressive alterations that disrupt cell and tissue homeostasis. Though, whereas many of those alterations can be induced by gene-specific mutations, faulty signals from the microenvironment are now assumed to act as inducers of tumor development and progression (Hanahan and Coussens, 2012).

As presented in Chapter 3, it is now generally accepted that a tumor is a heterogeneous entity composed of a wide range of cell populations in different stages of differentiation. One such population is comprised of CSCs, and recent findings indicated them as the only tumor fraction able to self-renew and produce phenotypically diverse populations (Marjanovic et al., 2013). The biology of CSCs has been exhaustively dissected during the last decades. It is now accepted that CSCs have a slower cell cycle and an asymmetric pattern of cellular division. These two characteristics, besides being very simple, are actually responsible for most of the malignant potential of this tumor population. Asymmetric division allows CSCs to keep providing the tumor with progenitor cells it may need, while keeping the pool of CSCs. On the other hand, the slower cell cycle protects these cells of DNA damage and increases their resistance to chemothera-

py. In fact, conventional chemo- and radiotherapy programs are designed to target proliferating cells, thus requiring active cycling to induce cellular apoptosis (Moore and Lyle, 2011). The origins of CSCs are still debatable, and it now seems that they may form from different sources. The most recently described strategy for CSCs formation was presented by Chaffer and colleagues, who provided the first experimental facts attesting that CSCs may arise by dedifferentiation of differentiated tumor cells. Besides authors popped the hypothesis that the formation of CSCs by dedifferentiation may involve EMT programs, this hypothesis has not, to the best of our knowledge, yet been assessed.

The main purpose of this study was to increase the malignant potential of the RenG2 system in order to exacerbate Cr(VI)-induced features as well as to fully characterized the attained systems. Finally, we want to scrutinize the involvement of CSCs on Cr(VI)-driven BEAS-2B cells' malignization.

7.1 Results

7.1.1 Increasing the malignant potential of the RenG2 cell line: the attainment of DRenG2 and DDRenG2 cellular systems

The *in vivo* studies performed to unveil the tumorigenic potential of RenG2 cell line showed that although the system was malignant, its potential was still very low, as it took circa two months for tumors to form.

To increase the malignant potential of RenG2 cells and thus exacerbate Cr(VI)-imprinted features, we decided to *in vivo* derive the RenG2 cell line as described in section 5.8 of Chapter 5. DRenG2 cells, the cells attained from the RenG2-induced tumor, turned out to be significantly more malignant than RenG2 cells as a tumor was already visible 30 days after injection. Tumors' resection was made when they reached a diameter of approximately 1 cm. Following resection, tumor was split and half of it was

sent to histopathological analysis, while the remaining specimen was used to establish the DDRenG2 system.

To prove that DDRenG2 cells were indeed more malignant than the DRenG2 system, the same number of cells from both cell lines was simultaneously injected into the subcutaneous compartment of two mice and allowed to grow. After 30 days both mice harbored tumors, even though the volume of the tumor induced by DDRenG2 cells was twice of that induced by DRenG2 (Figure 7.1).

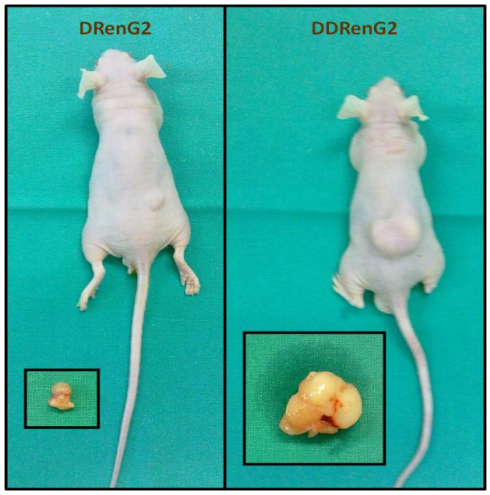

Figure 7.1 - Different tumorigenic potential of the derivative cellular systems. The size of the tumor induced by the same number of cells of the DDRenG2 system clearly depicts its higher malignant potential when compared to DRenG2 cells.

The time needed for tumor development was thus progressively lower as systems' malignancy increased, confirming their different tumorigenic potential.

7.1.2 Karyotypic study of the derivative systems

Similarly to what was done for the non-malignant and the RenG2 systems, the karyotype of both DRenG2 and DDRenG2 were also assessed. Not surprisingly, additional chromosomal alterations were observed, thus supporting the observations that GI accompanies malignant transformation (Potapova et al., 2013) and most importantly, Cr(VI)-induced transformation (Wise and Wise, 2012).

The alterations found in DRenG2 cells sum those already present in RenG2 cells. Moreover, besides the loss of the Y chromosome, which was found in all the analyzed cells, the other alterations were present as mosaics. From the 20 constructed karyotypes 60 % of them showed an isochromosome 9q with extra material at the terminal part of the chromosome [i(9)(q+)], 40 % showed a deletion of the terminal part of the short arm of chromosome 7 ($7p^-$), 20 % presented a similar alteration on the long arm of chromosome 7 ($7q^-$) and finally, 30 % had a chromosome 6 with additional material attached to its short arm ($6p^+$).

As to DDRenG2 cellular system, the observed alterations again sum to those found in the previous systems, exception made for $7q^-$. Moreover, the prevalence of $7p^-$ increased slightly to 27 %, the same percentage at which the chromosome 17 can be found with additional material on its short arm ($17p^+$). Finally, a translocation between chromosomes 7 and 14 [t(7;14)] was found in 40 % of the analyzed cells, while a derivative chromosome 12 [der(12)] only appeared in 20 %. Representative karyotypes of both cell lines are shown in Figure 7.2.

Figure 7.2 - Representative karyotypes of the DRenG2 and DDRenG2 derivative systems at #33. Karyotypes illustrated the new structural alterations present on DRenG2 (upper) cells, namely the i(9)(q^+) and the $7p^-$, and which were passed along to DDRenG2 cells (down). Moreover, they allowed the identification of $6p^+$ and $7q^-$ structural alterations as exclusive from DRenG2 cells and of $17p^+$, t(7;14) and der(12) as exclusive from the DDRenG2 system. At least 20 karyotypes were constructed for each cell passage analysed.

Independently of the alterations found, the chromosome number of both cell lines changed in comparison to RenG2 cells, as both carry 76 chromosomes. The number of chromosomes did not varied significantly among the analyzed cells.

7.1.3 Metabolic Studies using ^{18}FDG Uptake

Metabolic studies were performed in the five cell lines in order to highlight any differences that Cr(VI)-induced malignant transformation may have imprinted in the cells (Figure 7.3).

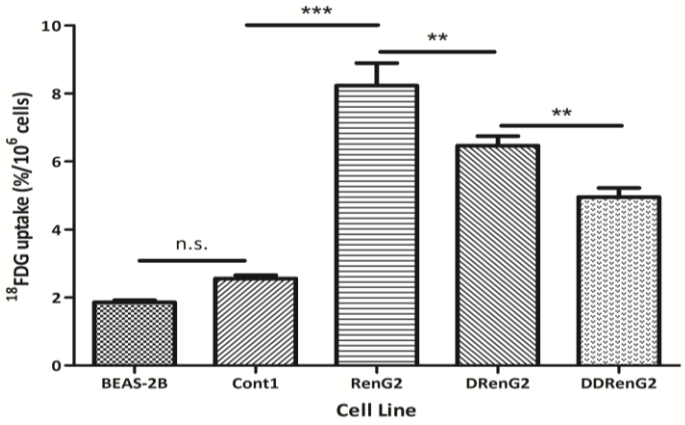

Figure 7.3 - ^{18}FDG uptake by malignant and non-malignant cellular systems. Malignant cells showed a considerably higher glucose uptake than non-malignant cells. Unexpectedly, however, as malignancy increased the glucose uptake decreased. Bars represent means ± SEM. Differences between the cell lines' means were evaluated by one-way ANOVA followed by a Bonferroni post test. n.s., no significant; *, $P \leq 0.05$; **, $P \leq 0.01$; ***, $P \leq 0.001$.

The malignant cells under study (RenG2, DRenG2 and DDRenG2) showed a much higher glucose uptake than their non-malignant common

progenitor, BEAS-2B, and the RenG2 non-malignant control, Cont1. This observation is believed to mirror their increased energetic demands, which is a common feature of malignant cells (Martins-Neves et al., 2012; Ren et al., 2013). In fact, the increased dependency of tumor cells upon glucose, even under high oxygen tensions, is known as the Warburg Effect and was recently considered an hallmark of cancer cells (Hanahan and Weinberg, 2011).

Surprisingly, however, was the progressive decrease of glucose consumption observed along the malignant systems (Figure 7.3). As a matter of fact, the DDRenG2 cell line showed a glucose uptake that, besides being considerably greater than that of BEAS-2B and Cont1 cells, was almost half of the uptake registered for RenG2 malignant cells. The glucose uptake of DRenG2 cells was situated between that of RenG2 and DDRenG2.

7.1.4 Doubling Times (DTs)

The DT calculation for all cell lines constituted a requirement to better understand the glucose-uptake results. Figure 7.4 illustrates each cell DT and highlights significant differences.

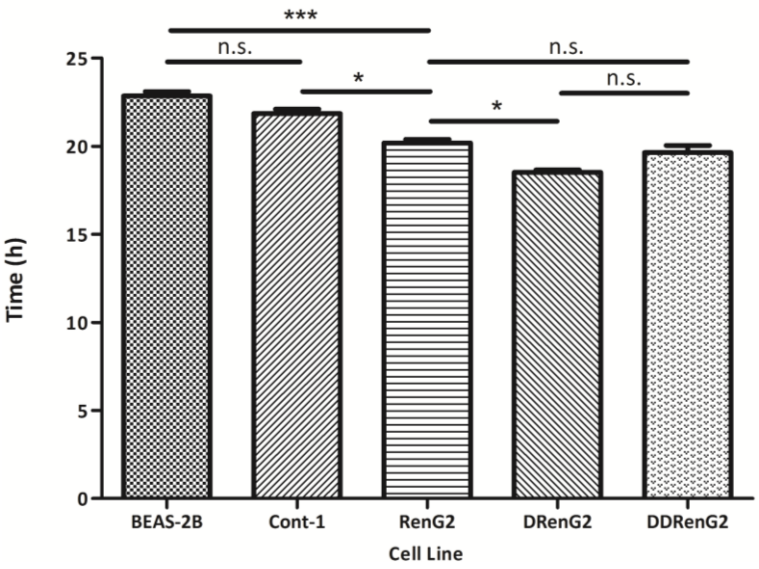

Figure 7.4 - Cellular duplication times. Malignant cells replicated significantly faster than their non-malignant progenitors. RenG2 DT was significantly different from that of DRenG2 cells, while no significance was observed when comparing DDRenG2 to its malignant counterparts. Data represent means ± SE. Differences between the means were evaluated by one-way ANOVA followed by a Bonferroni post test. n.s., no significant; *,$P \leq 0.05$; **, $P \leq 0.01$; ***, $P \leq 0.001$.

BEAS-2B cells showed a DT of approximately 23 h, which is in agreement with the observations of Costa and colleagues (Costa et al., 2010). Moreover, Cont1 cells showed no statistically significant differences in their DTs when compared to BEAS-2B cells' DT, thus corroborating their non-malignant nature. Malignant cell lines, however, were shown to replicate faster than non-malignant systems, particularly DRenG2 cells which showed a DT of roughly 18.5 h. No statistically significant differences were observed between DDRenG2 and either RenG2 or DRenG2 cells.

7.1.5 Clonogenic Ability of the Different Cellular Systems

To establish the portrait of cells' malignant signature, clonogenic assays were performed and the attained results are depicted at Table II.

Table II - Plating efficiency (PE) of the different cellular systems.

	BEAS-2B	Cont1	RenG2	DRenG2	DDRenG2
PE	0.37 ± 0.09	0.51 ± 0.17	3.41 ± 0.17***	3.78 ± 0.29***	3.87 ± 0.05***

Data are presented as mean ± SEM and one-way ANOVA followed by a Dunnett post test were used to identify differences between the cell lines. *,$P \leq 0.05$; **, $P \leq 0.01$; ***, $P \leq 0.001$.

The PE results from both BEAS-2B and Cont1 cell lines revealed little capacity to survive low density growth, further supporting their non-malignant nature. Conversely, BEAS-2B malignant progeny revealed single-cell independent growth ability, since all malignant cell lines were able to form colonies. Furthermore, the attained colonies, alike the ones from which RenG2 cells were isolated, displayed altered morphologies and a disordered growth pattern, thus corroborating the cells' malignant phenotype.

7.1.6 Migration Assay

A major characteristic of highly malignant cells is their enhanced migratory phenotype. In order to evaluate whether the derivative systems portrayed more pronounced migration ability than RenG2 and the non-malignant BEAS-2B and Cont1 cell lines, scratch assays were performed. Figure 7.5 combines several of the best photographs attained at key time points.

Figure 7.5 – Migration ability of the different cellular systems. Both BEAS-2B and Cont1 failed to close the scratch, even after 200 h. In the RenG2 dish, the wound was only grossly closed, while in both DRenG2 and DDRenG2 systems the scratch was clearly closed after 82 h. A magnification of 100x was used in all panels.

In agreement with their non-malignant phenotype, both BEAS-2B and Cont1 cell lines failed to close the wound after 200 h of the beginning of the assay, even though they displayed some residual migration ability. Comparatively, RenG2 cells displayed higher migration capacity even though by the end of the assay the wound closure was incomplete and gaps could still be observed. In contrast, the more malignant derivative systems closed the wound very fast. In fact, the wound made in the DRenG2 cells' monolayer was clearly closed 82 h after the beginning of the assay, while at 73 h timepoint the wound in DDRenG2 cells' monolayer was already closed.

7.1.7 Immunocytochemistry

The expression of α-SMA and Vimentin is widely used to monitor EMT. In fact, as reviewed by Kalluri and Weinberg, the lost of epithelial features towards a mesenchymal phenotype triggers the expression of α-SMA and increases that of Vimentin (Kalluri and Weinberg, 2009). To assess whether the more malignant cell lines portrayed a mesenchymal phenotype, immunocytochemistry analysis was performed using the abovementioned markers, and the results are illustrated in Figure 7.6.

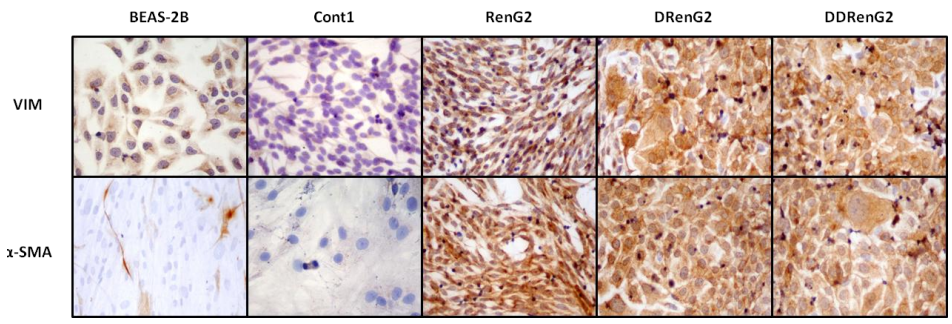

Figure 7.6 - Immunocytochemistry study of Vimentin and α-SMA. Both BEAS-2B and Cont1 non-malignant systems displayed a basal staining for

Vimentin. Conversely, α-SMA staining was negative in these cell lines. All the malignant systems, however, presented a strong staining for both Vimentin and α-SMA. A magnification of 400x was used in all panels. VIM, Vimentin.

Basal levels of Vimentin staining were found in BEAS-2B and Cont1 cells while BEAS-2B malignant progeny revealed an increased expression of this protein. As to α-SMA, not surprisingly this protein was only expressed in the malignant cell lines. Altogether, these results corroborated the observations of Weinberg's laboratory (Kalluri and Weinberg, 2009).

7.1.8 Therapy Resistance Studies

A widely accepted feature of cancer cells is that they are more resistant to conventional therapeutic drugs than normal cells. As a consequence, drug resistance assays are often performed to sustain cells' malignancy.

Applying a similar reasoning, drug resistance studies were performed in both the non-malignant and malignant cell lines under study. We selected three drugs that were normally used in the treatment of lung carcinomas, methotrexate (MTX), cisplatin (Cis) and gemcitabine (Gem). Following exposure of our cell lines to tree different concentrations of the drug, the cellular viability was measured by the MMT assay. Obtained results are shown in Figure 7.7.

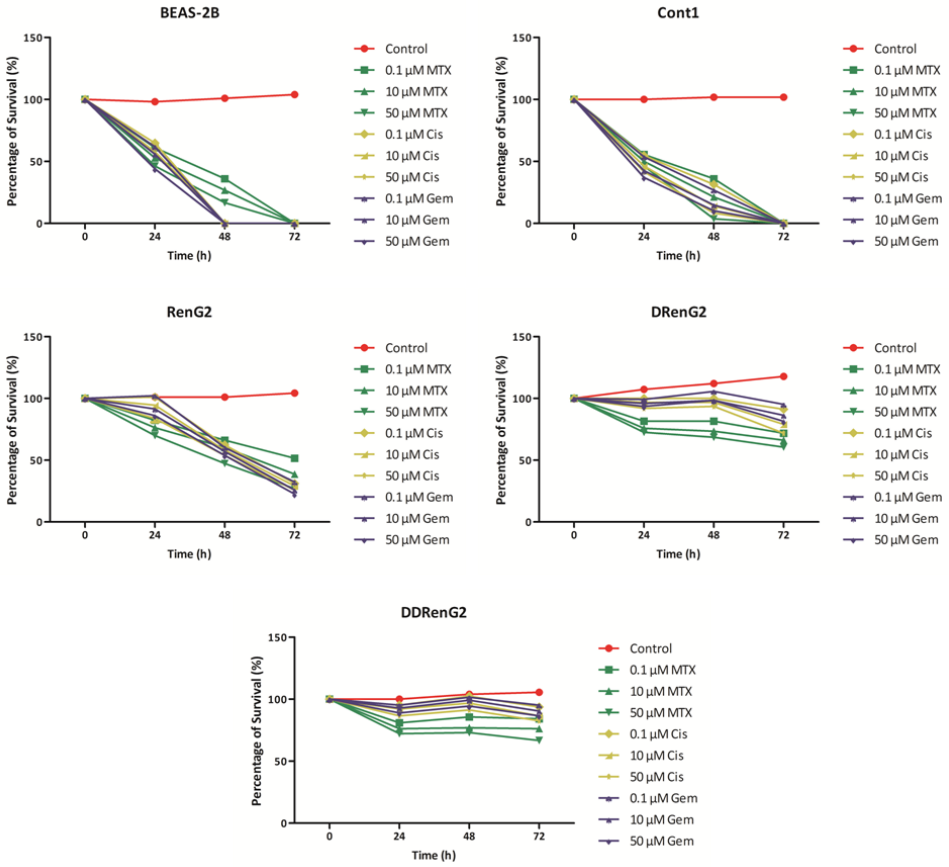

Figure 7.7 - Cell survival following drug treatment. The higher the degree of malignancy, the higher the resistance to the different drugs at all tested concentrations Derivative cell lines, in particular, were shown to be more sensitive to methotrexate than their non-malignant progenitor cells. Data represents mean ± SEM. When not visible error bars are smaller than the symbols. MTX, methotrexate; Cis, cisplatin; Gem, Gemcitabine.

The non-malignant BEAS-2B and Cont1 cell lines were shown to be very sensitive to the complete range of concentrations and drugs tested. However, Cont1 cells showed a more robust phenotype, as it took 72 h for both Cis and Gem drugs to eradicate these cells. Regarding BEAS-2B cells, results indicated that they were more resistant to MTX than to the other drugs under test.

Regarding BEAS-2B malignant progeny, none of the therapeutic regimens succeeded in completely eradicating them. Moreover, the higher the

malignancy of the system, the higher was the resistance to drugs. In fact, RenG2 cells showed a considerably lower resistance to the therapeutic regimens than the derivative systems, further supporting the hypothesis that RenG2 cells were only mildly malignant. In contrast, both the derivative systems distinctively succeed in surviving the entire repertoire of adopted therapeutic strategies, particularly DDRenG2 which was clearly more resistant than DRenG2. This observation further supported the premise that DDRenG2 cells were the more malignant cells under study. Finally, the results indicated that best therapeutic effectiveness was attained using MTX, while Gem and Cis showed less effectiveness and similar behavior.

7.1.9 CSCs Search using the Sphere-forming Assay

Medema's laboratory proposed that only CSCs are endowed with tumorigenic capacity and the ability to resist chemotherapy (Vermeulen et al., 2008b). By interpreting our results in light of Medema's theory, it became plausible to hypothesize that CSCs mediated BEAS-2B cells' malignization, and were liable for the malignant features of RenG2, DRenG2 and DDRenG2 cell lines. To test our hypothesis the sphere-forming assay was used as, according to Eramo and collaborators, it has the ability to specifically isolate CSCs from inside a an heterogeneous mixture of cells (Eramo et al., 2008, 2010).

The attained results were rather surprising as spheres only formed when DRenG2 and DDRenG2 cell lines were cultured at the restraining conditions of the sphere-forming assay (Figure 7.8). Moreover, the spheres attained with DDRenG2 cells were not only larger but also more numerous than those formed by DRenG2. This observation unveiled the higher stem potential of the DDRenG2 cellular system.

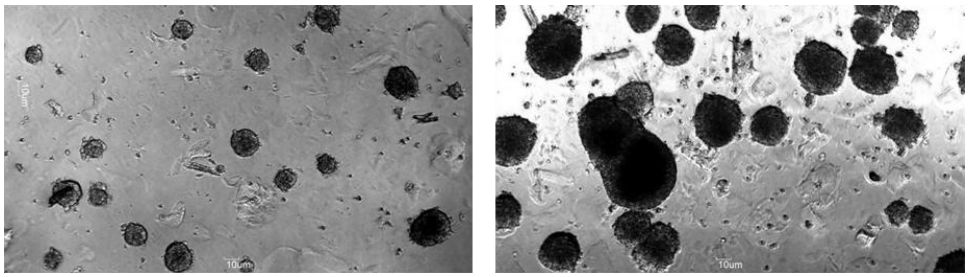

Figure 7.8 - Comparison of the spheres isolated from the derivative systems. DDRenG2 cell line formed more and larger spheres than its progenitor DRenG2 cell line. A magnification of 100x was used in both photographs.

The resulting DRenG2 and DDRenG2 spheres were then purified as described in section 5.16 of Chapter 5, in order to establish the CSC lines of each of the derivative systems, named SC-DRenG2 and SC-DDRenG2, respectively.

7.2 Discussion

The process of malignant transformation greatly differs among tissue types, even when the same set of genes is involved. For instance, *KRAS*-driven tobacco-induced lung adenocarcinomas need circa 30 years to evolve from preneoplastic lesions to the metastatic disease stage (Umar et al., 2012), while pancreatic adenocarcinomas, similarly driven by *KRAS* mutations, normally take less than 20 years to form metastasis (Yachida et al., 2010). These observations impose a great necessity of better understanding and characterizing the cellular physiology of the different tumors in order to design more adequate and effective therapeutic strategies against them.

Cells' aggressiveness and malignant potential are usually measured based on a wide range of factors, namely the time cells need to induce tumors in immunosuppressed mice, the volume of the tumors formed, and the extent of tissue damage observed in the tumor neighbourhoods (Musteanu et al., 2012). In light of

these observations, the results attained following *in vivo* derivation of the RenG2 system suggested that the malignant potential of these cells was successfully increased. Moreover, this assertion was further corroborated by the karyotypic studies on the derivative systems.

GI is recognized as a hallmark of malignant cells, which are usually regarded as having intricate genomes (Hanahan and Weinberg, 2011). GI is defined by the presence of gross structural chromosome alterations in the cells, and it may drive the formation of polyploid genomes (Fujiwara et al., 2005). As discussed in Chapter 6, Pellman's laboratory observed that tetraploid intermediates are frequently the reservoirs of this GI as they usually form during malignant transformation, subsequently evolving into aneuploid instable genomes (Ganem et al., 2009). Similarly, the results attained in the karyotypic study of BEAS-2B's malignant progeny corroborated Pellman's theory as all the malignant cell lines carried aneuploid genomes suggestive of being derived from a tetraploid intermediate. Moreover, they also confirmed that all the cell lines descended from BEAS-2B cells, as a chromosome signature was transversally present in BEAS-2B's progeny. Finally, derivative cells' karyotypes definitively supported their higher malignancy in comparison to RenG2 and the non-malignant cells, since some of the alterations found had already been associated to cancer. For instance, deletions of chromosome 7p have been identified in paediatric leukemias (Woo et al., 2009), while loss of chromosome Y as long been linked to LC (Center et al., 1993). Likewise, the deletion of chromosome 7q was already observed in breast cancer cells (Kristjansson et al., 1997) and the t(7;14) present in DDRenG2 cells' karyotype has very recently been found to be related with *EGFR* overexpression in multiple myeloma (Walker et al., 2013). It would be very interesting to assess whether *EGFR* alterations were involved in Cr(VI)-induced BEAS-2B malignization, as mutations in this gene were one of many drivers of lung carcinogenesis (da Cunha Santos et al., 2011).

Cells are social entities; they inhabit tissues, and they actually depend on their microenvironment to survive and sustain their physiology. As demonstrated

by Sassoli and collaborators using cardiac cells, paracrine and juxtacrine signalizations regulate tissues' homeostasis and fate (Sassoli et al., 2011). When normal cells are deprived of intercellular contacts, their internal circuitries are deregulated and the apoptotic cascades are triggered (Nelson and Bissell, 2006). Malignant cells, however, grow independently of these signalizations, and thus are able to survive following single-cell culture (Hanahan and Weinberg, 2011; Nelson and Bissell, 2006). The clonogenic assays' results evidenced the malignant nature of BEAS-2B's malignant progeny, as those cell lines were shown to give rise to significantly more cellular colonies than BEAS-2B and Cont1 cell lines. The capacity of these non-malignant systems to form colonies, although significantly lower than that of the malignant systems, potentially results from the immortalization with the SV40 virus, as was suggested by Yilmaz who observed similar features in immortalized human milk epithelial cells (Yilmaz et al., 1993).

The augmented clonogenic ability of the malignant systems sumed to their increased cellular motility, helping sustaining their malignant phenotype. Cellular motility is normally restrained to determined cellular populations in the body. As can easily be understood, lung bronchial epithelial cells are not one of those (Dertsiz et al., 2005). However, following malignization, these cells become motile in order to intravasate and disseminate throughout the organism (Joyce and Pollard, 2009). Paraphrasing Liang and colleagues, a scratch assay is a straightforward and economical method to study cell migration *in vitro* (Liang et al., 2007) and it is widely used in different cellular systems (Belo et al., 2013; Lee et al., 2013). In 2004, a high throughput platform was even designed to distinguish environmental perturbations that can affect cell migration, morphology, and division during the assay timeframe (Yarrow et al., 2004). The results attained in the scratch assay supported the assumption that RenG2 cells are the least malignant of BEAS-2B's progeny, as these cells only partially and disorderly closed the wound after 200 h. The fast wound closure observed in the derivative systems may suggest that wound closure relayed on cell division rather than on cell motility; how-

ever, the erratic pattern of closure along with the DTs calculated by the MTT assay strongly favored the migration theory. As a matter of fact, DDRenG2 cells showed no significant differences in DT when compared to RenG2 cells, yet they closed the wound in less than the half time and in a more ordered way then its progenitors.

The filamentous protein Vimentin, although often associated with mesenchymal cells, integrates the cytoskeleton of virtually all eukaryotic cells (Leader et al., 1987). Thus, its expression in BEAS-2B and Cont1 systems only illustrated its ubiquitousness. The absence of α-SMA staining in these non-malignant epithelial cells corroborated their epithelial nature. Conversely, the expression of α-SMA in the malignant systems sustained the EMT involvement in their formation. In agreement with Kalluri and Weinberg, this process of EMT is involved in the acquisition of motility properties by the malignant epithelial cells (Kalluri and Weinberg, 2009). Mendez and collaborators further identified Vimentin has the element responsible for the motility acquisition, through induction of the assembly of Vimentin intermediate filaments (Mendez et al., 2010). In light of these observations, immunocytochemistry results further supported scratch assay's results, as the more motile derivative cells showed a compatible mesenchymal phenotype.

Considering all the above mentioned results, the outcome of the therapy resistance studies was relatively predictable. Reflecting their non-malignant nature, both BEAS-2B and Cont1 cells succumbed to the employed therapeutic regimens and were killed soon after 48 h of treatment. The exceptional resistance shown by BEAS-2B cells to MTX treatment, rather than really meaning resistance, it most likely illustrated the different mechanism of action of the drugs used in this study. In fact, both Cis and Gem are predominantly cytotoxic agents while MTX is a cytostatic one. As cytotoxic agents, Gem and Cis affect cells at any stage of their cycle. MTX, on contrary, specifically interferes with DNA and RNA synthesis, acting preferably during the S-phase of the cell cycle during which these processes are crucial. As a consequence, cells cannot replicate their DNA and fail to divide

(Patanè et al., 2013). Overlapping the drug resistance results with those of the DTs, it became plausible to accept that slow-dividing non-malignant cells needed more time to progress through the cell cycle, thus delaying the entrance into S-phase and consequently, the toxic effects of MTX. This cycle phase-specificity of MTX may also justify its increased effectiveness in killing the cells of the derivative systems.

Highly proliferative cells such as cancer cells rely on glycolysis to support oxidative generation of ATP, regardless of oxygen availability, in a process called the Warburg effect (Warburg, 1956). Corroborating this observation, ^{18}FDG studies revealed that the malignant systems had a much higher demand of glucose than the non-malignant BEAS-2B and Cont1 cell lines (Vander Heiden et al., 2009). However, ^{18}FDG studies also unexpectedly revealed that the two derivative systems uptake significantly less glucose than RenG2 malignant cells, in spite of their higher malignant potential. These results indicated that DDRenG2 cells may need approximately half the energy required by RenG2 cells to sustain their malignant physiology. Moreover, because MTT assays showed that the three malignant systems have comparable DTs, the lower glucose demands cannot be ascribed to a slower proliferation. Instead, the metabolic profile of the more malignant cell lines suggested the existence of slow cycling and less glucose-requiring cellular subpopulations inside our derivative systems. Similar observations have been recently reported by Martins-Neves and collaborators using a human osteosarcoma cell line (Martins-Neves et al., 2012).

As discussed in Chapter 3, CSCs are characterized as being very tumorigenic and resistant to chemotherapy (Medema, 2013). Moreover, several other studies also showed that these cells also have lower glucose requirements, higher clonogenic efficiency and increased cellular mobility (Gottschling et al., 2012; Moore and Lyle, 2011; Visvader, 2011). Considering that we were able to find all these features in the derivative systems, it was hypothesized that CSCs mediated Cr(VI)-induced BEAS-2B cells' malignization. In line with the current literature, our initial

hypothesis was that a residual population of basal-like cells would have been retained in the BEAS-2B cell line during its immortalization. Subsequently, following exposure to Cr(VI), this population of cells would have been transformed into CSCs which had then driven the malignization process. Nonetheless, immunohistochemistry results did not corroborate the existence of such a basal-like cell population within BEAS-2B cells, and the sphere-forming revealed that only the derivative systems were able to produce spheres. Moreover, the fact that DDRenG2 cells formed more and bigger spheres, besides supporting the idea of their increased malignant potential, further suggested that the CSCs isolated from DRenG2 cultures were obtained through dedifferentiation of RenG2 cells and not by transformation of endogenous stem-like cells.

This hypothesis of dedifferentiation, although very appealing and not new, has only very recently been observed *in vitro* by Chaffer and colleagues (Chaffer et al., 2011). This group observed that differentiated mammary epithelial cells can reconvert to a stem-like state, in their opinion through an apparent stochastic process (Chaffer et al., 2011). Even though not excluding a random process, we rather believe that microenvironment cues were the major players in the dedifferentiation process. With that in mind it was reasoned that following injection of RenG2 cells in immunosuppressed mice a paracrine communication with mice subcutaneous stromal cells may have been established. This interaction with the microenvironment, as dissected in Chapter 3, is rather common among growing tumors and often results in microenvironment co-option and tumor outgrowth (Hanahan and Coussens, 2012). According to our rational, the soluble factors released by the mouse cells would have driven RenG2 cells dedifferentiation, thus leading to the formation of a CSC pool inside the DRenG2 system. Figure 7.9 presents the model proposed for CSCs-driven BEAS-2B cells' malignization following Cr(VI)-exposure.

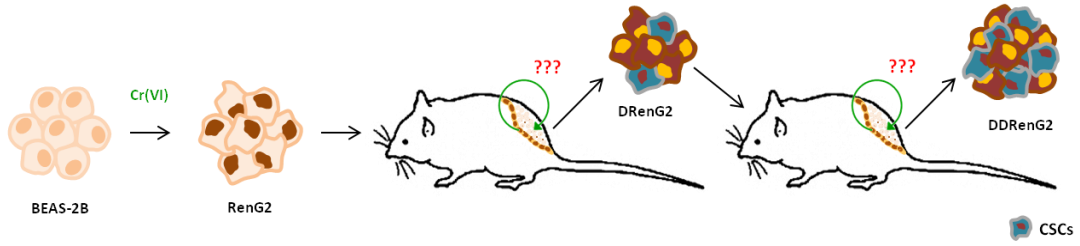

Figure 7.9 - Model for Cr(VI)-induced BEAS-2B cells' malignant transformation. Cr(VI) and low density culture rendered BEAS-2B malignant. According to our hypothesis, a subsequent communication between RenG2 cells and the subcutaneous mouse stromal cells would have driven the dedifferentiation of RenG2 cells with a specific set of Cr(VI)-induced mutations, and consequently, the formation of a CSC population inside DRenG2 cells. Further derivation of the system in a new mouse would have boosted the CSC sub-population in the DDRenG2 cell line.

The subsequent derivation of DRenG2 cells in a singenic mouse model would then have boosted the CSC sub-population, thus justifying the results attained in the sphere-forming assay. The comparative characterization of the attained stem systems would allow to clarify this hypothesis and understand the overall mechanism of Cr(VI)-induced BEAS-2B cells' malignization.

7.3 Conclusion

The process of *in vivo* derivation of the RenG2 cell line succeeded at increasing the malignant potential of the system. Moreover, it became evident that CSCs drove the boosted aggressiveness of the more malignant cell lines as a CSC sub-population was isolated from each of the derivative cell lines. Finally, the incapacity of RenG2 cells to yield spheres when cultured in restraining conditions indicated that CSCs were formed by dedifferentiation of the RenG2 cells while in the mouse subcutaneous compartment. The global chain of events further suggested that a paracrine communication between RenG2 and the mouse stromal cells may have driven the process of dedifferentiation.

Note

The results presented in this chapter are part of a manuscript in preparation:

Rodrigues, CFD, Val, M, Rodrigues IP, Fonseca, J, Gomes CMF, Abrunhosa, AJ, Paiva, A, Carvalho, L, Botelho, MF, Carreira, IM and Alpoim, MC. Stromal cells-released IL-6, G-CSF and Activin-A induce dedifferentiation of lung carcinoma cells into cancer stem cells.

Chapter 8

CSCs' Isolation and Characterization

8.1 Introduction

Intercellular crosstalk is probably the most important cellular event. In fact, it is through this process that cells keep their normal physiology, thus maintaining tissues' architecture and function, ultimately allowing the entire body homeostasis. As a consequence, it came as no surprise that this biological process is deeply affected by the malignant transformation course.

There are many ways through which cells may communicate; however, the most commonly employed strategies relay on paracrine and juxtacrine processes, and in the case of malignant cells, autocrine loops are also common. Regarding the mediators of the cellular dialogs, they mostly depend on the type of communication established. For instance, juxtacrine communication relays on intercellular membrane interaction through membrane-anchored molecules. Paracrine and autocrine loops, on contrary, depend upon the interaction of membrane-anchored cellular receptors with released soluble factors. Cytokines are often the mediators of paracrine and autocrine loops; these small molecules, although with different chemical structures, act over specific cellular receptors, activating intracellular signaling pathways that most frequently affect cells' expressome.

Co-culture strategies have been widely used to assess intercellular communication. There are many devices that can be used to co-culture cells, and their choice mostly depends upon the ultimate goal to be attained with the culture. When paracrine signalization is to be analyzed, Transwell® devices represent a good option as they may allow two different cellular populations to communicate without inter-population contact. As a consequence, soluble factors which enrich the correspondent conditioned media can subsequently be searched for using molecular biology techniques.

The aim of this study was to uncover the molecular mechanisms underlying CSCs-formation in the in DRenG2 and DDRenG2 cell lines, as a way of completing the molecular portrait of Cr(VI)-induced malignant transformation of BEAS-2B cells. High throughput strategies were used to identify the paracrine orchestrators of RenG2 cells' dedifferentiation, as well as the Cr(VI) role in the overall process.

8.2 Results

8.2.1 Karyotypic study of CSCs

To compare CSCs lines with their progenitors and identify genomic hallmarks of the dedifferentiation process, 20 karyotypes were constructed for both SC-DRenG2 and SC-DDRenG2 cells.

The karyotypic study of SC-DRenG2 cells revealed that, similarly to what was observed for DRenG2 and DDRenG2 cell lines, they harbored in all the analyzed karyotypes some of the features that were present in their progenitors, namely the $6p^+$ and the $i(9)(q^+)$. In addition, this CSCs line showed a reciprocal derivative of the short arms of chromosomes 1 and 2 (der 1p/2p) in 70 % of the analyzed cells, a similar derivative involving the long arms of the same chromosomes (der 1q/2q) in 33.3 % and a terminal

deletion in the long arm of chromosome 1 ($1q^-$) in 70 %, in the analyzed karyotypes (Figure 8.1).

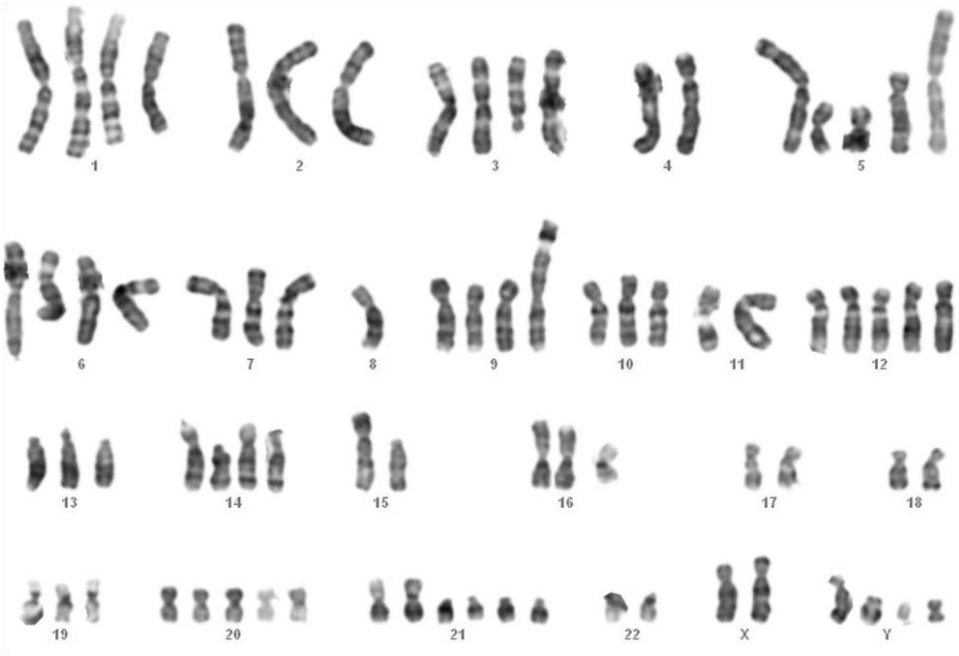

Figure 8.1 - Representative karyotype of SC-DRenG2 at #6. The karyotype showed new structural alterations relative to DRenG2 cells, namely the der(1p/2p), the der(1q/2q) and the $1p^-$. At least 20 karyotypes were constructed for each cell passage analysed.

SC-DDRenG2 cells also retained similar percentages of the $6p^+$, $7p^-$ and $17q^+$ from DDRenG2 cells. In addition, these cells' karyotype also showed an isochromosome of the short arm of chromosome 5 [i(5)(p10)] as well as a derivative chromosome involving parts of both chromosomes 5 and 7 (der5/7) in 100 % and 80 % of all the analyzed metaphases, respectively (Figure 8.2).

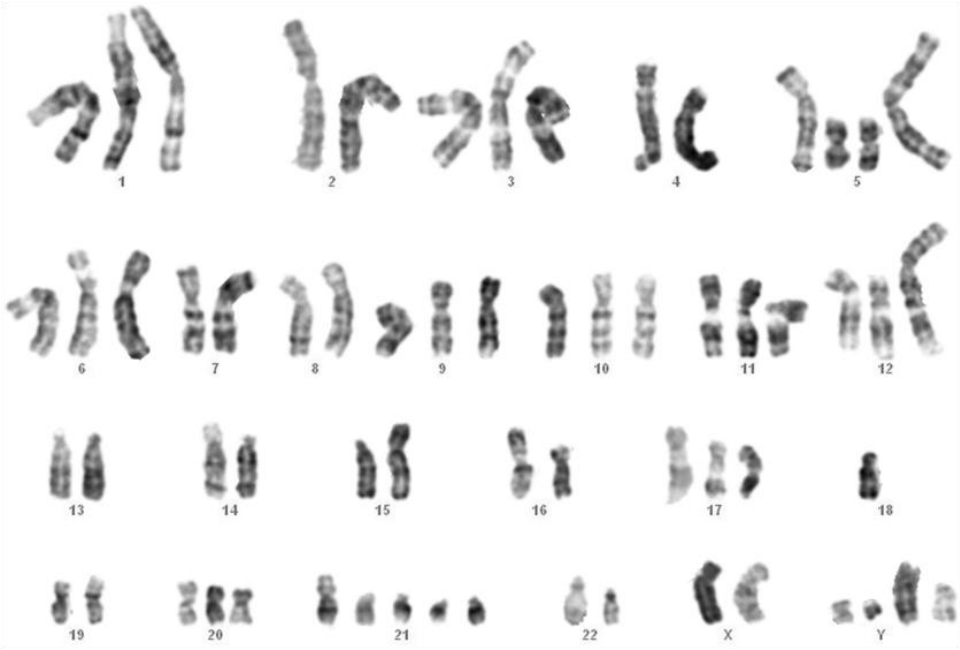

Figure 8.2 - Representative karyotype of SC-DDRenG2 at #6. The karyotype showed new structural alterations relative DDRenG2 cells, namely the i(5)(p10) and the der(5/7). At least 20 karyotypes were constructed for each cell passage analysed.

In terms of ploidy, both the CSC lines presented a reduced number of chromosomes when compared to their progenitors. As a matter of fact, SC-DRenG2 cells showed an average of 74 chromosomes, while SC-DDRenG2 normally presented circa 62 chromosomes.

8.2.2 Metabolic Studies using ^{18}FDG Uptake

CSCs are described as quiescent, slow dividing cell populations that consume less glucose than differentiated tumor cells (Moore and Lyle, 2011; Vlashi et al., 2011). Driven by these observations, the glucose uptake of both CSCs systems was assessed using ^{18}FDG (Figure 8.3).

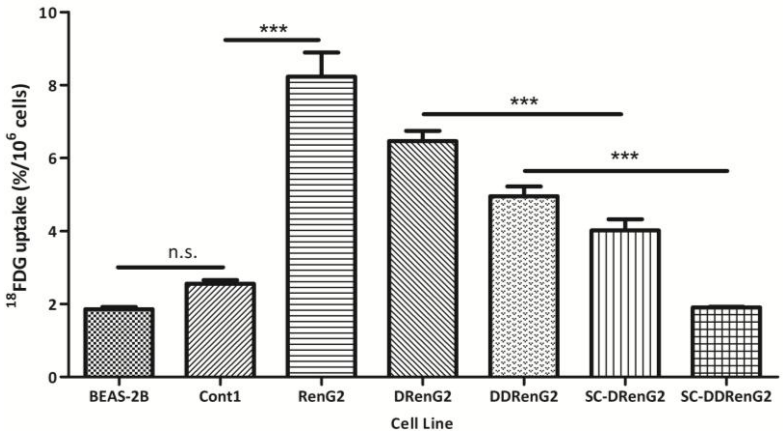

Figure 8.3 - Comparative analysis of ^{18}FDG uptake. Both SC-DRenG2 and SC-DDRenG2 cell lines uptake significantly less ^{18}FDG in comparison to the other malignant cell lines. Bars represent means ± SEM. Differences between the cell lines' means were evaluated by one-way ANOVA followed by a Bonferroni post test. n.s., no significant; *,$P \leq 0.05$; **, $P \leq 0.01$; ***, $P \leq 0.001$.

The attained results further corroborated the observations of Vlashi and colleagues as they showed that both our CSC systems had significantly lower glucose needs than RenG2, DRenG2 and DDRenG2 cell lines (Vlashi et al., 2011). In fact, the registered values of ^{18}FDG uptake for the stem cell lines were actually very close to those attained for the non-malignant BEAS-2B and Cont1 systems.

1.1.1. Doubling Times by MTT

To assess if the lower glucose requirements of the CSC systems paralleled an increased DT, MTT assay was performed as previously described. The attained results are summarized in Figure 8.4.

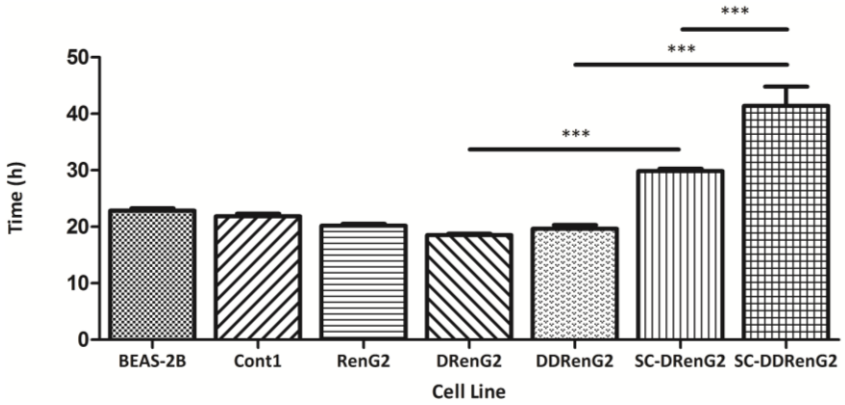

Figure 8.4 - Comparative study of cellular duplication times. Both SC-DRenG2 and SC-DDRenG2 had considerably higher replication times than their derivative progenitors. Moreover, SC-DDRenG2 needed even more time to replicate than SC-DRenG2. Data represent means ± SEM. Differences between the means were evaluated by one-way ANOVA followed by a Bonferroni post test. n.s., no significant; *,$P \leq 0.05$; **, $P \leq 0.01$; ***, $P \leq 0.001$.

Corroborating previous observations from other laboratories, the isolated CSCs populations had a longer cell cycle progression than the cell lines from which they were isolated (Dembinski and Krauss, 2010; Roesch et al., 2010). Moreover, trypan blue direct cell counting further confirmed that the increase observed in cellular viability did not result from an increase in cell number. Finally, the results attained in preliminary cell cycle studies with PI do corroborated the observations of Mackenzie and colleagues, according to whom CSCs isolated from epithelial tumors have a higher percentage of cells in G2 cell cycle phase (Harper et al., 2010).

8.2.3 Therapy Resistance Studies

Tumor resistance and consequent relapse is generally ascribed to CSCs as these cells show enhanced resistance to common therapeutic approaches. To test whether SC-DRenG2 and SC-DDRenG2 also had increased drug resistance, studies were performed using different concentrations of

MTX. The viability of the cell lines exposed to MTX was assessed along 72 h by the MTT assay (Figure 8.5).

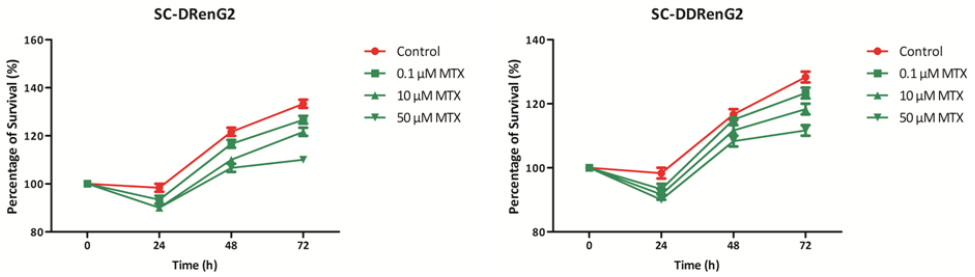

Figure 8.5 - CSCs' survival following MTX treatment. MTX not only failed at killing CSCs, but also was unable to block their division, as both SC-DRenG2 and SC-DDRenG2 grew in the presence of the drug. Data represents means ± SEM. When not visible error bars are smaller than the symbols.

On contrary to what was observed on Chapter 7 with the RenG2, DRenG2 and DDRenG2 malignant systems (see Figure 7.7), MTX failed to abrogate CSCs' cycle progression as the cells not only did not die, but kept dividing in the presence of the drug. This observation is consistent with previous studies demonstrating the higher resistance of CSCs to therapy (Barr et al., 2013; Gupta et al., 2009; Lee et al., 2011; Naujokata and Lauferc, 2013). Note that in both CSCs systems the drug treatment seemed to have had some degree of effectiveness 24 h following exposure, but this effectiveness was immediately abolished since 48 h following exposure cells were actively dividing again.

8.2.4 Gene expression profile by RT-qPCR

The gene expression analysis used to follow up BEAS-2B cells' malignization was globally recapitulated for the RenG2 progeny and for the

isolated CSCs systems, to highlight differences among them. The attained results are illustrated in Figure 8.6.

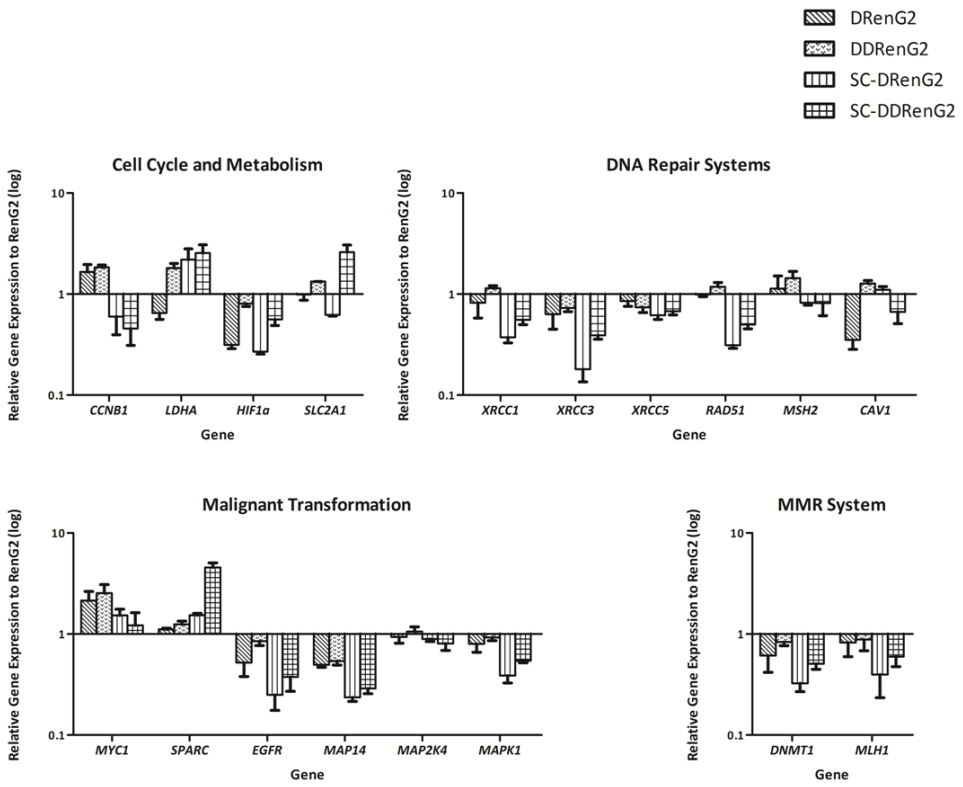

Figure 8.6 - Gene expression analysis of derivative and CSC systems. Altogether the results confirmed the higher malignancy of the derivative DRenG2 and DDRenG2 systems, as well as the stem nature of their isolated CSCs sub-populations. See text for specific analysis. Bars represent means ± SEM.

CCNB1 expression was significantly reduced in the CSCs systems, thus corroborating the cell cycle studies, according to which both SC-DRenG2 and SC-DDRenG2 divide slower than their progenitor derivative cells. As to *LDHA* gene, it was consistently overexpressed in CSCs in opposition to *HIF1α* gene, which was downregulated in both the derivative systems and in their isolated sub-populations. Moreover, *HIF1α* suppression was greater in the most malignant cell line (DDRenG2) and in its respective CSCs sub-population (SC-DDRenG2) (Figure 8.6).

DNA repair genes were globally downregulated, with the exception of *MSH2* and *XRCC1* in the derivative systems and *CAV1* in the DDRenG2 and CSCs systems. As to the genes involved in malignant transformation, all MAPKs tended to be downregulated in all the cell lines, in relation to the less malignant RenG2 cells, excepting *MAP2K4* which was slightly upregulated in DDRenG2 cells. *MYC* oncogene was greatly expressed in the more malignant systems, when compared to RenG2 cells. Surprisingly, however, its levels reached a peak in the derivative systems and were then inferior in both SC-DRenG2 and SC-DDRenG2 cells. *SPARC* showed a very significant up-regulation in the SC-CSCs, while the MMR system turned out to be silenced, as revealed by *DNMT1* and *MLH1* evident downregulation.

8.2.5 Comparative genomic analysis of all systems

Following karyotypic studies, aCGH was used to attained better understand the malignization process induced by Cr(VI). Using the Agilent 180 K platform, all our systems were compared to BEAS-2B cells. The results are illustrated in Figure 8.7.

An overview of the attained results allowed us to identify various genes potentially involved in the different steps of the cell lines' development. It was even possible to identify chromosome imbalances potentially correlated with viral-based BEAS-2B immortalization, like the observed point deletion at 1q34 in BEAS-2B, involving the zinc finger CCCH-type antiviral 1 (*ZC3HAV1)* gene, which codes for an anti-retroviral protein that inhibits viral replication (Cagliani et al., 2012). The low-density culture protocol did induced some degree of GI, as can be observed by the chromosome deletions at the distal part of the short arm of chromosome 4 and at the distal part of the long arm of chromosome 16 in both Cont1 and RenG2 cells (Figure 8.7).

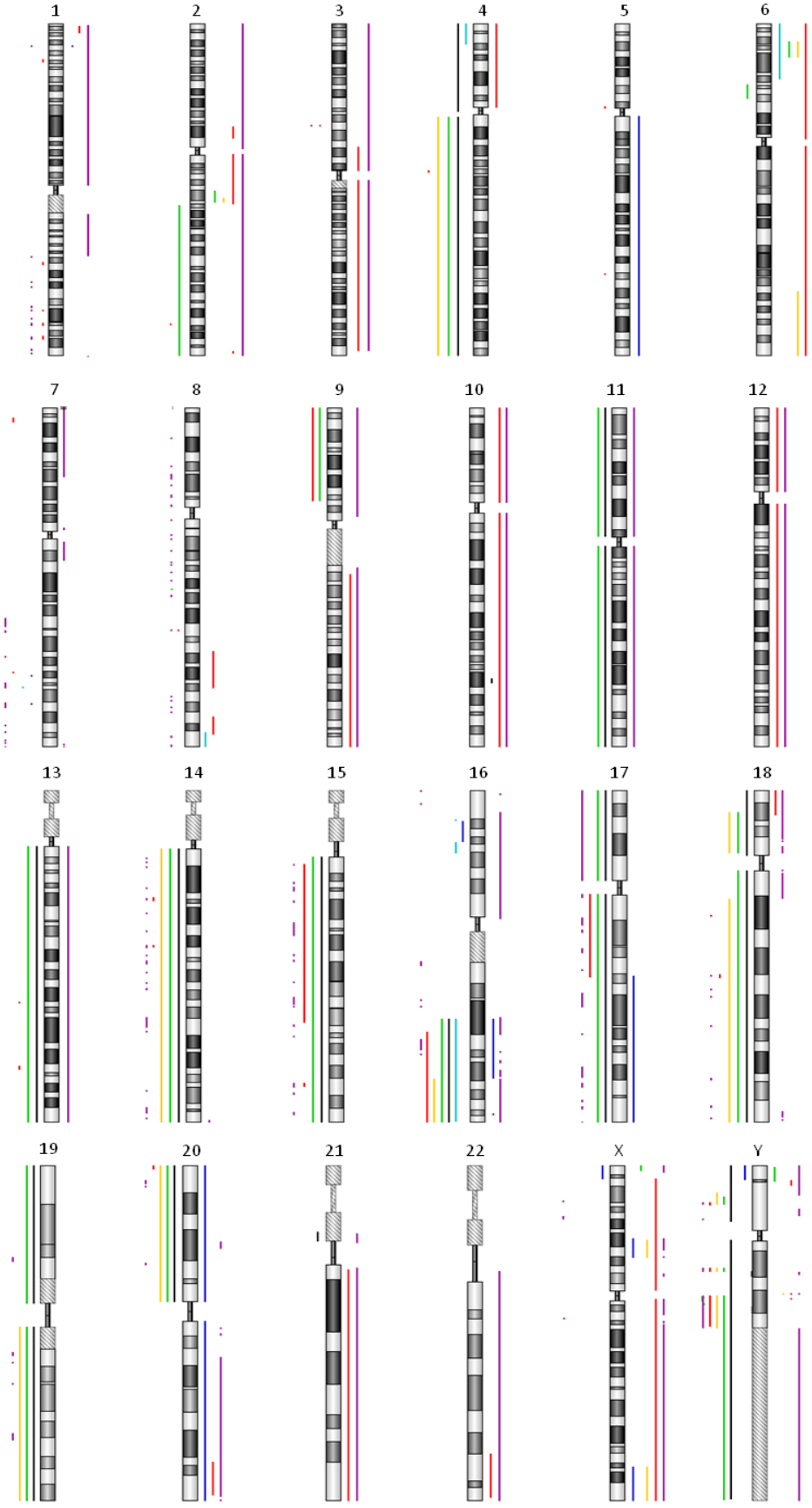
1
2
3
4
5
6
7
8
9
10
11
12
13
14
15
16
17
18
19
20
21
22
X
Y

Figure 8-7 - Ideogram representing chromosome imbalances in all cellular systems. It was possible to identify chromosome regions affected by low density culture, namely in chromosomes 4 and 16. A high degree of GI was found in the CSCs systems. Coloured lines represent the cell lines where imbalances occurred. When placed on the left of the chromosome they represent deletions, on contrary, when located on the right they represent amplifications. Dark blue BEAS-2B, light blue Cont1, black RenG2, green DRenG2, yellow DDRenG2, red SC-DRenG2 and violet SC-DDRenG2. The analysis software normalized the results to the most frequent ploidy displayed in each cell line in comparison to BEAS-2B cells.

In agreement with Borodyansky and Yang, the isolated CSCs systems showed a higher degree of GI when compared to the cell lines from which they were isolated (Li et al., 2009). In fact, analysis of the attained results revealed that both CSCs lines carried deletions on tumor suppressor genes, namely *TP53BP2*, *LIN9* and *RPS29*. Additionally, *WDR26* and *CDKL3*, two important genes in cell cycle progression were also shown to be deleted in both CSCs systems. Mitocondrial metabolism also seemed to be impaired as genes involved in mitochondria respiratory chain complexes' assembly were deleted. This was actually the case of *BCS1L*, involved in the assembly of complex III (Fernandez-Vizarra et al., 2007), *NUBPL*, involved in the assembly of complex I (Calvo et al., 2010; Kevelam et al., 2013), and *ATP5S*, needed for the regulation of ATP synthase (Belogrudov and Hatefi, 2002). Also deleted in both CSCs systems were various genes involved in intracellular MAPK-mediated signaling pathways, a gene involved in cellular differentiation, *ARID4B*, and two controllers of EMT, *TWIST2* and *PTPN14*. Regarding gene amplifications, they were shown to be significantly less frequent than deletions in the CSCs systems. Of relevance was the amplification of a wide range of cytokine genes (*CCL1*, *CCL2*, *CCL7*, *CCL8C*, *CCL11* and *CCL13*), of the *SKI* proto-oncogene and of genes involved in intercellular signal transduction affecting, for instance, NF_KB pathway (*PLEKHG5*), p53 pathway (*TP73*), PI3K pathway (*PRKCZ*) and RAF pathway (*KSR1*).

In addition to the above mentioned deletions and amplifications SC-DDRenG2 cells portrayed an even higher degree of GI when compared with SC-DRenG2. Especially relevant was the amplification of the genes *SRC*, Aurora kinase A and B (*AURKA* and *AURKB)*, Hypoxia-inducible factor 1β (HIF-1β), Snail homolog 3 (*SNAI3)*, Nuclear factor of activated T-cells, cytoplasmic, calcineurin-dependent 2 (*NFATC1* also known as *NFAT2)* and Ela-C homolog 2 (*ELAC2*).

8.2.6 Co-culture of RenG2 and FR: the last cue!

Following the confirmation of SC-DRenG2 and SC-DDRenG2 stem potential, it became evident that the mouse subcutaneous compartment drove RenG2 cells' dedifferentiation. To assess this hypothesis RenG2 cells were co-cultured with cirurgically isolated mouse FR cells for two months, and isolated RenG2 cells (iRenG2) were subsequently tested for their ability to grow under restraining conditions using the sphere-forming assay. Spheres formed soon after cells were plated in low-adherent wells, similarly to what was observed during the isolation of SC-DRenG2 and SC-DDRenG2 systems (section 7.1.9 of Chapter 7). To highlight differences and similarities between iRenG2 and RenG2, DRenG2 and SC-DRenG2, a gene expression analysis was performed using the same candidates. The obtained results are depicted at Figure 8.8.

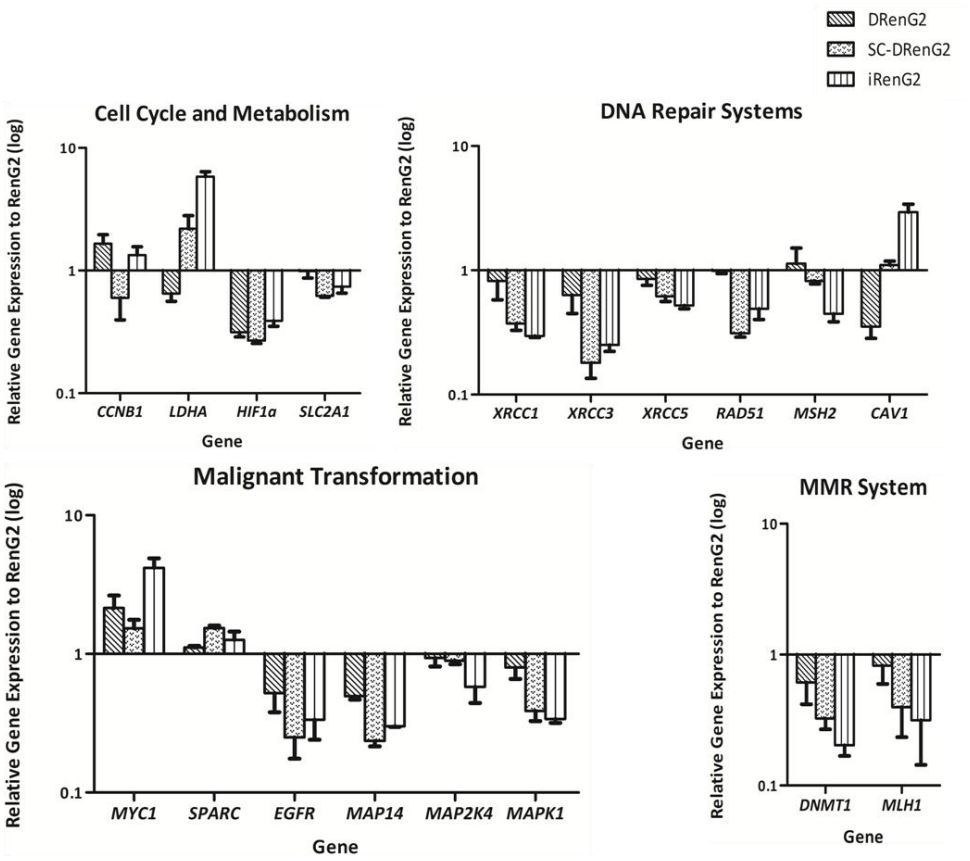

Figure 8.8 - Comparative gene expression analysis of iRenG2 cells. Globally, iRenG2 cells lost the expressome signature of RenG2 cells and adopted a new signature that lay in between those of DRenG2 and SC-DRenG2. Bars represent means ± SEM.

The attained results showed that iRenG2 cells no longer have RenG2's signature but rather adopted one that is somewhere in between those of DRenG2 and SC-DRenG2 cells. Furthermore, these observations were corroborated by the flow cytometry studies that used a selected panel of markers to compare the abovementioned cellular systems (Figure 8.9).

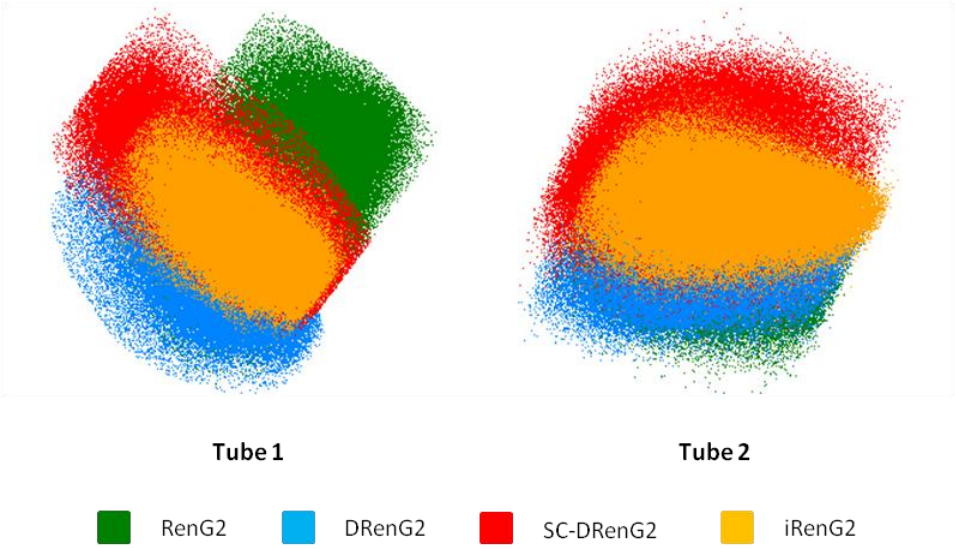

Figure 8.9 - Flow cytometry scattering plots comparing the iRenG2 cell line to both RenG2, DRenG2 and SC-DRenG2. In both tubes the yellow-represented iRenG2 cells were more close to both DRenG2 and SC-DRenG2 than to RenG2, illustrating their closer identity. Colored dots represent individual cells. RenG2 green, DRenG2 light blue, SC-DRenG2 red and iRenG2 yellow.

The scattering plots resulted from an integrative software analysis that combined the information of all the markers studied to assess the molecular signature of the cells. These plots revealed that iRenG2 cells are very close to both DRenG2 and SC-DRenG2 cells, but rather different from RenG2 cells. These observations prompted the hypothesis that a paracrine crosstalk may have driven the dedifferentiation of iRenG2 cells. To validate this hypothesis, additional control co- and monocultures were performed, as depicted in Figure 5.6 from Chapter 5. Subsequently, cytokine multiplex array and ELISA were carried out in the conditioned media of the different cultures (Figures 8.10 and 8.11).

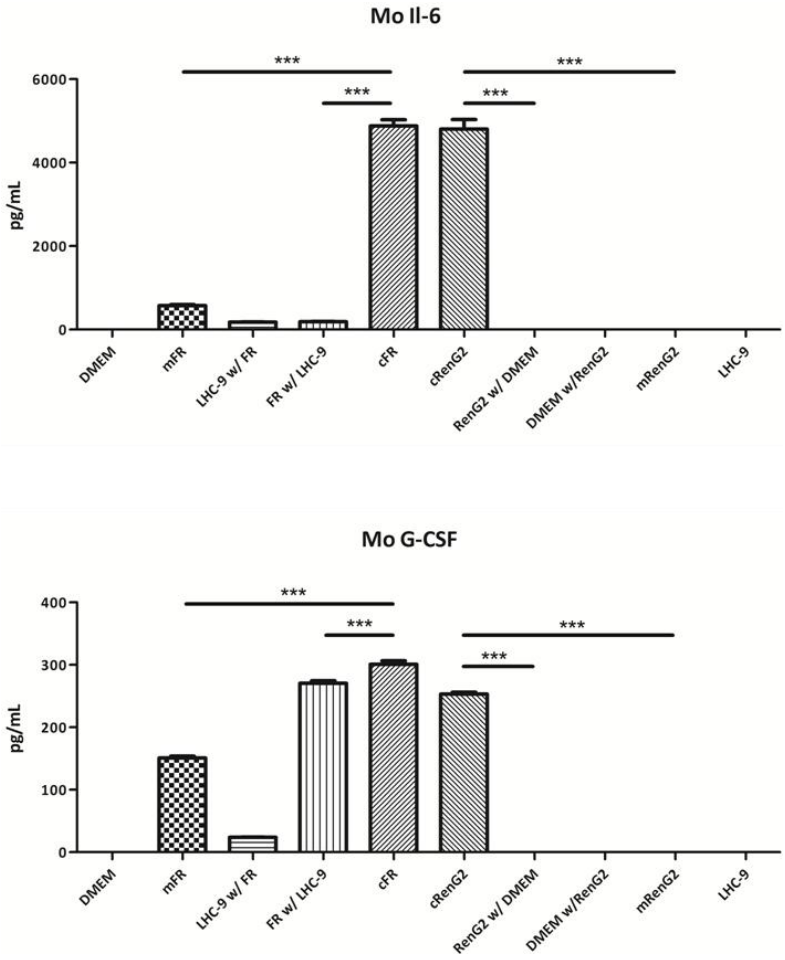

Figure 8.10 - IL-6 and G-CSF levels in the conditioned media of the RenG2-FR co-culture. The levels of both cytokines were significantly increased in the co-cultures relative to the controls. The use of an anti-mouse Ab allowed the detection of FR-produced cytokines in the upper compartment. Data represent means ± SEM. Differences between the means were evaluated by one-way ANOVA followed by a Bonferroni post test. Mo, mouse; mFR, monocultured FR cells; cFR, FR cells co-cultured with RenG2 cells; cRenG2, RenG2 cells co-cultured with FR cells; mRenG2, monocultured RenG2 cells; w/, co-cultured with; n.s., no significant; *,$P \leq 0.05$; **, $P \leq 0.01$; ***, $P \leq 0.001$.

Multiplex cytokine array is a very powerful and sensitive assay that allows detecting very low levels of cytokines. Non-significant variations

were detected in a wide range of cytokines, however, only the IL-6 and G-CSF levels in the co-culture conditioned media turned out to be elevated at a statistically significant level. Moreover, the specie-specificity of the Abs allowed to confirm that the FR-secreted cytokines were able to trespass the Transwell® membrane into the upper compartment, thus being available to affect RenG2 cells' physiology.

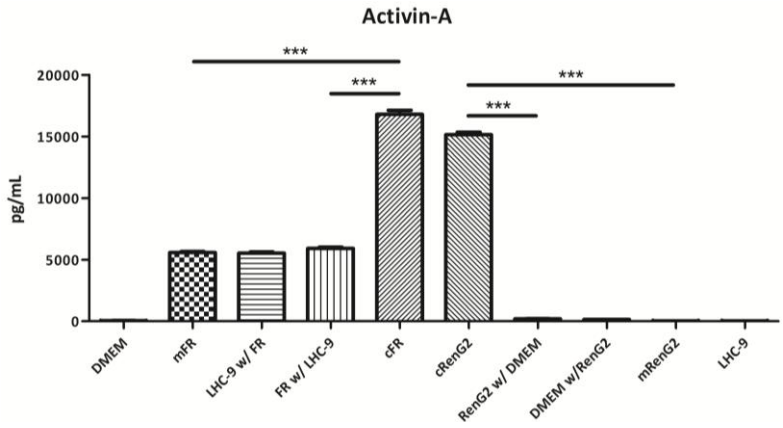

Figure 8.11 - Activin-A levels in the conditioned media of the RenG2-FR co-culture. A statistically significant increase on Activin-A levels was observed in the co-cultures relative to the controls. Data represent means ± SEM. Differences between the means were evaluated by one-way ANOVA followed by a Bonferroni post test. n.s., no significant; *,$P \leq 0.05$; **, $P \leq 0.01$; ***, $P \leq 0.001$.

The ELISA assay used to search for Activin-A in the co-cultures' conditioned media also suggested the involvement of this cytokine in RenG2 cells' dedifferentiation, as its levels were significantly increased compared to the one attained in control cultures. Nonetheless, although the inter-species cross-reactivity of the Ab used does not allow affirming definitely that Activin-A was produced by the FR feeder layer, the negligible produc-

tion of this molecule by RenG2 monocultures strongly supports this hypothesis.

8.3 Discussion

Independently of the tissue of origin and of the pathophysiology of the disease, malignant cells share a group of features that characterize them. The extent to which each of these characteristics is developed and their relative proportion further determines tumors' behavior. Gene expression usually underlies the development and expression of these characteristics, and it is actually believed to be their underlying driving force.

Alterations in cells' karyotype were commonly found in malignant cells as they very efficiently modulate gene expression. In fact, chromosome rearrangements may activate, silence, amplify or delete genes. For instance, *MYC* amplification was long encountered in a wide range of tumor cells (Collins and Groudine, 1982; Little et al., 1983), while *TP53* was found to be either deleted (Nigro et al., 1989) or mutated (Nigro et al., 1989). In both situations, malignant transformation was promoted either by the increased expression of an oncogene or by silencing of a tumor suppressor gene. Alternatively, the translocation of chromosome fragments, or even entire chromosome arms, may also be used by malignant cells to modulate their expressome. For example, acute lymphoblastic leukemias carrying a translocation affecting the mixed-lineage leukemia gene (*MLL*) portray a distinct gene expression profile that renders cells more resistant to chemotherapy (Armstrong et al., 2002).

aCGH is a very potent tool to assess numeric alterations in cancer cells. Nevertheless, the complexity of the chromosome rearrangements is such that sometimes it becomes very difficult to interpret and contextualize the results attained in the study of malignant cells. This task is further complicated by the software analysis which masks polyploid cells by transforming the probe intensity data

to a virtually diploid state (Gardina et al., 2008; Yau et al., 2010). As a consequence, the scrutiny of aCGH data needs special care and criticism. This fact justified the amplification/deletion of entire chromosomes attained in the present comparative study of the cell lines relative to their progenitor BEAS-2B cells.

According to manufacturer's instructions, the aCGH study of BEAS-2B cells was performed against a commercial control male genome. The control genome combines an average of the alterations found in the population, so it provides a standardized model against to which other male genomes can be compared. Following comparison to the control genome, BEAS-2B cells were shown to display a deletion at the q34 region of chromosome 7. Among the deleted genes was the *ZC3HAV1*, which encodes an antiretroviral protein. Although both SV40 and AD12 are DNA viruses, we reasoned that the specific deletion of this intrachromosomal region may have favored BEAS-2B immortalization.

The fact that the aCGH analysis was made against BEAS-2B cells, allowed the understanding of what alterations were introduced into the system by our manipulations. For example, the terminal deletions found in chromosomes 4 and 16 could be ascribed to low-density culture as they appeared in at least Cont1 and RenG2 cells, but not in BEAS-2B. An overview of the genes located in these regions, although identified genes that could have indirectly favored malignization, did not provide any real target for future dissection. Similarly, Cr(VI) also seemed to have had little GI-prone activity. In fact, contradicting the reports on the literature that described Cr(VI) as a highly mutagenic and genotoxic agent, the aCGH analysis only identified two small regions on chromosomes 10 and 21 that were amplified and deleted in RenG2 cells, respectively. The amplified region contained *SORCS1* that encodes for a family member of Vacuolar protein sorting 10 (VPS10), highly expressed in the central nervous system and which had been associated with diabetes (Goodarzi et al., 2007), Alzheimer (Lane et al., 2013) and more recently, renal disease (Lazar et al., 2013). Nonetheless, we were unable to find any link between *SORCS1*, VPS10 and cancer, so far. Regarding the deleted region on

chromosome 21, it contained only two genes, *TPT2*, which function is still unknown, and B melanoma antigen (*BAGE*), a tumor antigen discovered by Boël and collaborators in human melanoma samples (Boël et al., 1995). Later on, the protein coded by this gene was also found in benign and malignant neoplasms of the salivary glands (Nagel et al., 2003) and in ovarian cancer samples (Zhang et al., 2010). Although no relation was found between BAGE and either Cr(VI) and LC, it is rather surprising that this gene was shown to be deleted in RenG2 cells.

RenG2 cells' derivation in nude mice did not seem to have induced GI. In fact, the loss of entire chromosomes shown by aCGH for the cell lines is rather virtual and reflected the normalization performed by the software analysis (Yau et al., 2010). This observation further supported the theory presented in Chapter 6, according to which increased ploidy and consequent variations in gene dosage levels are mediators of malignant transformation (Duesberg and Li, 2003; Nguyen and Ravid, 2006). Nonetheless, and in agreement with their higher malignant potential, DDRenG2 cells did present some additional alterations, particularly in chromosome 6. Following analysis, the amplified regions in chromosome 6 revealed to contain genes that were potentially involved in the increased malignancy of the system. Among others we managed to found *CD83*, commonly expressed in human neoplasias (Ananiev et al., 2011; Zhang et al., 2007); the seventh member of the TBC1 domain family (*TBC1D7*) gene, whose activation is associated with lung carcinogenesis (Sato et al., 2010); endothelin-1 (*EDN1*), whose involvement is cancer has been recently reviewed by Rosanò and colleagues (Rosanò et al., 2013); the transcription factor AP-2α (*TFAP2A*) gene that seems to collaborate with *MYC* on the regulation of cell cycle progression (Wong et al., 2012a) and the MYC target 1 (*MYCT1*) gene that encodes the protein responsible for mediating many of MYC's actions (Yin et al., 2002).

Metabolic studies using ^{18}FDG revealed that the glucose requirements of CSC systems were comparable to those of non-malignant BEAS-2B and Cont1 cells, and thus significantly lower than that of RenG2, DRenG2 and DDRenG2 cells.

When interpreting these results in light of those from MTT-based cell DTs study, it became evident that the modest glucose necessities of CSCs portrayed their quiescent status, as these cell populations have a considerably longer cell cycle. Quiescence as long been associated with CSCs (Blanpain, 2012; Visvader and Lindeman, 2008), and it actually partially justifies their increased resistance to therapy, particularly to the agents that depend upon the cell cycle progression to target cells (Gottschling et al., 2012). SC-DRenG2 and SC-DDRenG2 cells' quiescence settlement was subsequently supported by RT-qPCR analysis showing underexpression of the *Cyclin B* gene (Figure 8.6), as well as by aCGH results revealing the deletion of genes involved in mitochondria oxidative metabolism (Figure 8.7). In fact, a dysfunctional mitochondria respiratory chain would render cells more dependent upon glycolysis as energy source. As a consequence, *HIF-1α* would have to be expressed and its levels stabilized to conjugate with HIF-1β, to induce the expression of target genes like *SLC2A1*, *GLUT3* and *LDHA*. Although aerobic respiration was not assessed, gene expression analysis of *HIF-1α* gene did not show its upregulation in the CSCs systems in comparison to the other malignant cell lines (Figure 8.6). *LDHA*, however, showed a marked overexpression, particularly in SC-DDRenG2 cells, as did *SLC2A1*.

The increase in the expression of the enzyme that catalyses the interconversion of pyruvate and lactate as been previously observed in bovine blastocyst development, and was correlated with the overexpression of *SLC2A1* but not *HIF-1α* (Harvey et al., 2007). Authors reasoned that the increased expression of these two genes depended upon HIF-2α-mediated response to oxygen concentration, sensed independently of HIF-1α (Harvey et al., 2007). Although this could have happened in DDRenG2 and SC-DDRenG2 systems, regarding the first derivative, only *LDHA* was shown to be overexpressed (Figure 8.6). In this case, the observed *LDHA* overexpression may have resulted from direct MYC stimulation, corroborating the observations of Dang's laboratory (Shim et al., 1997). In fact, MYC is able to activate LDHA, driving pyruvate away from mitochondria towards

the production of lactate (Gordan et al., 2007). This process allows regenerating nicotinamide adenine dinucleotide (NAD^+) from NADH, and provides a route for discarding the glucose-derived carbon molecules that are then extruded through lactate efflux, with the consequent lowering of the extracellular pH (Gordan et al., 2007; Shim et al., 1997). Although further experiments will be needed to directly assess MYC and HIF-1β involvement in gene expression regulation of our systems, upregulation of *MYC* expression in both CSC systems, along with the amplification of HIF-2β gene identified by aCGH in SC-DDRenG2 cells strongly support our hypothesis.

The increased ability of both SC-DRenG2 and SC-DDRenG2 to survive adverse growth conditions and methotrexate treatment further highlighted their CSCs signature. Furthermore, the very well established increased resistance of CSCs (Bertolini et al., 2009) laid the foundations of the theory of CSCs-driven tumor relapse (Frank et al., 2010). More recently, Visvader and Lindeman further introduced the concept of dormant CSCs, which seem to co-inhabit the tumors along with non-dormant CSCs, and are resistant to even targeted therapies (Visvader and Lindeman, 2012). This robustness of CSCs apparently relays on a very efficient activation of the DNA repair genes, as well as on the overexpression of drug efflux pumps like P-glycoprotein (Medema, 2013; Naujokata and Lauferc, 2013; Wilson et al., 2011a). However, whether other mechanisms are involved is still to be elucidated. In the present study RenG2's progeny showed a generalized underexpression of the DNA repair genes when cultured under normal conditions. This was not surprising, as they were kept under suitable conditions of nutrients and oxygen. Nonetheless, it would be interesting to assess the expression of those same genes following methotrexate treatment, and to evaluate the P-glycoprotein expression status.

The results attained regarding *MYC* expression may seem rather controversial. In fact, one would expect to find a progressively higher *MYC* overexpression along the malignant systems and not the opposite (Figure 8.6). However, Bártová's

laboratory recently showed that the same colony of mouse embryonic SCs (mESCs) harbored cells with distinct levels of OCT4 and MYC, resultant from different ratios of mono- and bi-allelic gene expression controlled by epigenetic modifications (Sustáčková et al., 2012). Earlier on, Niwa and collaborators further demonstrated that mESCs' pluripotency was dependent on a certain level of *OCT4* expression, and was lost whenever the gene was either up or downregulated (Niwa et al., 2000). Most probably, after a necessary initial boost to malignantly transform and derive BEAS-2B and RenG2 cells, respectively, *MYC* expression levels were then reduced to the values required by the CSC systems' to preserve a pluripotent phenotype. Furthermore, the group of Medema recently showed that WNT-pathway target genes are shown methylated in late stages of colon carcinogenesis, after a period of sustained overexpression (de Sousa E Melo et al., 2011), suggesting that gene expression signature alone is not enough to infer on CSCs' malignancy or even proportion inside tumors.

Conversely to *MYC*, *SPARC* showed a strong tendency for upregulation as malignancy increased (Figure 8.6). This same observation, already reported by other laboratories, was associated to decreased intercellular attachment and an increased metastatic ability (Jiang et al., 2013; Neuzillet et al., 2013; Said et al., 2013). The increased metastatic ability of the CSCs systems was also suggested by the aCGH results, as both *TWIST2* and *PTPN14* were equally amplified in the CSCs lines, and the *SCR*, *NFATC1* and *MMP9* were amplified solely in the more malignant SC-DDRenG2 cells. As amply dissected in Chapter 1, in order to intravasate tumor cells must acquire the ability to move and to destroy ECM and the intercellular connections. This capacity is acquired mainly by upregulating the expression of metalloproteinase genes, as shown in NSCLC (Safranek et al., 2009; Zheng et al., 2010). As revealed by Long and collaborators, SRC protein seems to have a key role in the process, as it interacts with specific transcription factors driving *MMP* genes' upregulation (Long et al., 2012). This observation may thus justify SRC expression found in nearly 60 % of all lung carcinomas (Mazurenko et al., 1992).

The involvement of *NFAT* genes in cancer has long been proposed. In 2006 Yiu and Toker demonstrated that NFTA induces the upregulation of *cyclooxygenase-2* (*COX-2*) gene and the synthesis of prostaglandins', driving breast cancer cells' invasion (Yiu and Toker, 2006). More recently, Oikawa and collaborators showed that the increased metastatic potential induced by *NFATC1* is mediated by TGF-β-independent upregulation of *SNAIL* and *ZEB1*, which subsequently downregulate *E-cadherin*, thus favoring EMT and a migratory phenotype (Oikawa et al., 2013). Additionally, *AURKA* and *AURKB* were also shown to be amplified in SC-DDRenG2 cells. According to Ice and colleagues, *AURKA* is overexpressed in 96 % of human cancers and is considered an independent marker of poor prognosis (Ice et al., 2013). Very recently, both these genes have been shown to be activated by *C-Abl Oncogene 1, Non-Receptor Tyrosine Kinase* (*BCR-ABL*) in leukemic cells (Yang et al., 2013), a gene from a 9q chromosome region that was amplified in both SC-DRenG2 and SC-DDRenG2 cells (Figure 8.7). In tumor cells *AURK* genes have already been associated with cell cycle alterations (Zhu et al., 2005), therapy resistance (Agnese et al., 2007), EMT and enhanced migration (Wan et al., 2008). Furthermore, Liu's group discovered that the increased metastatic ability of cells overexpressing *AURKA* relayed on *MAPK* downregulation (Wan et al., 2008). Taken together, these observations further support the higher malignant potential of SC-DDRenG2 cells', as they harbor both amplified AURKA and downregulated MAPK1. Finally, the groups of Scagliotti and Wang verified that particularly *AURKA* expression was associated with lung cancer histopathological classification, and more importantly with tumor dedifferentiation (Lo Iacono et al., 2011; Xu et al., 2006). In fact, both laboratories observed that AURKA amplification was associated with highly aggressive tumors that carry cells with less differentiated phenotypes.

Once confirmed the stem nature of SC-DRenG2 and SC-DDRenG2 isolated from DRenG2 and DDRenG2, respectively, it became unquestionable that a dedifferentiation process featured CSCs formation inside RenG2 cells while they were in the mouse lumbar subcutaneous compartment. This hypothesis was further sus-

tained by the progressive increment in CSCs sub-populations found along the derivative systems (DRenG2 and DDRenG2) (Figure 7.8, Chapter 7). Co-culture studies provided the final confirmation of this hypothesis, as iRenG2 cells, generated following co-culture of RenG2 with mouse stromal fibroblasts, portrayed the ability to form spheres when cultured in restraining conditions. Subsequent RT-qPCR and flow cytometry studies revealed that iRenG2 cells' signature, unlike their progenitor RenG2, was more similar to both DRenG2 and SC-DRenG2 signatures (Figures 8.8 and 8.9).

The multiplex array and ELISA experiments ultimately identified the drivers of RenG2 cells' dedifferentiation as being IL-6, G-CSF and Activin-A (Figures 8.10 and 8.11). The involvement of IL-6 in CSCs' formation have been previously suggested by the works of Levina and colleagues, who showed that CSC-derived tumors have increased levels this cytokine (Levina et al., 2008). The group of Struhl further sustained these suspicions by showing that IL-6 is sufficient to convert non-CSCs to CSCs in genetically different breast and prostate cell lines, and demonstrating that tumor heterogeneity involves an IL-6-mediated dynamic equilibrium between CSCs and non-CSCs (Iliopoulos et al., 2011). More recently, Xie and collaborators observed that EMT was involved in IL-6 driven CSCs' formation in breast cancer (Xie et al., 2012), while Kao's laboratory proved that IL-6-treated BEAS-2B cells displayed increased motility due to the activation of the AKT-pathway (Wang et al., 2012). Very recently, Kim and colleagues showed that breast cancer cells' dedifferentiation yielding CSCs relays on the activation of the IL-6-JAK1-STAT3-OCT-4 pathway (Kim et al., 2013b).

IL-6 is a pleiotropic cytokine produced by a myriad of cells with important roles in inflammatory response-based host defense (Kishimoto, 2010). It acts through its receptor (IL6R) activating JAK and subsequently STAT. STAT3, in particular, was shown to mediate the expression of various important genes in the context of cancer, namely *OCT-4*, *TWIST*, *SNAIL*, *VEGF* and *MMP-9* (Kim et al., 2013b). In addition, IL-6 was also shown to activate PI3K, NF_KB and MAPKs pathways (Kim

et al., 2013b; Lee et al., 2007). It is thus very plausible to admit the role of IL-6 in RenG2 cells' dedifferentiation, probably assisted by the amplification of *MMP-9*, *SNAI3*, *PRKCZ*, *PLEKHG5* and *TWIST2* genes revealed by aCGH study of the CSC systems (Figure 8.7).

Regarding G-CSF, it is considered a hematopoietic growth factor with important roles in neutrophils' differentiation (Baumann et al., 2005) and in response against bacterial infections (Nguyen-Jackson et al., 2010). Like IL-6, it is produced by a wide range of cells, including fibroblats, and is commonly present in tumors' stroma (Mueller and Fusenig, 2004). G-CSF was revealed to stimulate tumor angiogenesis (Shojaei et al., 2009) and, along with GM-CSF, to promote the malignant growth of some carcinomas (Gutschalk et al., 2006). Nonetheless, and perhaps more important in light of the attained results, IL-6 and G-CSF apparently work together on controlling the angiogenic potential of bone marrow resident monocytes. In agreement, Gregory and collaborators showed that tissue ischemia induced an increase of the systemic levels of both IL-6 and G-CSF (Gregory et al., 2010). As a consequence, these cytokines act over BM monocytes inducing their differentiation towards a TAM phenotype by stimulating the STAT3 pathway (Gregory et al., 2010; Yan et al., 2013). As presented in Chapter 1, hypoxia characterizes the majority of the tumors and represents one of body's great defenses against cancer (Denko, 2008). Tumor cells respond to hypoxia by releasing into circulation high levels of chemical mediators that will act over the endothelium and the BM to activate angiogenesis (Semenza, 2010). It is thus very likely that tumors also hijack this normal IL-6 and G-CSF-based physiological response to hypoxia to promote the angiogenic switch.

When cultured under the restraining sphere-forming assay condition, both the derivative cells underwent oxygen deprivation mainly as a consequence of the tridimensional sphere-form growth. It is plausible that G-CSF and IL-6 had been produced as a consequence of the hypoxic environment, ending up driving cells' dedifferentiation. Supporting this hypothesis, a group of the Baylor College of

Medicine showed that pancreatic cancer cells release high amounts of both IL-6 and G-CSF to their cell culture medium. Culture of $CD4^+$ monocytes in pancreatic cell-conditioned medium abrogated their differentiation into dendritic cells, thus favoring an undifferentiated phenotype (Bharadwaj et al., 2007).

Activin-A was identified as a mediator of RenG2 cells´ dedifferentiation. This TGF-β superfamily member acts in various biological processes ranging from cellular proliferation to differentiation and survival (Massague and Wotton, 2000). Its actions are mediated by the activin receptors I and II, each of which with two different isoforms. These receptors activate the SMAD2/SMAD3 intracellular complex, allowing its translocation into the nucleus and the activation of target genes (Tsuchida et al., 2009). With the discovery of SCs and iPS cells, new cell culture techniques were developed to maintain the stem potential of cells in culture. In the meantime, Beattie and colleagues discovered that Activin-A, abundantly secreted by fibroblasts feeder layers, had a potent stem-promoting action over human embryonic stem cells (hESCs) co-cultured with fibroblasts (Beattie et al., 2005). The same authors observed that supplementation of culture medium with Activin-A would avoid the need of a feeder layer on hESCs' culture. Rather simultaneously, the group of Pedersen showed that FGF pathway acts synergistically with Activin-A in mediating hESCs stemness under culture (Vallier et al., 2005). In pancreatic CSCs the upregulation of Activin-A pathway prompted CSCs' asymmetric division, thus contributing to their stem and increased malignant potential (Lonardo et al., 2011). Nonetheless, because the available literature reports provide antagonistic results, the role of this cytokine in tumor progression is still quite misunderstood. In fact, Activin-A has already been presented as a tumor suppressor and tumor promoting protein (reviewed by Antsiferova and Werner, 2012), and its function in tumor inflammation is rather controversial: while Zipori's laboratory observed that Activin-A actually antagonizes IL-6 pro-inflammatory actions (Zauberman et al., 2001), Jones and collaborators presented it as essential in tumor-promoting inflammatory responses (Jones et al., 2007). More recently, Hedg-

er and collaborators tried to meet consensus by proposing that Activin-A may be necessary to initiate inflammatory responses, but becomes dispensable during sustained inflammation (Hedger et al., 2011). Apart controversies, a strong correlation between increased systemic Activin-A levels and metastasis formation was reported in prostate and breast cancer patients (Incorvaia et al., 2007; Leto et al., 2006). Finally, previous work from Taketani's laboratory showed that some common tumor cytokines were able to mediate Activin-A overexpression in tumor cells, which in turn promoted IL-6 overexpression (Yoshino et al., 2011). As to G-CSF, no correlation was found between that cytokine and Activin-A.

The present results on the involvement of Activin-A in RenG2 cells' dedifferentiation, along with findings of Heeschen's and Taketani's groups, support a crucial role for Activin-A in cancer progression (Lonardo et al., 2011, Yoshino et al., 2011). Moreover, *ELAC2* amplification, a mediator of SMAD2 protein in Activin-A pathway (Noda et al., 2006), further consolidated the idea of a central role of this cytokine in RenG2 cells' dedifferentiation. Apparently, the Activin-A and IL-6 increased levels in the FR-RenG2 co-cultured cells were not arbitrary but rather a cause-consequence event.

8.4 Conclusion

The integrative strategy employed to characterize the SC-DRenG2 and SC-DDRenG2 systems yield a myriad of results that together provided clues on their formation and ultimately on the role played by Cr(VI) in the overall process. It is, to the best of our knowledge, the first time that increased Activin-A levels were associated with CSCs' formation, most particularly in lung cancer. Moreover, it now seems that Activin-A combined with IL-6 and G-CSF strongly shielded RenG2 cells from the attack of the aggressive mouse subcutaneous compartment environment. Acting cooperatively, these cytokines drove RenG2 cells' dedifferentia-

tion and rendered the resultant derivative systems considerably more resistant to hypoxia, starvation and death.

Note

The results presented in this chapter are part of a manuscript in preparation:

Rodrigues, CFD, Val, M, Rodrigues IP, Fonseca, J, Gomes CMF, Abrunhosa, AJ, Paiva, A, Carvalho, L, Botelho, MF, Carreira, IM and Alpoim, MC. Stromal cells-released IL-6, G-CSF and Activin-A induce dedifferentiation of lung carcinoma cells into cancer stem cells.

PART IV

General Discussion

Chapter 9

Final Integration

and Concluding Remarks

Even though chromium carcinogenesis is a very active field of research, no major steps have been taken in the recent years towards having an effective medical protocol to approach Cr(VI)-induced LC patients. In fact, despite the numerous reports in the literature indicating the fundamentally different genetic and pathophysiologic nature of chromate tumors, these neoplasias keep on being treated exactly the same way as tobacco or other carcinogen-induced LC.

Clinical advances relay on scientific knowledge generation and that, in turn, depends on the use of adequate laboratory disease models. As the rudimentary clinical approaches used in the treatment of chromate LC result from the inexistence of a reliable model for the study of such neoplasias, and consequently, from a bad bench-bedside correlation of the results attained *in vitro*, this project focused on developing a disease model. It was decided to depart from the immortalized normal human bronchial epithelial BEAS-2B cell line, as it better suited the present study, and to simply expose the cells to the sub-cytotoxic concentration of 1.0 μM Cr(VI). Nevertheless, as shown by Xie and collaborators, the Cr(VI)/cell ratio greatly limits Cr(VI)-uptake by the cells, which in turn modulates the carcinogenic actions of the oxyanion (Xie et al., 2004). As a consequence, it became evident that BEAS-2B would not be malignantly transformed by the first pro-

tocol we used, and therefore, a new low-density culture protocol was developed. Under these conditions, BEAS-2B cells' morphology deeply changed towards a malignant phenotype, being accompanied by the adoption of an expressome characteristic of malignant cells.

Against the observations of Zhitkovich's laboratory, Cr(VI)-driven BEAS-2B malignization did not involve MMR system inactivation nor MSI development (Reynolds et al., 2009). On contrary, BEAS-2B cells answered to the presence of Cr(VI) by overexpressing the genes coding for proteins of the DNA repair systems, thus indicating that the mutagenic effects of the oxyanion were at least approached by cellular repair machinery. Nonetheless, the near tetraploid karyotype of RenG2 cells suggested that cells may have taken too much time in repairing DNA lesions during S-phase, thus leading to cell division abrogation and formation of tetraploid cells carrying duplicated centrosomes. Most likely, the subsequent division of these cells drove the formation of the RenG2 cellular system, closely mimicking the results attained by Wise's group (Holmes et al., 2006). Preliminary immunocytochemistry results using a pericentrin Ab appear to validate this hypothesis, even though more studies are needed to assess centrosomes' role in BEAS-2B cells' malignization.

Tumorigenicity assays performed using RenG2 cells indicated that this cell line, though tumorigenic, was only mildly malignant. Following serial rounds of injection in athymic nude mice the derivative DRenG2 and DDRenG2 systems were attained. It was our rational that, by increasing RenG2 cells' malignant potential, Cr(VI) features imprinted in the cells would be exacerbated and thus better suitable for analysis. In fact, the derivation process *per si* promptly revealed the boosted malignant potential of the malignant systems as cells needed progressively less time to form tumors. Subsequently, the combination of assays selected in this project provided a group of results that altogether suggested the involvement of CSCs in BEAS-2B malignant transformation (Gottschling et al., 2012; Medema, 2013). Especially relevant were the glucose uptake studies performed using ^{18}FDG, which unveiled the lower glucose requirements of the more malignant derivative cell lines. Equally important were the drug resistance and the

migration assays that postulated the boosted resistance and migration ability of the newly attained cellular systems in comparison to RenG2 and the non-malignant BEAS-2B and Cont1 cell lines. The ultimate confirmation of CSCs' involvement was provided by the sphere-forming assay that showed that only the derivative systems (DRenG2 and DDRenG2) had the ability to form spheres under growth restraining conditions, particularly the DDRenG2 cell line. Moreover, these results also implied that a dedifferentiation process was involved in the formation of a CSC sub-population within the RenG2 system, although they provided no hint about the mechanisms or the orchestrators of this process.

After revisiting RenG2's formation protocol, it became evident that the dedifferentiation of RenG2 cells could only have occurred in the mice subcutaneous lumbar compartment, as it was the last place where RenG2 cells have been before giving rise to the DRenG2 cellular system. To validate this hypothesis a mouse lumbar fibroblasts' primary FR cell line was produced and co-culture experiments involving RenG2 and FR cells were performed using Transwell® devices. Once again, the sphere forming assay provided the final confirmation of FR-driven RenG2 cells' dedifferentiation, since this mildly malignant cellular population acquired the ability to form spheres following co-culture with FR cells.

Finally, beyond all experiments made to prove the similarities between iRenG2 cells and the DRenG2 and SC-DRenG2 cellular systems, the main efforts aimed at identifying the molecular orchestrators of the dedifferentiation process. As the protocol chosen to co-culture RenG2 and FR cells prevented physical contact between the two cellular populations, these orchestrators had to be paracrine soluble factors released by FR cells cultured in the bottom compartment. As paracrine communications are a potent weapon commonly hijacked by tumor cells to modulate their microenvironment, it was no surprise that such a mechanism was involved in RenG2 cells' dedifferentiation. The subsequent search for the guilty used sensitive molecular biology techniques and identified the IL-6, G-CSF and Activin-A cytokines as the molecular orchestrators of CSCs' for-

mation inside the RenG2 system. Mechanistically, literature hints suggest that IL-6 and Activin-A may have worked together to boost the survival of RenG2 cells' while they were inside the mice subcutaneous compartment, accidentally driving the activation of the IL-6-JAK1-STAT3-OCT-4 pathway, and consequently, their dedifferentiation (Kim et al., 2013b).

Altogether, the integrative strategy used in this process succeeded in attaining most of the initially established goals, namely:

- A new platform specifically tailored to examine the mechanisms underlying Cr(VI)-induced LC was produced;

- It became evident that the malignant transformation process triggered by low concentrations of soluble Cr(VI) rather involve the selection of Cr(VI)-resistant variants than the induction of DNA mutations;

- A dedifferentiation process leading to CSCs' formation was involved in the *in vi-vo* progression towards a more malignant phenotype of the first Cr(VI)-induced malignant system;

- The central role of the microenvironment in tumor biology was reinforced;

- IL-6 and Activin-A were identified as paracrine mediators of CSCs' formation, corroborating the observations made by other groups;

- G-CSF was implicated for the first time in the formation and maintenance of a CSC population;

- The dedifferentiation process was essentially chemical and specie-unspecific, as human cells can respond to mice cells-released molecules.

In conclusion, our results indicated that Cr(VI)-induced lung carcinogenesis is a very complex process that involves the activation of different cellular pathways and eventually the formation of CSCs. Unlike other neoplasias, ploidy unbalances rather than mutations seem to drive the transformation process, at least when low concentrations of chromium are used. Finally, the microenvironment plays a pivotal role in the overall process, acting like a maestro in mediating intercellular communications.

Chapter 10

Future Perspectives

The use of high throughput screenings for the analysis of biological samples usually provides an arsenal of information that more than delivering answers, opens new and numerous avenues of research. In fact, although a reliable model for the study of Cr(VI)-lung carcinogenesis has been established, it still has some edges that need to be polished. To that end, it would be very interesting to:

- Complete the characterization of the CSCs systems. Assess the presence of common CSCs markers of LC in SC-DRenG2 and SC-DDRenG2 cell lines, for instance CD133 and ALDH. In case they are not found, investigate new markers that may characterize Cr(VI)-induced malignant transformation. Evaluate the tumorigenic potential of all the cellular systems.

- Scrutinize the IL-6, G-CSF and Activin-A involvement in CSCs' formation. Dissect the IL-6-JAK1-STAT3-OCT-4 and Nodal-Activin pathways, and others that may seem relevant in CSCs' biology, perhaps by using iRNA technology to silence some of their key-players;

- Study the therapy-resistant cells. Preliminary observations made in our laboratory indicate that the cells that survived drug treatment have a boosted stem phenotype. Moreover, RenG2 cells appear to have acquired sphere-forming

ability following methotrexate treatment. Understanding the mechanisms of therapy resistance will most probably result in the design of a therapeutic approach for Cr(VI)-induced lung neoplasias;

- Deepen the analysis of aCGH results. Assess the role of some of the affected genes and understand how their deletion/amplification affected CSCs' dedifferentiation and the overall transformation process;
- Assess the metastatic potential of our entire repertoire of cellular systems. Confirm the hints provided by the many of the attaining results suggesting that the derivative systems are endowed with a higher migratory ability;

- Investigate the involvement of epigenetic events in BEAS-2B's malignization. According to the literature, epigenetic modulation of gene expression is an alternative avenue to attain malignant transformation. Considering that the Cr(VI) used in this study only induced a couple of chromosome alterations, it is plausible to admit that the epigenetic machinery may have contributed to the Cr(VI)-driven malignization process;

Finally, considering some promissory results attained using primary human bronchial fibroblats, it would be very interesting to reproduce at least parts of this project with a non-immortalized human bronchial epithelial system. Through this approach the distance between bench and bedside would be diminished and eventually patients' welfare would be ameliorated.

PART V

References

Adamson, I.Y., and Bowden, D.H. (1974). The type 2 cell as progenitor of alveolar epithelial regeneration. A cytodynamic study in mice after exposure to oxygen. Laboratory Investigation; a Journal of Technical Methods and Pathology *30*, 35–42.

Agnese, V., Bazan, V., Fiorentino, F.P., Fanale, D., Badalamenti, G., Colucci, G., Adamo, V., Santini, D., and Russo, a (2007). The role of Aurora-A inhibitors in cancer therapy. Annals of Oncology : Official Journal of the European Society for Medical Oncology / ESMO *18 Suppl 6*, vi47–52.

Alexander, J., and Aaseth, J. (1995). Uptake of chromate in human red blood cells and isolated rat liver cells: the role of the anion carrier. Analyst *120*, 931–933.

Al-Hajj, M., Becker, M.W., Wicha, M., Weissman, I., and Clarke, M.F. (2004). Therapeutic implications of cancer stem cells. Current Opinion in Genetics & Development *14*, 43–47.

Ames, B., and Gold, L. (1997). Environmental pollution, pesticides, and the prevention of cancer: misconceptions. The FASEB Journal *11*, 1041–1052.

Ananiev, J., Gulubova, M.V., and Manolova, I.M. (2011). Prognostic significance of CD83 positive tumor-infiltrating dendritic cells and expression of TGF-beta 1 in human gastric cancer. Hepato-gastroenterology *58*, 1834–1840.

Antsiferova, M., and Werner, S. (2012). The bright and the dark sides of activin in wound healing and cancer. Journal of Cell Science *125*, 3929–3937.

Arafat, K., Iratni, R., Takahashi, T., Parekh, K., Al Dhaheri, Y., Adrian, T.E., and Attoub, S. (2013). Inhibitory Effects of Salinomycin on Cell Survival, Colony Growth, Migration, and Invasion of Human Non-Small Cell Lung Cancer A549 and LNM35: Involvement of NAG-1. PloS One *8*, e66931.

Arakawa, H., Weng, M.-W., Chen, W.-C., and Tang, M. (2012). Chromium (VI) induces both bulky DNA adducts and oxidative DNA damage at adenines and guanines in the p53 gene of human lung cells. Carcinogenesis *33*, 1993–2000.

Armstrong, S.A., Staunton, J.E., Silverman, L.B., Pieters, R., den Boer, M.L., Minden, M.D., Sallan, S.E., Lander, E.S., Golub, T.R., and Korsmeyer, S.J. (2002). MLL translocations specify a distinct gene expression profile that distinguishes a unique leukemia. Nature Genetics *30*, 41–47.

Baeriswyl, V., and Christofori, G. (2009). The angiogenic switch in carcinogenesis. Seminars in Cancer Biology *19*, 329–337.

Bar, E.E., Chaudhry, A., Lin, A., Fan, X., Schreck, K., Matsui, W., Piccirillo, S., Vescovi, A.L., DiMeco, F., Olivi, A., et al. (2007). Cyclopamine-mediated hedgehog pathway inhibition depletes stem-like cancer cells in glioblastoma. Stem Cells (Dayton, Ohio) *25*, 2524–2533.

Barcellos-Hoff, M.H., Lyden, D., and Wang, T.C. (2013). The evolution of the cancer niche during multistage carcinogenesis. Nature Reviews. Cancer *13*, 511–518.

Barceloux, D. (1999). Chromium. Journal of Toxicology. Clinical Toxicology *37*, 173–194.

Barr, M.P., Gray, S.G., Hoffmann, A.C., Hilger, R. a, Thomale, J., O'Flaherty, J.D., Fennell, D. a, Richard, D., O'Leary, J.J., and O'Byrne, K.J. (2013). Generation and characterisation of cisplatin-resistant non-small cell lung cancer cell lines displaying a stem-like signature. PloS One *8*, e54193.

Baumann, M., Frye, T., Naqvi, T., and Gomez-Cambronero, J. (2005). Normal neutrophil maturation is associated with selective loss of MAP kinase activation by G-CSF. Leukemia Research *29*, 73–78.

Beattie, G.M., Lopez, A.D., Bucay, N., Hinton, A., Firpo, M.T., King, C.C., and Hayek, A. (2005). Activin A maintains pluripotency of human embryonic stem cells in the absence of feeder layers. Stem Cells (Dayton, Ohio) *23*, 489–495.

Beier, D., Hau, P., Proescholdt, M., Lohmeier, A., Wischhusen, J., Oefner, P.J., Aigner, L., Brawanski, A., Bogdahn, U., and Beier, C.P. (2007). CD133(+) and CD133(-) glioblastoma-derived cancer stem cells show differential growth characteristics and molecular profiles. Cancer Research *67*, 4010–4015.

Belo, A.I., van der Sar, A.M., Tefsen, B., and van Die, I. (2013). Galectin-4 Reduces Migration and Metastasis Formation of Pancreatic Cancer Cells. PloS One *8*, e65957.

Belogrudov, G.I., and Hatefi, Y. (2002). Factor B and the mitochondrial ATP synthase complex. The Journal of Biological Chemistry *277*, 6097–6103.

Bertolini, G., Roz, L., Perego, P., Tortoreto, M., Fontanella, E., Gatti, L., Pratesi, G., Fabbri, A., Andriani, F., Tinelli, S., et al. (2009). Highly tumorigenic lung cancer CD133+ cells display stem-like features and are spared by cisplatin treatment. Proceedings of the National Academy of Sciences of the United States of America *106*, 16281–16286.

Bharadwaj, U., Li, M., Zhang, R., Chen, C., and Yao, Q. (2007). Elevated interleukin-6 and G-CSF in human pancreatic cancer cell conditioned medium suppress dendritic cell differentiation and activation. Cancer Research *67*, 5479–5488.

Biedermann, K. a, and Landolph, J.R. (1990). Role of valence state and solubility of chromium compounds on induction of cytotoxicity, mutagenesis, and anchorage independence in diploid human fibroblasts. Cancer Research *50*, 7835–7842.

Blagosklonny, M. V (2002). Oncogenic resistance to growth-limiting conditions. Nature Reviews. Cancer *2*, 221–225.

Blanpain, C. (2012). Tracing the cellular origin of cancer. Nature Cell Biology *15*, 126–134.

Boël, P., Wildmann, C., Sensi, M.L., Brasseur, R., Renauld, J.C., Coulie, P., Boon, T., and van der Bruggen, P. (1995). BAGE: a new gene encoding an antigen recognized on human melanomas by cytolytic T lymphocytes. Immunity *2*, 167–175.

Bolós, V., Grego-Bessa, J., and de la Pompa, J.L. (2007). Notch signaling in development and cancer. Endocrine Reviews *28*, 339–363.

Borovski, T., De Sousa E Melo, F., Vermeulen, L., and Medema, J.P. (2011). Cancer stem cell niche: the place to be. Cancer Research *71*, 634–639.

Borthiry, G.R., Antholine, W.E., Myers, J.M., and Myers, C.R. (2008). Reductive activation of hexavalent chromium by human lung epithelial cells: generation of Cr(V) and Cr(V)-thiol species. Journal of Inorganic Biochemistry *102*, 1449–1462.

Bose, A., Barik, S., Banerjee, S., Ghosh, T., Mallick, A., Bhattacharyya Majumdar, S., Goswami, K.K., Bhuniya, A., Banerjee, S., Baral, R., et al. (2013). Tumor-derived vascular pericytes anergize Th cells. Journal of Immunology (Baltimore, Md. : 1950) *191*, 971–981.

Brooks, B., O'Brien, T.J., Ceryak, S., Wise, J.P., Wise, S.S., Defabo, E., and Patierno, S.R. (2008). Excision repair is required for genotoxin-induced mutagenesis in mammalian cells. Carcinogenesis *29*, 1064–1069.

Brooks, D.R., Austin, J.H.M., Heelan, R.T., Ginsberg, M.S., Shin, V., Olson, S.H., Muscat, J.E., and Stellman, S.D. (2005). Influence of type of cigarette on peripheral versus central lung cancer. Cancer Epidemiology, Biomarkers & Prevention : a Publication of the American Association for Cancer Research, Cosponsored by the American Society of Preventive Oncology *14*, 576–581.

Brown, J.R., and Thornton, J.L. (1957). Percivall Pott (1714-1788) and chimney sweepers' cancer of the scrotum. British Journal of Industrial Medicine *14*, 68–70.

Brugge, D., Durant, J.L., and Rioux, C. (2007). Near-highway pollutants in motor vehicle exhaust: a review of epidemiologic evidence of cardiac and pulmonary health risks. Environmental Health : a Global Access Science Source *6*, 23.

Buhard, O., Suraweera, N., Lectard, A., Duval, A., and Hamelin, R. (2004). Quasimonomorphic mononucleotide repeats for high-level microsatellite instability analysis. Disease Markers *20*, 251–257.

Cagliani, R., Guerini, F.R., Fumagalli, M., Riva, S., Agliardi, C., Galimberti, D., Pozzoli, U., Goris, a, Dubois, B., Fenoglio, C., et al. (2012). A trans-specific polymorphism in ZC3HAV1 is maintained by long-standing balancing selection and may confer susceptibility to multiple sclerosis. Molecular Biology and Evolution *29*, 1599–1613.

Cai, W.-Y., Wei, T.-Z., Luo, Q.-C., Wu, Q.-W., Liu, Q.-F., Yang, M., Ye, G.-D., Wu, J.-F., Chen, Y.-Y., Sun, G.-B., et al. (2013). The Wnt-β-catenin pathway represses let-7

microRNA expression through transactivation of Lin28 to augment breast cancer stem cell expansion. Journal of Cell Science *126*, 2877–2889.

Calvo, S.E., Tucker, E.J., Compton, A.G., Kirby, D.M., Crawford, G., Burtt, N.P., Rivas, M., Guiducci, C., Bruno, D.L., Goldberger, O.A., et al. (2010). High-throughput, pooled sequencing identifies mutations in NUBPL and FOXRED1 in human complex I deficiency. Nature Genetics *42*, 851–858.

Carmeliet, P., and Jain, R.K. (2011). Molecular mechanisms and clinical applications of angiogenesis. Nature *473*, 298–307.

Castedo, M., Coquelle, A., Vitale, I., Vivet, S., Mouhamad, S., Viaud, S., Zitvogel, L., and Kroemer, G. (2006). Selective resistance of tetraploid cancer cells against DNA damage-induced apoptosis. Annals of the New York Academy of Sciences *1090*, 35–49.

Center, R., Lukeis, R., Vrazas, V., and Garson, O.M. (1993). Y chromosome loss and rearrangement in non-small-cell lung cancer. International Journal of Cancer. Journal International Du Cancer *55*, 390–393.

Chaffer, C.L., Brueckmann, I., Scheel, C., Kaestli, A.J., Wiggins, P.A., Rodrigues, L.O., Brooks, M., Reinhardt, F., Su, Y., Polyak, K., et al. (2011). Normal and neoplastic nonstem cells can spontaneously convert to a stem-like state. Proceedings of the National Academy of Sciences of the United States of America *108*, 7950–7955.

Chen, C., Pore, N., Behrooz, A., Ismail-Beigi, F., and Maity, A. (2001). Regulation of glut1 mRNA by hypoxia-inducible factor-1. Interaction between H-ras and hypoxia. The Journal of Biological Chemistry *276*, 9519–9525.

Chen, R., Nishimura, M.C., Bumbaca, S.M., Kharbanda, S., Forrest, W.F., Kasman, I.M., Greve, J.M., Soriano, R.H., Gilmour, L.L., Rivers, C.S., et al. (2010). A hierarchy of self-renewing tumor-initiating cell types in glioblastoma. Cancer Cell *17*, 362–375.

Chen, Y.-C., Chen, Y.-W., Hsu, H.-S., Tseng, L.-M., Huang, P.-I., Lu, K.-H., Chen, D.-T., Tai, L.-K., Yung, M.-C., Chang, S.-C., et al. (2009). Aldehyde dehydrogenase 1 is a putative marker for cancer stem cells in head and neck squamous cancer. Biochemical and Biophysical Research Communications *385*, 307–313.

Cheng, N., Bhowmick, N., and Chytil, A. (2005). Loss of TGF-β type II receptor in fibroblasts promotes mammary carcinoma growth and invasion through upregulation of TGF-α-, MSP-and HGF-mediated signaling networks. Oncogene *24*, 5053–5068.

Chiang, A.C., and Massagué, J. (2008). Molecular basis of metastasis. The New England Journal of Medicine *359*, 2814–2823.

Chuang, S.M., and Yang, J.L. (2001). Comparison of roles of three mitogen-activated protein kinases induced by chromium(VI) and cadmium in non-small-cell lung carcinoma cells. Molecular and Cellular Biochemistry *222*, 85–95.

Clapp, R.W., Jacobs, M.M., and Loechler, E.L. (2008). Environmental and occupational causes of cancer: new evidence 2005-2007. Reviews on Environmental Health *23*, 1–37.

Clevers, H. (2006). Wnt/beta-catenin signaling in development and disease. Cell *127*, 469–480.

Collins, S., and Groudine, M. (1982). Amplification of endogenous myc-related DNA sequences in a human myeloid leukaemia cell line. Nature *298*, 679–681.

Coni, S., Infante, P., and Gulino, A. (2013). Control of stem cells and cancer stem cells by Hedgehog signaling: pharmacologic clues from pathway dissection. Biochemical Pharmacology *85*, 623–628.

Costa, N., Moreno, V., Prieto, J., Urbano, A.M., and Alpoim, M.C. (2010). Induction of Morphological Changes in BEAS-2B Human Bronchial Epithelial Cells Following Chronic Sub-Cytotoxic and Mildly Cytotoxic Hexavalent Chromium Exposures. MOLECULAR CARCINOGENESIS *49*, 582–591.

Coussens, L.M., Raymond, W.W., Bergers, G., Laig-Webster, M., Behrendtsen, O., Werb, Z., Caughey, G.H., and Hanahan, D. (1999). Inflammatory mast cells up-regulate angiogenesis during squamous epithelial carcinogenesis. Genes & Development *13*, 1382–1397.

Da Cunha Santos, G., Shepherd, F.A., and Tsao, M.S. (2011). EGFR mutations and lung cancer. Annual Review of Pathology *6*, 49–69.

Darai-Ramqvist, E., Diaz de Ståhl, T., Sandlund, A., Mantripragada, K., Klein, G., Dumanski, J., Imreh, S., and Kost-Alimova, M. (2006). Array-CGH and multipoint FISH to decode complex chromosomal rearrangements. BMC Genomics *7*, 330.

Davies, J.M. (1984). Lung cancer mortality among workers making lead chromate and zinc chromate pigments at three English factories. British Journal of Industrial Medicine *41*, 158–169.

DeBerardinis, R.J., Lum, J.J., Hatzivassiliou, G., and Thompson, C.B. (2008). The biology of cancer: metabolic reprogramming fuels cell growth and proliferation. Cell Metabolism *7*, 11–20.

Dembinski, J.L., and Krauss, S. (2010). A Distinct Slow-Cycling Cancer Stem-like Subpopulation of Pancreatic Adenocarcinoma Cells is maintained in Vivo. Cancers *2*, 2011–2025.

Denko, N.C. (2008). Hypoxia, HIF1 and glucose metabolism in the solid tumour. Nature Reviews. Cancer *8*, 705–713.

Dertsiz, L., Ozbilim, G., Kayisli, Y., Gokhan, G. a, Demircan, a, and Kayisli, U. a (2005). Differential expression of VASP in normal lung tissue and lung adenocarcinomas. Thorax *60*, 576–581.

Devesa, S.S., Bray, F., Vizcaino, a P., and Parkin, D.M. (2005). International lung cancer trends by histologic type: male:female differences diminishing and adenocarcinoma rates rising. International Journal of Cancer. Journal International Du Cancer *117*, 294–299.

Duesberg, P., and Li, R. (2003). Multistep carcinogenesis: a chain reaction of aneuploidizations. Cell Cycle (Georgetown, Tex.) *2*, 202–210.

Dvorak, H. (1986). Tumors: wounds that do not heal. Similarities between tumor stroma generation and wound healing. New England Journal of Medicine *315*, 1650–1659.

Eramo, a, Lotti, F., Sette, G., Pilozzi, E., Biffoni, M., Di Virgilio, a, Conticello, C., Ruco, L., Peschle, C., and De Maria, R. (2008). Identification and expansion of the tumorigenic lung cancer stem cell population. Cell Death and Differentiation *15*, 504–514.

Eramo, A., Haas, T.L., and De Maria, R. (2010). Lung cancer stem cells: tools and targets to fight lung cancer. Oncogene *29*, 4625–4635.

Erler, J., Bennewith, K., Cox, T., and Lang, G. (2009). Hypoxia-induced lysyl oxidase is a critical mediator of bone marrow cell recruitment to form the premetastatic niche. Cancer Cell *15*, 35–44.

Van Es, J.H., van Gijn, M.E., Riccio, O., van den Born, M., Vooijs, M., Begthel, H., Cozijnsen, M., Robine, S., Winton, D.J., Radtke, F., et al. (2005). Notch/gamma-secretase inhibition turns proliferative cells in intestinal crypts and adenomas into goblet cells. Nature *435*, 959–963.

Fakhrejahani, E., and Toi, M. (2012). Tumor angiogenesis: pericytes and maturation are not to be ignored. Journal of Oncology *2012*, 261750.

Fang, J.-Y., Cheng, Z.-H., Chen, Y.-X., Lu, R., Yang, L., Zhu, H.-Y., and Lu, L.-G. (2004). Expression of Dnmt1, demethylase, MeCP2 and methylation of tumor-related genes in human gastric cancer. World Journal of Gastroenterology : WJG *10*, 3394–3398.

Felton, J.S. (1997). The heritage of Bernardino Ramazzini. Occupational Medicine (Oxford, England) *47*, 167–179.

Fernandez-Vizarra, E., Bugiani, M., Goffrini, P., Carrara, F., Farina, L., Procopio, E., Donati, A., Uziel, G., Ferrero, I., and Zeviani, M. (2007). Impaired complex III assembly associated with BCS1L gene mutations in isolated mitochondrial encephalopathy. Human Molecular Genetics *16*, 1241–1252.

Figgitt, M., Newson, R., Leslie, I.J., Fisher, J., Ingham, E., and Case, C.P. (2010). The genotoxicity of physiological concentrations of chromium (Cr(III) and Cr(VI)) and cobalt (Co(II)): an in vitro study. Mutation Research *688*, 53–61.

Firket, J. (1958). The problem of cancer of the lung in the industrial area of Liège during recent years. Proceedings of the Royal Society of Medicine 347–352.

Folkins, C., Man, S., Xu, P., Shaked, Y., Hicklin, D.J., and Kerbel, R.S. (2007). Anticancer therapies combining antiangiogenic and tumor cell cytotoxic effects reduce the tumor stem-like cell fraction in glioma xenograft tumors. Cancer Research *67*, 3560–3564.

Frank, N.Y., Schatton, T., and Frank, M.H. (2010). The therapeutic promise of the cancer stem cell concept. The Journal of Clinical Investigation *120*, 41–50.

Franken, N. a P., Rodermond, H.M., Stap, J., Haveman, J., and van Bree, C. (2006). Clonogenic assay of cells in vitro. Nature Protocols *1*, 2315–2319.

Fujiwara, T., Bandi, M., Nitta, M., Ivanova, E. V, Bronson, R.T., and Pellman, D. (2005). Cytokinesis failure generating tetraploids promotes tumorigenesis in p53-null cells. Nature *437*, 1043–1047.

Gabrielson, E. (2006). Worldwide trends in lung cancer pathology. Respirology *2006*, 533–538.

Gaggioli, C., Hooper, S., Hidalgo-Carcedo, C., Grosse, R., Marshall, J., Harrington, K., and Sahai, E. (2007). Fibroblast-led collective invasion of carcinoma cells with differing roles for RhoGTPases in leading and following cells. Nature Cell Biology *9*, 1392–1400.

Ganem, N.J., Storchova, Z., and Pellman, D. (2007). Tetraploidy, aneuploidy and cancer. Current Opinion in Genetics & Development *17*, 157–162.

Ganem, N.J., Godinho, S. a, and Pellman, D. (2009). A mechanism linking extra centrosomes to chromosomal instability. Nature *460*, 278–282.

Gardina, P.J., Lo, K.C., Lee, W., Cowell, J.K., and Turpaz, Y. (2008). Ploidy status and copy number aberrations in primary glioblastomas defined by integrated analysis of allelic ratios, signal ratios and loss of heterozygosity using 500K SNP Mapping Arrays. BMC Genomics *9*, 489.

Garrison, F.H. (1926). The history of cancer. Bulletin of the New York Academy of Medicine *2*, 179–185.

Garvalov, B.K., and Acker, T. (2011). Cancer stem cells: a new framework for the design of tumor therapies. Journal of Molecular Medicine (Berlin, Germany) *89*, 95–107.

Giangreco, A., Reynolds, S.D., and Stripp, B.R. (2002). Terminal bronchioles harbor a unique airway stem cell population that localizes to the bronchoalveolar duct junction. The American Journal of Pathology *161*, 173–182.

Gocheva, V., Wang, H.-W., Gadea, B.B., Shree, T., Hunter, K.E., Garfall, A.L., Berman, T., and Joyce, J. a (2010). IL-4 induces cathepsin protease activity in tumor-associated macrophages to promote cancer growth and invasion. Genes & Development *24*, 241–255.

Godinho, S. a, Kwon, M., and Pellman, D. (2009). Centrosomes and cancer: how cancer cells divide with too many centrosomes. Cancer Metastasis Reviews *28*, 85–98.

Goldstraw, P., Ball, D., Jett, J.R., Chevalier, T. Le, Lim, E., Nicholson, A.G., and Shepherd, F.A. (2011). Non-small-cell lung cancer. The Lancet *378*, 1727 – 1740.

Gong, A., and Huang, S. (2012). FoxM1 and Wnt/β-catenin signaling in glioma stem cells. Cancer Research *72*, 5658–5662.

Goodarzi, M.O., Lehman, D.M., Taylor, K.D., Guo, X., Cui, J., Quiñones, M.J., Clee, S.M., Yandell, B.S., Blangero, J., Hsueh, W.A., et al. (2007). SORCS1: a novel human type 2 diabetes susceptibility gene suggested by the mouse. Diabetes *56*, 1922–1929.

Goodell, M.A. (2005). Stem cell identification and sorting using the Hoechst 33342 side population (SP). Current Protocols in Cytometry / Editorial Board, J. Paul Robinson, Managing Editor ... [et Al.] *Chapter 9*, Unit9.18.

Goodell, M.A., Brose, K., Paradis, G., Conner, A.S., and Mulligan, R.C. (1996). Isolation and functional properties of murine hematopoietic stem cells that are replicating in vivo. The Journal of Experimental Medicine *183*, 1797–1806.

Gordan, J.D., Thompson, C.B., and Simon, M.C. (2007). HIF and c-Myc: sibling rivals for control of cancer cell metabolism and proliferation. Cancer Cell *12*, 108–113.

Gordon, D.J., Resio, B., and Pellman, D. (2012). Causes and consequences of aneuploidy in cancer. Nature Reviews. Genetics *13*, 189–203.

Gottschling, S., Schnabel, P. a, Herth, F.J.F., and Herpel, E. (2012). Are we missing the target? Cancer stem cells and drug resistance in non-small cell lung cancer. Cancer Genomics & Proteomics *9*, 275–286.

Goubran, H. a, Burnouf, T., Radosevic, M., and El-Ekiaby, M. (2013). The platelet-cancer loop. European Journal of Internal Medicine *24*, 393–400.

Gregory, A.D., Capoccia, B.J., Woloszynek, J.R., and Link, D.C. (2010). Systemic levels of G-CSF and interleukin-6 determine the angiogenic potential of bone marrow resident monocytes. Journal of Leukocyte Biology *88*, 123–131.

Grlickova-Duzevik, E., Wise, S.S., Munroe, R.C., Thompson, W.D., and Wise, J.P. (2006). XRCC1 protects cells from chromate-induced chromosome damage, but does not affect cytotoxicity. Mutation Research *610*, 31–37.

Gupta, G., Nguyen, D., Chiang, A., Bos, P., Kim, J., Nadal, C., Gomis, R., Manova-Todorova, K., and Massagué, J. (2007). Mediators of vascular remodeling co-opted for sequential steps in lung metastasis. Nature *446*, 765–770.

Gupta, P.B., Onder, T.T., Jiang, G., Tao, K., Kuperwasser, C., Weinberg, R. a, and Lander, E.S. (2009). Identification of selective inhibitors of cancer stem cells by high-throughput screening. Cell *138*, 645–659.

Haddow, A. (1936). Historical Notes on Cancer from the MSS. of Louis Westenra Sambon. Proceedings of the Royal Society of Medicine *XXIX*, 19–32.

Hajdu, S.I. (2011a). A note from history: landmarks in history of cancer, part 1. Cancer *117*, 1097–1102.

Hajdu, S.I. (2011b). A note from history: landmarks in history of cancer, part 2. Cancer *117*, 2811–2820.

Hajdu, S.I. (2012a). A note from history: landmarks in history of cancer, part 3. Cancer *118*, 1155–1168.

Hajdu, S.I. (2012b). A note from history: landmarks in history of cancer, part 4. Cancer *118*, 4914–4928.

Hajdu, S.I., and Darvishian, F. (2013). A note from history: landmarks in history of cancer, part 5. Cancer *119*, 1450–1466.

Hanahan, D., and Coussens, L.M. (2012). Accessories to the crime: functions of cells recruited to the tumor microenvironment. Cancer Cell *21*, 309–322.

Hanahan, D., and Folkman, J. (1996). Patterns and emerging mechanisms of the angiogenic switch during tumorigenesis. Cell *86*, 353–364.

Hanahan, D., and Weinberg, R. (2000). The hallmarks of cancer. Cell *100*, 57–70.

Hanahan, D., and Weinberg, R.A. (2011). Hallmarks of cancer: the next generation. Cell *144*, 646–674.

Harada, M., Yokose, T., Yoshida, J., Nishiwaki, Y., and Nagai, K. (2002). Immunohistochemical neuroendocrine differentiation is an independent prognostic factor in surgically resected large cell carcinoma of the lung. Lung Cancer *38*, 177–184.

Harfe, B.D., and Jinks-Robertson, S. (2000). DNA mismatch repair and genetic instability. Annual Review of Genetics *34*, 359–399.

Harper, L.J., Costea, D.E., Gammon, L., Fazil, B., Biddle, A., and Mackenzie, I.C. (2010). Normal and malignant epithelial cells with stem-like properties have an extended G2 cell cycle phase that is associated with apoptotic resistance. BMC Cancer *10*, 166.

Harvey, a J., Kind, K.L., and Thompson, J.G. (2007). Regulation of gene expression in bovine blastocysts in response to oxygen and the iron chelator desferrioxamine. Biology of Reproduction *77*, 93–101.

Hecht, S.S. (1998). Biochemistry, biology, and carcinogenicity of tobacco-specific N-nitrosamines. Chemical Research in Toxicology *11*, 559–603.

Hedger, M.P., Winnall, W.R., Phillips, D.J., and de Kretser, D.M. (2011). The regulation and functions of activin and follistatin in inflammation and immunity. Vitamins and Hormones *85*, 255–297.

Vander Heiden, M.G., Cantley, L.C., and Thompson, C.B. (2009). Understanding the Warburg effect: the metabolic requirements of cell proliferation. Science (New York, N.Y.) *324*, 1029–1033.

Hermann, P.C., Huber, S.L., Herrler, T., Aicher, A., Ellwart, J.W., Guba, M., Bruns, C.J., and Heeschen, C. (2007). Distinct populations of cancer stem cells determine tumor growth and metastatic activity in human pancreatic cancer. Cell Stem Cell *1*, 313–323.

Hillen, F., and Griffioen, A.W. (2007). Tumour vascularization: sprouting angiogenesis and beyond. Cancer Metastasis Reviews *26*, 489–502.

Hirose, T., Kondo, K., Takahashi, Y., Ishikura, H., Fujino, H., Tsuyuguchi, M., Hashimoto, M., Yokose, T., Mukai, K., Kodama, T., et al. (2002). Frequent microsatellite instability in lung cancer from chromate-exposed workers. Molecular Carcinogenesis *33*, 172–180.

Hoey, T., Yen, W.-C., Axelrod, F., Basi, J., Donigian, L., Dylla, S., Fitch-Bruhns, M., Lazetic, S., Park, I.-K., Sato, A., et al. (2009). DLL4 blockade inhibits tumor growth and reduces tumor-initiating cell frequency. Cell Stem Cell *5*, 168–177.

Holash, J. (1999). Vessel Cooption, Regression, and Growth in Tumors Mediated by Angiopoietins and VEGF. Science *284*, 1994–1998.

Holmes, A.L., Wise, S.S., Sandwick, S.J., Lingle, W.L., Negron, V.C., Thompson, W.D., and Wise, J.P. (2006). Chronic exposure to lead chromate causes centrosome abnormalities and aneuploidy in human lung cells. Cancer Research *66*, 4041–4048.

Holmes, A.L., Wise, S.S., Pelsue, S.C., Aboueissa, A.-M., Lingle, W., Salisbury, J., Gallagher, J., and Wise, J.P. (2010). Chronic exposure to zinc chromate induces centrosome amplification and spindle assembly checkpoint bypass in human lung fibroblasts. Chemical Research in Toxicology *23*, 386–395.

Hong, K.U., Reynolds, S.D., Watkins, S., Fuchs, E., and Stripp, B.R. (2004). Basal cells are a multipotent progenitor capable of renewing the bronchial epithelium. The American Journal of Pathology *164*, 577–588.

Hovinga, K.E., Shimizu, F., Wang, R., Panagiotakos, G., Van Der Heijden, M., Moayedpardazi, H., Correia, A.S., Soulet, D., Major, T., Menon, J., et al. (2010). Inhibition of notch signaling in glioblastoma targets cancer stem cells via an endothelial cell intermediate. Stem Cells (Dayton, Ohio) *28*, 1019–1029.

Huang, C.-P., Tsai, M.-F., Chang, T.-H., Tang, W.-C., Chen, S.-Y., Lai, H.-H., Lin, T.-Y., Yang, J.C.-H., Yang, P.-C., Shih, J.-Y., et al. (2013). ALDH-positive lung cancer stem cells confer resistance to epidermal growth factor receptor tyrosine kinase inhibitors. Cancer Letters *328*, 144–151.

Huang, E., Hynes, M., Zhang, T., and Ginestier, C. (2009). Aldehyde dehydrogenase 1 is a marker for normal and malignant human colonic stem cells (SC) and tracks SC overpopulation during colon tumorigenesis. Cancer Research *69*, 3382–3389.

Huang, F.-T., Zhuan-Sun, Y.-X., Zhuang, Y.-Y., Wei, S.-L., Tang, J., Chen, W.-B., and Zhang, S.-N. (2012). Inhibition of hedgehog signaling depresses self-renewal of pancreatic cancer stem cells and reverses chemoresistance. International Journal of Oncology *41*, 1707–1714.

Huebner, R.J., and Todaro, G.J. (1969). Oncogenes of RNA tumor viruses as determinants of cancer. Proceedings of the National Academy of Sciences of the United States of America *64*, 1087–1094.

Hung, K., Hayashi, R., Lafond-Walker, a, Lowenstein, C., Pardoll, D., and Levitsky, H. (1998). The central role of CD4(+) T cells in the antitumor immune response. The Journal of Experimental Medicine *188*, 2357–2368.

Lo Iacono, M., Monica, V., Saviozzi, S., Ceppi, P., Bracco, E., Papotti, M., and Scagliotti, G. V (2011). Aurora Kinase A expression is associated with lung cancer histological-subtypes and with tumor de-differentiation. Journal of Translational Medicine *9*, 100.

Ice, R.J., McLaughlin, S.L., Livengood, R.H., Culp, M. V, Eddy, E.R., Ivanov, A. V, and Pugacheva, E.N. (2013). NEDD9 depletion destabilizes Aurora A kinase and heightens the efficacy of Aurora A inhibitors: implications for treatment of metastatic solid tumors. Cancer Research *73*, 3168–3180.

Incorvaia, L., Badalamenti, G., Rini, G., Arcara, C., Fricano, S., Sferrazza, C., Di Trapani, D., Gebbia, N., and Leto, G. (2007). MMP-2, MMP-9 and activin A blood levels in patients with breast cancer or prostate cancer metastatic to the bone. Anticancer Research *27*, 1519–1525.

Ishikawa, Y., Nakagawa, K., Satoh, Y., Kitagawa, T., Sugano, H., Hirano, T., and Tsuchiya, E. (1994a). “Hot spots” of chromium accumulation at bifurcations of chromate workers’ bronchi. Cancer Research *54*, 2342–2346.

Ishikawa, Y., Nakagawa, K., Satoh, Y., Kitagawa, T., Sugano, H., Hirano, T., and Tsuchiya, E. (1994b). Characteristics of chromate workers’ cancers, chromium lung deposition

and precancerous bronchial lesions: an autopsy study. British Journal of Cancer *70*, 160–166.

Ithimakin, S., Day, K.C., Malik, F., Zen, Q., Dawsey, S.J., Bersano-Begey, T.F., Quraishi, A.A., Ignatoski, K.W., Daignault, S., Davis, A., et al. (2013). HER2 drives luminal breast cancer stem cells in the absence of HER2 amplification: implications for efficacy of adjuvant trastuzumab. Cancer Research *73*, 1635–1646.

Izumiya, M., Kabashima, A., Higuchi, H., Igarashi, T., Sakai, G., Iizuka, H., Nakamura, S., Adachi, M., Hamamoto, Y., Funakoshi, S., et al. (2012). Chemoresistance is associated with cancer stem cell-like properties and epithelial-to-mesenchymal transition in pancreatic cancer cells. Anticancer Research *32*, 3847–3853.

Jackman, D.M., and Johnson, B.E. (2005). Small-cell lung cancer. The Lancet *366*, 1385–1396.

Jiang, Y., Zhu, Y., Shi, Y., He, Y., Kuang, Z., Sun, Z., and Wang, J. (2013). Downregulation of SPARC Expression Inhibits the Invasion of Human Trophoblast Cells In Vitro. PloS One *8*, e69079.

Jiang, Z., Jin, S., Yalowich, J.C., Brown, K.D., and Rajasekaran, B. (2010). The mismatch repair system modulates curcumin sensitivity through induction of DNA strand breaks and activation of G2-M checkpoint. Molecular Cancer Therapeutics *9*, 558–568.

Jones, K.L., Mansell, A., Patella, S., Scott, B.J., Hedger, M.P., de Kretser, D.M., and Phillips, D.J. (2007). Activin A is a critical component of the inflammatory response, and its binding protein, follistatin, reduces mortality in endotoxemia. Proceedings of the National Academy of Sciences of the United States of America *104*, 16239–16244.

Joo, K.M., Kim, S.Y., Jin, X., Song, S.Y., Kong, D.-S., Lee, J.-I., Jeon, J.W., Kim, M.H., Kang, B.G., Jung, Y., et al. (2008). Clinical and biological implications of CD133-positive and CD133-negative cells in glioblastomas. Laboratory Investigation; a Journal of Technical Methods and Pathology *88*, 808–815.

Joyce, J. a, and Pollard, J.W. (2009). Microenvironmental regulation of metastasis. Nature Reviews. Cancer *9*, 239–252.

Kalluri, R., and Weinberg, R.A. (2009). The basics of epithelial-mesenchymal transition. The Journal of Clinical Investigation *119*, 1420–1428.

Kamphorst, J.J., Cross, J.R., Fan, J., de Stanchina, E., Mathew, R., White, E.P., Thompson, C.B., and Rabinowitz, J.D. (2013). Hypoxic and Ras-transformed cells support growth by scavenging unsaturated fatty acids from lysophospholipids. Proceedings of the National Academy of Sciences of the United States of America *110*, 8882–8887.

Kemper, K., Sprick, M.R., de Bree, M., Scopelliti, A., Vermeulen, L., Hoek, M., Zeilstra, J., Pals, S.T., Mehmet, H., Stassi, G., et al. (2010). The AC133 epitope, but not the CD133 protein, is lost upon cancer stem cell differentiation. Cancer Research *70*, 719–729.

Kevelam, S.H., Rodenburg, R.J., Wolf, N.I., Ferreira, P., Lunsing, R.J., Nijtmans, L.G., Mitchell, A., Arroyo, H.A., Rating, D., Vanderver, A., et al. (2013). NUBPL mutations in patients with complex I deficiency and a distinct MRI pattern. Neurology *80*, 1577–1583.

Khazaie, K., Blatner, N.R., Khan, M.W., Gounari, F., Gounaris, E., Dennis, K., Bonertz, A., Tsai, F.-N., Strouch, M.J., Cheon, E., et al. (2011). The significant role of mast cells in cancer. Cancer Metastasis Reviews *30*, 45–60.

Khong, H.T., and Restifo, N.P. (2002). Natural selection of tumor variants in the generation of "tumor escape" phenotypes. Nature Immunology *3*, 999–1005.

Kim, C.F.B., Jackson, E.L., Woolfenden, A.E., Lawrence, S., Babar, I., Vogel, S., Crowley, D., Bronson, R.T., and Jacks, T. (2005). Identification of bronchioalveolar stem cells in normal lung and lung cancer. Cell *121*, 823–835.

Kim, H.-R., Roe, J.-S., Lee, J.-E., Cho, E.-J., and Youn, H.-D. (2013a). p53 regulates glucose metabolism by miR-34a. Biochemical and Biophysical Research Communications 1–7.

Kim, M., Trinh, B.N., Long, T.I., Oghamian, S., and Laird, P.W. (2004). Dnmt1 deficiency leads to enhanced microsatellite instability in mouse embryonic stem cells. Nucleic Acids Research *32*, 5742–5749.

Kim, S.-Y., Kang, J.W., Song, X., Kim, B.K., Yoo, Y.D., Kwon, Y.T., and Lee, Y.J. (2013b). Role of the IL-6-JAK1-STAT3-Oct-4 pathway in the conversion of non-stem cancer cells into cancer stem-like cells. Cellular Signalling *25*, 961–969.

Kishimoto, T. (2010). IL-6: from its discovery to clinical applications. International Immunology *22*, 347–352.

Kitamura, H., Okudela, K., Yazawa, T., Sato, H., and Shimoyamada, H. (2009). Cancer stem cell: implications in cancer biology and therapy with special reference to lung cancer. Lung Cancer (Amsterdam, Netherlands) *66*, 275–281.

Knowles, L.M., Malik, G., and Pilch, J. (2013). Plasma Fibronectin Promotes Tumor Cell Survival and Invasion through Regulation of Tie2. Journal of Cancer *4*, 383–390.

Kondo, K., Takahashi, Y., Ishikawa, S., Uchihara, H., Hirose, Y., Yoshizawa, K., Tsuyuguchi, M., Takizawa, H., Miyoshi, T., Sakiyama, S., et al. (2003). Microscopic analysis of chromium accumulation in the bronchi and lung of chromate workers. Cancer *98*, 2420–2429.

Kondo, K., Takahashi, Y., Hirose, Y., Nagao, T., Tsuyuguchi, M., Hashimoto, M., Ochiai, A., Monden, Y., and Tangoku, A. (2006). The reduced expression and aberrant methylation of p16(INK4a) in chromate workers with lung cancer. Lung Cancer (Amsterdam, Netherlands) *53*, 295–302.

Koo, K.H., Kim, H., Bae, Y.-K., Kim, K., Park, B.-K., Lee, C.-H., and Kim, Y.-N. (2013). Salinomycin induces cell death via inactivation of Stat3 and downregulation of Skp2. Cell Death & Disease *4*, e693.

Kotaś, J., and Stasicka, Z. (2000). Chromium occurrence in the environment and methods of its speciation. Environmental Pollution (Barking, Essex : 1987) *107*, 263–283.

Kristjansson, A.K., Eiriksdottir, G., Ragnarsson, G., Sigurdsson, A., Gudmundsson, J., Barkardottir, R.B., Jonasson, J.G., Egilsson, V., and Ingvarsson, S. (1997). Loss of heterozygosity at chromosome 7q in human breast cancer: association with clinical variables. Anticancer Research *17*, 93–98.

Lane, R.F., Steele, J.W., Cai, D., Ehrlich, M.E., Attie, A.D., and Gandy, S. (2013). Protein sorting motifs in the cytoplasmic tail of SorCS1 control generation of Alzheimer's amyloid-β peptide. The Journal of Neuroscience : the Official Journal of the Society for Neuroscience *33*, 7099–7107.

Langård, S. (1990). One hundred years of chromium and cancer: a review of epidemiological evidence and selected case reports. American Journal of Industrial Medicine *17*, 189–215.

Lapidot, T., Sirard, C., Vormoor, J., Murdoch, B., Hoang, T., Caceres-Cortes, J., Minden, M., Paterson, B., Caligiuri, M. a, and Dick, J.E. (1994). A cell initiating human acute myeloid leukaemia after transplantation into SCID mice. Nature *367*, 645–648.

Lazar, J., O'Meara, C.C., Sarkis, A.B., Prisco, S.Z., Xu, H., Fox, C.S., Chen, M.-H., Broeckel, U., Arnett, D.K., Moreno, C., et al. (2013). SORCS1 contributes to the development of renal disease in rats and humans. Physiological Genomics *45*, 720–728.

Leader, M., Collins, M., Patel, J., and Henry, K. (1987). Vimentin: an evaluation of its role as a tumour marker. Histopathology *11*, 63–72.

Lee, H.E., Kim, J.H., Kim, Y.J., Choi, S.Y., Kim, S.-W., Kang, E., Chung, I.Y., Kim, I. a, Kim, E.J., Choi, Y., et al. (2011). An increase in cancer stem cell population after primary systemic therapy is a poor prognostic factor in breast cancer. British Journal of Cancer *104*, 1730–1738.

Lee, S.-H., Kim, J.K., Kim, D.W., Hwang, H.S., Eum, W.S., Park, J., Han, K.H., Oh, J.S., and Choi, S.Y. (2013). Antitumor activity of methyl gallate by inhibition of focal adhesion formation and Akt phosphorylation in glioma cells. Biochimica et Biophysica Acta *1830*, 4017–4029.

Lee, Y.J., Heo, J.S., Suh, H.N., Lee, M.Y., and Han, H.J. (2007). Interleukin-6 stimulates alpha-MG uptake in renal proximal tubule cells: involvement of STAT3, PI3K/Akt, MAPKs, and NF-kappaB. American Journal of Physiology. Renal Physiology *293*, F1036–46.

Leto, G., Incorvaia, L., Badalamenti, G., Tumminello, F.M., Gebbia, N., Flandina, C., Crescimanno, M., and Rini, G. (2006). Activin A circulating levels in patients with bone metastasis from breast or prostate cancer. Clinical & Experimental Metastasis *23*, 117–122.

Levina, V., Marrangoni, A.M., DeMarco, R., Gorelik, E., and Lokshin, A.E. (2008). Drug-selected human lung cancer stem cells: cytokine network, tumorigenic and metastatic properties. PloS One *3*, e3077.

Levina, V., Marrangoni, A., Wang, T., Parikh, S., Su, Y., Herberman, R., Lokshin, A., and Gorelik, E. (2010). Elimination of human lung cancer stem cells through targeting of the stem cell factor-c-kit autocrine signaling loop. Cancer Research *70*, 338–346.

Li, G.-M. (2008). Mechanisms and functions of DNA mismatch repair. Cell Research *18*, 85–98.

Li, L., Borodyansky, L., and Yang, Y. (2009). Genomic instability en route to and from cancer stem cells. Cell Cycle (Georgetown, Tex.) *8*, 1000–1002.

Li, R., Yerganian, G., Duesberg, P., Kraemer, a, Willer, a, Rausch, C., and Hehlmann, R. (1997). Aneuploidy correlated 100% with chemical transformation of Chinese hamster cells. Proceedings of the National Academy of Sciences of the United States of America *94*, 14506–14511.

Li, T., Su, L., Zhong, N., Hao, X., Zhong, D., Singhal, S., and Liu, X. (2013). Salinomycin induces cell death with autophagy through activation of endoplasmic reticulum stress in human cancer cells. Autophagy *9*, 1057–1068.

Liang, C.-C., Park, A.Y., and Guan, J.-L. (2007). In vitro scratch assay: a convenient and inexpensive method for analysis of cell migration in vitro. Nature Protocols *2*, 329–333.

Little, C.D., Nau, M.M., Carney, D.N., Gazdar, A.F., and Minna, J.D. (1983). Amplification and expression of the c-myc oncogene in human lung cancer cell lines. Nature *306*, 194–196.

Loeb, L. (1989). Endogenous carcinogenesis: molecular oncology into the twenty-first century—presidential address. Cancer Research *49*, 5489–5496.

Loeb, L. a, Bielas, J.H., and Beckman, R. a (2008). Cancers exhibit a mutator phenotype: clinical implications. Cancer Research *68*, 3551–7; discussion 3557.

Lonardo, E., Hermann, P.C., Mueller, M.-T., Huber, S., Balic, A., Miranda-Lorenzo, I., Zagorac, S., Alcala, S., Rodriguez-Arabaolaza, I., Ramirez, J.C., et al. (2011).

Nodal/Activin signaling drives self-renewal and tumorigenicity of pancreatic cancer stem cells and provides a target for combined drug therapy. Cell Stem Cell *9*, 433–446.

Lonardo, F., Rusch, V., Langenfeld, J., Dmitrovsky, E., and Klimstra, D.S. (1999). Overexpression of cyclins D1 and E is frequent in bronchial preneoplasia and precedes squamous cell carcinoma development. Cancer Research *59*, 2470–2476.

Long, W., Foulds, C.E., Qin, J., Liu, J., Ding, C., Lonard, D.M., Solis, L.M., Wistuba, I.I., Tsai, S.Y., Tsai, M., et al. (2012). ERK3 signals through SRC-3 coactivator to promote human lung cancer cell invasion. The Journal of Clinical Investigation *122*, 1869–1880.

Loughery, J.E.P., Dunne, P.D., O'Neill, K.M., Meehan, R.R., McDaid, J.R., and Walsh, C.P. (2011). DNMT1 deficiency triggers mismatch repair defects in human cells through depletion of repair protein levels in a process involving the DNA damage response. Human Molecular Genetics *20*, 3241–3255.

Lu, X., and Kang, Y. (2009). Cell fusion as a hidden force in tumor progression. Cancer Research *69*, 8536–8539.

Lyden, D., Hattori, K., Dias, S., Costa, C., Blaikie, P., Butros, L., Chadburn, a, Heissig, B., Marks, W., Witte, L., et al. (2001). Impaired recruitment of bone-marrow-derived endothelial and hematopoietic precursor cells blocks tumor angiogenesis and growth. Nature Medicine *7*, 1194–1201.

MacDonald, B.T., Tamai, K., and He, X. (2009). Wnt/beta-catenin signaling: components, mechanisms, and diseases. Developmental Cell *17*, 9–26.

Malanchi, I., Peinado, H., Kassen, D., Hussenet, T., Metzger, D., Chambon, P., Huber, M., Hohl, D., Cano, A., Birchmeier, W., et al. (2008). Cutaneous cancer stem cell maintenance is dependent on beta-catenin signalling. Nature *452*, 650–653.

Mani, S., Guo, W., Liao, M., and Eaton, E. (2008). The epithelial-mesenchymal transition generates cells with properties of stem cells. Cell *133*, 704–715.

Maniotis, a J., Folberg, R., Hess, a, Seftor, E. a, Gardner, L.M., Pe'er, J., Trent, J.M., Meltzer, P.S., and Hendrix, M.J. (1999). Vascular channel formation by human melanoma cells in vivo and in vitro: vasculogenic mimicry. The American Journal of Pathology *155*, 739–752.

Marjanovic, N.D., Weinberg, R. a, and Chaffer, C.L. (2013). Cell plasticity and heterogeneity in cancer. Clinical Chemistry *59*, 168–179.

Marshall, B.J., and Warren, J.R. (1984). Unidentified curved bacilli in the stomach of patients with gastritis and peptic ulceration. Lancet *1*, 1311–1315.

Martin, G.S. (2004). The road to Src. Oncogene *23*, 7910–7917.

Martin, A., and Scharff, M.D. (2002). AID and mismatch repair in antibody diversification. Nature Reviews. Immunology *2*, 605–614.

Martins-Neves, S.R., Lopes, Á.O., do Carmo, A., Paiva, A. a, Simões, P.C., Abrunhosa, A.J., and Gomes, C.M.F. (2012). Therapeutic implications of an enriched cancer stem-like cell population in a human osteosarcoma cell line. BMC Cancer *12*, 139.

Marxer, M., Ma, H.T., Man, W.Y., and Poon, R.Y.C. (2013). p53 deficiency enhances mitotic arrest and slippage induced by pharmacological inhibition of Aurora kinases. Oncogene.

Massague, J., and Wotton, D. (2000). Transcriptional control by the TGF-β/Smad signaling system. EMBO Journal *19*, 1745–1754.

Mazurenko, N.N., Kogan, E.A., Zborovskaya, I.B., and Kisseljov, F.L. (1992). Expression of pp60c-src in human small cell and non-small cell lung carcinomas. European Journal of Cancer (Oxford, England : 1990) *28*, 372–377.

Medema, J.P. (2013). Cancer stem cells: The challenges ahead. Nature Cell Biology *15*, 338–344.

Medema, J.P., and Vermeulen, L. (2011). Microenvironmental regulation of stem cells in intestinal homeostasis and cancer. Nature *474*, 318–326.

Van Meerloo, J., Kaspers, G.J.L., and Cloos, J. (2011). Cell sensitivity assays: the MTT assay. Methods in Molecular Biology (Clifton, N.J.) *731*, 237–245.

Mendez, M.G., Kojima, S.-I., and Goldman, R.D. (2010). Vimentin induces changes in cell shape, motility, and adhesion during the epithelial to mesenchymal transition. FASEB Journal : Official Publication of the Federation of American Societies for Experimental Biology *24*, 1838–1851.

Monge, J., Kricun, M., Radovčić, J., Radovčić, D., Mann, A., and Frayer, D.W. (2013). Fibrous Dysplasia in a 120,000+ Year Old Neandertal from Krapina, Croatia. PLoS ONE *8*, e64539.

Moon, R.T., Kohn, A.D., De Ferrari, G. V, and Kaykas, A. (2004). WNT and beta-catenin signalling: diseases and therapies. Nature Reviews. Genetics *5*, 691–701.

Moore, N., and Lyle, S. (2011). Quiescent, slow-cycling stem cell populations in cancer: a review of the evidence and discussion of significance. Journal of Oncology *2011*.

Mueller, M.M., and Fusenig, N.E. (2004). Friends or foes - bipolar effects of the tumour stroma in cancer. Nature Reviews. Cancer *4*, 839–849.

Murphree, a L., and Benedict, W.F. (1984). Retinoblastoma: clues to human oncogenesis. Science (New York, N.Y.) *223*, 1028–1033.

Musah, S., Chen, J., and Hoyle, G. (2012). Repair of tracheal epithelium by basal cells after chlorine-induced injury. Respiratory Research *13*, 107.

Musteanu, M., Blaas, L., Zenz, R., Svinka, J., Hoffmann, T., Grabner, B., Schramek, D., Kantner, H.-P., Müller, M., Kolbe, T., et al. (2012). A mouse model to identify cooperating signaling pathways in cancer. Nature Methods *9*, 897–900.

Nagel, H., Laskawi, R., Eiffert, H., and Schlott, T. (2003). Analysis of the tumour suppressor genes, FHIT and WT-1, and the tumour rejection genes, BAGE, GAGE-1/2, HAGE, MAGE-1, and MAGE-3, in benign and malignant neoplasms of the salivary glands. Molecular Pathology : MP *56*, 226–231.

Nakamura, H., and Saji, H. (2013). A worldwide trend of increasing primary adenocarcinoma of the lung. Surgery Today.

Naujokata, C., and Lauferc, S. (2013). Targeting cancer stem cells with defined compounds and drugs. Journal of Cancer Research *2*, 36–67.

Nelson, C.M., and Bissell, M.J. (2006). Of extracellular matrix, scaffolds, and signaling: tissue architecture regulates development, homeostasis, and cancer. Annual Review of Cell and Developmental Biology *22*, 287–309.

Neuzillet, C., Tijeras-Raballand, A., Cros, J., Faivre, S., Hammel, P., and Raymond, E. (2013). Stromal expression of SPARC in pancreatic adenocarcinoma. Cancer Metastasis Reviews.

Nguyen, H.G., and Ravid, K. (2006). Tetraploidy/aneuploidy and stem cells in cancer promotion: The role of chromosome passenger proteins. Journal of Cellular Physiology *208*, 12–22.

Nguyen, D.X., Bos, P.D., and Massagué, J. (2009). Metastasis: from dissemination to organ-specific colonization. Nature Reviews. Cancer *9*, 274–284.

Nguyen-Jackson, H., Panopoulos, A.D., Zhang, H., Li, H.S., and Watowich, S.S. (2010). STAT3 controls the neutrophil migratory response to CXCR2 ligands by direct activation of G-CSF-induced CXCR2 expression and via modulation of CXCR2 signal transduction. Blood *115*, 3354–3363.

Nickens, K.P., Patierno, S.R., and Ceryak, S. (2010). Chromium genotoxicity: A double-edged sword. Chemico-biological Interactions *188*, 276–288.

Nickens, K.P., Han, Y., Shandilya, H., Larrimore, A., Gerard, G.F., Kaldjian, E., Patierno, S.R., and Ceryak, S. (2012). Acquisition of mitochondrial dysregulation and resistance to mitochondrial-mediated apoptosis after genotoxic insult in normal human fibroblasts: a possible model for early stage carcinogenesis. Biochimica et Biophysica Acta *1823*, 264–272.

Nigro, J.M., Baker, S.J., Preisinger, A.C., Jessup, J.M., Hostetter, R., Cleary, K., Bigner, S.H., Davidson, N., Baylin, S., and Devilee, P. (1989). Mutations in the p53 gene occur in diverse human tumour types. Nature *342*, 705–708.

Niwa, H., Miyazaki, J., and Smith, a G. (2000). Quantitative expression of Oct-3/4 defines differentiation, dedifferentiation or self-renewal of ES cells. Nature Genetics *24*, 372–376.

Noda, D., Itoh, S., Watanabe, Y., Inamitsu, M., Dennler, S., Itoh, F., Koike, S., Danielpour, D., ten Dijke, P., and Kato, M. (2006). ELAC2, a putative prostate cancer susceptibility gene product, potentiates TGF-beta/Smad-induced growth arrest of prostate cells. Oncogene *25*, 5591–5600.

Nolan, D.J., Ciarrocchi, A., Mellick, A.S., Jaggi, J.S., Bambino, K., Gupta, S., Heikamp, E., McDevitt, M.R., Scheinberg, D.A., Benezra, R., et al. (2007). Bone marrow-derived endothelial progenitor cells are a major determinant of nascent tumor neovascularization. Genes & Development *21*, 1546–1558.

O'Brien, C. a, Pollett, A., Gallinger, S., and Dick, J.E. (2007). A human colon cancer cell capable of initiating tumour growth in immunodeficient mice. Nature *445*, 106–110.

O'Brien, T., Ceryak, S., and Patierno, S. (2003). Complexities of chromium carcinogenesis: role of cellular response, repair and recovery mechanisms. Mutation Research/Fundamental and Molecular Mechanisms of Mutagenesis *533*, 3–36.

O'Brien, T.J., Brooks, B.R., and Patierno, S.R. (2005). Nucleotide excision repair functions in the removal of chromium-induced DNA damage in mammalian cells. Molecular and Cellular Biochemistry *279*, 85–95.

Oikawa, T., Nakamura, A., Onishi, N., Yamada, T., Matsuo, K., and Saya, H. (2013). Acquired Expression of NFATc1 Downregulates E-Cadherin and Promotes Cancer Cell Invasion. Cancer Research *73*, 5100–5109.

Okazaki, T., Ebihara, S., Asada, M., Kanda, A., Sasaki, H., and Yamaya, M. (2006). Granulocyte colony-stimulating factor promotes tumor angiogenesis via increasing circulating endothelial progenitor cells and Gr1+CD11b+ cells in cancer animal models. International Immunology *18*, 1–9.

Ornitz, D., Hammer, R., Messing, A., Palmiter, R., and Brinster, R. (1987). Pancreatic neoplasia induced by SV40 T-antigen expression in acinar cells of transgenic mice. Science *238*, 188–193.

Ouillette, P., Saiya-Cork, K., Seymour, E., Li, C., Shedden, K., and Malek, S.N. (2013). Clonal evolution, genomic drivers, and effects of therapy in chronic lymphocytic leukemia. Clinical Cancer Research : an Official Journal of the American Association for Cancer Research *19*, 2893–2904.

Padilla-Nash, H.M., Hathcock, K., McNeil, N.E., Mack, D., Hoeppner, D., Ravin, R., Knutsen, T., Yonescu, R., Wangsa, D., Dorritie, K., et al. (2012). Spontaneous transformation of murine epithelial cells requires the early acquisition of specific chromosomal aneuploidies and genomic imbalances. Genes, Chromosomes & Cancer *51*, 353–374.

Padua, D., Zhang, X.H., Wang, Q., Nadal, C., Gerald, W.L., Gomis, R.R., and Massagué, J. (2008). TGF β primes breast tumors for lung metastasis seeding through angiopoitin-like 4. *133*, 66–77.

Pàez-Ribes, M., Allen, E., and Hudock, J. (2009). Antiangiogenic therapy elicits malignant progression of tumors to increased local invasion and distant metastasis. Cancer Cell *15*, 220–231.

Paget, S. (1889). The distribution of secondary growths in cancer of the breast. The Lancet *133*, 571–573.

De Palma, M., and Hanahan, D. (2012). The biology of personalized cancer medicine: facing individual complexities underlying hallmark capabilities. Molecular Oncology *6*, 111–127.

Palumbo, J.S., Talmage, K.E., Massari, J. V, La Jeunesse, C.M., Flick, M.J., Kombrinck, K.W., Jirousková, M., and Degen, J.L. (2005). Platelets and fibrin(ogen) increase metastatic potential by impeding natural killer cell-mediated elimination of tumor cells. Blood *105*, 178–185.

Paoli, P., Giannoni, E., and Chiarugi, P. (2013). Anoikis molecular pathways and its role in cancer progression. Biochimica et Biophysica Acta.

Papavramidou, N., Papavramidis, T., and Demetriou, T. (2010). Ancient Greek and Greco-Roman methods in modern surgical treatment of cancer. Annals of Surgical Oncology *17*, 665–667.

Pardal, R., Clarke, M., and Morrison, S. (2003). Applying the principles of stem-cell biology to cancer. Nature Reviews Cancer *3*.

Parkin, D.M., Bray, F., Ferlay, J., and Pisani, P. (2005). Global cancer statistics, 2002. CA: a Cancer Journal for Clinicians *55*, 74–108.

Patanè, M., Ciriaco, M., Chimirri, S., Ursini, F., Naty, S., Grembiale, R.D., Gallelli, L., De Sarro, G., and Russo, E. (2013). Interactions among Low Dose of Methotrexate and Drugs Used in the Treatment of Rheumatoid Arthritis. Advances in Pharmacological Sciences *2013*, 313858.

Patel, M., Lu, L., Zander, D.S., Sreerama, L., Coco, D., and Moreb, J.S. (2008). ALDH1A1 and ALDH3A1 expression in lung cancers: correlation with histologic type and potential precursors. Lung Cancer (Amsterdam, Netherlands) *59*, 340–349.

Pavlides, S., Vera, I., Gandara, R., Sneddon, S., Pestell, R.G., Mercier, I., Martinez-Outschoorn, U.E., Whitaker-Menezes, D., Howell, A., Sotgia, F., et al. (2012). Warburg meets autophagy: cancer-associated fibroblasts accelerate tumor growth and metastasis via oxidative stress, mitophagy, and aerobic glycolysis. Antioxidants & Redox Signaling *16*, 1264–1284.

Pawelek, J., and Chakraborty, A. (2008). Fusion of tumour cells with bone marrow-derived cells: a unifying explanation for metastasis. Nature Reviews Cancer *8*, 377–386.

Pellman, D. (2007). Aneuploidy and cancer. Nature *446*, 38–39.

Peterson-Roth, E., Reynolds, M., Quievryn, G., and Zhitkovich, A. (2005). Mismatch repair proteins are activators of toxic responses to chromium-DNA damage. Molecular and Cellular Biology *25*, 3596–3607.

Pistoia, V., Morandi, F., Bianchi, G., Pezzolo, A., Prigione, I., and Raffaghello, L. (2013). Immunosuppressive microenvironment in neuroblastoma. Frontiers in Oncology *3*, 167.

Potapova, T. a, Zhu, J., and Li, R. (2013). Aneuploidy and chromosomal instability: a vicious cycle driving cellular evolution and cancer genome chaos. Cancer Metastasis Reviews.

Psaila, B., and Lyden, D. (2009). The metastatic niche: adapting the foreign soil. Nature Reviews Cancer *9*, 285–293.

Ralph, S.J., Rodríguez-Enríquez, S., Neuzil, J., Saavedra, E., and Moreno-Sánchez, R. (2010). The causes of cancer revisited: “mitochondrial malignancy” and ROS-induced oncogenic transformation - why mitochondria are targets for cancer therapy. Molecular Aspects of Medicine *31*, 145–170.

Rawlins, E.L., Okubo, T., Xue, Y., Brass, D.M., Auten, R.L., Hasegawa, H., Wang, F., and Hogan, B.L.M. (2009). The Role of Scgb1a1 + Clara Cells in the Long-Term Maintenance and Repair of Lung Airway, but Not Alveolar, Epithelium. Cell Stem Cell *4*, 525–534.

Reddel, R.R., Ke, Y., Gerwin, B.I., McMenamin, M.G., Lechner, J.F., Su, R.T., Brash, D.E., Park, J.B., Rhim, J.S., and Harris, C.C. (1988). Transformation of human bronchial epithelial cells by infection with SV40 or adenovirus-12 SV40 hybrid virus, or transfection via strontium phosphate coprecipitation with a plasmid containing SV40 early region genes. Cancer Research *48*, 1904–1909.

Ren, H., Zhao, T., Sun, J., Wang, X., Liu, J., Gao, S., Yu, M., and Hao, J. (2013). The CX3CL1/CX3CR1 reprograms glucose metabolism through HIF-1 pathway in pancreatic adenocarcinoma. Journal of Cellular Biochemistry *114*, 2603–2611.

Reynolds, M., and Zhitkovich, A. (2007). Cellular vitamin C increases chromate toxicity via a death program requiring mismatch repair but not p53. Carcinogenesis *28*, 1613–1620.

Reynolds, M., Stoddard, L., Bespalov, I., and Zhitkovich, A. (2007). Ascorbate acts as a highly potent inducer of chromate mutagenesis and clastogenesis: linkage to DNA breaks in G2 phase by mismatch repair. Nucleic Acids Research *35*, 465–476.

Reynolds, M., Armknecht, S., Johnston, T., and Zhitkovich, A. (2012). Undetectable role of oxidative DNA damage in cell cycle, cytotoxic and clastogenic effects of Cr(VI) in human lung cells with restored ascorbate levels. Mutagenesis *27*, 437–443.

Reynolds, M.F., Peterson-Roth, E.C., Bespalov, I. a, Johnston, T., Gurel, V.M., Menard, H.L., and Zhitkovich, A. (2009). Rapid DNA double-strand breaks resulting from processing of Cr-DNA cross-links by both MutS dimers. Cancer Research *69*, 1071–1079.

Rivera, C., Rivera, S., Loriot, Y., Vozenin, M.-C., and Deutsch, E. (2011). Lung cancer stem cell: new insights on experimental models and preclinical data. Journal of Oncology *2011*, 549181.

Robertson, A.B., Klungland, A., Rognes, T., and Leiros, I. (2009). DNA repair in mammalian cells: Base excision repair: the long and short of it. Cellular and Molecular Life Sciences : CMLS *66*, 981–993.

Robinson, B.D., Sica, G.L., Liu, Y.-F., Rohan, T.E., Gertler, F.B., Condeelis, J.S., and Jones, J.G. (2009). Tumor microenvironment of metastasis in human breast carcinoma: a potential prognostic marker linked to hematogenous dissemination. Clinical Cancer Research : an Official Journal of the American Association for Cancer Research *15*, 2433–2441.

Rodova, M., Fu, J., Watkins, D.N., Srivastava, R.K., and Shankar, S. (2012). Sonic hedgehog signaling inhibition provides opportunities for targeted therapy by sulforaphane in regulating pancreatic cancer stem cell self-renewal. PloS One *7*, e46083.

Roesch, A., Fukunaga-Kalabis, M., Schmidt, E.C., Zabierowski, S.E., Brafford, P. a, Vultur, A., Basu, D., Gimotty, P., Vogt, T., and Herlyn, M. (2010). A temporarily distinct subpopulation of slow-cycling melanoma cells is required for continuous tumor growth. Cell *141*, 583–594.

Rosanò, L., Spinella, F., and Bagnato, A. (2013). Endothelin 1 in cancer: biological implications and therapeutic opportunities. Nature Reviews. Cancer *13*, 637–651.

Rous, P., and Kidd, J.G. (1941). CONDITIONAL NEOPLASMS AND SUBTHRESHOLD NEOPLASTIC STATES : A STUDY OF THE TAR TUMORS OF RABBITS. The Journal of Experimental Medicine *73*, 365–390.

Safranek, J., Pesta, M., Holubec, L., Kulda, V., Dreslerova, J., Vrzalova, J., Topolcan, O., Pesek, M., Finek, J., and Treska, V. (2009). Expression of MMP-7, MMP-9, TIMP-1 and TIMP-2 mRNA in lung tissue of patients with non-small cell lung cancer (NSCLC) and benign pulmonary disease. Anticancer Research *29*, 2513–2517.

Said, N., Frierson, H.F., Sanchez-Carbayo, M., Brekken, R.A., and Theodorescu, D. (2013). Loss of SPARC in bladder cancer enhances carcinogenesis and progression. The Journal of Clinical Investigation *123*, 751–766.

Salnikow, K., and Zhitkovich, A. (2008). Genetic and epigenetic mechanisms in metal carcinogenesis and cocarcinogenesis: nickel, arsenic, and chromium. Chemical Research in Toxicology *21*, 28–44.

Sassoli, C., Pini, A., Mazzanti, B., Quercioli, F., Nistri, S., Saccardi, R., Zecchi-Orlandini, S., Bani, D., and Formigli, L. (2011). Mesenchymal stromal cells affect cardiomyocyte growth through juxtacrine Notch-1/Jagged-1 signaling and paracrine mechanisms: clues for cardiac regeneration. Journal of Molecular and Cellular Cardiology *51*, 399–408.

Sato, N., Koinuma, J., Ito, T., Tsuchiya, E., Kondo, S., Nakamura, Y., and Daigo, Y. (2010). Activation of an oncogenic TBC1D7 (TBC1 domain family, member 7) protein in pulmonary carcinogenesis. Genes, Chromosomes & Cancer *49*, 353–367.

Schiavoni, G., Gabriele, L., and Mattei, F. (2013). The Tumor Microenvironment: A Pitch for Multiple Players. Frontiers in Oncology *3*, 1–15.

Schreiber, R.D., Old, L.J., and Smyth, M.J. (2011). Cancer immunoediting: integrating immunity's roles in cancer suppression and promotion. Science (New York, N.Y.) *331*, 1565–1570.

Seidel, S., Garvalov, B.K., Wirta, V., Stechow, L. Von, Schänzer, A., Meletis, K., Wolter, M., Sommerlad, D., Henze, A., Nistér, M., et al. (2010). A hypoxic niche regulates glioblastoma stem cells through hypoxia inducible factor 2 a. Brain *133*, 983–995.

Semenza, G.L. (2010). HIF-1: upstream and downstream of cancer metabolism. Current Opinion in Genetics & Development *20*, 51–56.

Sharma, R., Sharma, M., and Sharma, V. (2013). The impact of incinerators on human health and environment. Reviews on Environmental Health *28*, 67–72.

Shaykhiev, R., Wang, R., Zwick, R.K., Hackett, N.R., Leung, R., Moore, M. a S., Sima, C.S., Chao, I., Downey, R.J., Strulovici-Barel, Y., et al. (2013). Airway Basal Cells of Healthy Smokers Express an Embryonic Stem Cell Signature Relevant to Lung Cancer. Stem Cells (Dayton, Ohio) 1–19.

Shi, Q., and King, R.W. (2005). Chromosome nondisjunction yields tetraploid rather than aneuploid cells in human cell lines. Nature *437*, 1038–1042.

Shim, H., Dolde, C., Lewis, B.C., Wu, C.S., Dang, G., Jungmann, R.A., Dalla-Favera, R., and Dang, C. V (1997). c-Myc transactivation of LDH-A: implications for tumor metabolism and growth. Proceedings of the National Academy of Sciences of the United States of America *94*, 6658–6663.

Shuck, S., Short, E., and Turchi, J. (2008). Eukaryotic nucleotide excision repair: from understanding mechanisms to influencing biology. Cell Research *18*, 64–72.

Siegel, M., ; Deepa Naishadham, M., and ; Ahmedin Jemal, D. (2013). Cancer statistics, 2013. … Cancer Journal for Clinicians *63*, 11–30.

Singh, A., and Settleman, J. (2010). EMT, cancer stem cells and drug resistance: an emerging axis of evil in the war on cancer. Oncogene *29*, 4741–4751.

Society, American.Cancer. (2011). Global Cancer Facts & Figures 2nd Edition.

Society, American.Cancer., and Livestrong (2010). The global economic cost of cancer.

Soda, Y., Marumoto, T., Friedmann-Morvinski, D., Soda, M., Liu, F., Michiue, H., Pastorino, S., Yang, M., Hoffman, R.M., Kesari, S., et al. (2011). Transdifferentiation of glioblastoma cells into vascular endothelial cells. Proceedings of the National Academy of Sciences of the United States of America *108*, 4274–4280.

Soto, A.M., and Sonnenschein, C. (2004). The somatic mutation theory of cancer: growing problems with the paradigm? BioEssays : News and Reviews in Molecular, Cellular and Developmental Biology *26*, 1097–1107.

De Sousa E Melo, F., and Medema, J.P. (2012). Axing Wnt signals. Cell Research *22*, 9–11.

De Sousa E Melo, F., Colak, S., Buikhuisen, J., Koster, J., Cameron, K., de Jong, J.H., Tuynman, J.B., Prasetyanti, P.R., Fessler, E., van den Bergh, S.P., et al. (2011). Methylation of cancer-stem-cell-associated Wnt target genes predicts poor prognosis in colorectal cancer patients. Cell Stem Cell *9*, 476–485.

Spiro, S.G., and Silvestri, G. a (2005). One hundred years of lung cancer. American Journal of Respiratory and Critical Care Medicine *172*, 523–529.

Stackpole, M.M., Wise, S.S., Goodale, B.C., Duzevik, E.G., Munroe, R.C., Thompson, W.D., Thacker, J., Thompson, L.H., Hinz, J.M., and Wise, J.P. (2007). Homologous recombination repair protects against particulate chromate-induced chromosome instability in Chinese hamster cells. Mutation Research *625*, 145–154.

Stehelin, D., Varmus, H., Bishop, J., and Vogt, P. (1976). DNA related to the transforming gene (s) of avian sarcoma viruses is present in normal avian DNA. Nature *260*, 170–173.

Stellman, S.D., Muscat, J.E., Hoffmann, D., and Wynder, E.L. (1997). Impact of filter cigarette smoking on lung cancer histology. Preventive Medicine *26*, 451–456.

Sudhakar, A. (2009). History of Cancer, Ancient and Modern Treatment Methods. Journal of Cancer Science & Therapy *1*, 1–4.

Sustáčková, G., Legartová, S., Kozubek, S., Stixová, L., Pacherník, J., and Bártová, E. (2012). Differentiation-independent fluctuation of pluripotency-related transcription factors and other epigenetic markers in embryonic stem cell colonies. Stem Cells and Development *21*, 710–720.

Takahashi, Y., Kondo, K., Hirose, T., Nakagawa, H., Tsuyuguchi, M., Hashimoto, M., Sano, T., Ochiai, A., and Monden, Y. (2005). Microsatellite instability and protein expression of the DNA mismatch repair gene, hMLH1, of lung cancer in chromate-exposed workers. Molecular Carcinogenesis *42*, 150–158.

Taniguchi, T., Garcia-Higuera, I., Andreassen, P.R., Gregory, R.C., Grompe, M., and D'Andrea, A.D. (2002). S-phase-specific interaction of the Fanconi anemia protein, FANCD2, with BRCA1 and RAD51. Blood *100*, 2414–2420.

Thompson, C.M., Fedorov, Y., Brown, D.D., Suh, M., Proctor, D.M., Kuriakose, L., Haws, L.C., and Harris, M. a (2012). Assessment of Cr(VI)-induced cytotoxicity and genotoxicity using high content analysis. PloS One *7*, e42720.

Thun, M.J., Lally, C.A., Flannery, J.T., Calle, E.E., Flanders, W.D., and Heath, C.W. (1997). Cigarette smoking and changes in the histopathology of lung cancer. Journal of the National Cancer Institute *89*, 1580–1586.

Todaro, M., Alea, M.P., Di Stefano, A.B., Cammareri, P., Vermeulen, L., Iovino, F., Tripodo, C., Russo, A., Gulotta, G., Medema, J.P., et al. (2007). Colon cancer stem cells dictate tumor growth and resist cell death by production of interleukin-4. Cell Stem Cell *1*, 389–402.

Trosko, J., and Chang, C. (1989). Stem cell theory of carcinogenesis. Toxicology Letters, 49 283–295.

Tsuchida, K., Nakatani, M., Hitachi, K., Uezumi, A., Sunada, Y., Ageta, H., and Inokuchi, K. (2009). Activin signaling as an emerging target for therapeutic interventions. Cell Communication and Signaling : CCS *7*, 15.

Umar, A., Dunn, B.K., and Greenwald, P. (2012). Future directions in cancer prevention. Nature Reviews. Cancer *12*, 835–848.

Urbano, a M., Ferreira, L.M.R., and Alpoim, M.C. (2012). Molecular and cellular mechanisms of hexavalent chromium-induced lung cancer: an updated perspective. Current Drug Metabolism *13*, 284–305.

Urbano, A.M., Rodrigues, C.F.D., and Alpoim, M.C. (2008). Hexavalent chromium exposure , genomic instability and lung cancer Review Article. Gene Therapy and Molecular Biology *12*, 219–238.

Valastyan, S., and Weinberg, R. a (2011). Tumor metastasis: molecular insights and evolving paradigms. Cell *147*, 275–292.

Vallier, L., Alexander, M., and Pedersen, R. a (2005). Activin/Nodal and FGF pathways cooperate to maintain pluripotency of human embryonic stem cells. Journal of Cell Science *118*, 4495–4509.

Vermeulen, L., Todaro, M., de Sousa Mello, F., Sprick, M.R., Kemper, K., Perez Alea, M., Richel, D.J., Stassi, G., and Medema, J.P. (2008a). Single-cell cloning of colon cancer stem cells reveals a multi-lineage differentiation capacity. Proceedings of the National Academy of Sciences of the United States of America *105*, 13427–13432.

Vermeulen, L., Sprick, M.R., Kemper, K., Stassi, G., and Medema, J.P. (2008b). Cancer stem cells - old concepts, new insights. Cell Death and Differentiation *15*, 947–958.

Vermeulen, L., De Sousa E Melo, F., van der Heijden, M., Cameron, K., de Jong, J.H., Borovski, T., Tuynman, J.B., Todaro, M., Merz, C., Rodermond, H., et al. (2010). Wnt activity defines colon cancer stem cells and is regulated by the microenvironment. Nature Cell Biology *12*, 468–476.

Vermeulen, L., de Sousa e Melo, F., Richel, D.J., and Medema, J.P. (2012). The developing cancer stem-cell model: clinical challenges and opportunities. The Lancet Oncology *13*, e83–9.

Vesely, M.D., and Schreiber, R.D. (2013). Cancer immunoediting: antigens, mechanisms, and implications to cancer immunotherapy. Annals of the New York Academy of Sciences *1284*, 1–5.

Vilcheck, S.K., O'Brien, T.J., Pritchard, D.E., Ha, L., Ceryak, S., Fornsaglio, J.L., and Patierno, S.R. (2002). Fanconi anemia complementation group A cells are hypersensitive to chromium(VI)-induced toxicity. Environmental Health Perspectives *110 Suppl* , 773–777.

Visvader, J.E. (2011). Cells of origin in cancer. Nature *469*, 314–322.

Visvader, J.E., and Lindeman, G.J. (2008). Cancer stem cells in solid tumours: accumulating evidence and unresolved questions. Nature Reviews. Cancer *8*, 755–768.

Visvader, J.E., and Lindeman, G.J. (2012). Cancer stem cells: current status and evolving complexities. Cell Stem Cell *10*, 717–728.

Vlashi, E., Lagadec, C., Vergnes, L., Matsutani, T., Masui, K., Poulou, M., Popescu, R., Della Donna, L., Evers, P., Dekmezian, C., et al. (2011). Metabolic state of glioma stem cells and nontumorigenic cells. Proceedings of the National Academy of Sciences of the United States of America *108*, 16062–16067.

Walker, B.A., Wardell, C.P., Ross, F.M., and Morgan, G.J. (2013). Identification of a novel t(7;14) translocation in multiple myeloma resulting in overexpression of EGFR. Genes, Chromosomes & Cancer *52*, 817–822.

Walter, J.B., and Pryce, D.M. (1955). The histology of lung cancer. Thorax *10*, 107–116.

Wan, X.-B., Long, Z.-J., Yan, M., Xu, J., Xia, L.-P., Liu, L., Zhao, Y., Huang, X.-F., Wang, X.-R., Zhu, X.-F., et al. (2008). Inhibition of Aurora-A suppresses epithelial-mesenchymal transition and invasion by downregulating MAPK in nasopharyngeal carcinoma cells. Carcinogenesis *29*, 1930–1937.

Wang, L., Huang, X., Zheng, X., Wang, X., Li, S., Zhang, L., Yang, Z., and Xia, Z. (2013). Enrichment of prostate cancer stem-like cells from human prostate cancer cell lines by culture in serum-free medium and chemoradiotherapy. International Journal of Biological Sciences *9*, 472–479.

Wang, R., Chadalavada, K., Wilshire, J., Kowalik, U., Hovinga, K.E., Geber, A., Fligelman, B., Leversha, M., Brennan, C., and Tabar, V. (2010). Glioblastoma stem-like cells give rise to tumour endothelium. Nature *468*, 829–833.

Wang, W.-C., Kuo, C.-Y., Tzang, B.-S., Chen, H.-M., and Kao, S.-H. (2012). IL-6 augmented motility of airway epithelial cell BEAS-2B via Akt/GSK-3β signaling pathway. Journal of Cellular Biochemistry *113*, 3567–3575.

Warburg, O. (1956). On the origin of cancer cells. Science *123*, 309–314.

Weis, S.M., and Cheresh, D. a (2011). Tumor angiogenesis: molecular pathways and therapeutic targets. Nature Medicine *17*, 1359–1370.

Welte, Y., Adjaye, J., Lehrach, H.R., and Regenbrecht, C.R. (2010). Cancer stem cells in solid tumors: elusive or illusive? Cell Communication and Signaling : CCS *8*, 6.

Wicha, M.S., Liu, S., and Dontu, G. (2006). Cancer stem cells: an old idea--a paradigm shift. Cancer Research *66*, 1883–90; discussion 1895–6.

Wilson, B.J., Schatton, T., Zhan, Q., Gasser, M., Ma, J., Saab, K.R., Schanche, R., Waaga-Gasser, A.-M., Gold, J.S., Huang, Q., et al. (2011a). ABCB5 identifies a therapy-refractory tumor cell population in colorectal cancer patients. Cancer Research *71*, 5307–5316.

Wilson, E.B., El-Jawhari, J.J., Neilson, A.L., Hall, G.D., Melcher, A. a, Meade, J.L., and Cook, G.P. (2011b). Human tumour immune evasion via TGF-β blocks NK cell activation but not survival allowing therapeutic restoration of anti-tumour activity. PloS One *6*, e22842.

Wise, S.S., and Wise, J.P. (2012). Chromium and genomic stability. Mutation Research *733*, 78–82.

Wise, S.S., Holmes, A.L., Qin, Q., Xie, H., Katsifis, S.P., Thompson, W.D., and Wise, J.P. (2010). Comparative genotoxicity and cytotoxicity of four hexavalent chromium compounds in human bronchial cells. Chemical Research in Toxicology *23*, 365–372.

Wong, P.-P., Miranda, F., Chan, K. V, Berlato, C., Hurst, H.C., and Scibetta, A.G. (2012a). Histone demethylase KDM5B collaborates with TFAP2C and Myc to repress the cell cycle inhibitor p21(cip) (CDKN1A). Molecular and Cellular Biology *32*, 1633–1644.

Wong, V., Armknecht, S., and Zhitkovich, A. (2012b). Metabolism of Cr(VI) by ascorbate but not glutathione is a low oxidant-generating process. Journal of Trace Elements in Medicine and Biology : Organ of the Society for Minerals and Trace Elements (GMS) *26*, 192–196.

Woo, K.-S., Kim, K.-E., Kim, K.-H., Kim, S.-H., Park, J.-I., Shaffer, L.G., and Han, J.-Y. (2009). Deletions of chromosome arms 7p and 7q in adult acute myeloid leukemia: a marker chromosome confirmed by array comparative genomic hybridization. Cancer Genetics and Cytogenetics *194*, 71–74.

Wu, K.-J., and Yang, M.-H. (2011). Epithelial-mesenchymal transition and cancer stemness: the Twist1-Bmi1 connection. Bioscience Reports *31*, 449–455.

Wu, J., Issa, J.P., Herman, J., Bassett, D.E., Nelkin, B.D., and Baylin, S.B. (1993). Expression of an exogenous eukaryotic DNA methyltransferase gene induces transformation of NIH 3T3 cells. Proceedings of the National Academy of Sciences of the United States of America *90*, 8891–8895.

Wynder, E.L., and Muscat, J.E. (1995). The changing epidemiology of smoking and lung cancer histology. Environmental Health Perspectives *103 Suppl* , 143–148.

Xie, G., Yao, Q., Liu, Y., Du, S., Liu, A., Guo, Z., Sun, A., Ruan, J., Chen, L., Ye, C., et al. (2012). IL-6-induced epithelial-mesenchymal transition promotes the generation of breast cancer stem-like cells analogous to mammosphere cultures. International Journal of Oncology *40*, 1171–1179.

Xie, H., Holmes, A.L., Wise, S.S., Gordon, N., and Wise, J.P. (2004). Lead chromate-induced chromosome damage requires extracellular dissolution to liberate chromium ions but does not require particle internalization or intracellular dissolution. Chemical Research in Toxicology *17*, 1362–1367.

Xie, H., Wise, S.S., Holmes, A.L., Xu, B., Wakeman, T.P., Pelsue, S.C., Singh, N.P., and Wise, J.P. (2005). Carcinogenic lead chromate induces DNA double-strand breaks in human lung cells. Mutation Research *586*, 160–172.

Xu, C., Xie, D., Yu, S.-C., Yang, X.-J., He, L.-R., Yang, J., Ping, Y.-F., Wang, B., Yang, L., Xu, S.-L., et al. (2013). β-Catenin/POU5F1/SOX2 Transcription Factor Complex Mediates IGF-I Receptor Signaling and Predicts Poor Prognosis in Lung Adenocarcinoma. Cancer Research *73*, 3181–3189.

Xu, H.-T., Ma, L., Qi, F.-J., Liu, Y., Yu, J.-H., Dai, S.-D., Zhu, J.-J., and Wang, E.-H. (2006). Expression of serine threonine kinase 15 is associated with poor differentiation in lung squamous cell carcinoma and adenocarcinoma. Pathology International *56*, 375–380.

Yachida, S., Jones, S., Bozic, I., Antal, T., and Leary, R. (2010). Distant metastasis occurs late during the genetic evolution of pancreatic cancer. Nature *467*, 1114–1117.

Yamanaka, S., and Blau, H.M. (2010). Nuclear reprogramming to a pluripotent state by three approaches. Nature *465*, 704–712.

Yan, B., Wei, J.-J., Yuan, Y., Sun, R., Li, D., Luo, J., Liao, S.-J., Zhou, Y.-H., Shu, Y., Wang, Q., et al. (2013). IL-6 cooperates with G-CSF to induce protumor function of neutrophils in bone marrow by enhancing STAT3 activation. Journal of Immunology (Baltimore, Md. : 1950) *190*, 5882–5893.

Yang, J., Ikezoe, T., Nishioka, C., Udaka, K., and Yokoyama, A. (2013). Bcr-Abl activates AURKA and AURKB in chronic myeloid leukemia cells via AKT signaling. International Journal of Cancer. Journal International Du Cancer 1–49.

Yang, L., Pang, Y., and Moses, H.L. (2010). TGFβ and immune cells: an important regulatory axis in the tumor microenvironment and progression. Trends in Immunology *31*, 220–227.

Yarrow, J.C., Perlman, Z.E., Westwood, N.J., and Mitchison, T.J. (2004). A high-throughput cell migration assay using scratch wound healing, a comparison of image-based readout methods. BMC Biotechnology *4*, 21.

Yau, C., Mouradov, D., Jorissen, R.N., Colella, S., Mirza, G., Steers, G., Harris, A., Ragoussis, J., Sieber, O., and Holmes, C.C. (2010). A statistical approach for detecting genomic aberrations in heterogeneous tumor samples from single nucleotide polymorphism genotyping data. Genome Biology *11*, R92.

Yeung, J., Esposito, M.T., Gandillet, A., Zeisig, B.B., Griessinger, E., Bonnet, D., and So, C.W.E. (2010). β-Catenin mediates the establishment and drug resistance of MLL leukemic stem cells. Cancer Cell *18*, 606–618.

Yilmaz, a, Gaide, a C., Sordat, B., Borbenyi, Z., Lahm, H., Imam, a, Schreyer, M., and Odartchenko, N. (1993). Malignant progression of SV40-immortalised human milk epithelial cells. British Journal of Cancer *68*, 868–873.

Yin, X., Grove, L., Rogulski, K., and Prochownik, E. V (2002). Myc target in myeloid cells-1, a novel c-Myc target, recapitulates multiple c-Myc phenotypes. The Journal of Biological Chemistry *277*, 19998–20010.

Yiu, G.K., and Toker, A. (2006). NFAT induces breast cancer cell invasion by promoting the induction of cyclooxygenase-2. The Journal of Biological Chemistry *281*, 12210–12217.

Yoshino, O., Izumi, G., Shi, J., Osuga, Y., Hirota, Y., Hirata, T., Harada, M., Nishii, O., Koga, K., and Taketani, Y. (2011). Activin-A is induced by interleukin-1β and tumor necrosis factor-α and enhances the mRNA expression of interleukin-6 and protease-

activated receptor-2 and proliferation of stromal cells from endometrioma. Fertility and Sterility *96*, 118–121.

Youlden, D.R., Cramb, S.M., and Baade, P.D. (2008). The International Epidemiology of Lung Cancer: geographical distribution and secular trends. Journal of Thoracic Oncology : Official Publication of the International Association for the Study of Lung Cancer *3*, 819–831.

Zauberman, A., Lapter, S., and Zipori, D. (2001). Smad proteins suppress CCAAT/enhancer-binding protein (C/EBP) beta- and STAT3-mediated transcriptional activation of the haptoglobin promoter. The Journal of Biological Chemistry *276*, 24719–24725.

Zecevic, A., Menard, H., Gurel, V., Hagan, E., DeCaro, R., and Zhitkovich, A. (2009). WRN helicase promotes repair of DNA double-strand breaks caused by aberrant mismatch repair of chromium-DNA adducts. Cell Cycle (Georgetown, Tex.) *8*, 2769–2778.

Zhang, G.-N., Liang, Y., Zhou, L.-J., Chen, S.-P., Chen, G., Zhang, T.-P., Kang, T., and Zhao, Y.-P. (2011). Combination of salinomycin and gemcitabine eliminates pancreatic cancer cells. Cancer Letters *313*, 137–144.

Zhang, S., Zhou, X., Yu, H., and Yu, Y. (2010). Expression of tumor-specific antigen MAGE, GAGE and BAGE in ovarian cancer tissues and cell lines. BMC Cancer *10*, 163.

Zhang, S., Wang, Y., Mao, J.-H., Hsieh, D., Kim, I.-J., Hu, L.-M., Xu, Z., Long, H., Jablons, D.M., and You, L. (2012). Inhibition of CK2α down-regulates Hedgehog/Gli signaling leading to a reduction of a stem-like side population in human lung cancer cells. PloS One *7*, e38996.

Zhang, X.-P., Zheng, G., Zou, L., Liu, H.-L., Hou, L.-H., Zhou, P., Yin, D.-D., Zheng, Q.-J., Liang, L., Zhang, S.-Z., et al. (2008). Notch activation promotes cell proliferation and the formation of neural stem cell-like colonies in human glioma cells. Molecular and Cellular Biochemistry *307*, 101–108.

Zhang, Z., Borecki, I., Nguyen, L., Ma, D., Smith, K., Huettner, P.C., Mutch, D.G., Herzog, T.J., Gibb, R.K., Powell, M.A., et al. (2007). CD83 gene polymorphisms increase susceptibility to human invasive cervical cancer. Cancer Research *67*, 11202–11208.

Zhao, C., Chen, A., and Jamieson, C. (2009). Hedgehog signalling is essential for maintenance of cancer stem cells in myeloid leukaemia. Nature *458*, 776–779.

Zheng, S., Chang, Y., Hodges, K.B., Sun, Y., Ma, X., Xue, Y., Williamson, S.R., Lopez-Beltran, A., Montironi, R., and Cheng, L. (2010). Expression of KISS1 and MMP-9 in non-small cell lung cancer and their relations to metastasis and survival. Anticancer Research *30*, 713–718.

Zhu, H., and Gooderham, N. (2002). Neoplastic transformation of human lung fibroblast MRC-5 SV2 cells induced by benzo[a]pyrene and confluence culture. Cancer Research *62*, 4605–4609.

Zhu, J., Abbruzzese, J.L., Izzo, J., Hittelman, W.N., and Li, D. (2005). AURKA amplification, chromosome instability, and centrosome abnormality in human pancreatic carcinoma cells. Cancer Genetics and Cytogenetics *159*, 10–17.

Zirath, H., Frenzel, A., Oliynyk, G., Segerström, L., Westermark, U.K., Larsson, K., Munksgaard Persson, M., Hultenby, K., Lehtiö, J., Einvik, C., et al. (2013). MYC inhibition induces metabolic changes leading to accumulation of lipid droplets in tumor cells. Proceedings of the National Academy of Sciences of the United States of America *110*, 10258–10263.

Appendix A

Solutions' Preparation

2.5 mM $K_2Cr_2O_7$ stock solution

This stock solution was prepared by dissolving 73,5 mg of $K_2Cr_2O_7$ in 100 ml of milli-Q water. Syringe filtration was subsequently used to guarantee the sterilization of the solution.

2 % BSA solution

This solution was prepared by diluting 2 g of BSA in 100 ml of milli-Q water under mild agitation. Syringe filtration was subsequently used to guarantee the sterilization of the solution.

Progesterone solution

Dissolve 0.003 g of progesterone in 1 ml of water in order to prepare an initial stock solution of 10 mM. The final 10 mM solution used in cell culture medium's preparation is made by mixing 100 µl of the stock solution with 900 µl of water.

2 % methylcellulose solution

To prepare 300 ml of a 2 % methylcellulose solution pre-heat 100 ml of water until it reaches the final temperature of 80 ºC, always keeping a mild stirring. Then dissolve 6 g of methylcellulose on the warm water and wait until the cellulose particles are dispersed to add the remaining 200 ml of water. This turn the water should has been previously cold until 4 ºC. The temperature of the solution should be brought to around 4 ºC, which is aided by placing the solution cup into ice. After reaching the desired temperature, agitation should be kept for approximately 20 min in order to ensure complete dissolution of the methylcellulose particles. Sterilization is attained by conventional autoclaving.

RT-qPCR primers' information

Table III - RT-qPCR primers' information.

Gene Primer	Catalogue number
GAPDH_2_SG	QT 01192646
TOP1_1_SG	QT 00068915
CCNB1_1_SG	QT 00006615
LDHA_1_SG	QT 00001687
HIF1α_1_SG	QT 00083664
SLC2A1_1_SG	QT 00068957
MYC_1_SG	QT 00035406
SPARC_1_SG	QT 00018620
EGFR_1_SG	QT 00085701
MAPK14_1_SG	QT 00079345
MAP2K4_1_SG	QT 00082530
MAPK1_1_SG	QT 00065933
XRCC1_1_SG	QT 00016688
XRCC3_1_SG	QT 00095921
XRCC5_1_SG	QT 00052731
RAD51_1_SG	QT 00072688
MSH2_1_SG	QT 00032466
CAV1_1_SG	QT 00012607
DNMT1_1_SG	QT 00034335
MLH1_1_SG	QT 00028833

Articles

Mutation Research 670 (2009) 42–52

Contents lists available at ScienceDirect

Mutation Research/Fundamental and Molecular Mechanisms of Mutagenesis

journal homepage: www.elsevier.com/locate/molmut
Community address: www.elsevier.com/locate/mutres

Human bronchial epithelial cells malignantly transformed by hexavalent chromium exhibit an aneuploid phenotype but no microsatellite instability

C.F.D. Rodrigues[a,b], A.M. Urbano[a,c,d], E. Matoso[a,e], I. Carreira[a,e,f], A. Almeida[g], P. Santos[g], F. Botelho[a,f], L. Carvalho[a,f], M. Alves[h], C. Monteiro[h], A.N. Costa[i], V. Moreno[i], M.C. Alpoim[a,b,c,*]

[a] Centro de Investigação em Meio Ambiente, Genética e Oncobiologia (CIMAGO), Faculdade de Medicina, Universidade de Coimbra, Coimbra, Portugal
[b] Centro de Neurociências e Biologia Celular, Universidade de Coimbra, Coimbra, Portugal
[c] Departamento de Bioquímica, Faculdade de Ciências e Tecnologia, Universidade de Coimbra, Coimbra, Portugal
[d] Unidade de Química Física Molecular, Faculdade de Ciências e Tecnologia, Universidade de Coimbra, Coimbra, Portugal
[e] Serviço de Citogenética, Instituto de Biologia Médica, Faculdade de Medicina, Universidade de Coimbra, Coimbra, Portugal
[f] Faculdade de Medicina, Universidade de Coimbra, Coimbra, Portugal
[g] Centro de Histocompatibilidade do Centro, Coimbra, Portugal
[h] Faculdade de Farmácia, Universidade de Lisboa, Lisboa, Portugal
[i] Departament de Química Inorgànica, Facultat de Química, Universitat de Barcelona, Barcelona, Spain

ARTICLE INFO

Article history:
Received 20 January 2009
Received in revised form 19 May 2009
Accepted 9 July 2009
Available online 16 July 2009

Keywords:
Hexavalent chromium
Lung cancer
BEAS-2B cells
Malignant transformation
Microsatellite instability
Mismatch repair system

ABSTRACT

Hexavalent chromium [Cr(VI)] is a well-recognized human lung carcinogen. In order to gain further insight into Cr(VI)-induced carcinogenesis, we have established an adequate *in vitro* cellular model for the study of this process. To this end, BEAS-2B cells were used. Chronic exposure of cells to 1 μM Cr(VI) induced changes in the cells' ploidy and a decrease in cloning efficiency, although cultures continued to progress to confluence. After prolonged exposure (12 passages), the culture became heterogeneous, exhibiting areas where apparently normal epithelial cells and morphologically altered cells coexisted. Subsequent culture at a very low density strongly accentuated the Cr(VI)-induced changes in morphology and pattern of growth. Three individual colonies were then ring-cloned and expanded into three subclonal aneuploid cell lines. These subclonal cell lines showed changes in growth pattern and morphology, as well as a karyotype drift concomitant with the overexpression of genes commonly involved in malignant transformation (c-*MYC*, *EGFR*, *HIF-1*α and *LDH-A*). Moreover, when one of these cell lines (RenG2) was injected into nude mice, it showed the ability to induce tumors. This cell line revealed no microsatellite instability (MSI), which points to the expression of a functional MLH1 protein and an active mismatch repair (MMR) system. Therefore, the progression to malignancy of the BEAS-2B cells involved Cr(VI)-induced transformants that retained the ability to repair DNA damage, suggesting that genotoxicity underlies the ongoing carcinogenic process.

1. Introduction

Epidemiologic studies revealed that there is a direct relationship between chronic exposure to Cr(VI) compounds (chromates) and lung cancer development [1]. Occupational exposure to Cr(VI) affects several million workers worldwide and non-occupational exposures to particulate chromates are increasing, due to industrial waste disposal, concrete pavement and fuel combustion, among other uses of Cr(VI). Important studies on Cr(VI) biochemistry revealed that the chromate structural affinity to sulphate and phosphate allows its quick movement across the cell membrane [2]. Once inside the cells, Cr(VI) is rapidly reduced to Cr(III) through mechanisms dependent on the reducing conditions [3,4]. Binary and ternary Cr(III)–DNA adducts were the most important DNA lesions detected in *in vitro* experiments [3]. Other forms of Cr(VI)-induced DNA damage include Cr(III)–DNA–protein crosslinks, DNA interstrand crosslinks, as well as DNA–protein crosslinks (DPCs) [2], which apparently represent the major obstacle for the replication and transcription processes [5]. In cellular systems, Cr(VI)-induced DNA lesions can easily generate not only single-strand breaks, but also the very mutagenic double-strand breaks, due to an abnormal procession of primary lesions by DNA repair systems, such as nucleotide excision repair (NER) and the methyl directed mismatch repair (MMR) [4], genome-surveillance systems that maintain the genomic integrity of mammalian organisms [6]. Accumulation of unrepaired double-strand breaks usually leads to apoptosis, while

* Corresponding author at: Departamento de Bioquímica, Faculdade de Ciências e Tecnologia, Universidade de Coimbra, Apartado 3126, 3001-401 Coimbra, Portugal. Tel.: +351 239853603; fax: +351 239853607.
E-mail address: mcalpoim@gmail.com (M.C. Alpoim).

0027-5107/$ – see front matter © 2009 Elsevier B.V. All rights reserved.
doi:10.1016/j.mrfmmm.2009.07.004

their abnormal processing by the non-homologous end joining system (NHEJ) generates chromosome rearrangements and thus genomic instability [7]. Cr(VI)-induced genomic instability can also result from uncoupling of centrosome duplication from the cell cycle, as a consequence of prolonged arrest at either S or G2 phases to repair double-strand breaks [8].

As revealed by post-mortem studies, the squamous lung cancer induced by inhalation of Cr(VI) compounds is different from the lung cancer induced by cigarette smoke and asbestos [9–11]. In fact, in contrast to other squamous lung carcinomas, Cr(VI)-induced lung cancer exhibits MSI, loss of expression of MLH1, aberrant methylation of $p16^{INK4}$ and low incidence of p53 mutations [9–11]. Furthermore, whenever p53 appeared mutated, it was found that it presented an unusual mutation pattern [9].

Recently, following the observation that MMR-deficient cells were highly tolerant to Cr(VI), another path has been evoked as the major pathway leading to Cr(VI)-induced lung cancers [4]. According to the proposal, chronic exposure to toxic doses of Cr(VI) may result in the selective outgrowth of MMR-deficient cells. Since MMR-deficient cells exhibit very high rates of spontaneous mutagenesis [12] and impaired MMR can give rise to malignancies exhibiting MSI [13], this model can account for the lack of expression of MLH1, a key protein of the MMR system, and the high incidence of MSI found in chromate lung cancers [9,10,14].

In spite of relevant studies on Cr(VI)-induced lung carcinogenesis that yielded important information on this subject (see, for instance, references [15–17]), it must be noted that very few utilized epithelial lung cells, the main targets of Cr(VI) carcinogenicity, and that, to the best of our knowledge, none of them involved continuous, long-term exposure to this carcinogen. Ideally, one should use primary cultures. However, the short lifespan of these cultures is not compatible with prolonged exposures to sub-lethal Cr(VI)-doses. For this reason the option for the BEAS-2B cell line (SV40 immortalized) [18] used in the present study to evaluate: (i) if the *in vivo* process of malignancy induced by chronic exposure to Cr(VI) could be mimicked *in vitro*; (ii) if the malignant transformation induced by Cr(VI) exposure was due to a process of selection of *MMR*-deficient, Cr(VI)-resistant and genetically unstable populations; (iii) if MSI was involved on Cr(VI)-induced malignant transformation; (iv) if this process of malignant transformation involved changes in the expression of genes commonly associated with carcinogenesis, namely, c-*MYC* [19], *HIF-1α* [20], *LDH-A* [21], *EGFR* [22], *DNMT1* [23], the cyclins *CCND1* and *CCNB1* [24], the MaP kinases *JNK*, *ERK* and *p38* [2,25], and the proteins involved in DNA repair *MLH1*, *RAD51*, *XRCC5*, *XRCC1*, *XRCC3* and *OGG1* [8,10,26,27]. Our study revealed that it is possible to induce *in vitro* the malignant transformation of bronchial epithelial cells by Cr(VI), and that this process was accomplished by a large karyotype drift and the overexpression of all genes under scrutiny, including *MLH1*. In spite of the extensive genomic instability induced by Cr(VI), the absence of MSI clearly showed that the progression to malignancy of the BEAS-2B cells did not involve the selection of *MLH1*-deficient cells.

2. Materials and methods

2.1. Cells and cell culture

BEAS-2B cells were obtained from the European Collection of Animal Cell Cultures (Salisbury, UK; ECCAC no. 95102433). Cells, grown as adherent monolayers, were maintained in Clonetics® BEGM medium supplemented with bovine insulin, bovine pituitary extract, epinephrine, human epidermal growth factor, hydrocortisone, retinoic acid, triiodothyronine, transferrin and the antibiotics amphotericin-B sulphate and gentamicin (Lonza, Barcelona, Spain) at 37 °C in a 95% air/5% CO_2 incubator. Vented culture flasks (Corning, Lowell, MA) were covered with a solution of type-B gelatin from bovine skin (Sigma–Aldrich, Sintra, Portugal) 2 h before use. Except otherwise stated, cells were seeded at an initial density of 4×10^3 cells/cm^2 and sub-cultured with a 0.25% trypsin–1 mM EDTA solution (Sigma–Aldrich, Sintra, Portugal) when cultures reached 80% confluence. Continuous cultivation in the presence of 1.0 μM Cr(VI) started at passage (#) 4. Cr(VI) was added as a 50 μM potassium dichromate aqueous solution, which was filter sterilized before use. Control cultures, grown in the absence of Cr(VI), were maintained in parallel.

2.2. Clonogenic assays

Cr(VI)-exposed cells from different passages were seeded onto 100 mm Petri dishes (Corning, Lowell, MA) at a cell density of 13 cells/cm^2. Cultures were then allowed to grow for 10 days both in the absence and in the presence of 1 μM Cr(VI). Control cells were subjected to the same treatment, except that Cr(VI) was always absent from the medium. Surviving colonies (containing more than 10 cells) were scored to assess cloning efficiency. Dense clumps, present in Cr(VI)-treated cultures, were also scored. Cells from these clumps exhibited clearly altered morphologies. Clonogenic experiments were repeated at least three times.

2.3. Generation of subclonal cell lines

For the generation of subclonal cell lines, several dense clumps obtained when passage 12 cultures were submitted to the clonogenic assay in the presence of Cr(VI) were isolated, using glass cloning rings (Sigma–Aldrich, Sintra, Portugal), reseeded onto 150 mm Petri dishes (Corning, Lowell, MA) and cultured again in the presence of 1 μM Cr(VI). Ten days later, three morphologically altered colonies were isolated and transferred into 3 different wells of a 6-well plate (Corning, Lowell, MA). When cultures reached near 80% confluence, cells were trypsinized and reseeded onto 25 cm^2 culture flasks (Corning, Lowell, MA), again in the presence of 1 μM Cr(VI). In the case of control cultures, where no dense clumps formed during the clonogenic assays, the cloning rings were used to isolate randomly chosen colonies. The cells thus isolated were subjected to the same treatment as the Cr(VI)-treated cells, except that Cr(VI) was always absent from the medium. All subclonal cell lines obtained were maintained as previously described.

2.4. Cytogenetic analysis

For cytogenetic analysis, cells were cultivated in 75 cm^2 flasks and allowed to reach approximately 75% confluence. The preparation of metaphase chromosomes was carried out according to standard procedures optimized to our cultures [28].

Metaphase spreads were GTG-banded and, for each passage, at least 30 metaphases were analyzed and 15 karyotypes constructed using a Nikon microscope (Nikon Portugal, Lisbon, Portugal) coupled with Applied Imaging® CytoVision® software (Genetix, New Milton, UK).

2.5. Gene expression analysis

For RNA isolation, 1×10^6 cells were initially collected in RNA*later*® RNA Stabilization Reagent (Qiagen, Madrid, Spain) and stored at −20 °C. RNA isolation was then carried out using the RNeasy® Mini Kit (Qiagen, Madrid, Spain), which allows for the isolation of total RNA from animal cells. To quantify the RNA extracted and verify its integrity, samples were analyzed using the RNA 6000 Nano Chip® Kit in an Agilent 2100 Bioanalyzer with the 2100 Expert Software (Agilent Technologies, Böblingen, Germany), according to the manufacturer's instructions.

One microgram of total RNA was reverse transcribed using the SuperScript™ III First-Strand Synthesis System for RT-PCR (Invitrogen, Barcelona, Spain). The reactions were carried out in a GeneAmp PCR System 9600 Thermal Cycler (PerkinElmer, Waltham, MA). Reaction products were digested with 1 μl RNase H and finally eluted with 30 μl Rnase-free water and stored at −20 °C.

Relative quantification of gene expression by Real-Time PCR was performed in a 7900 HT Sequence Detection System (Applied Biosystems, Foster City, CA). For normalization purposes, optimal housekeeping genes for this study were selected using the geNorm™ Housekeeping Gene Selection Kit (PrimerDesign, Southampton, UK) and the geNorm™ software (Ghent University Hospital, Ghent, Belgium). Real-time PCR reactions used QuantiTect® Primer Assays (Qiagen, Madrid, Spain) for each of the different genes. Real-time PCR reactions were carried using 100 ng of cDNA sample, 1× QuantiTect® Primer Assay and 1× QuantiTect® SYBR Green PCR Master Mix (Qiagen, Madrid, Spain), in a total volume of 50 μl, using the following thermal profile: 15 min at 95 °C (PCR initial activation step) and 40 cycles of 15 s at 94 °C, 30 s at 55 °C and 30 s at 72 °C. Real-time PCR results were analyzed with the SDS 2.1 Software (Applied Biosystems, Foster City, CA) and quantified using the $2^{-\Delta\Delta Ct}$ method [29].

2.6. Microsatellite analysis

Five mononucleotide repeats (NR-21, NR-24, NR-27, BAT-25 and BAT-26) were amplified in a pentaplex PCR reaction using a Biometra T3 Thermocycler (Göttingen, Germany). Primer sequences were as previously described [30]. All the reverse primers (Thermo Scientific, Ulm, Germany) were 5′-labelled with a fluorescent tag – HEX for markers NR-24, NR-27 and BAT-26, and 6-FAM for markers NR-21 and BAT-25 – to allow for microsatellite detection using an Applied Biosystems 3730XL DNA Analyzer (Applied Biosystems, Foster City, CA). The PCR reaction was carried out in a total volume of 25 μl that contained 1× GoTaq® Flexi Buffer (Promega, Madison, WI), 0.2 mM dNTPs, 2.5 mM $MgCl_2$, 8 pmol of primers NR-21, NR-24 and NR-27, 10 pmol of

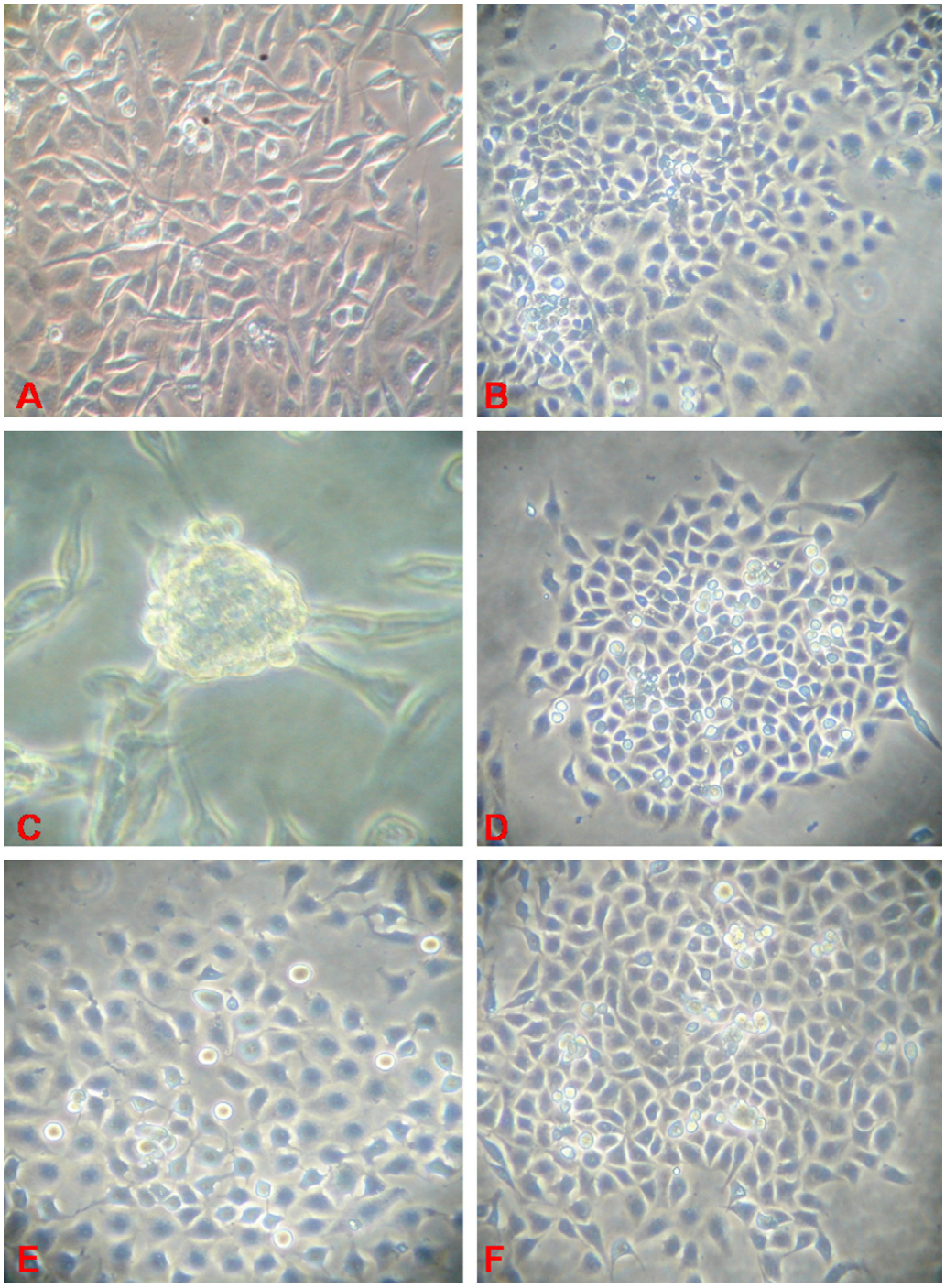

Fig. 1. Effect of Cr(VI) on the morphology and growth pattern of BEAS-2B cells. (A) Representative image of BEAS-2B cultures that were cultivated for 8 passages in the presence of 1 μM Cr(VI). (B) As (A), but with cells grown in the absence of Cr(VI) (control cultures). (C) Representative image of colonies obtained when cells from the cultures represented in (A) were cultivated at very low density (13 cells/cm^2) in the presence of 1 μM Cr(VI). (D) Representative image of colonies obtained when cells from the cultures represented in (B) were cultivated at very low density (13 cells/cm^2) in the absence of Cr(VI). (E) Representative image of the RenG2 subclonal cell line. (F) Representative image of a control subclonal culture.

primer BAT-25, 12 pmol of primer BAT-26, 0.75 U of GoTaq® Flexi A DNA Polymerase (Promega, Madison, WI) and 5 μl of genomic DNA. Genomic DNA was extracted from the cells with the Puregene® DNA Isolation Kit (Gentra Systems, Minneapolis, MN), according to the manufacturer's instructions. After an initial denaturation at 95 °C for 5 min, PCR steps were as follows: 35 cycles of denaturation at 94 °C for 30 s, annealing at 54 °C for 45 s and extension at 72 °C for 30 s. Final extension was carried out at 72 °C for 10 min. Successful amplification was confirmed by electrophoresis on a 3.5% agarose gel and PCR products were sent to Macrogen Inc. (Seoul, Republic of Korea) (http://www.macrogen.com) for fragment analysis. Allelic sizes estimation and MSI analysis were made using the GeneMarker® software (SoftGenetics, State College, PA). The Cr(VI)-exposed cell line would be considered MSI positive if, at least, 2 out of 5 markers showed band shifting, when compared to the control, non-exposed one.

2.7. *In vivo tumorigenicity assay*

All experiments were performed according to EU guidelines on the ethical use of experimental animals (86/609/EEC). The tumorigenicity assay was performed by s.c. injection of 10^7 cells suspended in 100 μl of sterile saline solution into four 6 weeks old BALB/c-nu/nu mice. Animals were inspected weekly for the appearance of tumors. Two months after the injection, tumors were removed and fixed in formalin. Two additional mice were s.c. injected with 10^7 and 2×10^7 BEAS-2B control cells.

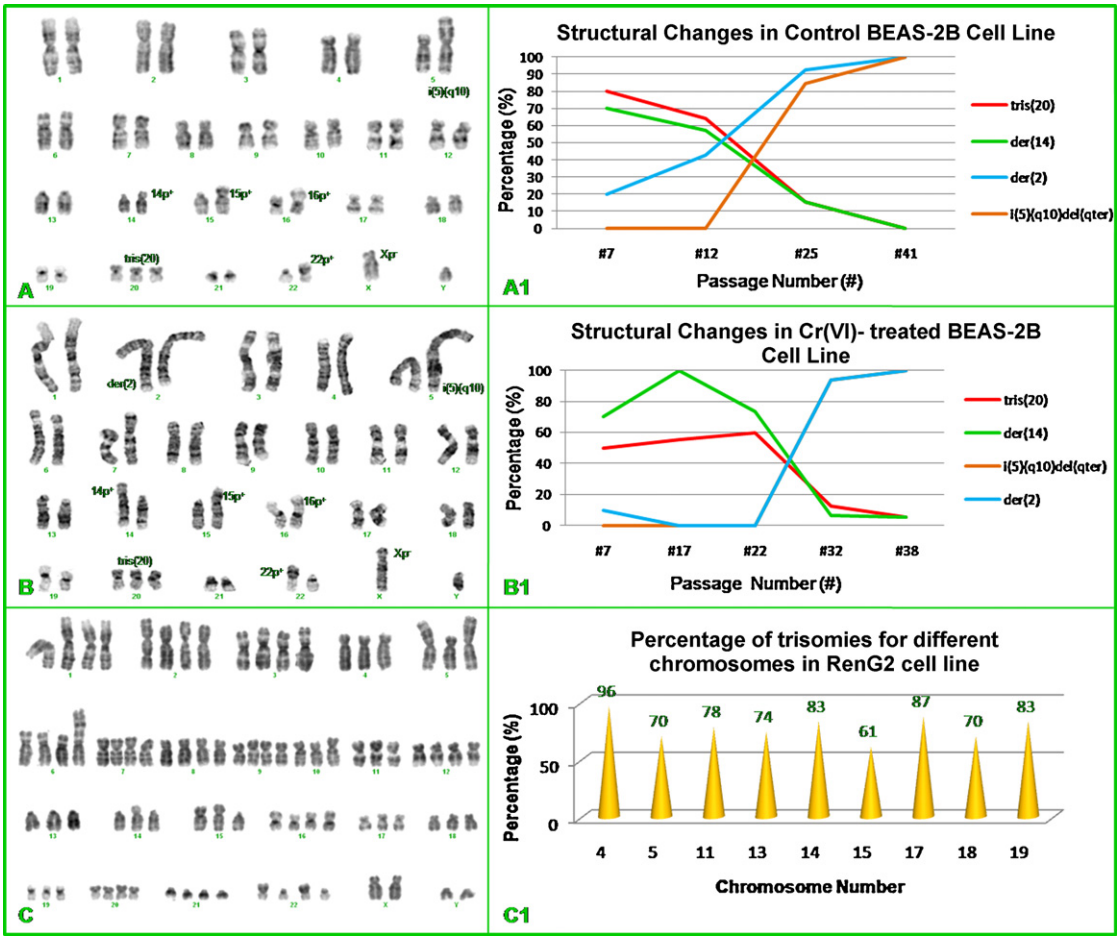

Fig. 2. Representative karyotype of BEAS-2B cells (at passage 7). (A) Cultures grown in the absence of Cr(VI). (B) Cultures grown in the presence of 1 μM Cr(VI), showing alterations in various chromosomes: i(5)(q10), $14p^+$, $15p^+$, $16p^+$, trisomy 20, $22p^+$ and Xp^-. (A1) Evolution of the karyotype along time in culture for control BEAS-2B cells. (B1) Evolution of the karyotype along time in culture for BEAS-2B cells exposed to 1 μM Cr(VI). It was observed a gradual disappearance of trisomy 20 and of the 14 mosaicism and an increase on der(2) as well as i(5)(q10)del(5)(qter) both in control and Cr(VI)-treated BEAS-2B cells. Percentages were relative to the initial karyotype variations documented in (A) and (B). (C) Representative karyotype of Cr(VI)-transformed subclonal cell line RenG2 (#4). (C1) Percentage of trisomies for different chromosomes in the RenG2 cell line. The presented percentages were calculated from the evaluation of 20 karyotypes of the RenG2 cell line.

For the determination of their histological classification, tumors were embedded in paraffin. Three micrometer sections were stained with hematoxylin and eosin for microscopic evaluation and were examined by a pathologist. Immunohistochemistry was performed for LCA (lymphoma marker; clone 2B11 + PD7/26), HMB-45 (melanosome marker), MNF116 (cytokeratin antibody marker for carcinomas; clone MNF116), and vimentin (mesenchymal marker; clone Vim 3B4). All clones were obtained from Dako Corporation (Carpinteria, CA).

2.8. Digital image

Throughout this study, cell morphology and growth pattern were continuously monitored by microscopic observation. Inverted phase micrographs were obtained using a Sony Cyber Shot digital camera DSC-S600.

3. Results

3.1. Establishment of subclonal cell lines

In an attempt to establish malignantly transformed subclonal cell lines, we have continuously exposed BEAS-2B cells to 1 μM Cr(VI), a dose previously found by us to be only slightly cytotoxic (submitted for publication).

Up to *ca.*10 passages in culture, both control and Cr(VI)-treated BEAS-2B cells displayed similar morphologies when cultivated at the regular cell density (4000 cells/cm^2). However, upon Cr(VI) exposure, cells became increasingly less resistant to trypsinization, as compared to control cells. By passage 12, the Cr(VI)-exposed culture became non-homogeneous (Fig. 1A), with discrete collections of cells displaying a growth pattern and/or morphologic appearance distinct from those of the normal diamond-shaped epithelial cells (Fig. 1B), a behaviour identical to that observed by our group on a previous study (submitted for publication).

Clonogenicity assays carried out at different passages (between 5 and 13) confirmed the low cytotoxicity of the Cr(VI) dose used in this study. In fact, when the assay was carried out in the absence of Cr(VI), the clonogenic survival of Cr(VI)-exposed BEAS-2B cells was only slightly lower (by less that 10% at all passages tested) than that of the control cells. Addition of Cr(VI) to the growth medium during the assay resulted in a higher decrease of the clonogenic survival of Cr(VI)-treated cells (results not shown). This decreased clonogenic efficiency was likely the result of the reported higher duplication time exhibited by BEAS-2B cells exposed to 1 μM Cr(VI) (submitted for publication), as prolonged exposure to this Cr(VI) dose did not result in significant cell death (submitted for publication). Cultivation of these Cr(VI)-treated cells at a very low cell density (13 cells/cm^2), again in the presence of Cr(VI), deeply accentuated the observed Cr(VI) effects, with cultures showing many areas of cells with profoundly changed morphologies and with growth pattern features resembling those of malignantly transformed cells. It was also possible to observe several dense clumps containing cells with clearly altered morphologies (Fig. 1C). Cultivation of control cells at the same low cell density had no effect on the morphology

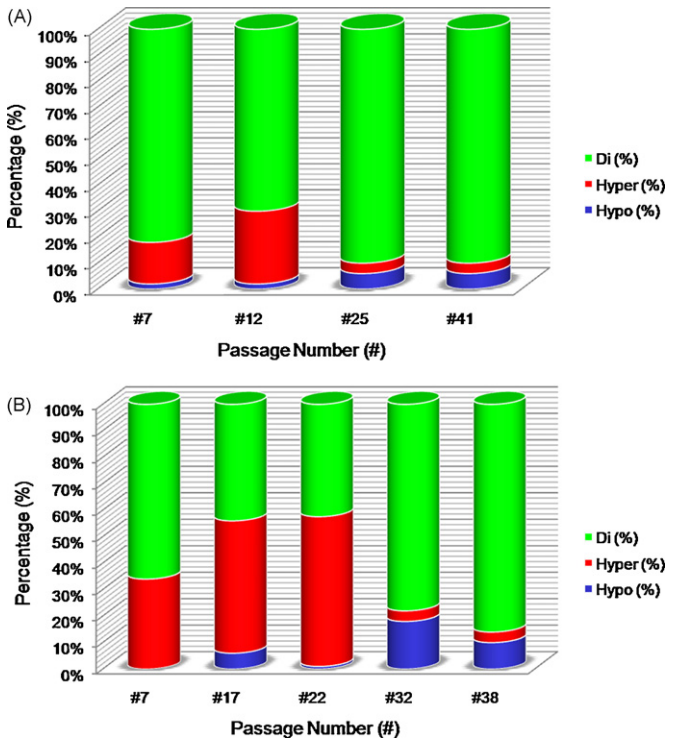

Fig. 3. Representative changes in cells' ploidy along time in culture. (A) BEAS-2B cells grown in the absence of Cr(VI). (B) BEAS-2B cells grown in the presence of 1 μM Cr(VI) (B). Although a similar pattern was observed for both control and Cr(VI)-exposed BEAS-2B cells, Cr(VI) treatment exacerbated the increase in the percentage of hyperdiploid metaphases (between 46 and 96) in early passages and the increase in the number of hypodiploid metaphases (less than 46 chromosomes) in late passages. At least 30 metaphases were analyzed for each passage.

and pattern of growth of the cells (Fig. 1D). Thus, cultivation at a very low density and in the presence of Cr(VI) of cells that were being chronically exposed to this carcinogen set the stage for the emergence and evolution of cells portraying some of the biological hallmarks of tumor progression (e.g. foci formation, decreased cell–cell interactions). Three subclonal cell lines [RenG1, RenG2 (Fig. 1E) and CrossG1] were established from these Cr(VI)-exposed cultures (see the Materials and Methods section for the detailed protocol). Control cultures also gave rise to three control subclonal cell lines [Cont1 (Fig. 1F), Cont2 and Cont3].

3.2. Karyotype evolution

Lack of detailed information on the cytogenetic constitution of BEAS-2B cells prompted the study of the evolution of the karyotype of this cell line along time in culture. At the beginning of this study, with cultures at very low passages, all cells analyzed showed an isochromosome 5 [i(5)(q10)], a terminal deletion of the short arm of chromosome X (Xp^-) and additional material on the short arm of chromosomes 15 (15p+), 16 (16p+) and 22 (22p+) (Fig. 2A). In addition, this cell line exhibited a trisomy of chromosome 20 in nearly 80% of the metaphases analyzed, the presence of a derivative chromosome 14 with additional material on the short arm [der(14)] on 70% of the metaphases, as well as structural alterations of the banding pattern along the long arm of chromosome 2 [der(2)] on 20% of the metaphases. Karyotype evolution along the time in culture (up to #42) showed a decrease in the percentage of cells with trisomy 20 and with der(14). Increases in the percentage of cells with der(2) and the emergence of a terminal deletion on i(5)(q10) [i(5)(q10)del(qter)] were also observed (Fig. 2A1).

As illustrated in Fig. 3, in the early stages of exposure to Cr(VI), there was an increase in the number of hyperdiploid cells relative to the control. However, the evolution pattern of the cell line karyotype in the presence of Cr(VI) (Figs. 2B and 3B) was quite similar to that observed in control cells (Figs. 2A and 3A), *i.e.* there was a decrease in the number of cells with trisomy 20 and chromosome 14 mosaicism, as well as an increase in der(2) and i(5)(q10)del(qter) (Fig. 2B and B1). More prolonged cultivation (>#25) in the presence of Cr(VI) lead to an increase in hypodiploid cells (Fig. 3B), similar to what was found in human bronchial fibroblasts exposed to Cr(VI) [31]. The control subclonal cell line had a karyotype rather similar to that of the initial cell line. In contrast, the subclonal cell lines derived from Cr(VI)-exposed BEAS-2B cultures showed a marked karyotypic change. Fig. 2C and C1 illustrates the aneuploid phenotype (*ca.* 80 chromosomes in over 90% of the metaphases analyzed) of one of these subclonal cell lines (RenG2) at passage 4. Between passages 1 and 4, a duplication of the chromosome complement of the RenG2 subclonal cell line must have taken place, followed by a gradual loss of chromosomes towards the aneuploid phenotype observed at passage 4. This latter phenotype remained stable along time in culture. It has been suggested that this chromosomal evolution reflects the earliest steps on a long process toward malignancy [32–34]. As karyotype analysis revealed that all Cr(VI)-subclonal cell lines were identical, only one of them (RenG2) was selected for subsequent studies.

3.3. Evolution of the expression of biomarkers of malignant transformation

In non-small cell lung cancer (NSCLC), as well as in bronchial preneoplasia, the epidermal growth factor receptor (*EGFR*) is frequently overexpressed, and its autocrine loop is considered fundamental in regulating epithelial carcinogenesis [22,35]. *CCND1* (cyclin D1) is also frequently overexpressed in the early stages of lung carcinogenesis *in vivo* [24] and several studies revealed that *CCND1* transcriptional activation in response to *EGFR* activation is mediated by diverse pathways, such as the mitogen-activated protein kinase (MaP kinase) pathway [25]. Therefore, it was reasonable to hypothesize that during the process of BEAS-2B malignant transformation these genes would be constitutively up-regulated.

The Warburg effect, the ability of cancer cells to overproduce lactic acid aerobically as a consequence of exacerbated glycolysis, was recognized long ago [36]. The basis for the Warburg effect is likely to include activated oncogenes, inactivated tumor suppressors and the hypoxia-inducible transcription factor HIF-1, a heterodimeric transcription factor composed of HIF-1α and HIF-1β/aryl hydrocarbon nuclear translocator subunits [21]. HIF-1α is the regulatory component of the HIF-1 complex and is unique to the hypoxic response and metal stress [37]. Under normoxic conditions, HIF-1α is virtually undetectable in many normal cells [38]. However, *HIF-1* is induced by the expression of oncogenes such as *v-SRC*, *RAS* and *c-MYC* [39] and is overexpressed in many human cancers [21]. In fact, its activity in cells correlates with tumorigenicity and angiogenesis [40]. HIF-1α regulates the expression of many genes, including lactate dehydrogenase A (*LDH-A*) [21]. LDH-A, which participates in normal anaerobic glycolysis, has been used as a marker of neoplastic transformation [21]. The LDH-A gene, frequently overexpressed in human cancers, was identified as a c-MYC-responsive target [19]. Transgenic animals constructed to overexpress c-MYC in the liver have increased levels of glycolytic liver enzymes and overproduce lactic acid [41].

Unequivocal evidence from numerous cellular experimental systems indicates that oncogenic factors including c-MYC [19], HIF-1α [20] and LDH-A [21] are prevalent in many types of cancers, being associated with cellular response to stress and demonstrating pleiotropic properties. As illustrated in Fig. 4A cultivation of BEAS-

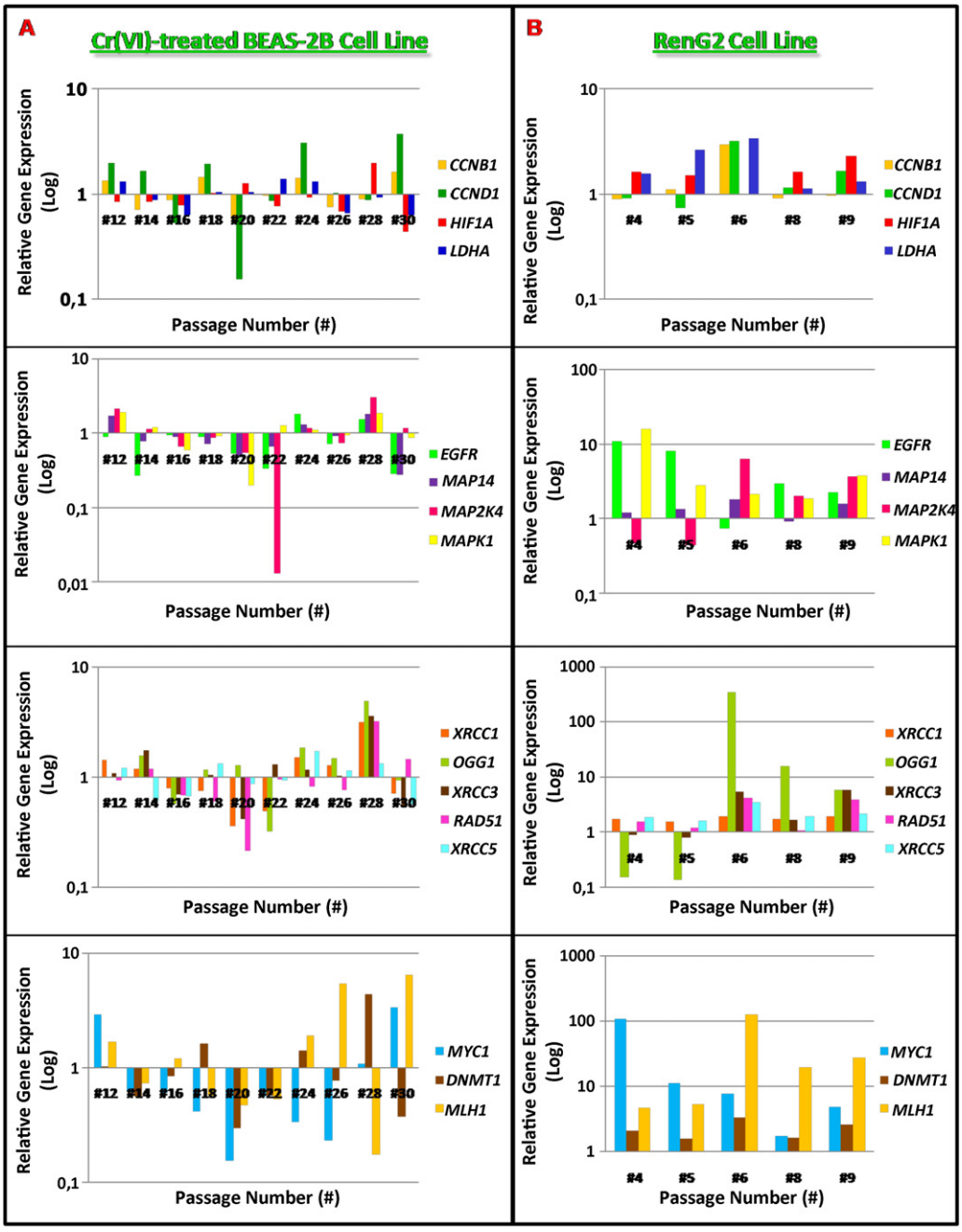

Fig. 4. Variations in gene expression profiles between Cr(VI)-treated BEAS-2B and RenG2 cell line. These images establish a parallel between the expression profiles of *CCNB1*, *CCND1*, *DNMT1*, *EGFR*, *HIF-1α*, *LDH-A*, *MAPK14*, *MAP2K4*, *MAPK1*, *c-MYC*, *MLH1*, *OGG1*, *RAD51*, *XRCC3*, *XRCC1* and *XRCC5* genes in both Cr(VI)-exposed BEAS-2B and RenG2 cells. The same color is used in the corresponding graphs to represent the same gene. (For interpretation of the references to color in this figure legend, the reader is referred to the web version of the article.)

2B cells in the presence of Cr(VI) yielded no consistent changes on the overall expression of genes c-*MYC*, *HIF-1α* and *LDH-A*, as well as of genes such as *EGFR*, *CCND1* and of the MaP kinases JNK (*MAP2K4*), ERK (*MAPK1*) and p38 (*MAPK14*). However, in the RenG2 subclonal cell line, the expression of all these genes was consistently up-regulated along time in culture (Fig. 4B).

3.4. Evolution of the expression of the genes that code for proteins of the DNA repair systems and of DNMT1

As mentioned before, it has been suggested that deficiencies in DNA repair due to inactivation of DNA repair systems and/or to their abnormal processing of DNA lesions may be implicated in Cr(VI)-induced lung cancer. DNA methyltransferases (DNMTs), which catalyze the covalent addition of methyl groups to cytosines in the CpG dinucleotide context, were reported to play an important role in the inactivation of DNA repair systems [42], in genomic instability with increased loss of heterozygosity [43], in the activation of tumor suppressors and in the activation of oncogenes [44]. Moreover, they have been directly implicated in the epigenetic drift observed in malignant transformed tissues [44]. Therefore, it was important to explore their involvement in Cr(VI)-induced lung cancer.

In BEAS-2B cells exposed to Cr(VI), the expression of the genes that code for proteins involved on DNA repair, namely *RAD51*, *XRCC3* and *OGG1* [homologous recombination (HR)], *XRCC1* [base excision

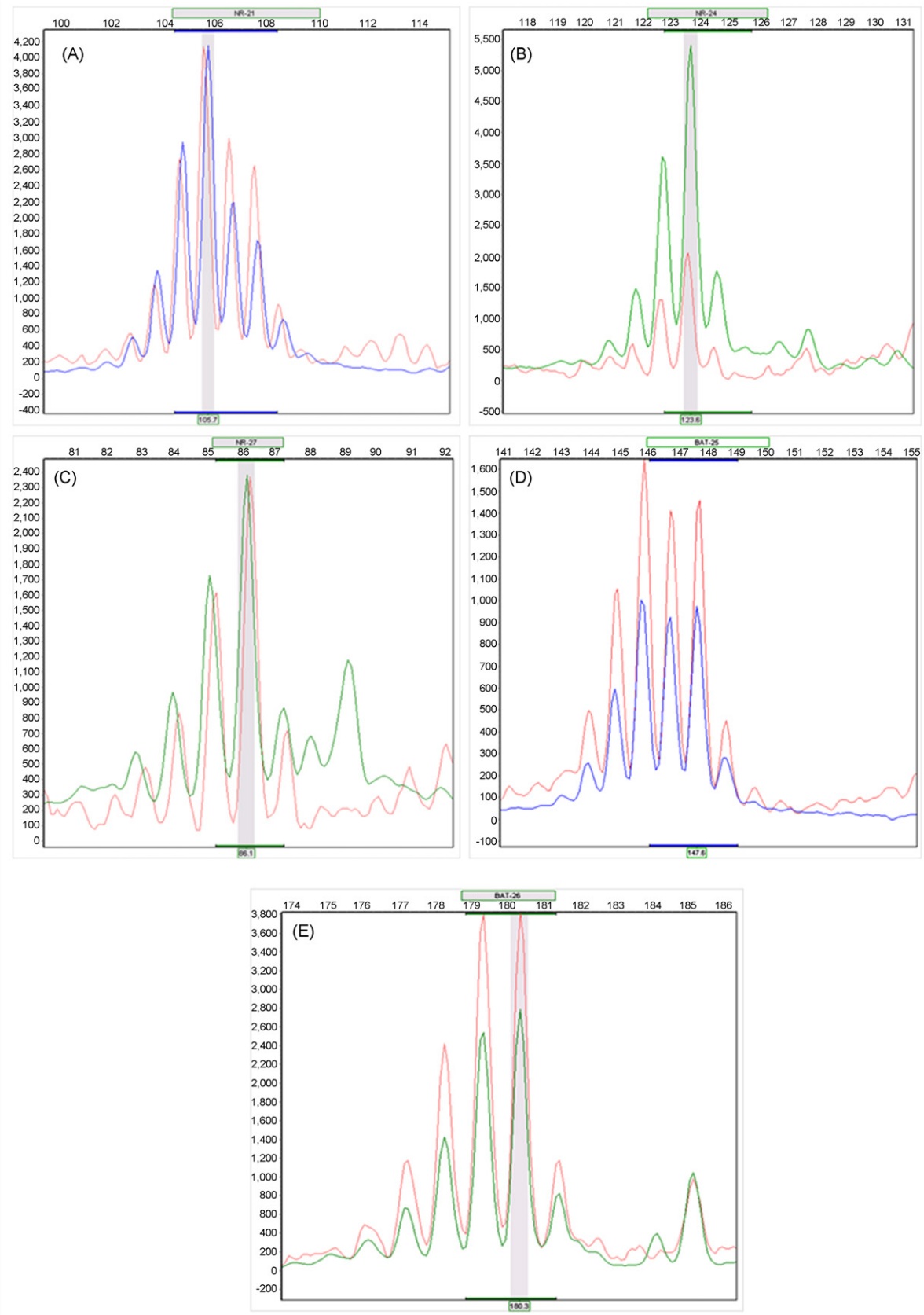

Fig. 5. Chromatograms showing absence of instability for the microsatellite markers (A) NR-21, (B) NR-24, (C) NR-27, (D) BAT-25 and (E) BAT-26. Red peaks correspond to the BEAS-2B control cell line whereas blue/green correspond to the RenG2 Cr(VI)-transformed subclonal cell line. (For interpretation of the references to color in this figure legend, the reader is referred to the web version of the article.)

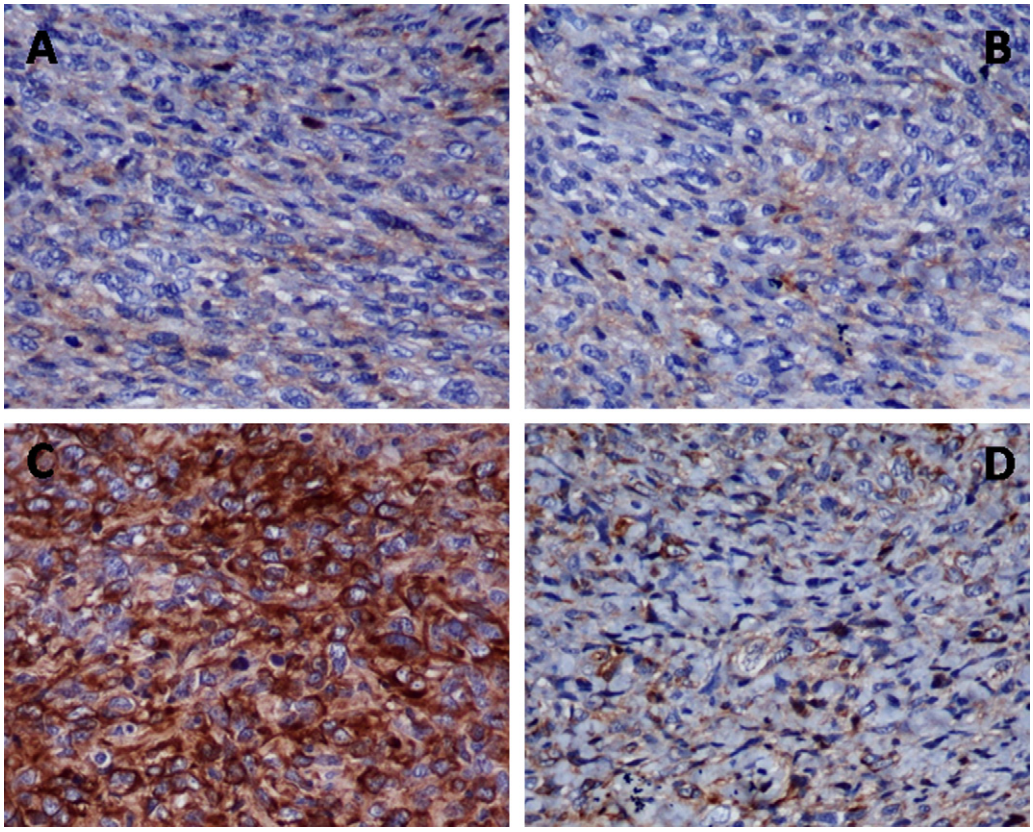

Fig. 6. Immunohistological analysis of the tumors induced by RenG2 cells upon s.c. injection into nude mice. The negative staining for LCA (400×) (A) and HMB45 (400×) (B) and the positive staining for MNF116 (400×) (C) revealed the malignant epithelial nature of the tumors. Vimentin staining (400×) (D) showed a ubiquitous distribution of this protein, typical of normal tissue, confirming the epithelial origin of the tumor.

repair (BER)], *XRCC5* (NHEJ) and *MLH1* (MMR), as well as that of the *DNMT1*, changed randomly with exposure time (Fig. 4A). The continuous and random variation of the expression of the aforementioned genes possibly reflects the phenotypic diversity that resulted from exposure to Cr(VI). In contrast, the expression of all the above mentioned genes in RenG2 was consistently up-regulated (Fig. 4B).

3.5. Microsatellite analysis

Microsatellites are short, tandemly repeated nucleotide sequences that are widely distributed throughout the genome [45]. Because of their repetitive nature, microsatellites are particularly prone to errors during replication. Length alterations in microsatellite repeats are termed MSI [45]. Frequent somatic variations in the size of microsatellites is a characteristic of the replication error phenotype (RER) [46], which is most commonly caused by a deficiency of the DNA MMR system attributable to mutation in one of the human DNA MMR genes: h*MLH1*, h*MSH2*, h*MSH3*, h*MSH6*, h*PMS1* and h*PMS2* [42,45]. The recently introduced pentaplex polymerase chain reaction of five mononucleotide repeats to establish the MSI status of human tumors was shown to be 100% sensitive and specific [30]. In the present study, the microsatellite analysis of the RenG2 cell line with the pentaplex mononucleotide panel showed no MSI at any marker, when compared with control BEAS-2B cells (Fig. 5). All electrophoretograms of mononucleotide markers showed a number of less intense stutter peaks at 1 bp intervals from the true allele peak, due to polymerase slippage during PCR amplification of each STR marker. Therefore, the RenG2 cell line does not have an MSI phenotype because, according to the consensus meeting guidelines, a tumor is considered MSI-H (MSI phenotype) when at least 3 out of 5 mononucleotide repeats show instability [30].

3.6. Tumorigenicity results

None of the two male nude mice s.c. injected with control BEAS-2B cells developed tumors, which is in agreement with what was previously reported by Reddel et al. [18]. Concerning the RenG2 subclonal cell line, 3 out of 4 injected mice developed one tumor each. The immunohistological analysis of the tumor cells induced by RenG2 in nude mice revealed negative staining for LCA and HMB45, and positive staining for MNF116 (Fig. 6), clearly showing characteristics of carcinoma.

4. Discussion

In the present work, a tumorigenic cell line was established by cultivating at a very low density and in the presence of 1 μM Cr(VI) cells that had been exposed to this dose of the carcinogen for several passages. Such treatment did not induce microsatellite instability, but lead to changes in chromosome number, to decreased cell–cell interactions, as well as to alterations in the cells' morphology and growth pattern and in the expression of genes commonly associated with malignant transformation. Moreover, when cells from one of the subclonal cell lines obtained were injected into nude mice, it induced tumors.

Frequently, the diploid to aneuploid transition is associated with the biological progression from phenotypically normal to malignant cells [32–34]. The induction of aneuploidy and the correlated ability to induce morphological transformation observed in this study parallels the results obtained with other human and rodent

SV40-immortalized cells [47,48] and with a SV40-transgenic mouse model [49] following exposure to a chemical carcinogen. These findings may suggest that immortalization by SV40, which leads to the sequestration of p53 [50], a protein that has been correlated to the onset of tetraploidy [33], may induce malignant transformation. Nevertheless, the results of the present work confirm that immortalization by SV40 is not sufficient for the neoplastic transformation of BEAS-2B cells, as non-treated BEAS-2B cells are not malignant. However, we cannot exclude that p53 deficiency may pre-dispose Cr(VI)-damaged cells to aneuploidy because cells with DNA damage may continue to divide, being subject to asymmetric chromosome segregation every time this happens [51].

Even though the mutagenic effect of carcinogens is generally accepted as the driving force of transformation, a new theory has recently emerged pointing that changes in ploidy and the consequent imbalance in gene expression may also play an important role [52]. As recent work showed, in cell lines with relatively high spontaneous rates of chromosome non-disjunction in late mitosis, the fate of the majority of cells is to become tetraploid [32]. Therefore, cancer development may not necessarily require mutations in cancer related genes at the DNA level, but an imbalance in the dosage of thousands of normal genes, caused by chromosomal gains or losses by random aneuploidization [53]. Thus, cells may become transformed before mutations on tumor suppressor genes and/or oncogenes occur [52].

The malignant transformation of BEAS-2B cells following prolonged exposure and low density cultivation in the presence of Cr(VI) cannot be ascribed solely to Cr(VI) effects on chromosome segregation and genetic instability. The finding that the transcription of genes that code for proteins involved in DNA repair (*RAD51*, *XRCC3*, *OGG1*, *XRCC1*, *XRCC5* and *MLH1*) is up-regulated in the subclonal RenG2 cell line suggests that DNA damage played an important role in the process of transformation. This assumption is reinforced by the fact that chronic exposure of BEAS-2B cells to Cr(VI) increased their duplication time (results submitted to publication), which may reflect the time spent by the cells repairing DNA damage. Additionally, BEAS-2B cells exposed for lower periods (5 passages) to Cr(VI) preserved a normal phenotype even when cultivated at a very low cell density (results not shown), supporting the premise that prolonged DNA damage is a major event in the progression to malignancy.

Recent data obtained with human epithelial colon HCT116 cells ($MLH1^{-/-}$ and $MLH1^{+/+}$) and also with MMR-deficient human lung fibroblasts and epithelial cells strongly suggested that chronic exposure to toxic doses of Cr(VI) may result in the selective outgrowth of MMR-deficient cells [4,7]. As MMR-deficient cells exhibit very high rates of spontaneous mutagenesis, this model could explain the high incidence of MSI found in chromate cancers [9,10,14], thereby leading to the hypothesis that Cr(VI)-associated cancer cells express the mutator phenotype (the tendency to undergo a cascade of further mutations) [54] caused by the loss of the DNA most important mutation prevention system, MMR [4]. However, our data contradicts this hypothesis, since the malignant RenG2 subclonal cell line has high *MLH1* transcript levels and does not exhibit MSI. Additionally, the findings that the *DNMT1* gene is overexpressed in RenG2 subclonal cell line further confirms that the pathway involved in malignant transformation of BEAS-2B by Cr(VI) does not appoint to MSI, since reduction of *DNMT1* activity was reported to reduce MMR efficiency and to increase MSI [55]. Besides, increased *DNMT1* transcript levels were reported to correlate with c-*MYC* mRNA levels in gastric cancers [56] and to transformation of NIH 3T3 cells [23].

In the RenG2 subclonal cell line, the genes of the most important DNA repair systems (BER, HR and NHEJ) were also actively transcribed, which goes against the assertion that genomic instability only builds up in cells whose DNA repair pathways are seriously compromised, as was the case with HR- [26], BER- [27] and FANCA-(Falconi anemia) [57] deficient cells exposed to Cr(VI), which exhibited increased chromosomal damage and aberrations.

The absence of neoplastic transformation of BEAS-2B cells after prolonged exposure (>#12) to Cr(VI) at normal cell density indicates that the low cell density setting provided adequate conditions for selection of variants that were susceptible to Cr(VI) transformation. Cellular Cr(VI) uptake has been reported to be very fast, with a maximum load being reached within the first 3 h of exposure [58]. In this study, we observed that Cr(VI)-treatment weakened cell adhesion to the substratum. The ratio Cr(VI)/cell was much lower at normal cell density than in the low density cultures. Thus, in low density cultures, Cr(VI) pressure selects the most resistant phenotypes, through a multi-stage process which, similarly to the acquisition of drug resistance, is associated with genomic instability. In fact, genetic instability provides a supply of mutants from which the environment selects favourable variants to its growth-limiting conditions [59]. As recently emerged, mutations themselves are irrelevant if there is not a microenvironment change that selects the cells carrying such mutations [60]. Thus, the nature of the cellular microenvironment must have determined the cells to be selected.

Activation of MaP kinases pathways has a pivotal function in controlling cell growth, survival, differentiation and apoptosis [61]. The results obtained in the present study are in agreement with a critical role for ERK in mitogenesis and differentiation [62]. As to JNK and p38, our data revealed that their activation does not correlate with cytotoxicity. *JNK* and *p38* were also persistently activated [63] in human lung carcinoma cells continuously exposed to Cr(VI), which raises the hypothesis that activation of these kinases may support cell survival and carcinogenesis. This goes against the common association of their activation to growth arrest and apoptosis [64].

Finally, our data indicates that *in vitro* Cr(VI)-induced malignant transformation of BEAS-2B is mediated by *EGFR* activation, similarly to what was reported in *in vivo* human bronchial pre-neoplastic and malignant lung lesions [24].

In conclusion, similarly to chronic exposure to cigarette smoke, the effects of prolonged exposure to Cr(VI) may also include DNA damage and growth inhibition. These effects run in parallel with the emergence of altered cells resistant to cytotoxicity. The development of Cr(VI) resistance, more than the mutagenic potential of Cr(VI), paves the way to the accumulation of mutations through the selection of the most resistant variants. Thus, our findings in fact suggest that the resistance phenotype pathway plays an important role in the onset of the chromate lung cancer.

Conflict of interest

The authors declare that there are no conflicts of interest.

Acknowledgements

This research was supported by Centro de Investigação em Meio Ambiente, Genética e Oncobiologia (CIMAGO; Research grant 16/06), by Fundação para a Ciência e Tecnologia, Portugal (FCT; Research grant POCTI/CBO/48631/2002; co-financed by FEDER) and by Ministério de Educación y Ciência, Spain (Research grant BQU-2005-01834). CFDR and ANC acknowledge PhD grants from FCT, Portugal (grants SFRH/BD/48072/2008 and SFRH/BD/37194/2007, respectively).

References

[1] R.M. Park, J.F. Bena, L.T. Stayner, R.J. Smith, H.J. Gibb, P.S. Lees, Hexavalent chromium and lung cancer in the chromate industry: a quantitative risk assessment, Risk Anal. 24 (2004) 1099–1108.

[2] T.J. O'Brien, S. Ceryak, S.R. Patierno, Complexities of chromium carcinogenesis: role of cellular response, repair and recovery mechanisms, Mutat. Res. 533 (2003) 3–36.
[3] A. Zhitkovich, Importance of chromium-DNA adducts in mutagenicity and toxicity of chromium(VI), Chem. Res. Toxicol. 18 (2005) 3–11.
[4] K. Salnikow, A. Zhitkovich, Genetic and epigenetic mechanisms in metal carcinogenesis and cocarcinogenesis: nickel, arsenic, and chromium, Chem. Res. Toxicol. 21 (2008) 28–44.
[5] M. Schnekenburger, G. Talaska, A. Puga, Chromium cross-links histone deacetylase 1-DNA methyltransferase 1 complexes to chromatin, inhibiting histone-remodeling marks critical for transcriptional activation, Mol. Cell. Biol. 27 (2007) 7089–7101.
[6] M.J. Schofield, P. Hsieh, DNA mismatch repair: molecular mechanisms and biological function, Annu. Rev. Microbiol. 57 (2003) 579–608.
[7] M. Reynolds, A. Zhitkovich, Cellular vitamin C increases chromate toxicity via a death program requiring mismatch repair but not p53, Carcinogenesis 28 (2007) 1613–1620.
[8] A.M. Urbano, C.F.D. Rodrigues, M.C. Alpoim, Hexavalent chromium exposure, genomic instability and lung cancer, Gene Ther. Mol. Biol. 12 (2008) 219–238.
[9] K. Kondo, N. Hino, M. Sasa, Y. Kamamura, S. Sakiyama, M. Tsuyuguchi, M. Hashimoto, T. Uyama, Y. Monden, Mutations of the p53 gene in human lung cancer from chromate-exposed workers, Biochem. Biophys. Res. Commun. 239 (1997) 95–100.
[10] Y. Takahashi, K. Kondo, T. Hirose, H. Nakagawa, M. Tsuyuguchi, M. Hashimoto, T. Sano, A. Ochiai, Y. Monden, Microsatellite instability and protein expression of the DNA mismatch repair gene, hMLH1, of lung cancer in chromate exposed workers, Mol. Carcinog. 42 (2005) 150–158.
[11] K. Kondo, Y. Takahashi, Y. Hirose, T. Nagao, M. Tsuyuguchi, M. Hashimoto, A. Ochiai, Y. Monden, A. Tangoku, The reduced expression and aberrant methylation of p16(INK4a) in chromate workers with lung cancer, Lung Cancer 53 (2006) 295–302.
[12] E. Avdievich, C. Reiss, S.J. Scherer, Y. Zhang, S.M. Maier, B. Jin, H. Hou Jr., A. Rosenwald, H. Riedmiller, R. Kucherlapati, P.E. Cohen, W. Edelmann, B. Kneitz, Distinct effects of the recurrent Mlh1G67R mutation on MMR functions, cancer, and meiosis, Proc. Natl. Acad. Sci. U.S.A. 105 (2008) 4247–4252.
[13] M.L. Veigl, L. Kasturi, J. Olechnowicz, A. Ma, J.D. Lutterbaugh, S. Periyasamy, G.-M. Li, J. Drummond, P.L. Modrich, W.D. Sedwick, S.D. Markowitz, Biallelic inactivation of hMLH1 by epigenetic gene silencing, a novel mechanism causing human MSI cancers, Proc. Natl. Acad. Sci. U.S.A. 95 (1998) 8698–8702.
[14] T. Hirose, K. Kondo, Y. Takahashi, H. Ishikura, H. Fujino, M. Tsuyuguchi, M. Hashimoto, T. Yokose, K. Mukai, T. Kodama, Y. Monden, Frequent microsatellite instability in lung cancer from chromate-exposed workers, Mol. Carcinog. 33 (2002) 172–180.
[15] K.A. Biedermann, J.R. Landolph, Induction of anchorage independence in human diploid foreskin fibroblasts by carcinogenic metal salts, Cancer Res. 47 (1987) 3815–3823.
[16] S.R. Patierno, D. Banh, J.R. Landolph, Transformation of C3H/10T1/2 mouse embryo cells to focus formation and anchorage independence by insoluble lead but not soluble calcium chromate: relationship to mutagenesis and internalization of lead chromate particles, Cancer Res. 48 (1988) 5280–5288.
[17] K.A. Biedermann, J.R. Landolph, Role of valence state and solubility of chromium compounds on induction of cytotoxicity, mutagenesis, and anchorage independence in diploid human fibroblasts, Cancer Res. 50 (1990) 7835–7842.
[18] R.R. Reddel, Y. Ke, B.I. Gerwin, M.G. McMenamin, J.F. Lechner, R.T. Su, D.E. Brash, J.B. Park, J.S. Rhim, C.C. Harris, Transformation of human bronchial epithelial cells by infection with SV40 or adenovirus-12 SV40 hybrid virus, or transfection via strontium phosphate co-precipitation with a plasmid containing SV40 early region genes, Cancer Res. 48 (1988) 1904–1909.
[19] H. Shim, C. Dolde, B.C. Lewis, C.S. Wu, G. Dang, R.A. Jungmann, R. Dalla-Favera, C.V. Dang, c-Myc transactivation of LDH-A: implications for tumor metabolism and growth, Proc. Natl. Acad. Sci. U.S.A. 94 (1997) 6658–6663.
[20] I.F. Robey, A.D. Lien, S.J. Welsh, B.K. Baggett, R.J. Gillies, Hypoxia inducible factor-1α and the glycolytic phenotype in tumors, Neoplasia 7 (2005) 324–330.
[21] G.L. Semenza, Hypoxia-inducible Factor 1 and Human Cancer, Asco Educational Book, 2008, pp. 548–551.
[22] V. Rush, D. Klimstra, I. Linkov, E. Dmitrovsky, Aberrant expression of p53 or the epidermal growth factor receptor is frequent in early bronchial neoplasia and coexpression precedes squamous cell carcinoma development, Cancer Res. 55 (1995) 1365–1372.
[23] J. Wu, J. Issa, J. Herman, D.E. Bassett Jr., B.D. Nelkin, S.B. Baylin, Expression of an exogenous eukaryotic DNA methyltransferase gene induces transformation of NIH 3T3 cells, Proc. Natl. Acad. Sci. U.S.A. 90 (1993) 8891–8895.
[24] F. Lonardo, V. Rusch, J. Langenfeld, E. Dmitrovsky, D.S. Klimstra, Overexpression of cyclins D1 and E is frequent in bronchial preneoplasia and precedes squamous cell carcinoma development, Cancer Res. 59 (1999) 2470–2476.
[25] J.F. Sah, R.L. Eckert, R.A. Chandraratna, E.A. Rorke, Retinoids suppress epidermal growth factor-associated cell proliferation by inhibiting epidermal growth factor receptor-dependent ERK1/2 activation, J. Biol. Chem. 277 (2002) 9728–9735.
[26] M.M. Stackpole, S.S. Wise, B.C. Goodale, E.G. Duzevika, R.C. Munroe, W.D. Thompson, J. Thackerd, L.H. Thompsone, J.M. Hinze, J.P. Wise Sr., Homologous recombination repair protects against particulate chromate-induced chromosome instability in Chinese hamster cells, Mutat. Res. 625 (2007) 145–154.
[27] E. Grlickova-Duzevik, S.S. Wise, R.C. Munroe, W.D. Thompson, J.P. Wise Sr., XRCC1 protects cells from chromate-induced chromosome damage, but does not affect cytotoxicity, Mutat. Res. 610 (2006) 31–37.
[28] D.E. Rooney, B.H. Czepulkowski (Eds.), Human Cytogenetics: A Practical Approach, 2nd ed., Oxford University Press, Oxford, 1992.
[29] K. Livak, T. Schmittgen, Analysis of relative gene expression data using real-time quantitative PCR and the $2^{-\Delta\Delta Ct}$, Methods 25 (2001) 402–408.
[30] O. Buhard, N. Suraweera, A. Lectard, A. Duval, R. Hamelin, Quasimonomorphic mononucleotide repeats for high level microsatellite instability analysis, Dis. Markers 20 (2004) 251–257.
[31] A.L. Holmes, S.S. Wise, S.J. Sandwick, W.L. Lingle, V.C. Negron, W.D. Thompson, J.P. Wise Sr., Chronic exposure to lead chromate causes centrosome abnormalities and aneuploidy in human lung cells, Cancer Res. 66 (2006) 4041–4048.
[32] Q. Shi, R.W. King, Chromosome nondisjunction yields tetraploid rather than aneuploid cells in human cell lines, Nature 437 (2005) 1038–1042.
[33] T. Fujiwara, M. Bandi, M. Nitta, E.V. Ivanova, R.T. Bronson, D. Pellman, Cytokinesis failure generating tetraploids promotes tumorigenesis in p53-null cells, Nature 437 (2005) 1043–1047.
[34] N.J. Ganem, S. Storchova, D. Pellman, Tetraploidy, aneuploidy and cancer, Curr. Opin. Genet. Dev. 17 (2007) 157–162.
[35] J. Mendelsohn, J. Baselga, Status of epidermal growth factor receptor antagonists in the biology and treatment of cancer, J. Clin. Oncol. 21 (2003) 2787–2799.
[36] O. Warburg, On the origin of cancer cells, Science 123 (1956) 309–314.
[37] K. Salnikow, K.S. Kasprzak, Ascorbate depletion: a critical step in nickel carcinogenesis? Environ. Med. 113 (2005) 577–584.
[38] S. Salceda, J. Caro, Hypoxia-inducible factor-1alpha (HIF-1alpha) protein is rapidly degraded by the ubiquitin proteasome system under normoxic conditions. Its stabilization by hypoxia depends on redox-induced changes, J. Biol. Chem. 272 (1997) 22642–22647.
[39] N.M. Mazure, E.Y. Chen, K.R. Laderoute, A.J. Giaccia, Induction of vascular endothelial growth factor by hypoxia is modulated by a phosphatidylinositol 3-kinase/Akt signaling pathway in Ha-ras-transformed cells through a hypoxia inducible factor-1 transcriptional element, Blood 90 (1997) 3322–3331.
[40] P.H. Maxwell, G.U. Dachs, J.M. Gleadle, L.G. Nicholls, A.L. Harris, I.J. Stratford, O. Hankinson, C.W. Pugh, P.J. Ratcliffe, Hypoxia-inducible factor-1 modulates gene expression in solid tumors and influences both angiogenesis and tumor growth, Proc. Natl. Acad. Sci. U.S.A. 94 (1997) 8104–8109.
[41] A. Valera, A. Pujol, X. Gregori, E. Riu, J. Visa, F. Bosch, Evidence from transgenic mice that myc regulates hepatic glycolysis, FASEB J. 9 (1995) 1067–1078.
[42] M. Esteller, R. Levine, S.B. Baylin, L.H. Ellenson, J.G. Herman, MLH1 promoter hypermethylation is associated with the microsatellite instability phenotype in sporadic endometrial carcinomas, Oncogene 16 (1998) 2413–2417.
[43] R.Z. Chen, U. Pettersson, C. Beard, L. Jackson-Grusby, R. Jaenisch, DNA hypomethylation leads to elevated mutation rates, Nature 395 (1998) 89–93.
[44] S.B. Baylin, J.E. Ohm, Epigenetic gene silencing in cancer: a mechanism for early oncogenic pathway addiction? Nat. Rev. Cancer 6 (2006) 107–116.
[45] B. Iacopetta, R. Hamelin, Evaluation of tumor microsatellite instability using five quasimonomorphic mononucleotide repeats and pentaplex PCR, Gastroenterology 123 (2002) 1804–1811.
[46] S.N. Thibodeau, G. Bren, D. Schaid, Microsatellite instability in cancer of the proximal colon, Science 260 (1993) 816–819.
[47] H. Zhu, N. Gooderham, Neoplastic transformation of human lung fibroblast MRC-5 SV2 cells induced by benzo[a]pyrene and confluence culture, Cancer Res. 62 (2002) 4605–4609.
[48] R. Li, G. Yerganian, P. Duesberg, A. Kraemer, A. Willer, C. Rausch, R. Hehlmann, Aneuploidy correlated 100% with chemical transformation of Chinese hamster cells, Proc. Natl. Acad. Sci. U.S.A. 94 (1997) 14506–14511.
[49] D.M. Ornitz, R.E. Hammer, A. Messing, R.D. Palmiter, R.L. Brinster, Pancreatic neoplasia induced by SV40 T-antigen expression in acinar cells of transgenic mice, Science 238 (1987) 188–193.
[50] T.A. Lehman, R. Modali, P. Boukamp, J. Stanek, W.P. Bennett, J.A. Welsh, R.A. Metcalf, M.R. Stampfer, N. Fusenig, E.M. Rogan, C.C. Harris, p53 mutations in human immortalized epithelial cell lines, Carcinogenesis 14 (1993) 833–839.
[51] R. Holliday, Chromosome error propagation and cancer, Trends Genet. 5 (1989) 42–45.
[52] H.G. Nguyen, K. Ravid, Tetraploidy/Aneuploidy and stem cells in cancer promotion: the role of chromosome passenger proteins, J. Cell Physiol. 208 (2006) 12–22.
[53] P. Duesberg, R. Li, Multistep carcinogenesis: a chain reaction of aneuploidizations, Cell Cycle 2 (2003) 202–210.
[54] J.H. Bielas, L.A. Loeb, Mutator phenotype in cancer: timing and perspectives, Environ. Mol. Mutagen. 45 (2005) 206–213.
[55] M. Kim, B.N. Trinh, T.I. Long, S. Oghamian, P.W. Laird, Dnmt1 deficiency leads to enhanced microsatellite instability in mouse embryonic stem cells, Nucleic Acids Res. 32 (2004) 5742–5749.
[56] J.-Y. Fang, Z.-H. Cheng, Y.-X. Chen, R. Lu, L. Yang, H.-Y. Zhu, L.-G. Lu, Expression of Dnmt1, demethylase, MeCP2 and methylation of tumor-related genes in human gastric cancer, World J. Gastroenterol. 10 (2004) 3394–3398.
[57] S.K. Vilcheck, T.J. O'Brien, D.E. Pritchard, L. Ha, S. Ceryak, J.L. Fornsaglio, S.R. Patierno, Fanconi anemia complementation group A cells are hypersensitive to chromium(VI)-induced toxicity, Environ. Health Perspect. 110 (2002) 773–777.
[58] H. Xie, A.L. Holmes, S.S. Wise, N. Gordon, J.P. Wise Sr., Lead chromate-induced chromosome damage requires extracellular dissolution to liberate chromium ions but does not require particle internalization or intracellular dissolution, Chem. Res. Toxicol. 17 (2004) 1362–1367.
[59] M.V. Blagosklonny, Oncogenic resistance to growth-limiting conditions, Nat. Rev. Cancer 2 (2002) 221–224.

[60] E. Laconia, S. Doratiottoa, P. Vineis, The microenvironments of multistage carcinogenesis, Semin. Cancer Biol. 18 (2008) 322–329.
[61] T.P. Garrington, G.L. Johnson, Organization and regulation of mitogen-activated protein kinase signaling pathways, Curr. Opin. Cell. Biol. 11 (1999) 211–218.
[62] C.S. Hill, R. Treisman, Transcriptional regulation by extracellular signals: mechanisms and specificity, Cell 80 (1995) 199–211.
[63] S.-M. Chuang, J.-L. Yang, Comparison of roles of three mitogen-activated protein kinases induced by chromium(VI) and cadmium in non-small-cell lung carcinoma cells, Mol. Cell. Biochem. 222 (2001) 85–95.
[64] A.J. Whitmarsh, R.J. Davis, Transcription factor AP-1 regulation by mitogen-activated protein kinase signal transduction pathways, J. Mol. Med. 74 (1996) 589–607.